HYDROGELS CONTAINING LINEAR AND CYCLIC POLYETHERS

HELEN RACHEL OXLEY

Doctor of Philosophy

THE UNIVERSITY OF ASTON IN BIRMINGHAM

April 1991

THE UNIVERSITY OF ASTON IN BIRMINGHAM

HYDROGELS CONTAINING LINEAR AND CYCLIC POLYETHERS

HELEN RACHEL OXLEY

Submitted for the Degree
of Doctor of Philosophy

April 1991

SUMMARY

Hydrogels are a unique class of polymer which swell, but do not dissolve in, water. A range of 2-hydroxyethyl methacrylate based copolymer hydrogels containing both cyclic and linear polyethers have been synthesised and are described in this thesis. Initially, cyclic polyethers were occluded within the polymer matrix and the transport properties investigated. The results indicated that the presence of an ionophore can be used to modulate ion transport and that ion transport is described by a dual-sorption mechanism. However, these studies were limited due to ionophore loss during hydration. Hence, the synthesis of a range of acrylate based crown ether monomers was considered. A pure sample of 4-acryolylaminobenzo-15-crown-5 was obtained and a terpolymer containing this monomer was prepared. Transport studies illustrated that the presence of a 'bound' ionophore modulates ion transport in a similar way to the occluded systems. The transport properties of a series of terpolymers containing linear polyethers were then investigated. The results indicated that the dual-sorption mechanism is observed for these systems with group II metal cations while the transport of group I metal cations, with the exception of sodium, is enhanced.

Finally, the equilibrium water contents (EWC) surface and mechanical properties of these terpolymers containing linear polyethers were examined. Although subtle variations in EWC are observed as the structure of the polyether side chain varies, generally EWC is enhanced due to the hydrophilicity of the polyether side chain. The macroscopic surface properties were investigated using a sessile drop technique and FTIR spectroscopy. At a molecular level surface properties were probed using an *in vitro* ocular spoilation model and preliminary cell adhesion studies. The results indicate that the polyethylene oxide side chains are expressed at the polymer surface thus reducing the adhesion of biological species.

Keywords: **hydrogel, cyclic polyether, linear polyether, transport properties, surface properties**

To my family

ACKNOWLEDGEMENTS

I would like to take this opportunity to express my thanks to the following:

Firstly, I would like to thank my supervisor Dr. Ann Jarvie and my associate supervisor Dr. Brian Tighe for their advice, encouragement and enthusiasm throughout the course of this work.

Dr. Val Franklin for undertaking the *in vitro* ocular spoilation studies, Dr. Mike Perry for running the NMR spectra, Dr. Steve Holding at RAPRA for performing the GPC's and Miss Helen Fitton for completing the cell adhesion studies described in this thesis.

Dr. Colin Hamilton, Dr. Sheila Murphy and Dr. Megan Davies for their help during the early months of this work.

All the staff and students who have worked with me in the Speciality Materials Group for helping to make my time at Aston so enjoyable.

SERC for financial support.

Finally, special thanks go to Dr. Phil Corkhill for his patience, support and understanding during the course of this work and in particular while I have been 'writing up'.

LIST OF CONTENTS

		Page
TITLE PAGE		1
SUMMARY		2
DEDICATION		3
ACKNOWLEDGEMENTS		4
LIST OF CONTENTS		5
LIST OF TABLES		12
LIST OF FIGURES		15
LIST OF ABBREVIATIONS		22
CHAPTER 1	INTRODUCTION AND LITERATURE SURVEY	23
1.1	General Introduction	24
1.2	Hydrogels	25
1.3	Water in Hydrogels	26
1.4	Biocompatibility of Hydrogels	29
1.5	Ionophores for Group I and II Metal Cations	32
1.5.1	Nomenclature of Crown Ethers	36
1.5.2	Characteristics of Crown Ethers	37
1.5.3	Synthesis of Crown Ethers	37
1.5.4	Crown Ethers in Polymers	38
1.6	The Transport Properties of Hydrogels	44
1.6.1	The Fundamentals of Permeation and Diffusion	44
1.6.2	Transport and Permeability Phenomena in Hydrogels	47

		Page
1.7	Aims and Scopes of the Project	51
CHAPTER 2	MATERIALS AND METHODS	53
2.1	Introduction	54
2.2	Reagents	54
2.2.1	Crown Ethers	54
2.2.2	Miscellaneous Reagents Used in Monomer Synthesis	56
2.2.3	Salts	56
2.2.4	Reagents Used in Polymer Synthesis	56
2.3	The Preparation of 4-acryloylaminobenzo-15-crown-5	59
2.3.1	The Preparation of 4-nitrobenzo-15-crown-5	59
2.3.2	The Preparation of 4-aminobenzo-15-crown-5	60
2.3.3	The Preparation of 4-acryloylaminobenzo-15-crown-5	62
2.4	The Preparation of 4-acetylbenzo-15-crown-5	63
2.5	The Preparation of 4-acryloylmethylbenzo-15-crown-5	64
2.5.1	The Synthesis of 4-formylbenzo-15-crown-5	64
2.5.2	The Preparation of 4-hydroxybenzo-15-crown-5	65
2.5.3	The Preparation of 4-acryloylmethyl-benzo-15-crown-5	67
2.6	The Synthesis of 4,4'-diacryloylaminodibenzo-18-crown-6	67

		Page
2.6.1	The Synthesis of 4,4'-dinitrodibenzo-18-crown-6	67
2.6.2	The Preparation of *trans* 4,4'-diamino-dibenzo-18-crown-6	69
2.7	The Preparation of 4,4'diacryloylmethyldibenzo-18-crown-6	69
2.7.1	The Preparation of 4,4'-diformyldibenzo-18-crown-6	70
2.7.2	The Preparation of 4,4'-dihydroxymethyl-dibenzo-18-crown-6	70
2.7.3	The Preparation of 4,4'diacryloylmethyl-dibenzo-18-crown-6	71
2.8	The Preparation of Hydrogel Membranes	72
2.9	Determination of Equilibrium Water Content (EWC)	73
2.9.1	The Effect of Salt on EWC	74
2.9.2	The Measurement of Partition Coefficients	74
2.9.3	The Leaching of Membrane Components	76
2.10	Measurement of Surface Properties	76
2.11	Permeability Studies	77
2.11.1	Design and Set-Up of the Ion Permeability Apparatus	77
2.11.2	Operation of the Ion Permeability Apparatus	80
2.11.3	Errors Associated with the measurement of Permeability Coefficients	81
2.12	Measurement of Mechanical Properties	82

		Page
CHAPTER 3	TRANSPORT PROPERTIES OF UNMODIFIED AND CROWN MODIFIED HYDROGEL MEMBRANES	84
3.1	Introduction	85
3.2	Ion Permeation Studies Through a Crosslinked HEMA Membrane	86
3.2.1	Effect of Cation Variation on the Transport of Chloride Salts	86
3.2.2	Permeation of a Mixed Salt Solution	90
3.2.3	Effect of Anion Variation on the Transport of Potassium Ions	92
3.3	Transport Phenomena in Hydrogels Containing Occluded Crown Ethers	94
3.3.1	Effect of Cation Variation on the Transport of Chloride Salts Through a dicyclohexyl-18-crown-6 Modified Membrane	94
3.3.2	Effect of Anion variation on the Transport of Potassium Through dicyclohexano-18-crown-6 Modified Membranes	97
3.3.3	Occlusion of Other Crown Ethers in Hydrogel Membranes	101
3.4	Conclusions	103

		Page
CHAPTER 4	SYNTHESIS AND PRELIMINARY TRANSPORT STUDIES OF MONOMERIC CROWN ETHERS	105
4.1	Introduction	106
4.2	Synthesis of Crown Monomers	106
4.3	Summary of Monomer Synthesis	113
4.4	Hydrogels Containing 4-acryloylamino-benzo-15-crown-5	113
4.5	Conclusions	118
CHAPTER 5	CHARACTERISATION OF 2-HYDROXYETHYL METHACRYLATE COPOLYMERS CONTAINING LINEAR POLYETHERS	119
5.1	Introduction	120
5.2	Assessment of the Purity of Linear Polyether Monomers	122
5.3	The Effect of Linear Polyethers on EWC	122
5.3.1	Effect of Linear Polyethers on the EWC of HEMA:EGDM (99:1)	122
5.3.2	Effect of Linear Polyether on the EWC of HEMA:EGDM (90:10)	128
5.3.3	Effect of Crosslinker Content on EWC	133
5.4	Effect of Salt on EWC	134
5.5	Partition Coefficients of HEMA:EGDM (90:10) Containing Linear Polyethers	138

		Page
5.6	Mechanical Properties of Hydrogels Containing Linear Polyethers	142
5.7	Conclusions	144
CHAPTER 6	TRANSPORT STUDIES OF LINEAR POLYETHER MODIFIED HYDROGEL MEMBRANES	145
6.1	Introduction	146
6.2	Effect of Linear Polyethers on the Transport of Group I Metal Cations Across HEMA:EGDM (90:10)	147
6.3	Effect of MPEG 200 MA Content on Sodium Transport Across HEMA:EGDM (90:10)	155
6.4	Effect of Linear Polyethers on the Transport of Group II Metal Cations Across HEMA:EGDM (90:10)	157
6.5	Discussion and Conclusions	165
CHAPTER 7	SURFACE PROPERTIES OF HYDROGELS MODIFIED WITH LINEAR POLYETHERS	168
7.1	Introduction	169
7.2	Determination of Surface Energy	170
7.3	Horizontal ATR FTIR of Poly (ethylene oxide) Terpolymers	177
7.4	Lipid and Protein Deposition Studies	181
7.4.1	Effect of Poly (ethylene oxide) Chain Length on Ocular Spoilation	186

		Page
7.4.2	Effect of Crosslinker Content on the Deposition of Proteins and Lipids	190
7.4.3	Effect of Structural Variations in the Polyether Side Chain on Ocular Compatibility	192
7.4.4	Ocular Spoilation Studies on Novel Soft Contact Lenses	196
7.5	Cell Adhesion to Poly (ethylene oxide) Terpolymers	198
7.6	Conclusions	199
CHAPTER 8	CONCLUSIONS AND SUGGESTIONS FOR FURTHER WORK	203
8.1	Conclusions	204
8.2	Suggestions for Further Work	209
APPENDICES		
Appendix 1	Nomenclature of Crown Ethers	212
Appendix 2	Spectral Data for Synthesis of Crown Ether Monomers	214
Appendix 3	Gel Permeation Chromatograms for Linear Polyether Monomers	222
LIST OF REFERENCES		227

LIST OF TABLES

		Page
Table 2.1	Crown ethers used in this work	54
Table 2.2	Reagents used in monomer synthesis	56
Table 2.3	Molecular weights and suppliers of monomers	57
Table 3.1	Permeability coefficients for cation transport across HEMA:EGDM (90:10)	88
Table 3.2	Ionic radii for Group I and II metal cations	89
Table 3.3	Permeability coefficients for the transport of potassium salts across HEMA:EGDM (90:10)	93
Table 3.4	Permeability coefficients P_1 and P_2 for cation transport across a dicyclohexano-18-crown-6 modified membrane	96
Table 3.5	Extended 'lag-times' for the transport of cations across a dicyclohexano-18-crown-6 modified membrane	96
Table 3.6	Effect of anion variation on the 'lag-time' for potassium transport across a dicyclohexano-18-crown-6 modified membrane	98
Table 3.7	Permeability coefficients P_1 and P_2 for the transport of potassium salts across a dicyclohexano-18-crown-6 modified membrane	99
Table 3.8	Effective reduction in the permeability coefficient for the transport of potassium across a dicyclohexano-18-crown-6 modified membrane	100

		Page
Table 4.1	The effect of bound crown on the EWC of HEMA:EGDM (90:10)	114
Table 4.2	The effect of 4-acryloylaminobenzo-15-crown-5 on the EWC of HEMA:EGDM (90:10)	116
Table 4.3	The effect of 0.25M NaCl on the EWC of HEMA:EGDM (90:10)	116
Table 5.1	The effect of polyether content on the EWC of HEMA:EGDM (99:1)	123
Table 5.2	The effect of increasing HPHPMA content on EWC	127
Table 5.3	Effect of polyether chain length on the EWC of HEMA:EGDM (90:10)	129
Table 5.4	The effect polyethers on the EWC of HEMA:EGDM (90:10)	131
Table 5.5	The effect of salt on the EWC of HEMA:EGDM (90:10)	134
Table 5.6	The effect of salt on the EWC of MPEGMA modified membranes	137
Table 5.7	Partition coefficients, Sm, for 0.25M solutions of NaCl and $CaCl_2$	140
Table 5.8	The effect of MPEG 200 MA content on the EWC of modified HEMA:EGDM (90:10) in 0.25M NaCl at room temperature	142
Table 6.1	The effect of polyether chain length on the calculated permeability coefficients, P, for the transport of 0.25 M solutions of NaCl, KCl and LiCl across HEMA:EGDM (90:10)	150

		Page
Table 6.2	Effect of MPEG 200 MA content on the permeability coefficient for the transport of 0.25M NaCl at 37°C across HEMA:EGDM (90:10)	156
Table 6.3	Calculated values of the permeability coefficients, P_1 and P_2 for the transport of group II metal chlorides across HEMA:EGDM (90:10) modified terpolymers	161
Table 6.4	Extended 'lag-times' for the permeation of group II chlorides through MPEG MA modified membranes	163
Table 7.1	Polar and dispersive components of water and methylene iodide	171
Table 7.2	Polar, dispersive and total surface energies for dehydrated poly (ethylene oxide) modified copolymers	172
Table 7.3	Calculated values for the polar, dispersive and total surface free energies of hydrated poly (ethylene oxide) modified terpolymers in their hydrated state	176
Appendix 1		
Table 1	Nomenclature of crown ethers	213

LIST OF FIGURES

		Page
Figure 1.1	A diagramatic representation of the three phase model of imbibed water	28
Figure 1.2	The interaction of blood components with hydrated poly (ethylene oxide) chains at the polymer surface	31
Figure 1.3	dibenzo-18-crown-6	33
Figure 1.4	[2,2,2] cryptand	34
Figure 1.5	bis-tetrakis (hydroymethyl) ethylene or bis-THYME	34
Figure 1.6	valinomycin	35
Figure 1.7	p-tert-butylcalix[4]arene	35
Figure 1.8	The synthesis of dibenzo-18-crown-6	38
Figure 1.9	The synthesis of 18-crown-6	39
Figure 1.10	An immobilised crown ether	42
Figure 2.1	Structures of crown ethers	54
Figure 2.2	Structures of reagents used in polymer synthesis	58
Figure 2.3	Membrane mould	72
Figure 2.4	Diagramatic representation of the permeability cell	78
Figure 2.5	Schematic representation of permeability apparatus	79
Figure 3.1	Primary data for the transport of group I metal chlorides across HEMA:EGDM (90:10)	87
Figure 3.2	Primary data for the transport of group II metal chlorides across HEMA:EGDM (90:10)	87

		Page
Figure 3.3	Primary data for the transport of a mixed salt solution across HEMA:EGDM (90:10)	91
Figure 3.4	Effect of anion variation on cation transport through HEMA:EGDM (90:10)	93
Figure 3.5	Effect of cation variation on ion transport through a dicyclohexano-18-crown-6 modified membrane	95
Figure 3.6	Effect of anion variation on potassium ion transport across a dicyclohexano-18-crown-6 modified membrane	98
Figure 3.7	Transport of sodium chloride across a benzo-15-crown-5 modified membrane	102
Figure 3.8	Average weight loss from unmodified and benzo-15-crown-5 modified membranes	103
Figure 4.1	The synthesis of 4-acryloylaminobenzo-15-crown-5	107
Figure 4.2	The synthesis of 4-acryloylacetylbenzo-15-crown-5	109
Figure 4.3	The synthesis of 4-acryloylmethylbenzo-15-crown-5	110
Figure 4.4	The synthesis of 4,4'-diacryloylaminodibenzo-18-crown-6	111
Figure 4.5	The synthesis of 4,4'-diacryloylmethyldibenzo-18-crown-6	112
Figure 4.6	Transport of NaCl across HEMA:EGDM (90:10) modified with 2.5% 4-acryloylaminobenzo-15-crown-5	115
Figure 4.7	Transport of NaCl across HEMA:EGDM (90:10) modified with 5% 4-acryloylaminobenzo-15-crown-5	117
Figure 5.1	Structures of poly (ethylene oxide) monomers	121
Figure 5.2	Effect of polyether chain length on the EWC of HEMA:EGDM (99:1)	124

		Page
Figure 5.3	Effect of hydroxy vs methoxy end groups on the EWC of terpolymers with 4,5 repeating ether groups in the polyether side chain	126
Figure 5.4	Effect of hydroxy vs methoxy end groups on the EWC of terpolymers with 9,10 repeating ether groups in the polyether side chain	126
Figure 5.5	Effect of HPHPMA on the EWC of HEMA:EGDM (99:1)	128
Figure 5.6	Effect of polyether chain length on the EWC of HEMA:EGDM (90:10)	130
Figure 5.7	Effect of polyether content on the EWC of HEMA:EGDM (90:10)	131
Figure 5.8	Effect of crosslinker concentration on the EWC of polyether terpolymers	133
Figure 5.9	Effect of salt on the EWC of HEMA:EGDM (90:10)	135
Figure 5.10	Effect of salt on the EWC of MPEG 200 MA modified HEMA:EGDM (90:10)	136
Figure 5.11	Effect of salt on the EWC of MPEG 400 MA modified HEMA:EGDM (90:10)	136
Figure 5.12	Effect of salt on the EWC of MPEG 1000 MA modified HEMA:EGDM (90:10)	137
Figure 5.13	Typical load / extension curves for (a) HEMA:EGDM (99:1) and (b) HEMA:EGDM (99:1) + 5% MPEG 1000 MA	143
Figure 6.1	The structure of the MPEG MA's used in this study	146

		Page
Figure 6.2	Primary transport data for the permeation of NaCl across methoxy polyethylene glycol methacrylate modified HEMA:EGDM (90:10)	148
Figure 6.3	Primary transport data for the permeation of KCl across methoxy polyethylene glycol methacrylate modified HEMA:EGDM (90:10)	148
Figure 6.4	Primary transport data for the permeation of LiCl across methoxy polyethylene glycol methacrylate modified HEMA:EGDM (90:10)	149
Figure 6.5	Plot of P vs H for the transport of group I metal chlorides through MPEG MA modified membranes	151
Figure 6.6	Plot of LnP vs 1/H for the transport of group I metal chlorides through MPEG MA modified membranes	153
Figure 6.7	Effect of composition on the permeability coefficients, P, for the transport of group I metal cations across modified and unmodified HEMA:EGDM (90:10)	154
Figure 6.8	Effect of MPEG 200 MA content on the transport of NaCl	156
Figure 6.9	Plot of Ln P vs 1/H for the transport of NaCl across MPEG 200 MA modified terpolymers	157
Figure 6.10	Primary transport data for the permeation of $CaCl_2$ across methoxy polyethylene glycol methacrylate modified HEMA:EGDM (90:10)	158
Figure 6.11	Primary transport data for the permeation of $MgCl_2$ across methoxy polyethylene glycol methacrylate modified HEMA:EGDM (90:10)	159

		Page
Figure 6.12	Primary transport data for the permeation of $BaCl_2$ across methoxy polyethylene glycol methacrylate modified HEMA:EGDM (90:10)	159
Figure 6.13	Plot of LnP_2 vs 1/H for the transport of group II metal chlorides through MPEG MA modified membranes	162
Figure 6.14	Effect of composition on the permeability coefficient, P, for the transport of group II metal cations across modified and unmodified HEMA:EGDM (90:10)	164
Figure 7.1	Effect of composition on γ_s^d of poly (ethylene oxide) terpolymers	173
Figure 7.2	Effect of composition on γ_s^p of poly (ethylene oxide) terpolymers	173
Figure 7.3	Effect of composition on γ_s^t of poly (ethylene oxide) terpolymers	174
Figure 7.4	Horizontal ATR FTIR of HEMA:EGDM (99:1)	178
Figure 7.5	Horizontal ATR FTIR of HEMA:EGDM (99:1) modified with 5% MPEG 200 MA	179
Figure 7.6	Horizontal ATR FTIR subtraction spectra for HEMA:EGDM (99:1) with 5% MPEG 200 MA and HEMA:EGDM (99:1)	180
Figure 7.7	Fluorescence spectra excited at 360nm	184
Figure 7.8	Fluorescence spectra excited at 280nm	185
Figure 7.9	Typical deposition of lipid on a poly (ethylene oxide) modified HEMA copolymer with time	186
Figure 7.10	Effect of polyether chain length on lipid deposition to methoxy polyethylene glycol methacrylate modified HEMA:EGDM (99:1) terpolymers	187

		Page
Figure 7.11	Effect of polyether chain length on lipid deposition to methoxy polyethylene glycol methacrylate modified HEMA:EGDM (90:10) terpolymers	188
Figure 7.12	Effect of polyether chain length on protein deposition to methoxy polyethylene glycol methacrylate modified HEMA:EGDM (99:1) terpolymers	189
Figure 7.13	Effect of polyether chain length on protein deposition to methoxy polyethylene glycol methacrylate modified HEMA:EGDM (90:10) terpolymers	190
Figure 7.14	Effect of crosslinker concentration on lipid deposition to methoxy polyethylene glycol methacrylate modified terpolymers	191
Figure 7.15	Effect of crosslinker concentration on protein deposition to methoxy polyethylene glycol methacrylate modified terpolymers	191
Figure 7.16	Effect of hydroxy vs methoxy end groups on lipid deposition to poly (ethylene oxide) modified HEMA:EGDM (99:1)	193
Figure 7.17	Effect of hydroxy vs methoxy end groups on protein deposition to poly (ethylene oxide) modified HEMA:EGDM (99:1)	194
Figure 7.18	Effect of a methyl substituent in the polyether side chain on lipid deposition to poly (ethylene oxide) modified HEMA:EGDM (99:1)	195
Figure 7.19	Effect of a methyl substituent in the polyether side chain on protein deposition to poly (ethylene oxide) modified HEMA:EGDM (99:1)	196

Page

Figure 7.20 Deposition of lipid with time on novel contact lenses containing poly (ethylene oxides) 197

Figure 7.21 Adhesion of 3T3 cells to poly (ethylene oxide) modified terpolymers 199

APPENDICES

Appendix 1

Figure 1 Infra-red spectrum of 4-nitrobenzo-15-crown-5 216

Figure 2 ^{1}H nmr spectrum of 4-nitrobenzo-15-crown-5 217

Figure 3 ^{13}C spectrum of 4-nitrobenzo-15-crown-5 218

Figure 4 A two dimensional COSY spectrum of 4-nitrobenzo-15-crown-5 219

Figure 5 ^{13}C spectrum of 4-formylbenzo-15-crown-5 220

Figure 6 Infra-red spectrum of contaminated 4-acryloylaminobenzo-15-crown-5 221

Appendix 3

Figure 1 Gel permeation chromatograms for the methoxy polyethylene glycol methacrylates (MPEG MA's) 223

Figure 2 Gel permeation chromatogram for ethoxylated hydroxyethyl methacrylate (HEMA 4,5 EO) 224

Figure 3 Gel permeation chromatogram for polyethylene glycol methacrylate (PEGMA 10 EO) 225

Figure 4 Gel permeation chromatogram for hexapropoxylated hydroxypropyl methacrylate (HPHPMA) 226

LIST OF ABBREVIATIONS

AZBN	Azo-bis-isobutyronitrile	B-15-C-5	benzo-15-crown-5
COSY	Correlation Spectroscopy	DB-18-C-6	dibenzo-18-crown-6
DCH-18-C-6	dicyclohexano-18-crown-6	DSC	Differetial Scannining Calorimetry
DTA	Differential Thermal Analysis	E	Youngs modulus
ε_b	Elongation to break	EMA	Ethyl methacrylate
EGDM	Ethylene glycol dimethacrylate	EWC	Equilibrium Water Content
γ^d	Dispersive component of surface free energy	γ^p	Polar component of the surface free energy
γ^t	Total surface free energy	GPC	Gel Permeation Chromatogram
HPHPMA	Hexapropoxylated hydroxypropyl methacrylate	HEMA	2-Hydroxyethyl methacrylate
HEMA 4,5 EO	Ethoxylated hydroxyethyl methacrylate	MMA	Methyl methacrylate
MPEGMA	Methoxy poly ethylene glycol methacrylate	NMR	Nuclear magnetic resonance spectroscopy
PEGMA 10 EO	Polyethylene glycol monomethacrylate 10 moles EO	Sm	Partition coefficient
σ_b	Tensile strength	TFA	Trifluoracetic acid

CHAPTER 1

Introduction and Literature Survey

1.1 General Introduction

Hydrogels are a unique class of polymer which swell, but do not dissolve, in water. Hence many naturally occurring materials, such as gelatin, may be classed as hydrogels. The preparation of a synthetic hydrogel was first reported in the early 1960's by two Czechoslovakian workers Wichterle and Lim[1]. These workers synthesised a poly hydroxy methacrylate, namely poly 2-hydroxyethyl methacrylate or poly HEMA and highlighted the potential biomedical applications of this material. Since this discovery synthetic hydrogels have been used for a wide variety of biomedical applications ranging from contact lenses[2], drug delivery systems[3], wound dressings[4] and fertility control devices[5] through to synthetic articular cartilage[6].

However, poly HEMA is not a universally compatible biomaterial[7]. Thus, although the fabrication of soft contact lenses is one of the most successful applications of these materials, ocular incompatibility is observed with the formation of 'white surface films'[8] and 'white spots'[9] on the lens surface. There have been many attempts to improve the biocompatibility of poly HEMA by copolymerising it with a range of vinyl monomers. To date no universally compatible material has been found but both Graham[10] and Merrill[11] have described hydrogels containing poly(ethylene oxide) which exhibit enhanced biocompatibility.

The imbibed water present in hydrogels plays a significant role not only in contributing to the overall structure of these materials but also in influencing their surface, transport and mechanical properties. Water structuring effects within hydrogels are known to play an important role in influencing the biocompatibility of these materials. Although water structuring in hydrogels has not been investigated experimentally in this thesis, the water binding properties of hydrogels containing both poly(ethylene oxides)[10] and poly

hydroxyalkyl acrylates and methacrylates[7] have been discussed in the literature. This thesis is primarily concerned with attempts to harness both the water-structuring properties and enhanced biocompatibility of poly (ethylene oxide) units in vinyl based hydrogels. As both cyclic and linear polyethers form complexes with metal cations, this property may be advantageous in the design of permselective membranes, particularly for use in sensor applications. However, if these ligands sequester metal cations, particularly calcium ions, from biological solutions, this may lead to biointolerence. Hence, particular emphasis has been placed on the transport properties of these materials. This introductory chapter will, therefore, discuss some of the fundamental properties of hydrogels including their transport properties and review some aspects of the coordination chemistry of group I and II metal cations.

1.2 Hydrogels

The term hydrogel has been used to describe a variety of materials ranging from naturally occurring polymers such as gelatin, through semi-synthetic materials such as cellulose acetate, to those entirely synthetic in nature. A small family of polyether-polyurethane copolymers is included in this last category. However, most synthetic hydrogels are based on the poly hydroxy acrylates and methacrylates. The common characteristics that all these materials possess are that they are hydrophilic in nature and exhibit the ability to form water swollen gels. This work is predominantly concerned with synthetic, crosslinked hydrogel networks based on poly(2-hydroxyethyl methacrylate) often abbreviated to poly HEMA with ethylene glycol dimethacrylate (EGDM) acting as the crosslinking agent.

Many of the properties of hydrogels are influenced by the water within the polymer matrix. It is the ability of this water to facilitate the transport of aqueous species,

particularly group I and II metal cations, which is of most interest within the context of this project. Thus, one of the most important properties of a hydrogel is its equilibrium water content (EWC) whereby;

$$EWC = \frac{\text{weight of water present in the hydrated gel}}{\text{total weight of hydrated gel}} \times 100\,(\%) \quad (1.1)$$

The equilibrium water content of a hydrogel is in turn governed to a large extent by chemical structure. Copolymerisation of HEMA with more hydrophilic monomers, such as N-vinyl pyrrolidone, increases the EWC, conversely copolymerisation with hydrophobic monomers, for example styrene, will cause a net decrease in EWC. Other factors such as environment, temperature, pH and tonicity can all affect the EWC.

Variations in the EWC have pronounced effects on the bulk, surface, mechanical and transport properties of the gel. The effect of EWC on transport properties will be discussed in more detail in Section 1.6, while Barnes and coworkers[12] have discussed the variation in bulk, surface and mechanical properties with EWC. At this point it is sufficient to note that as EWC increases, there is generally a fall in tensile strength of the hydrogel. Furthermore, an increase in surface energy is observed as EWC increases due to the contribution of the polar water molecules.

1.3 Water in Hydrogels

The nature of water imbibed within a hydrogel matrix is important since it not only influences the surface and interfacial properties of the material, but also affects the transport of aqueous species across the polymer matrix. Hence, it is important to have some understanding of the interactions involved between the polymer and the imbibed water.

A variety of techniques have been used to study water in hydrogels[13-35]. These include specific conductivity[13], differential scanning calorimetry, (DSC)[22-27], differential thermal analysis, (DTA)[28, 29], dilatometry[30] and nuclear magnetic resonance spectroscopy, (NMR)[31-35].

There is a great deal of evidence to suggest that water in hydrogel membranes can exist in more than one state[13-37]. Initially, studies were restricted to cellulosic membranes, in particular cellulose acetate membranes, which are of interest in reverse osmosis applications. Workers generally agreed that at least two different states of water are present in such membranes. The first of these states involves 'non-freezing' water or 'bound' water which is thought to interact strongly with or bind to the polymer. The second involves freezing water which has only weak interactions with the polymer backbone. Frommer and Lancet[23] illustrated that in such cellulosic membranes the proportion of 'non-freezing' or 'bound' water is dependent upon the polymer morphology and increases with decreasing packing density of the polymer membrane. However, Taniguchi and Horigome[36] suggested that there might be as many as four states of water within these membranes. The first three of these states can interact with salts and are classified as completely free water, free water which interacts weakly with the polymer and bound water which can contain salts. Finally, the last of these states involved bound water which rejects salts.

Andrade, Jhon and coworkers [13,17-19,37] have studied synthetic hydrogels of the type considered in these studies. These workers favour a model which contains three distinct phases of water classified by the letters, X, Y and Z, where X represents bound water, Y represents interfacial water and Z represents bulk water. This model is represented by Figure 1.1 and has been confirmed by a variety of experimental techniques.

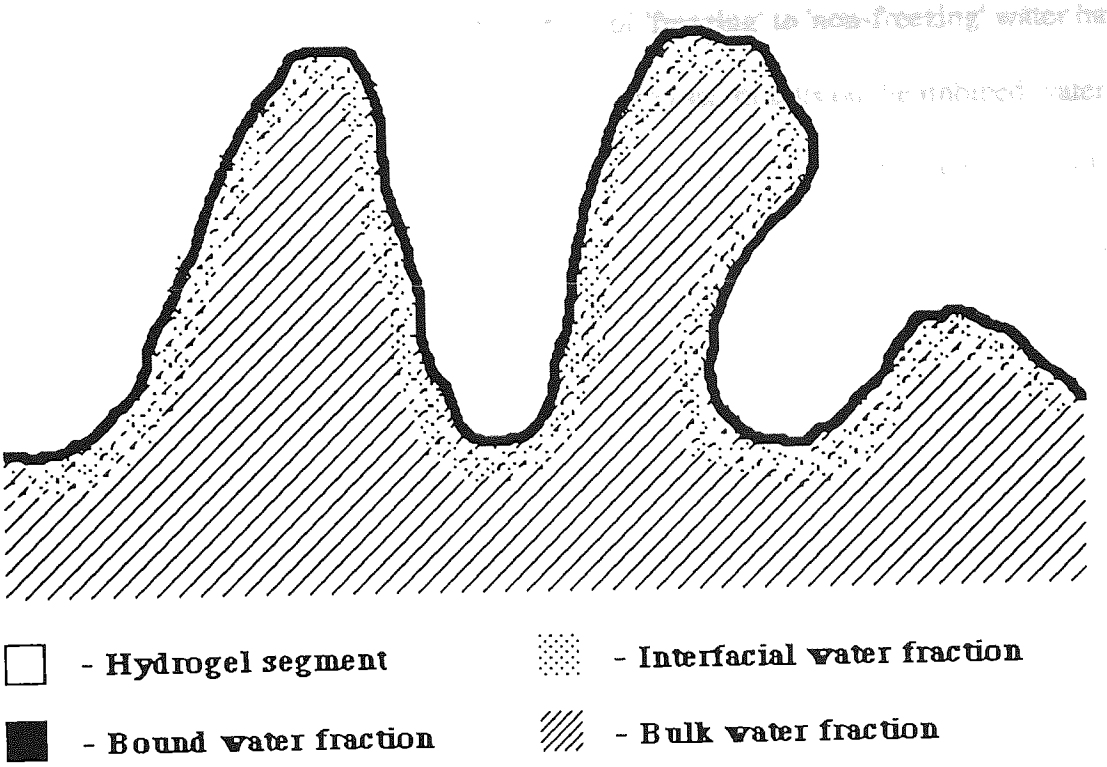

Figure 1.1 A diagramatic representation of the three phase model of imbibed water (redrawn from reference 39)

Several Dutch workers have recently suggested that the presence of non-freezing water within poly HEMA is not a thermodynamic phenomenon caused by interactions or 'bonding' between the polymer and water [28,29,35]. These workers attribute the presence of such water to kinetic factors and suggest that since the polymers are well below their Tg at the temperatures used for DSC studies water molecules are prevented from diffusing to the ice crystals forming within the gel and hence remain unfrozen[29]. Further evidence to support this theory is provided by their NMR relaxation studies which suggest that there are no thermodynamically different classes of water within the gels studied irrespective of their crystalline water content[35]. However, these workers have concentrated on poly HEMA and have neglected the contributions that variations in chemical structure will have on both the water binding and the Tg of the polymer.

To date studies of the effect of salts on the ratio of 'freezing' to 'non-freezing' water have been limited. Hamilton[39,40] studied the effect of potassium salts on the imbibed water in poly HEMA using DSC. He found that structure making anions such as Cl^- and SO_4^{2-} reduce the free or freezing water content, whereas structure breaking anions for example I^- increase the freezing water content.

These studies have in the main been concerned with polymers containing hydroxyl as the dominant water-structuring group. Since this thesis is concerned with hydrogels containing poly(ethylene oxide) units, it is important to consider the contributions this group will make to the overall water-structuring of these hydrogels. The interactions of poly ethylene glycols with water have been studied by numerous workers[41-57]. Several studies have illustrated that both mono and trihydrates are formed between each ether unit and water molecules[41,46,52]. More recently, Schreiner and coworkers have studied the stoichiometry of poly (ethylene glycol 400) hydrates using proton NMR[55]. These studies indicated that two water molecules are associated with each ether group. In addition, other workers have suggested that poly(ethylene oxide) exists in a helical conformation in water[45,56,57]. Finally, Graham and coworkers have studied the interactions of water with poly (ethylene oxide) based hydrogels[51,53,54] and have illustrated that both mono and trihydrates are present in these hydrogels.

1.4 Biocompatibility of Hydrogels

Since the thromboresistant properties of poly HEMA were first reported by Wichterle and Lim[1], there have been extensive studies of the interaction of body fluids with hydrogel surfaces. To date, there is no clear cut theory which may be used to predict whether a material will be biocompatible or biotolerant, however, several workers have indicated that the surface energy may be an important parameter. In 1970, Baier and coworkers

suggested that blood compatibility might be dependent upon a material having a moderate surface energy[58]. This theory was based on measurements of the surface tension of materials which exhibit reasonable biotolerance. Such measurements indicated that these materials all have a critical surface tension in the range of 20-30 mN/m, thus suggesting that materials which have a critical surface tension in this range will exhibit biocompatibility. However, there are several exceptions to this theory including hydrogels.

Andrade[58] proposed an alternative hypothesis of minimal interfacial energy, which suggested that a low interfacial tension between the implant material and the host environment would improve biocompatibility. Ratner and coworkers[60] studied the interaction of blood with a range of HEMA:EMA (ethyl methacrylate) copolymers and suggested that since the non-thrombogenic reactions were improved in these copolymers a balance between the apolar and polar sites might lead to enhanced biotolerance. Andrade and coworkers[61] have more recently studied a range of surfaces including HEMA:MMA (methyl methacrylate) copolymers and concluded that their results could not be accounted for on the basis of a minimum free energy. They indicated that whilst a multi parameter approach may be required to rationalise these results, an optimum balance between apolar and polar sites is important for biocompatibility.

It has been known for some time that poly(ethylene oxide) plays a significant role in reducing the adsorption of biological species to substrates[62]. These properties have been exploited by numerous workers in the fabrication of a range of hydrogels based on poly (ethylene oxides) and polyurethanes[10,11,63-66]. More recently, poly (ethylene oxides) have been grafted onto a variety of polymers including polyurethanes[67], copolyether urethanes[68], poly(vinyl chloride)[69,70], HEMA:styrene copolymers[71] and poly

ethylene[72]. Nagaoaka, Nakao and coworkers have studied the interaction of blood components with hydrogel copolymers based on methoxy poly(ethylene oxide) monomethacrylates and methyl methacrylate[73]. These workers suggest that the presence of long (at least 100 repeating OCH_2CH_2 units in the polyether side chain) flexible poly(ethylene oxide) chains at the surface restrict protein adsorption and hence reduce thrombogenic reactions. This process may be visualised as illustrated in Figure 1.2 with the flexible poly ethylene oxides providing an excluded volume which prevents the adsorption of protein molecules at the polymer surface.

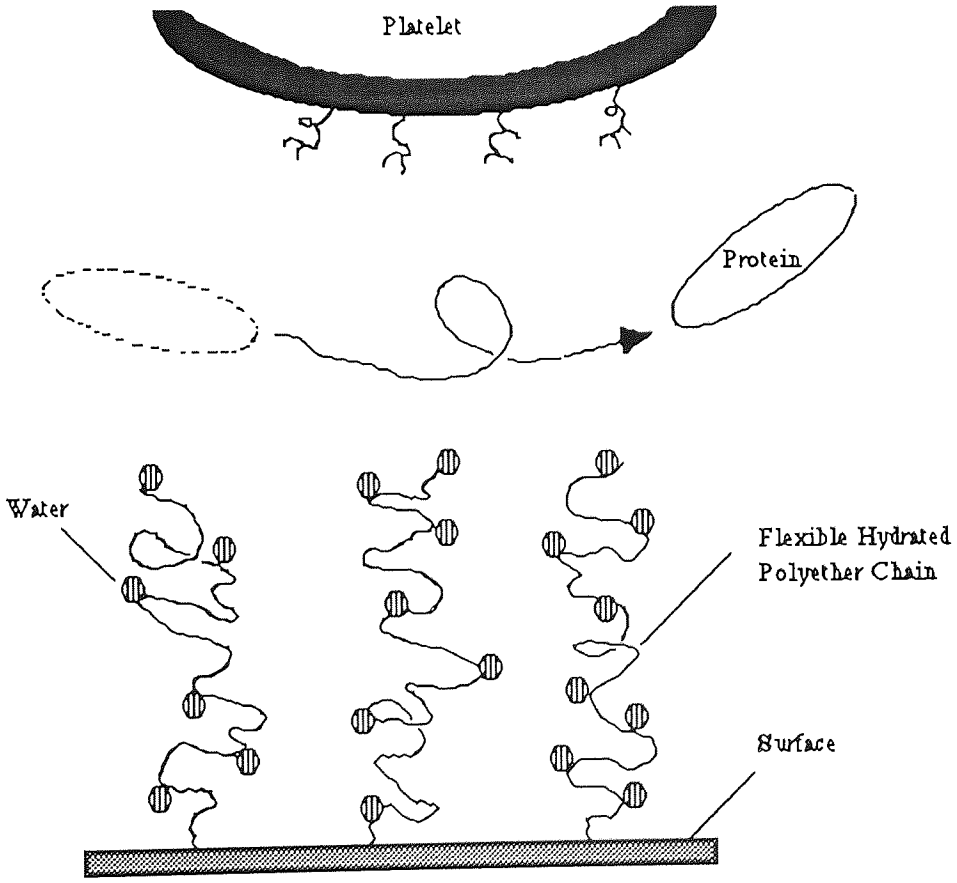

Figure 1.2 The interaction of blood components with hydrated poly (ethylene oxide) chains at the polymer surface (redrawn from reference 70)

Finally, Andrade and coworkers have prepared a range of copolymers of alkyl methacrylates with methoxy (polyethylene glycol) monomethacrylates[74]. These copolymers were studied as both protein resistant coatings and as polymeric surfactants for the removal of proteins.

Having discussed hydrogels and linear polyethers the next section will examine some aspects of the chemistry of cyclic polyethers.

1.5 Ionophores for Group I and II Metal Cations

The term ionophore when strictly translated means 'ion-bearer', but in this thesis it is used to describe a neutral chelating agent which facilitates the selective binding and transport of a specific ion. For many years little was known about the coordination chemistry of solvated group I and II metal cations because of the lack of convenient magnetic and spectroscopic properties available to study such interactions. However, the occurrence of weak interactions between these ions and ethereal solutions such as tetrahydrofuran, ethylene and diethylene glycol were well known. This situation radically changed with the discovery of a class of ionophoric cyclic ethers, known as crown ethers, in 1967 by Pedersen[75,76], which form stable complexes with metal cations. For example Frensdorff and Pedersen[77,78] measured the stability constants (K) for the formation of potassium complexes between 18-crown-6 and its open chain analogue, pentaglyme; values for log K of 6.1 and 2.2 were obtained respectively indicating the enhanced stability of the metal cation:crown ether complex. Soon many other macrocyclic chelating systems were reported in the literature. This chemistry has recently been reviewed by Bajaj and Poonia[79] and several books have also been dedicated to this topic[80-83].

Crown ethers are a unique class of cyclic compounds which are built up from repeating

OCH_2CH_2 units, an example, dibenzo-18-crown-6, is illustrated in Figure 1.3. The oxygen atoms may then be successively replaced by nitrogen or sulphur atoms to give a range of azacrown ethers and thiacrown ethers respectively. Macrocyclic crown ethers containing oxygen, nitrogen and sulphur are known as azathiacrown ethers. Systems based on these ligands have been synthesised with an increasing degree of sophistication. A range of crowns incorporating heterocyclic donor groups such as tetrahydrofuran and furan have been reported[84]. Several workers have synthesised and studied crowns containing interannular donor atoms[85,86] and pendant donor groups, a class known as the lariat ethers[87,88]. More recently, crown ether systems containing chromophoric groups have been synthesised by Vogtle and Dix to allow the colourimetric determination of group I and II metal cations[89,90].

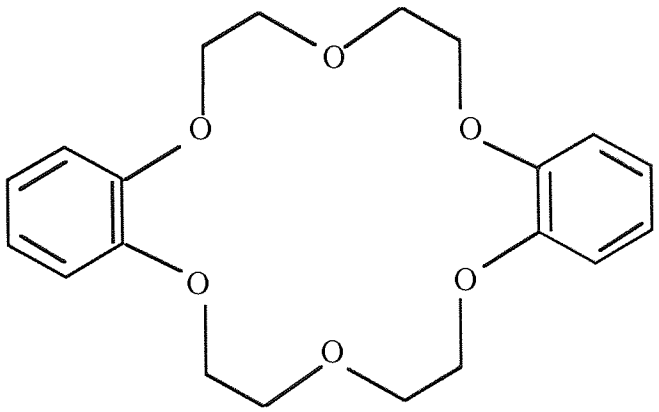

Figure 1.3 dibenzo-18-crown-6

Further progress was made by Lehn and coworkers, with the synthesis of multicyclic crown compounds known as cryptands or cryptanoids[91]. These compounds have a cage like structure which is held in place by two tertiary amino groups at the bridgehead. An example of this type of compound is represented in Figure 1.4.

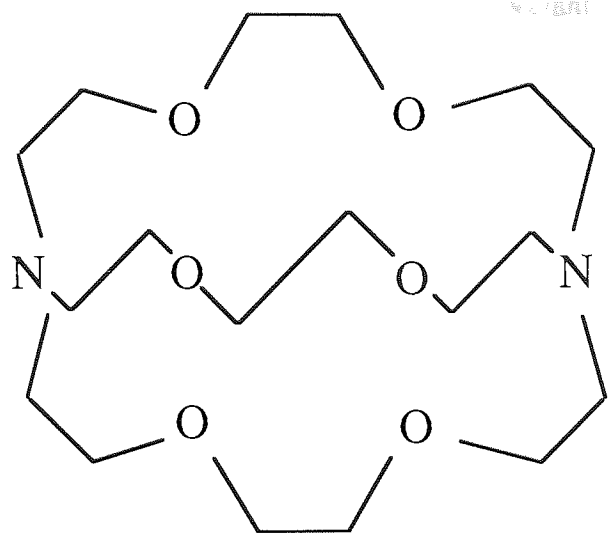

Figure 1.4 [2,2,2] cryptand

This class of compounds not only exhibits a higher ion selectivity than crown ethers, but also forms more stable complexes. The cavity type structure of cryptands has recently been adapted in the synthesis of a three dimensional analogue of 18-crown-6, the bis-tetrakis (hydroxymethyl) ethylene or bis-THYME cylinder[92]. The structure of this molecule is illustrated in Figure 1.5.

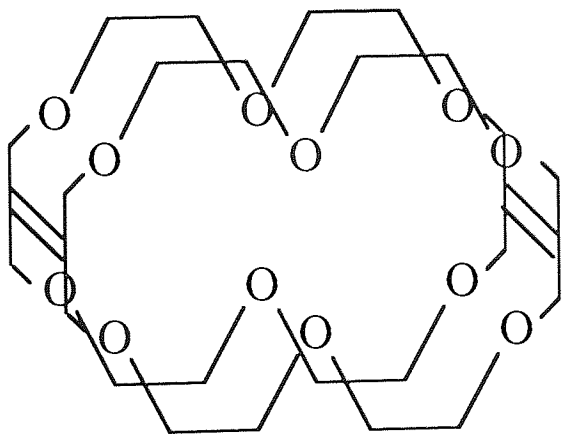

Figure 1.5 bis-tetrakis (hydroxymethyl) ethylene or bis-TYHME

Other macrocyclic ionophores for the group I and II metal cations include several naturally occurring antibiotics, containing repeating ester or amide linkages. Of this group

valinomycin (Figure 1.6) is perhaps the most important. This compound binds selectively to potassium[93] and hence has been used extensively in the fabrication of potassium ion-selective electrodes.

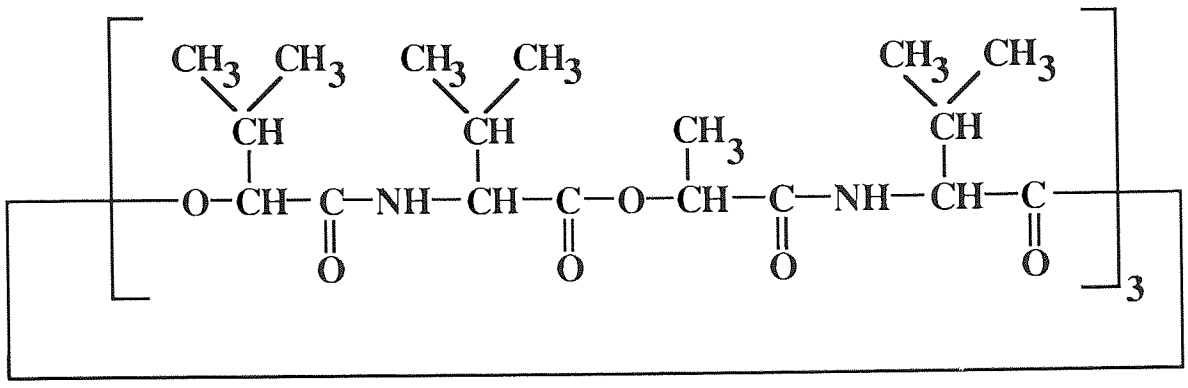

Figure 1.6 valinomycin

A further range of ligands known as the calixarenes are obtained via an internal cyclisation, condensation reaction between phenol and formaldehyde[92-94]. An example of this type of compound is illustrated below in Figure 1.7.

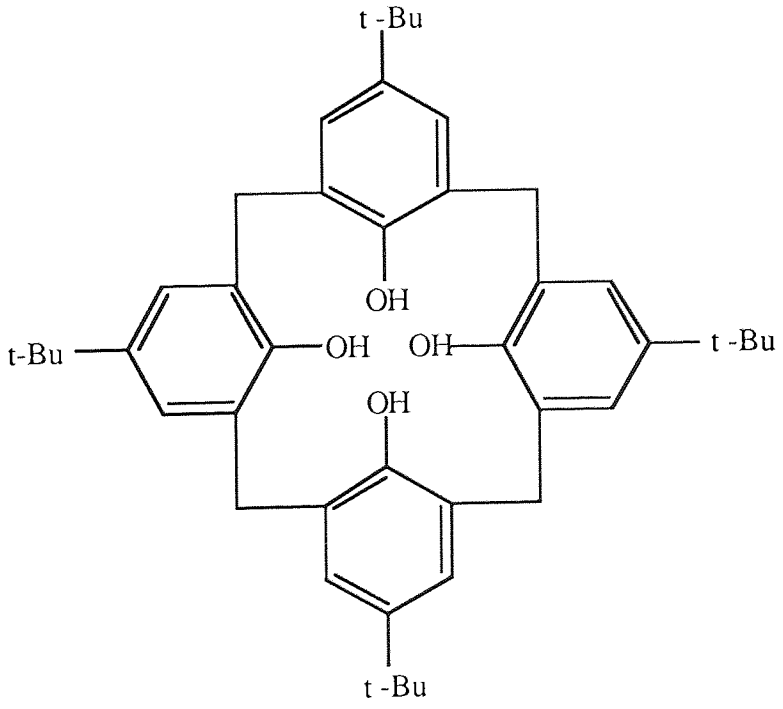

Figure 1.7 p-tert-butylcalix[4]arene

If the phenolic hydroxyl groups are reacted with an alkyl acetate, a further sub-class of compounds known as the alkyl calixaryl acetates are obtained[97,98]. Recently an ion-selective electrode for sodium based on such a compound, p-tert-butylcalix[4] aryl acetate, has been fabricated by Diamond *et al* [99].

Finally, a further range of ionophores based on a non-cyclic crown ether, which forms a cavity on complexation has been studied[100]. Of all these ionophores crown ethers are most readily available from chemical suppliers and hence their chemistry has been studied extensively.

1.5.1 Nomenclature of Crown Ethers

The term 'crown' was first applied to cyclic polyethers by Pedersen[75,76]. Such terminology resulted from the physical appearance of their molecular models and the fact that the cyclic polyether sits on the cation rather like a crown on a head.

The naming then consists of, in order:

i) the number and kind of hydrocarbon ring,

ii) the total number of atoms in the polyether ring,

iii) the class name, crown and finally,

iv) the number of oxygens in the ring.

For example a cyclic ether containing 6 oxygen atoms in an 18 member ring would be 18-crown-6. In most cases the placement of hydrocarbon rings and oxygen atoms are symmetrical, the exceptions, however are indicated by the prefix *asym.* Names derived from Pedersen's nomenclature rapidly replaced those derived from the more accurate IUPAC nomenclature, due to their ease of use and brevity.

Unfortunately Pedersen's nomenclature can lead to confusion thus an alternative nomenclature was proposed, by Weber and Vogtle[101], to circumvent such problems. In this terminology, multidentate monocyclic ligands with any type of donor atom, are referred to as coronands. The different types of nomenclature are illustrated in Table 1, Appendix I.

1.5.2 Characteristics of Crown Compounds.

The most important characteristic of a crown compound is the ability to form stable complexes with cations. The complexation process involves the cationic portion of either a metal salt, ammonium salt or an ionic organic species, the 'guest', being held in place by donor atoms, such as O, N and S, within the crown, the 'host ', thus giving rise to the concept of 'guest-host' interactions. The stability of the resulting complex is dependent on various factors:

i) the relative sizes of the diameter of the cavity within the crown and the diameter of the cation,

ii) the charge and 'hardness' of the cations and finally,

iii) the nature of the donor atoms within the crown; this affects the 'hardness' and the basicity of the donor atom.

In addition, the structures of these complexes may vary in the ratio of crown ether:cation over the range 1:1, 2:1, 3:2 and 1:2. This is dependent upon the relative sizes of the crown cavity and the ionic diameter of the cation.

1.5.3 Synthesis of Crown Ethers

Crown ethers may be synthesised via a relatively simple condensation reaction (Williamsons synthesis). Cyclisation typically involves the nucleophilic displacement of

either halide or tosylate ions from a disubstituted ethylene oxide by alkoxide or pheonoxide ions. An example of this synthesis is given in Figure 1.8 which illustrates the preparation of dibenzo-18-crown-6.

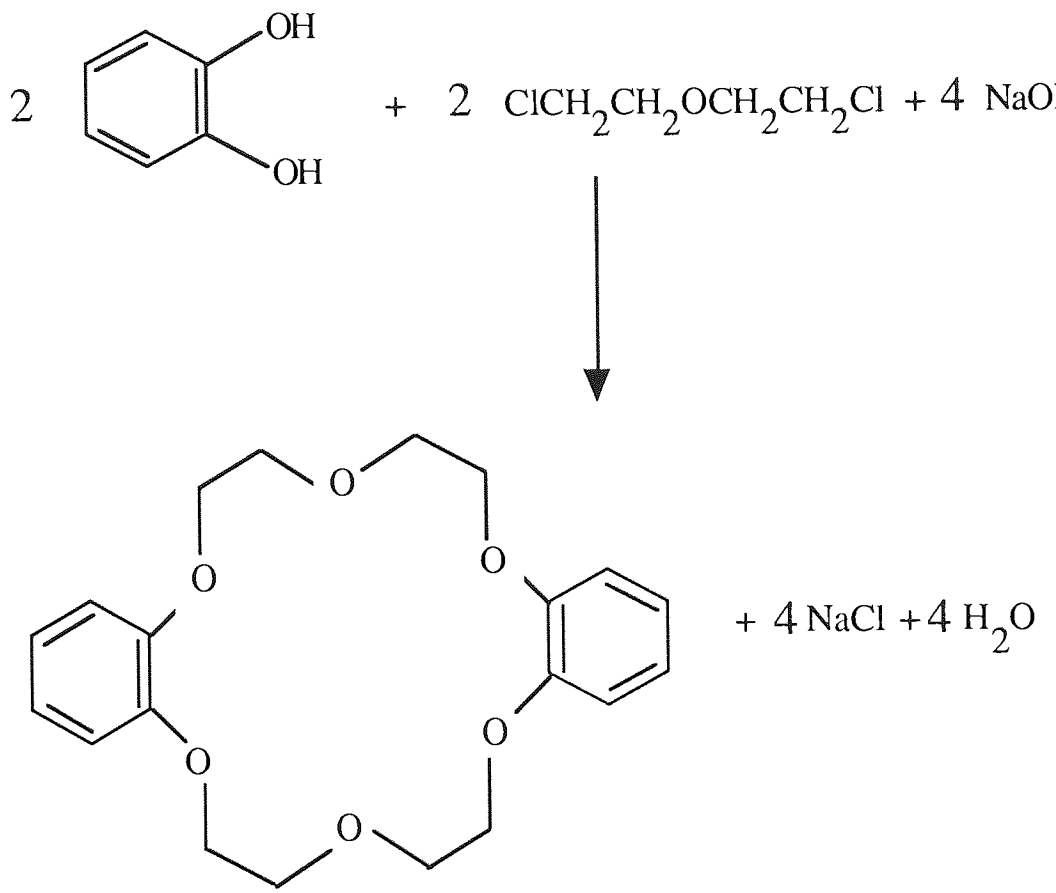

Figure 1.8 The synthesis of dibenzo-18-crown-6

Alternatively, alkali metal cations may be used in the reaction to play a template role. An example is given in Figure 1.9 where the synthesis of 18-crown-6 is illustrated.

1.5.4 Crown Ethers in Polymers.

Crown ethers are relatively inexpensive ionophores but their generally high solubility in both water and organic solvents means that it is often necessary to recycle these

ionophores to reduce the costs of using them on an industrial scale.

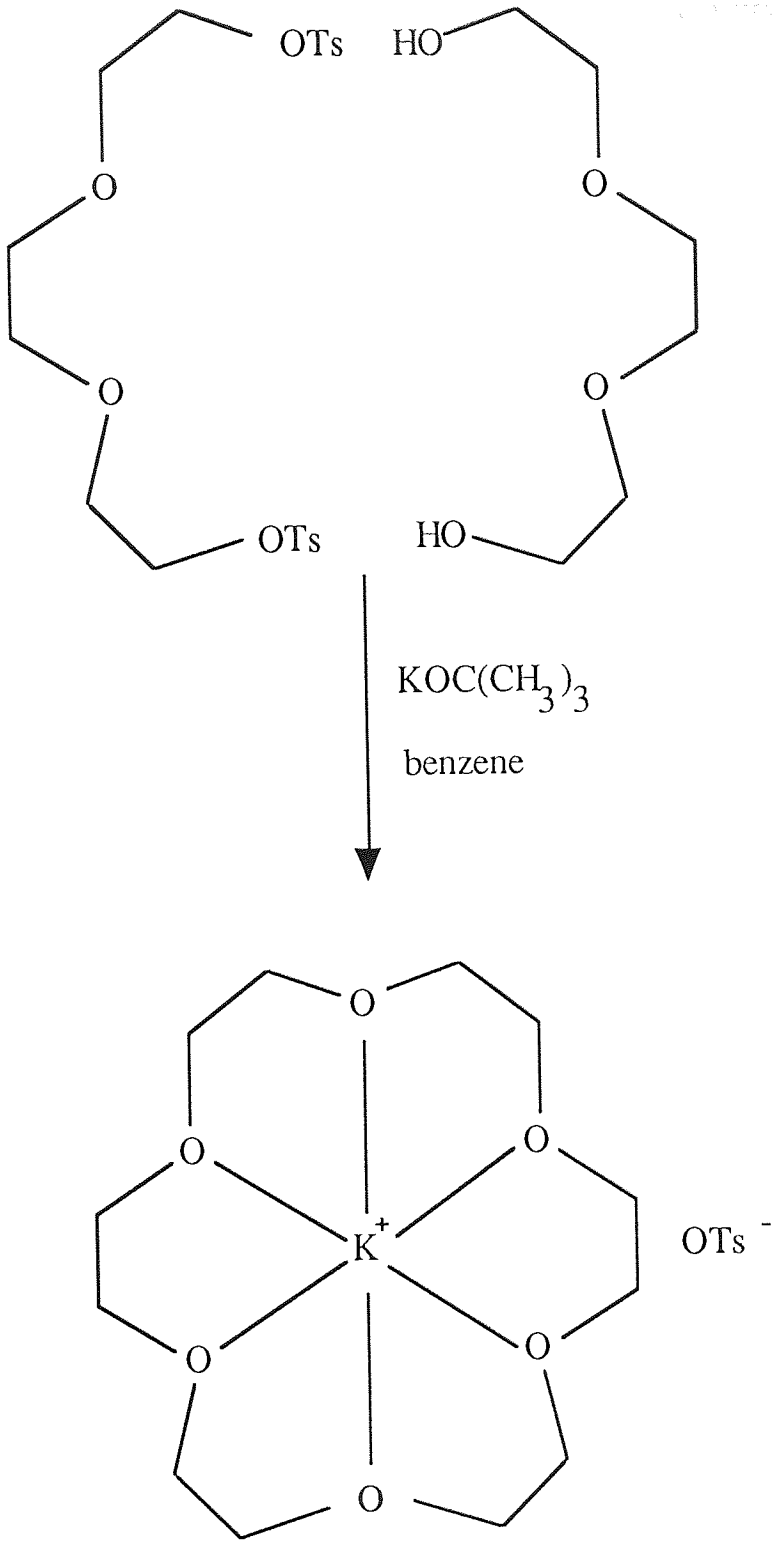

Figure 1.9 The synthesis of 18-crown-6

To circumvent this problem several workers have considered the synthesis of polymeric or immobilised crown systems and the interest in this chemistry has been sufficient to warrant its inclusion in several books[80-83].

Immobilised crown ether systems have been considered for use in a broad range of applications including: reverse osmosis membranes[102,103], ion selective electrodes[104], solid state electrolytes[105], chromatographic stationary phases[106,107] and liquid crystal polymers[108,109]. Crown ethers have also been immobilised to produce photoreactive polymers[110-112] and to provide artificial ion channels in a synthetic biomembranes[113]. However, to date crown ethers have almost exclusively been immobilised within hydrophobic polymer matrices.

Polymeric crown ethers have been obtained using a variety of methods and starting materials but these methods generally fall into the following categories

i) polymerisation reactions involving the polycondensation or polyaddition reactions of diaminodibenzo-18-crown-6

ii) polymerisation or copolymerisation of vinyl derivatives either by free radical or ionic polymerisation

ii) utilisation of the reactions of functional groups on either the crown ethers or the polymer substrate and finally

iv) forming a crown ether in the polymer backbone during the polymerisation.

These methods will now be discussed in greater detail.

One of the first attempts at binding a crown ether into a polymer matrix was reported by Feigenbaum and Michel[114]. This work involved the synthesis of various polyamides via a polycondensation reaction with the two isomeric forms of diaminodibenzo-18-crown-6.

These polyamides along with film cast poly (vinyl pyrrolidone) blends or 'alloys' have been studied for potential use as reverse osmosis membranes by Shchori and Jagur-Gradinski[102,103]. Diaminodibenzo-18-crown-6 has also been used to prepare both polyurea and polyurethane based polymers[82]. More recently, a polyimide containing diaminodibenzo-18-crown-6 has been prepared by Ergozhin coworkers using N'N-bismaleimides[115].

A further range of polymeric crown ethers have been obtained by polymerising a range of vinyl derivatives. Smid and coworkers reported the synthesis and cation binding properties of a range of polymers based on the vinyl derivatives of monobenzo-15-crown-5, dibenzo-18-crown-6 and monobenzo-18-crown-6[116-118]. In general, these workers observed an increase in the cation binding abilities with the polymeric crown ethers and suggested that this might be attributable to the formation of 2:1 crown ether to metal cation complexes. Vinyl derivatives of benzo-15-crown-5 and benzo-18-crown-6 have also been used by these workers to produce a range of styrene copolymers[118]. Liquid membranes were then prepared from these copolymers and the diffusion of sodium picrates studied. Poly (vinylbenzo-15-crown-5) and its styrene copolymers were found to be more effective at extracting potassium than 15-crown-5, due to the preferential formation of a 2:1 crown:cation complex with potassium. Finally, various other routes to vinyl derivatives have been reported by Reinhoudt[119], Kikukawa and coworkers[120] and Tomoi *et al* [121].

A variety of poly crown acrylates and methacrylates have also been reported in the literature [122-126]. These monomers have all been prepared by reacting the corresponding amino or hydroxy crown with methacryloyl chloride or acryloyl chloride. Smid and coworkers reported that the cation binding abilities of polymers derived from acrylate and

methacylate derivatives of benzo-15-crown-5 and monobenzo-18-crown-6 were similar to those obtained for the poly vinyl crown ether styrene based copolymers[122].

Chujo and coworkers[127] used mercapto-16-crown-5 as a chain transfer agent and produced an alternative route to a poly(methylmethacrylate) terminated crown ether. These workers reported the selective extraction of sodium cations using this thioester terminated poly (methylmethacrylate). However, the efficiency of the extraction was reported to be strongly influenced by the molecular weight, Mn, of the polymer with increases in Mn above $1x10^4$, giving rise to a decrease in the efficiency of the extraction process.

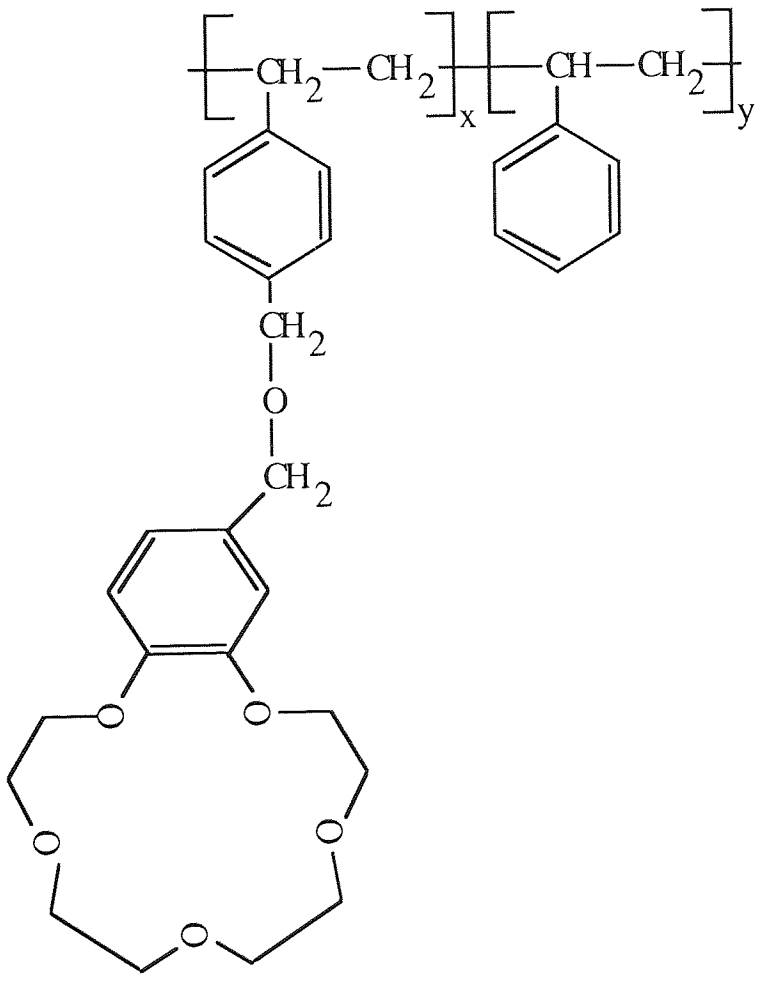

Figure 1.10 An immobilised crown ether

Immobilised crown ethers have also been synthesised by utilising the reactive functional groups of polymers (Figure 1.10). Molinari, Montanri and Tundo immobilised a crown ether on polystyrene via a condensation reaction with a chloromethylated polystyrene, commercially available as Merrifields resin, and a ω ethylaminononyl-18-crown-6[128]. The polymer was then evaluated for phase transfer catalytic activity. However, the reaction rates were noticeably slower for the immobilised systems because of the difficulties associated with bringing the reactive species into contact with the catalytic site. Similarly polymers of the type illustrated in Figure 1.10 can be prepared by reacting either a hydroxy crown ether or a poly ethylene glycol with Merrifields resin[129,130]. Alternatively, the crown ether unit may be formed as a pendant group, by reacting pendant catechol groups with an α,ω-glycol dihalide. This idea has been exploited by Kahana *et al* [130].

Finally, a range of chiral polymers containing chiral crown ethers have also been produced by Kakuchi and coworkers[131-133]. These polymers were all synthesised via the cationic polymerisation of optically active divinyl ethers producing polymers containing crown ethers within the polymer backbone. In the long term it was hoped that such polymers might be developed to separate racemic mixtures.

This literature survey has illustrated that the immobilisation of crown ethers within hydrophobic membranes is well established. Hydrophilic polymers can imbibe water and therefore facilitate the transport of aqueous species. Thus, it is suprising to note that there have been few attempts to exploit the unique properties of both hydrophilic polymers and the selective chelating agents, crown ethers, in the design of permselective membranes. Kimura and coworkers, however, have produced an interesting range of crown ether containing polymers via a 'pseudo grafting' type reaction [134]. This involved the reaction

of a formyl derivative of the crown with poly (vinyl alcohol) in the presence of p-toluenesulphonic acid. Membranes were cast from these polymers and the transport of alkali metal picrates studied. These workers reported that the transport of alkali metals was retarded when compared with the results obtained for the unmodified polymer, poly (vinyl alcohol). The authors attributed this to the formation of intramolecular sandwich-type complexes. Yagi and coworkers produced a range of hydrophilic polymers based on methacrylamide derivatives of benzo-15-crown-5 and dibenzo-18-crown-6[123]. Finally, preliminary studies within the Speciality Materials Group at Aston have illustrated that it is possible to occlude certain crown ethers within hydrogel membranes[39]. Transport studies on membranes containing dicyclohexano-18-crown-6 indicated that potassium ion transport is suppressed. However, these studies are limited due to ionophore loss during hydration.

1.6 The Transport Properties of Hydrogels

An understanding of the transport properties of hydrogels is important in a wide variety of applications including controlled release systems, contact lenses, reverse osmosis, haemodialysis and the design of permselective membranes. However, before the results obtained from transport studies can be rationalised it is important to understand some of the fundamentals of permeation and diffusion.

1.6.1 The Fundamentals of Permeation and Diffusion

The term 'permeation' is generally used to define the mass transport of a certain species or component through another species. Diffusion is an example of a permeation process and in this case the driving force is a concentration gradient. Under such conditions, the random motion of molecules, causes matter to be transferred from the region of highest concentration to that of the lowest. This statement may be described mathematically using

Fick's First Law of Diffusion (Equation 1.2)[135]. Here the quantity of material diffusing across a plane of unit area in unit time is the flux, J_x. This flux is proportional to the concentration gradient normal to this plane (dc/dx), giving rise to the equation;

$$J_x = - D \frac{dc}{dx} = - \frac{F}{S} \qquad (1.2)$$

where D is the diffusion coefficient or the diffusivity,

F is the total flow rate and finally,

S is the area.

For membrane diffusion when a steady state is attained then Equation 1.2 may be rewritten to give;

$$F = \frac{DS (\Gamma_2 - \Gamma_1)}{L} \qquad (1.3)$$

where, Γ_1 is the concentration of solute just inside the membrane at the low side,

Γ_2 is the concentration of solute just inside the membrane at the high side and finally L is the membrane thickness.

Additionally, if Henry's Law is applicable then ;

$$\Gamma_1 = S_m C_1. \qquad (1. 4)$$

and

$$\Gamma_2 = S_m C_2 \qquad (1.5)$$

where, S_m is the partition coefficient

C_1 is the concentration of the bulk solution at the low side and finally,

C_2 is the concentration of the bulk solution at the high side.

Furthermore, since the partition coefficient is defined by Equation 1.6,

$$P = D\,S_m \qquad (1.6)$$

where, P is the permeability coefficient, then Equation 1.3 may be rewritten and rearranged to give an expression for P of the form,

$$P = \frac{F\,L}{S\,(C_2 - C_1)} \qquad (1.7)$$

In this thesis permeability has been studied using the apparatus outlined in Section 2.13. Here C_1 relates to the concentration of species present at the low side of the permeability cell, and since this is significantly lower than the concentration at the high side Equation 1.7 is effectively reduced to;

$$P = \frac{F \times L}{S\,C_2} \qquad (1.8)$$

Additionally, the flow rate, F, may be obtained from the gradient, G, of a graph showing concentration at the low side with time, and the volume, V, of the permeability half cell by substitution into the following equation;

$$F = G\,V \qquad (1.9)$$

thus the permeability coefficient may be calculated from the equation;

$$P = \frac{GVL}{SC_2} \qquad (1.10)$$

1.6.2 Transport and Permeability Phenomena in Hydrogels.

Several studies have been made of the transport properties of hydrogels particularly for the transport of small molecular species[136-157]. A universally acceptable model for transport is yet to be realised, however, all models derived to date relate permeability or diffusivity to the overall equilibrium water content of the matrix. For example, Tighe and Ng noted that the logarithm permeability coefficient for the transport dissolved of oxygen is proportional to the EWC and is unaffected by the chemical nature of the polymer[142]. This empirical relationship was later confirmed by Refojo and Leong[143].

The first studies of transport properties were prompted by an interest in the design of membranes for desalination and haemodialysis applications. Yasuda and coworkers studied the diffusion of sodium chloride[138] and water soluble organics[139] through hydrogels. Membranes were cast from a broad range of hydrophilic polymers and copolymers and the partition, diffusion and permeability coefficients calculated. The results were then examined using a model based on the free volume of diffusion theory in which it is assumed that :

i) the effective free volume for diffusion corresponds to the free volume of the aqueous phase,

ii) the solute permeates through 'holes' which fluctuate both in size and in location with time and finally,

iii) the solute permeates through the aqueous phase only, implying that the solute-polymer interactions are minimal.

The diffusion constant D, is then related to the degree of hydration, H, by the equation

$$\log D = \log D_o - C((1/H) - 1) \qquad (1.11)$$

where D_o is the diffusion constant for the solute in pure water at a defined temperature

C is the constant of proportionality and is related to the characteristic volume and the free volume occupied by the water.

This theory, therefore, predicts a linear relationship between log D and 1/H, which has been observed for a range of solutes[138,139].

The relationship between the partition coefficient, S_m, and the degree of hydration was found to be more complex, with S_m being more dependent on polymer structure. At higher values of H, S_m is nearly equal to H whereas at lower values of H, S_m deviates significantly from the value of H. Since the permeability coefficient, P, is defined as the product of the diffusion constant and the partition coefficient, then log P exhibits a linear relationship with 1/H at higher values of H, but deviations are observed with lower values of H due to the dependence of S_m on 1/H.

According to Yasuda *et al* [157] the free volume model also predicts a linear relationship between the hydraulic permeability, K_w, and the degree of hydration, H, (above H = 0.4) of the form;

$$K_w / H = A \exp (BHV_{fw}) \qquad (1.12)$$

where A and B are constants

V_{fw} is the free volume function of water in the membrane.

Kojima and coworkers tried to extend this free volume model to data obtained from the permeability of water through poly (vinyl alcohol) membranes[148,149]. However, with these membranes the expected linear relationships between log P and 1/H and K_w/H and H were not obtained. These workers found that a linear relationship was obtained for permeability studies on a range of membranes with H between the limits 0.4 and 0.9. This may be described by Equation (1.13)

$$\text{Ln } K_w / H = A + BH \qquad (1.13)$$

where A and B are again constants.

By recalling Ogstons[159] model for the diffusion of spheres through a random suspension of fibrils, the authors expanded Equation 1.13 as follows;

$$K_w / H = K_w^{o} \exp [- (1-H) (1+r / R_f)^2] \qquad (1.14)$$

where r is the radius of the solute

R_f is the radius of the fibre in the membrane and

K_w^{o} is the reduced permeability of water in the hydrogel.

This equation predicts a linear relationship between Ln K_w / H and 1-H and has been successfully applied to the permeation of the NaCl, congo red and sunset yellow through poly (vinyl alcohol) membranes[149].

More recently, Peppas and Moynihan[151] derived a further model which extends the free

volume model to incorporate topological characteristics of the membrane. An equation was derived which links the diffusion coefficient to the equilibrium swelling, the hydrodynamic radius of the solute, the number average molecular weight Mn between crosslinks and a function of the mesh size which accounts for barriers due to crosslinks and chain entanglements. This theory was later applied to the diffusion of phenylalanine through poly HEMA[152].

These transport models tend to relate the permselectivity to the overall EWC. However in Section 1.3 the experimental evidence which suggests water in hydrogels exists in more than one state was discussed. Several workers have, therefore, attempted to study the effect that water structuring within the hydrogel network has on the transport properties[23,25,145,153,158]. Wisienski and Kim studied the diffusion of a variety of water soluble species through poly HEMA and poly HEMA containing 1% EGDM crosslinker[145] and concluded that the solute permeation occurs in the freezing or free water fraction of the gels imbibed water. Uragami and coworkers illustrated that hydrophilic solutes such as NaCl require the presence of freezing water in order to partition in the membrane[153]. Similarly, the ratio of freezing water to non-freezing water strongly influences the transport properties of hydrogels, for example it has been known for a long time that salt rejection is enhanced when freezing water content is low[23]. Oxygen transport was also found to be negligible in styrene-HEMA copolymers which have no freezing water[25].

In this thesis the transport of group I and II cationic species is of particular interest. A systematic study of the permeability of poly HEMA based hydrogels to a range of group I and II metal cations has been reported by Hamilton and coworkers[156]. Here it was found that the counter anion has a significant role to play in the permeability process. Metal

cations with counter anions which act as structure-breakers, for example SCN^-, I^- and Br^- are observed to permeate more rapidly than those with structure-making anions e.g F^- and SO_4^{2-}. Furthermore, the general order of salt permeability decreases in the order of a spectrochemical series, given below, similar to the Hofmeister series.

$$SCN^- > I^- > NO_3^- > Br^- > Cl^- > F^- > SO_4^{2-}$$

The transport properties of a range of copolymers based on poly HEMA with either styrene or methyl methacrylate have been studied by Murphy and coworkers[40]. In these studies the permeability of a range of group I and II metal cations were studied in the presence of a fixed anion, chloride. The results from this work indicated that both the cation size and the water structuring phenomena within the polymer matrix (which is controlled by the combined water structuring effects of the anion, the cation and the polymer itself) contributed to the overall transport process and that situations arise when either can play a dominant role. The free volume model was found to account reasonably well for differences in cation permeation in which diffusional size effects are a critical factor. However, the deviations from the free volume model observed at lower EWC's could be accounted for by water-structuring effects since decreases in EWC are mirrored by decreases in the fraction of 'free' or 'unbound' water.

1.7 Aims and Scopes of the Project

The initial aim of this project was to synthesise a range of vinyl based hydrogels containing poly(ethylene oxide) units. The reasons for this were twofold; the literature survey had illustrated that poly(ethylene oxide) units can enhance the biocompatibility of hydrogels, hence by combining this property with the synthetic versatility offered by vinyl monomers it should be possible to prepare a novel range of hydrogels with interesting and

varied surface properties. In addition, both linear polyethers and cyclic polyethers can complex with metal cations, thus their presence within a hydrogel matrix may have a significant effect on the transport properties of these materials. In particular since the cyclic crown ethers selectively chelate with metal cations their inclusion may produce permselective membranes which are of interest for aqueous separations in general but in particular for use in the design of chemical sensors.

Initially, crown ethers were occluded within hydrogel membranes and the transport properties of these materials were studied. However, the range of ionophores which could be used was limited by ionophore loss during hydration. Hence attempts were made to synthesise monomeric crown ethers and to study the effects these 'bound' crowns have on the transport properties. Finally, a range of hydrogels were prepared containing a variety of linear polyethers and a systematic study of the effects of both variations in the polyether concentration and polyether chain length on the transport properties were studied. The linear polyethers used in this study were chosen so that the effect of structural variations in the polyether side chain on the EWC, surface and mechanical properties of a range of HEMA based copolymers could also be evaluated.

CHAPTER 2

Materials and Methods

2.1 Introduction

This chapter deals with the synthetic details for the preparation of the monomers based on crown ethers outlined in Figures 4.1-4.5, Section 4.2 and lists the reagents involved. It also includes details of membrane fabrication and discusses the techniques used to characterise these membranes. Particular attention has been paid to the design and operation of the permeability apparatus and the measurement of contact angles.

2.2 Reagents

2.2.1 Crown Ethers

The crown ethers supplied were refrigerated until required and used without any further purification. These compounds are listed in Table 2.1 and their structures are illustrated in Figure 2.1.

Table 2.1 Crown ethers used in this work

Crown Ether	MWt (g/mole)	Abbreviation	Supplier
Benzo-15-crown-5	268.3	B-15-C-5	Aldrich
Dibenzo-18-crown-6	360.4	DB-18-C-6	Aldrich
Dicyclohexano-18-crown-6	372.5	DCH-18-C-6	Lancaster
4-Nitrobenzo-15-crown-5	314.3	————	Aldrich

Figure 2.1 Structures of crown ethers used in this work

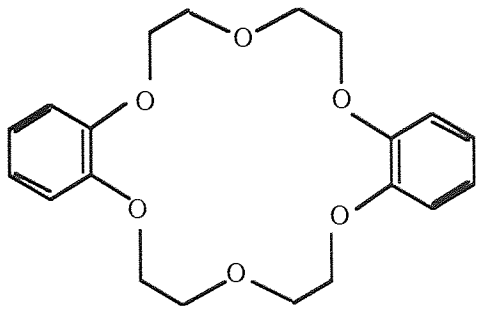

dibenzo-18-crown-6

Figure 2.1 (continued) Structures of crown ethers used in this work

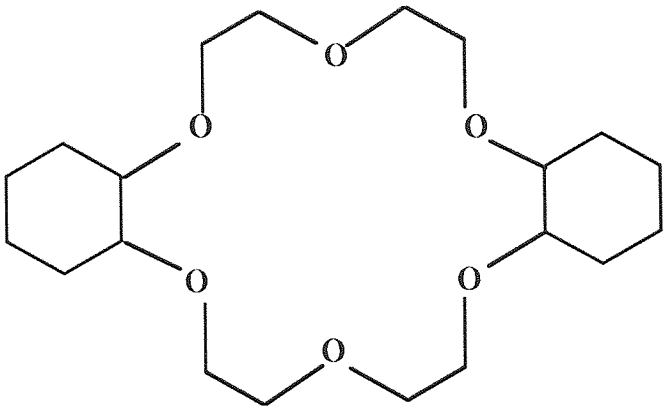

dicylohexano-18-crown-6

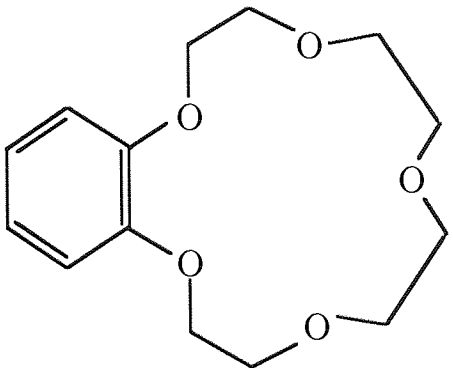

benzo-15-crown-5

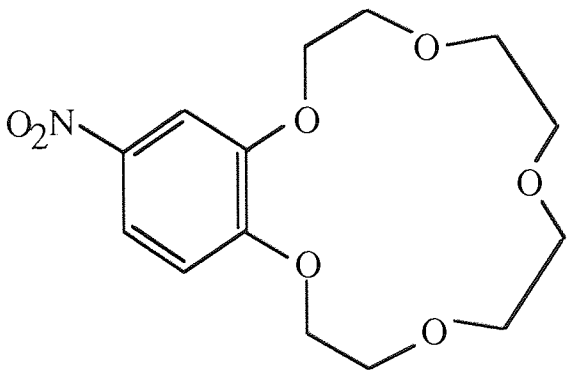

4-nitrobenzo-15-crown-5

2.2.2 Miscellaneous Reagents Used in Monomer Synthesis

The reagents tabulated in Table 2.2 were used as supplied.

Table 2.2 Reagents used in monomer synthesis

Compound	MWt (g/mole)	Abbreviation	Supplier
Acetic acid	61.1	——	BDH
Acetyl chloride	78.1	——	BDH
Acryloyl chloride	90.5	——	Aldrich
Lithium aluminium hydride	38.0	$LiAlH_4$	BDH
Sodium borohydride	37.8	$NaBH_4$	BDH
Nitric acid	60.0	HNO_3	BDH
Palladium charcoal	——	Pd/C	BDH
Triethylamine	101.2	Et_3N	Aldrich
Trifluoroacetic acid	114.0	TFA	Lancaster

2.2.3 Salts

All salts used in this study were of analytical grade and were supplied either by Fisons or BDH. The salts were used without any further purification. Salt solutions were prepared using distilled water of conductivity 1.3 $\mu S\ cm^{-1}$.

2.2.4 Reagents Used in Polymer Synthesis

Optically pure 2-hydroxyethyl methacrylate, HEMA was supplied by Ubichem Ltd. The crosslinking agent ethylene glycol dimethacrylate , EGDM (BDH) and the initiator α- azo-bisisobutyronitrile, AZBN (Aldrich) were refrigerated until required and used as supplied. Methoxy polyethylene glycol monomethacrylates of nominal molecular weights 200, 400 and 1,000 (Polysciences) were used without further purification. Methoxypolyethylene gylcol-550-methacrylate, ethoxylated hydroxyethyl methacrylate (HEMA 4,5 EO) and hexaproxylated hydroxypropylmethacrylate (HPHPMA) were obtained from Röhm

GMBH (UK distributors Cornelius Chemicals Co. Ltd) and used without further purification. These reagents are summarised in Table 2.3 and their structures are illustrated in Figure 2.2.

Table 2.3 Molecular weights and suppliers of monomers

Monomer	MWt (g/mole)	Abbreviation	Supplier
ethylene glycol dimethacrylate	198	EGDM	BDH
α-azo-bisisobutyronitrile	164	AZBN	Aldrich
2-hydroxyethyl methacrylate	130	HEMA	Ubichem Ltd
methoxy polyethylene glycol 200 methacrylate	330*	MPEG 200 MA	Polysciences
methoxy polyethylene glycol 400 methacrylate	710*	MPEG 400 MA	Polysciences
methoxy polyethylene glycol 550 methacrylate	910*	MPEG 550 MA	Röhm GMBH
methoxy polyethylene glycol 1000 methacrylate	1650*	MPEG 1000 MA	Polysciences
polyethylene glycol monomethacrylate 10 moles EO	540**	PEGMA 10 EO	Polysciences
ethoxylated hydroxyethyl methacrylate	450*	HEMA 4,5 EO	Röhm GMBH
hexapropoxylated hydroxypropyl methacrylate	7740	HPHPMA	Röhm GMBH

[*Values are polystyrene equivalent molecular masses as determined by GPC at RAPRA using a PL gel 2 x mixed gel column, tetrahydrofuran as the solvent, a flow rate of 1 ml/min and a refractive index detector. ** This value is a polyethylene glycol/poly (ethylene oxide) molecular weight as determined at RAPRA using the same column, flow rate and detector but DMF as the solvent]

Figure 2.2 Structures of reagents used in polymer synthesis

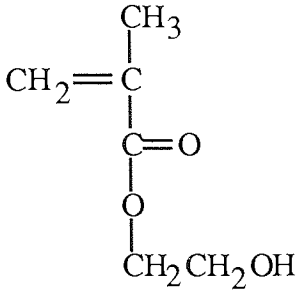

2 - hydroxyethyl methacrylate

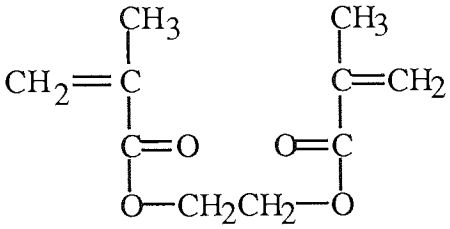

ethylene glycol dimethacrylate

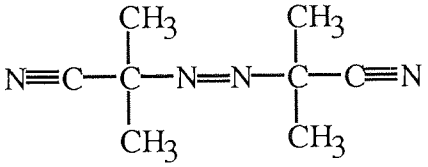

azo-bis-isobutyronitrile

methoxy polyethylene glycol monomethacrylates (PEG MA)

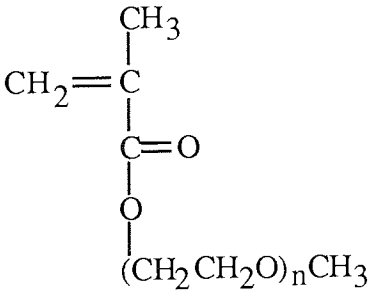

n=4 to 5 MPEG 200 MA
n=9 to 10 MPEG 400 MA
n=12 to 13 MPEG 550 MA
n=22 to 23 MPEG 1000 MA

ethoxylated hydroxyethyl methacrylate (HEMA 4,5,EO) and polyethylene glycol methacrylate 10 moles EO

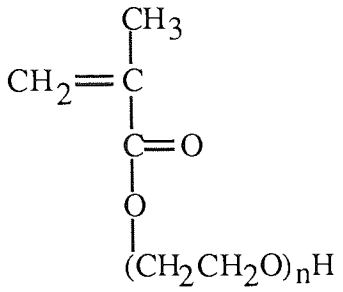

n=5 to 6 HEMA 4,5 EO

n=10 PEGMA 10 EO

hexapropoxylated hydroxypropyl methacrylate (HPHPMA)

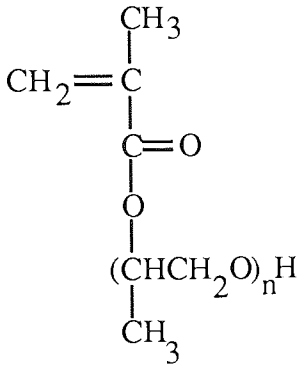

n = 7 HPHPMA

2.3 The Preparation of 4-acryloylaminobenzo-15-crown-5

This Section is concerned with the synthesis of the compounds outlined in Figure 4.1.

2.3.1 The Preparation of 4-nitrobenzo-15-crown-5

The synthesis of this compound closely follows that reported by Ungaro *et al* [160].

Benzo-15-crown-5 (20.0g, 75 mmol) was dissolved in chloroform (500 cm^3). Acetic acid (240 cm^3) was added. This mixture was then stirred whilst, nitric acid (68 cm^3, 70%) was added, and the resulting mixture stirred at room temperature overnight. TLC ($CHCl_3$ and silica gel / iodine stain) indicated the presence of starting material so the mixture was stirred for a further 4 days. The reaction was neutralised with sodium

bicarbonate and the organic layer separated. The aqueous phase was extracted with chloroform (3x300 cm^3) and the combined organic extracts dried over $CaCl_2$. Evaporation gave a pale yellow oil which rapidly crystallised to give a pale yellow solid. This solid was recrystallised from ethanol.

Yield: 18.7g (80%); m.p.95-96°C (Ref[160] m.p. 84-85°C)

IR: 3083cm^{-1} (aromatic C-H stretch), 2868cm^{-1} - 2928cm^{-1} (alkane C-H stretch), 1587cm^{-1} and 1516cm^{-1} (aromatic C=C stretch and N=O stretch).

^1H NMR, ($CDCl_3$), δ 1.1 and 2.4 (impurities), 3.7 (CH impurity in $CDCl_3$), 3.8 (t, $-CH_2$), 4.1 (t, $-CH_2$), 6.8 (d, aromatic H), 7.2 (impurity), 7.6 (d, aromatic H) and finally 7.8 (d d, aromatic H).

^{13}C NMR ($CDCl_3$) 68.74, 68.80, 68.88, 68.93, 70.00, 70.07 and 70.98 ppm. ('secondary', CH_2 , C atoms in the crown ring), 108.22, 111.12 and 117.88 ppm. ('tertiary', CH, C atoms in the aromatic ring) and finally 142.5, 148.47 and 154.53 ppm ('quaternary' C atoms in the aromatic ring).

Elemental analysis:	C	H	N	O
Found (%):	53.68	6.13	4.43	34.26
Calculated (%):	53.67	6.07	4.47	35.78

2.3.2 The Preparation of 4-aminobenzo-15-crown-5

Two methods were used to prepare this compound.

Method A: Reduction with tin and hydrochloric acid.

4-Nitrobenzo-15-crown-5 (1.0 g, 3.16 mmol) and tin (3.0 g, 25.3 mmol) were placed in a round bottomed flask. This mixture was then stirred whilst concentrated HCl (10 cm^3) was slowly added. The resulting mixture was refluxed for 2 hours, allowed to cool and

neutralised with ammonium hydroxide. This mixture was then extracted with chloroform (3x30 cm^3). The combined organic extracts were dried over $MgSO_4$ and evaporated to leave a brown oil which was used without further purification.

Yield: 0.18g, (20%); the sample melted over a broad temperature range (Ref[160] m.p. 73-74°C)

IR: 3431 cm^{-1}, 3554 cm^{-1} and 3224 cm^{-1} (NH stretch for a primary amine), 2925 cm^{-1} and 2871 cm^{-1} (alkane CH stretch), 1613 cm^{-1} and 1536 cm^{-1} (NH def and aromatic C=C stretch) and finally 1515 cm^{-1} (aromatic C=C stretch).

Method B: Catalytic hydrogenation of 4-nitrobenzo-15-crown-5.

4-Nitrobenzo-15-crown-5 (2.0 g , 6.4 mmol) and palladium on charcoal, Pd/C, (0.32 g , 10 %) were placed in a hydrogenation flask. The sides of the flask were washed down with ethanol (50 cm^3). The mixture was then hydrogenated under reduced pressure and the IR spectrum of a sample of this mixture was taken at regular intervals. The reaction appeared to be complete when approximately 1.7L of hydrogen had been adsorbed. The flask was then removed and the mixture filtered. The solvent was removed under vacuum to yield a pinky, brown oil. A pinky brown solid was obtained on scratching in diethylether.

Yield: 1.23g (63%); m.p 72-74°C (Ref[160] m.p. 73-74°C)

IR: 3395 cm^{-1}, 3345 cm^{-1} and 3224 cm^{-1} (NH stretch of primary amine) 2921cm^{-1} and 2878cm^{-1} (alkane CH stretch) 1613 and 1590 cm^{-1}(NH deformation and aromatic C=C stretch) and finally 1575 cm^{-1} (aromatic C=C stretch)

^1H NMR ($CDCl_3$) δ 1.9 (impurity), δ 3.4 (NH), δ 3.7 (impurity in $CDCl_3$), δ 3.8-3.9 (multiplet, CH_2 protons in crown ring), δ 6.1 (d,d aromatic CH proton), δ 6.2 (d,

aromatic CH proton), δ 6.7 (d, aromatic CH proton) and finally δ 7.2 (aromatic impurity).

^{13}C NMR ($CDCl_3$) 68.55, 69.85, 70.37, 70.68, 70.75 and 70.85 ppm ('secondary' CH_2 C atoms in the crown ring), 102.47, 107.14 and 117.39 ppm ('tertiary', CH, C atoms in the aromatic ring) and finally 141.51, 141.78 and 150.39 ppm ('quaternary' C atoms in the aromatic ring)

Elemental analysis:	C	H	N	O
Found (%):	60.94	7.46	4.85	28.04
Calculated (%):	59.35	7.47	4.94	28.21

2.3.3 The Preparation of 4-acryloylaminobenzo-15-crown-5

4-Aminobenzo-15-crown-5 (1.0 g, 3.5 mmol) was placed in a 3 neck round bottomed flask, equipped with two dropping funnels and a condenser. The amine was then dissolved in dry tetrahydrofuran, THF, (50 cm^3, dried over sodium wire and distilled from $LiAlH_4$). Dry triethylamine (0.3 cm^3, 2.2 mmol, dried over KOH pellets) was dissolved in dry THF (20cm^3) and was added to the flask via a dropping funnel. Nitrogen gas was then blown over the top of the mixture via the condenser. Acryloyl chloride (0.29 cm^3, 3.5 mmol) was dissolved in dry THF (20cm^3). This mixture was added slowly via the second dropping funnel over a period of approximately 15 minutes and the resulting mixture was stirred at room temperature overnight. The reaction mixture was centrifuged to remove the triethylamine hydrochloride. This precipitate was washed twice with THF, (2x10 cm^3). The combined organic phases were evaporated to give a pale brown solid. This material was used without further purification.

Yield: 0.92g (78%); m.p. 127-130°C

IR: 3273 cm^{-1} (NH stretch for a primary amine), 2936 cm^{-1} and 2861 cm^{-1} (alkane -CH stretch), 1658 cm^{-1} (carbonyl from amide C=O), 1631 cm^{-1} (C=C stretch), 1607 cm^{-1} and 1515 cm^{-1} (aromatic C=C stretch) and 1135 cm^{-1} (C-O stretch).

^{1}H NMR ($CDCl_3$) δ 0 (impurity), δ 1.3 and 2.1 (impurities), δ 3.(0 9 impurity or NH proton), δ 3.7 (impurity in $CDCl_3$) δ 3.8 and 4.0 (multiplets, CH_2 protons in crown ring), δ 5.6 (d,d vinylic CH proton), δ 6.3 (multiplet, vinylic CH_2 protons), δ 6.7 and 6.9 (d, coupled aromatic CH protons), δ 7.2 (impurity), δ (s, aromatic CH proton) and finally δ 7.9 (impurity or NH proton)

^{13}C NMR ($CDCl_3$) 2.55 ppm (Si impurity), 34.77 ppm (impurity), 57.56, 58.27, 58.43, 58.51, 59.24, 59.39, 59.77, and 59.86 ppm ('secondary' CH_2, C atoms in the crown ring), 98.84, 101.33, 103.56 and 120.21 ppm ('tertiary' CH, aromatic and vinylic C atoms), 116.17 ppm ('secondary' CH_2, vinylic C atom), 121.14, 134.62 and 138.11 ppm ('quaternary' aromatic C atoms) and finally 152.44 ppm (carbonyl C atom).

Elemental analysis:	C	H	N
Found (%):	60.53	6.82	4.15
Calculated (%):	59.99	6.93	4.14

2.4 The Preparation of 4-acetylbenzo-15-crown-5

In this Section the synthetic details for the preparation of 4-acetylbenzo-15-crown-5 will be given. This compound is the first intermediate in the synthesis of 4'-acryloylacetylbenzo-15-crown-5 which is outlined in Figure 4.2.

Aluminium chloride (0.33g, 2.48 mmol), was added to dichloromethane (5 cm^3). This solution was cooled in an ice-water bath and stirred for thirty minutes. Acetyl chloride

solution was cooled in an ice-water bath and stirred for thirty minutes. Acetyl chloride (0.14 cm^3, 2.0 mmol) in dichloromethane (2.5 cm^3) was added slowly and stirred for fifteen minutes, before a solution of benzo-15-crown-5 (0.5g, 1.86mmol) in dichloromethane (2.5 cm^3) was added. This mixture was then stirred at this temperature for half an hour and then for twenty four and a half hours at room temperature. A mixture of ice and concentrated HCl (1g, 0.5 cm^3) was added and the resulting mixture stirred for fifteen minutes. The organic phase was separated from the aqueous phase which was then washed with dichloromethane (3x25 cm^3). The combined organic extracts were then dried over $MgSO_4$ and evaporated to leave a pale yellow oil which rapidly solidified to give pale yellow crystals.

Yield: 0.17g, (29%); m.p. 80-81°C (Ref[119] m.p. 96-97°C)

IR: 3300 cm^{-1}- 3500 cm^{-1} (C=O overtone), 2880 cm^{-1} and 2960 cm^{-1} (alkane C-H stretch), 1680 cm^{-1} (small ill-defined C=O stretch), 1600 cm^{-1} and 1500 cm^{-1} (aromatic C=C stretch) and 740 cm^{-1} (C-H def. for o substituted benzene)

2.5 The Preparation of 4-acryloylmethylbenzo-15-crown-5

This Section is concerned with the synthesis outlined in Figure 4.3.

2.5.1 The Synthesis of 4-formylbenzo-15-crown-5

The synthesis of this compound follows the method reported by Wada *et al*[161].

Benzo-15-crown-5 (2.0g, 7.5 mmol), was dissolved in dry THF (10 cm^3). The solution was purged with nitrogen. Hexamethylenetetraamine, hexamine, (2.0g, 5 mmol) in THF (10 cm^3) was added followed by a solution of trifluoroacetic acid, TFA, (32 cm^3) in THF (10 cm^3). This mixture was refluxed for 36 hours under a N_2 atmosphere. The THF and

water (150 cm^3) for 90 minutes. The aqueous phase was extracted with toluene (3x100 cm^3) and the combined organic extracts dried over $MgSO_4$. Evaporation gave a pale browny orange oil which solidified on standing. This material was extracted with hot n-heptane (3x100 cm^3) using a Soxhlet to leave a very pale yellow oil which solidified on standing.

Yield: 0.51g (22%); m.p. 78-80°C (Ref[161] m.p 78-80°C)

IR: 3508 cm^{-1} (C=O overtone or water), 2927 cm^{-1} and 2869 cm^{-1} (alkane -CH stretch), 1784 cm^{-1} (C=O stretch), 1595 cm^{-1} and 1505 cm^{-1} (aromatic C=C stretch)

2.5.2 The Preparation of 4-hydroxymethylbenzo-15-crown-5

Two methods were used to effect this synthesis.

Method A: Reduction of 4-formylbenzo-15-crown-5 with lithium aluminum hydride.

Lithium aluminium hydride, lithal, (0.04 g, 1 mmol) was added to dry diethyl ether (20 cm^3). This mixture was then stirred, whilst a solution of 4-formylbenzo-15-crown-5 (0.2g) in dry diethyl ether (30 cm^3) was added slowly over a period of 5 minutes. The resulting mixture was then refluxed for five hours. The excess lithal was decomposed with ice-water (20 cm^3). The resulting solid was filtered off and the aqueous phase was then extracted with diethyl ether (3x25 cm^3). The combined organic extracts were dried over $MgSO_4$ and evaporated to leave a trace amount of a clear oil which crystallised on standing.

Yield: 0.1g (50%); m.p. 78-80°C (Ref[122], m.p. 80°C).

IR: 3200 cm^{-1} - 3490 cm^{-1} (OH stretch), 3031 cm^{-1} and 3002 cm^{-1} (aromatic CH stretch), 2953 cm^{-1} and 2916 cm^{-1} (alkane CH stretch), 1596 cm^{-1} and 1505 cm^{-1} (aromatic C = C stretch).

NMR

^{1}H ($CDCl_3$) δ 1.3 (s), 3.9 (t, CH_2), 4.1 (t, CH_2), 6.8 (d, d, CH).

^{13}C ($CDCl_3$) 29.9 ppm (impurity), 68.99 ppm, 69.56 ppm, 70.46 ppm, and 70.99 ppm ('secondary', CH_2, C atoms within the crown ring), 114.15 ppm and 121.32 ppm ('tertiary', CH , C atoms in the benzene ring), and finally 149.11 ppm ('quaternary', C, atoms in the benzene ring).

Method B: Reduction with sodium borohydride.

The method followed is based on that outlined by Varma in the literature[122]. 4-Formylbenzo-15-crown-5 (0.26g, 0.9 mmol), was dissolved in ethanol (10 cm^3). Sodium borohydride (0.4 g, 1.1 mmol) was added and this mixture was then stirred at room temperature for 24 hours. The reaction mixture was poured onto water (7.5 cm^3) and neutralised with acetic acid (25 %). The resulting solution was extracted with chloroform, (4x10 cm^3) and the combined organic extracts dried over $MgSO_4$. Evaporation of the filtered solution gave a very pale pink coloured oil from which pink crystals were precipitated on addition of petroleum ether 60-80 (10 cm^3). The pink coloured impurity was removed by recrystallisation from a hot, filtered solution of chloroform and decolourising charcoal.

Yield : 0.11g (42%); m.p. 78-80°C (Ref[122] m.p. 80°C)

IR : 3300-3600 cm^{-1} (OH stretch), 2920 cm^{-1} and 2860 cm^{-1} (alkane CH stretch), 1730 cm^{-1} (C=O stretch), finally 1595 cm^{-1} and 1505 cm^{-1} (aromatic C=C stretch).

NMR

^{1}H ($CDCl_3$) δ 1.8 (small OH peak), 3.7 (impurity in $CDCl_3$), 3.9 (t, CH_2), 4.1 (t, CH_2), 6.8 (aromatic CH) and 7.2 (impurity).

^{13}C The spectrum obtained matched that obtained for the previous product.

2.5.3 The Preparation of 4-acryloylmethylbenzo-15-crown-5

The synthesis of this compound was attempted using the procedure outlined by Varma[122] Acryoyl chloride (0.1 cm^3, 1.2 mmol) was dissolved in THF (5 cm^3). A solution of 4-hydroxybenzo-15-crown-5 (0.1 g, 0.34 mmol) and triethylamine (0.7 cm^3, 0.48 mmol) in THF (10 cm^3) was added dropwise to the solution containing the acryloyl chloride. The mixture was then stirred for four hours at room temperature and heated for a further hour on a water bath. After cooling, the mixture was filtered. The THF was removed and the residue partitioned between chloroform and water (20 cm^3 of each). The aqueous phase was then extracted with chloroform (2x15 cm^3). The organic phases were dried and evaporated to leave a clear oil which crystalised when petroleum ether was added.

Yield: 0.02 g, (17%) ; m.p. 67-68 ^oC (Ref[122] m.p. 49-50 ^oC)

IR: 2910 cm^{-1} and 2840 cm^{-1} (alkane CH stretch), 1730 cm^{-1} (C =O stretch), 1590 cm^{-1} and 1490 cm^{-1} (aromatic C = C stretch).

2.6 The Synthesis of 4,4'-diacyloylaminodibenzo-18-crown-6

This Section deals with the synthesis of the functionalised crown ether, dibenzo-16-crown-6 illustrated in Figure 4 4.

2.6.1 The Synthesis of 4,4'-dinitrodibenzo-18-crown-6

This compound was synthesised following the procedure outlined by Feigenbaum and Michel[114].

Dibenzo-18-crown-6 (3.0 g, 8.3 mmol) was placed in a round bottomed flask and

dissolved in chloroform (10 cm^3). Glacial acetic acid (90 cm^3) was added and then fuming nitric acid (9 cm^3, 98%) was added dropwise over a period of about ten minutes. The temperature was maintained at room temperature by immersing the flask in a water bath. This mixture was then stirred at room temperature for 24 hours. The chloroform layer was reduced and a tan solid precipitated on standing. This was removed by filtration. The mother liquor was poured onto water (100 cm^3) and neutralised with sodium bicarbonate. This mixture was washed with chloroform (3x100 cm^3) and the combined organic extracts dried over $MgSO_4$. Evaporation of the organic extracts yielded an orange coloured solid. All solid fractions were then combined and the mixture boiled in 2-methoxyethanol. The hot solution was filtered to remove the insoluble tan coloured crystals, the *trans* isomer. Evaporation of the 2-methoxyethanol gave the pale yellow *cis* derivative.

Yield: 2.63g, (70%)

trans Isomer

Yield: 2.32g; m.p. 237-245°C (Ref[114] m.p. 237-246°C)

IR: 3631 cm^{-1} and 3417 cm^{-1} (water from KBr), 3092 cm^{-1} (aromatic CH stretch), 2953 cm^{-1} 2063 cm^{-1} (alkane CH stretch), 1754 cm^{-1} and 1673 cm^{-1} (impurity), 1591 cm^{-1} and 1510 cm-1 (aromatic C = C and NO_2)

NMR

^1H (DMSO) δ 2.5 (s, DMSO), 3.3 (d, CH_2 in the crown ring), 3.9 (d, CH_2 in the crown ring), 4.2 (d, CH_2 in the crown ring), 7.1 (d, CH in the aromatic ring), 7.2 (d, CH in the aromatic ring), 7.8 (d, d, CH in the aromatic ring).

^{13}C (DMSO) 38.67 ppm-40.34 ppm (DMSO), 67.96 ppm, 68.32 ppm, and 66.46 ppm ('secondary', CH_2, C atoms in the crown ring), 106.52 ppm, 111.17 ppm, 117.54 ppm ('tertiary', CH, C atoms in the benzene ring), 140.54 ppm, 147.63 ppm, and153.71 ppm

('quaternary', C atoms in the benzene ring)

cis Isomer

Yield: 0.31g; m.p. 220-230 ^{o}C (Ref[102] m.p. 206-232 ^{o}C)

IR: The IR obtained for this sample is similar to that obtained for the *trans* isomer.

NMR

^{1}H ($CDCl_3$) δ 0.9, 1.3, 2.1, 2.8, and 2.9 (impurities), 2.7 (d, small peak assigned to CH_2 in the crown ring),4.0 (d,d, CH_2 in the crown ring), 4.2 (d,d, CH_2 in the crown ring), 6.8 (t, t, CH in the aromatic ring)

^{13}C ($CDCl_3$) 68.45 ppm, 68.59 ppm and 68.21 ppm ('secondary', CH_2, C atoms in crown ring), 107.19 ppm, 110.56 ppm and 117.61 ppm ('tertiary', CH, C atoms in benzene ring), 141.42 ppm, 148.16 ppm and 153.88 ppm ('quarternary', C atoms in the benzene ring).

2.6.2 The Preparation of *trans* 4,4' diaminodibenzo-18-crown-6

trans-Dinitrodibenzo-18-crown-6 (1.5 g, 0.52 mmol), was placed in a hydrogenation flask with Pd/C (0.15 g) and DMF (180 cm^3). This mixture was then hydrogenated under pressure. Hydrogenation was terminated once 400 cm^3 of H_2 had been absorbed, (theoretical volume required 236 cm^3). The mixture was filtered and the solvent removed by distillation. A glassy tar was obtained. This was redissolved water and chloroform (150 cm^3 of each). The aqueous phase was extracted with chloroform (4x100 cm^3) then the combined organic phases were dried over $MgSO_4$ and evaporated to leave a trace amount of a brown oil from which it was impossible to obtain an IR spectra.

2.7 The Preparation of 4,4' diacryloylmethyldibenzo-18-crown-6

The preparation of the compounds illustrated in Figure 4.5 are described below.

2.7.1 The Preparation of 4,4'-diformyldibenzo-18-crown-6

Dibenzo-18-crown-6 (1.0 g, 2.8 mmol), was dissolved in dry THF (15 cm^3). A solution of hexamine (0.79 g, 5.6 mmol) in THF (5 cm^3) was then added followed by a solution of trifluoroacetic acid, TFA (0.5 cm^3, 5.6 mmol) in THF (5 cm^3). This reaction mixture was stirred and heated under a N_2 atmosphere for 2 hours. More (35 cm^3) solvent was added since most of the initial solvent had evaporated. This mixture was then heated for a further 14 hours. The reaction mixture was poured onto water (30 cm^3) and the resulting mixture was stirred for an hour at room temperature. A white precipitate was obtained which was filtered off. The aqueous phase was extracted with toluene (3x75 cm^3) and the combined extracts were then dried over $MgSO_4$. Evaporation left a pale yellow solid. This material was combined with the white precipitate obtained earlier and extracted with hot n-heptane in Soxhlet extractor. On cooling a white crystalline product was obtained.

Yield: 0.82g, (70%); m.p. 162-164 ^oC.

IR: 3433 cm^{-1} (impurity), 3064 cm^{-1} and 3087 cm^{-1} (aromatic CH stretch), 2949 cm^{-1} - 2745 cm^{-1} (alkane CH stretch), 1736 cm^{-1} (small, ill-defined C = O stretching band), 1597 cm^{-1} and 1510 cm^{-1} (aromatic C = C stretch).

NMR

^1H ($CDCl_3$) δ 1.7 (impurity), 4.0 (d,d, CH_2), 4.1 (d,d, CH_2), 6.8 (t,t, aromatic CH) , 7.2 (s, aromatic CH).

^{13}C ($CDCl_3$) 68.8 ppm and 69.9 ppm ('secondary', CH_2, C atoms in the crown ring), 113.6 ppm and 121.ppm ('tertiary ', CH, C atoms in the aromatic ring) and finally 149.8 ppm ('quaternary' C atom in the aromatic ring).

2.7.2 The Preparation of 4,4'-dihydroxymethyldibenzo-18-crown-6

The experimental procedure used to synthesise this compound is outlined in Section

2.5.1. However, in this case 4',4-diformyldibenzo-18-crown-6 (0.54 g, 1.2 mmol) was used with sodium borohydride, $NaBH_4$ (0.104 g, 2.8 mmol). The mixture was refluxed for 2 hours after stirring for 24 hours. Approximately 0.5 g of $NaBH_4$ were added and the mixture refluxed for a further 2 hours. The resulting mixture was then worked up as outlined in Section 2.4.1. A white crystalline material was obtained.

Yield: 0.44g, (88%); m.p. 160-163 ^oC

IR: 3410 cm^{-1} (OH stretch), 3065 cm^{-1} (aromatic CH stretch), 2950 cm^{-1} - 2890 cm^{-1} (alkane CH stretch), 1740 cm^{-1} (small, ill-defined C = O stretching band), 1600 cm^{-1} and 1510 cm^{-1} (aromatic C = C stretch).

NMR

^1H ($CDCl_3$) δ 0.9, 1.3 and 2.0 (impurities), 4.1 (d,d, CH_2), 6.8 (t,t, aromatic CH), 7.2 (s, aromatic C).

^{13}C ($CDCl_3$) 68.8 ppm and 69.9 ppm ('secondary', CH_2, C atoms in the crown ring), 113.6 ppm and 121.ppm ('tertiary ', CH, C atoms in the aromatic ring) and finally 149.8 ppm ('quaternary' C atom in the aromatic ring).

2.7.3. The Preparation of 4,4'-diacryloylmethyldibenzo-18-crown-6.

The experimental method used to synthesise this compound is outlined in Section 2.5.3. However, 4',4-dihydroxydibenzo-18-crown-6 (0.3 g, 0.71 mmol) was used in place of 4'-formylbenzo-15-crown-5. This diol was then reacted with acryloyl chloride (0.12 cm^3, 1.43 mmol) and triethylamine (0.2 cm^3, 0.12 mmol) to obtain the diacryolyl derivative. A white solid was obtained.

Yield: 0.14g, (77%); m.p. 162-164 ^oC.

IR: the spectrum matches dibenzo-18-crown-6.

2.8 The Preparation of Hydrogel Membranes

Hydrogel membranes were prepared by a free radical, bulk polymerisation of the constituent monomers in a membrane mould which is illustrated in Figure. 2.3.

Figure 2.3 Membrane mould (reproduced form reference 39)

Two glass sheets (8x13 cm^2) were each covered by a Melinex (polyethylene terephthalate) sheet. This eases the separation of the plates once the polymerisation process is complete and also provides a smooth, clean surface. The covered plates were then wiped with acetone and placed together with three polyethylene gaskets (each 0.2 mm thick with a

rectangular hole 5x9 cm^2) separating the Melinex sheets. A G22 syringe needle was inserted between the gaskets and the whole mould was held together using bulldog clips.

The monomer mixtures used were based on solutions containing HEMA and a crosslinking agent, EGDM. These monomers were used in ratios of either 90:10, 95:5 or 99:1 wt/wt HEMA:EGDM. A free radical initiator, azo-bis-isobutyronitrile 0.5 % wt/wt was added to the HEMA mixture. Other monomers were then added in varying amounts to this basic mixture (usually in 5 to 20% wt/wt of HEMA comonomer mix). Once a homogeneous solution had been obtained the solution was outgassed with nitrogen for 10 minutes. The mixture was then slowly injected into the gasket, taking care to ensure that air bubbles were not introduced to the mould. Once the cavity was almost full the mould was laid horizontally and the needle was removed, thus allowing the monomer solution to fill the mould. The mould was then placed in an air oven at 60 ^{o}C for 3 days followed by 2/3 hours postcuring at 90 ^{o}C.

After postcuring, the mould was removed from the oven and the membrane was carefully removed from the Melinex sheets and allowed to soak in distilled water. Care was taken to ensure that this process was completed efficiently whilst the mould was still warm otherwise the membrane stuck to the Melinex sheets. When this problem arose the hydrogel was generally released from the Melinex sheets by soaking in distilled water. All hydrogel membranes were then soaked in distilled water for 3 weeks prior to use (NB for the first week the soaking water was changed daily).

2.9 Determination of Equilibrium Water Content (EWC)

A gravimetric technique has been used to determine the EWC of hydrogel samples. A cork borer (size 7) was used to cut five discs from a hydrogel sample which had generally

been hydrated for at least three weeks. However, in the case where the membrane contained an unbound crown ether, hydration was assumed to be complete after a few hours. These discs were then placed in distilled water overnight. A disc was transferred to a piece of filter paper and the surface water was removed from the exposed surface by running a piece of filter paper over it. This process was repeated for the other surface. The sample was then weighed and its hydrated weight, W_h , recorded. Once all the discs had been weighed they were dehydrated in a microwave oven for 10 minutes. The dehydrated weight, W_d, was then obtained for each disc. The equilibrium water content could then be calculated using Equation 1.1, Section 1.2.1 whereby;

$$EWC = \frac{\text{total weight of water present in the hydrogel}}{\text{total weight of hydrated hydrogel}} \times 100\ (\%)$$

$$= \frac{W_h - W_d}{W_h} \times 100\ (\%)$$

Previously, this technique has been used for a statistical analysis of 100 samples of poly HEMA[39]. The results indicated that a mean EWC of 37.6 % is obtained with Σ_{n-1}=0.42. Similar errors were obtained in these determinations with Σ_{n-1}=0.5.

2.9.1 The Effect of Salt on EWC

The method outlined in Section 2.9 was followed, however, in this case the discs were initially wiped to remove the surface water and then allowed to equilibrate overnight in the salt solution prior to the determination of EWC.

2.9.2 The Measurement of Partition Coefficients

The partition coefficient, S_m, is defined in Equation 2.1 and has been determined using

the methods outlined by Yasuda and coworkers[138] and Hamilton[39].

$$Sm = \frac{\text{concentration of salt in membrane / (mMole/g)}}{\text{concentration of salt in equilibrating solution / (mMole/g)}} \qquad (2.1)$$

A disc (size 7 cork borer) was cut from the hydrated membrane. The surface water was removed and the disc transferred to 10 cm^3 of a 250 mM solution of the test salt. The sample was then allowed to equilibrate at either room temperature or 37 ^oC for a few days. The disc was then removed, the salt solution carefully wiped from the surface and the weight of the membrane and its thickness were determined. The disc was placed in 10 cm^3 of distilled water and left at 37^oC for a few days to allow the salt to leach out. The concentration of leached salt was then determined conductimetrically. Since the volume of water added was known, the amount of salt present in the membrane could be calculated, assuming of course that all the salt is leached from the membrane. Finally, if the amount of salt present in the membrane was assumed to have no effect on the overall concentration of the soaking solution then the partition coefficient could be determined using the equation derived by Yasuda and coworkers (Equation 2.2)

$$Sm = \frac{\text{weight of salt in membrane / volume of membrane}}{\text{weight of salt / volume of solution}} \qquad (2.2)$$

and the equation used by Hamilton (Equation 2.3)

$$Sm = \frac{\text{moles of salt in the membrane / weight of membrane}}{\text{moles of salt /g of equilibrating solution}} \qquad (2.3)$$

The partition coefficient was determined using three discs from each sample in each of salt solutions and the average value was then taken as the partition coefficient.

2.9.3 The Leaching of Membrane Components.

When a hydrogel is hydrated components are leached from the membrane. These include not only unreacted monomers and crosslinker, but perhaps more significantly in this study 'unbound' components such as crown ethers. Hence, it is important to study the leaching properties of these membranes. This property has been studied in this work by determining weight loss during leaching.

Membranes were prepared as outlined in Section 2.8, however, in these studies smaller gaskets (1cm by 4cm) were used and an aliquot (5% wt/wt) of B-15-C-5 was added to the basic mixture, HEMA:EGDM (90:10) before polymerisation. The leaching profile was then obtained by determining the dry weight of the sample after specific leaching times.

2.10 Measurement of Surface Properties

This Section deals with the experimental techniques used to measure contact angles. The theory used to determine the surface energies from contact angles, however, will be dealt with in Chapter 7.

The surface energies of the hydrogels studied were determined in the dehydrated state using the conventional sessile drop technique. Before any measurements were made the polymer surface was cleaned. The sample was first washed with a Teepol detergent solution, rinsed with distilled water and allowed to soak thoroughly in distilled water. The hydrogel samples were then dehydrated in a microwave oven for ten minutes and left in a desiccator overnight. The contact angles with both distilled water and methylene iodide were measured directly using a Rame-Hart contact angle Goniometer (model 100-00). A minimum of four measurements were made and the average value determined.

The experimental error on this data was of the order of ± 2°. The surface energy was then calculated using Macintosh Works™ which had been programmed with the Owens and Wendt equation.

2.11 Permeability Studies

The permeability cell used in these studies is designed so that the membrane is held vertically. This is important since it reduces the hydrostatic head and bubble formation. The surface layer is constantly stirred by means of magnetic couples linked to an external mechanical stirrer motor. This is particularly important since it reduces the stagnant layer formation at the membrane surface.

2.11.1 Design and Set-Up of the Ion Permeability Apparatus

The original permeability cell used was obtained from D.C Sammon of AERE Harwell. Later, copies were made to this design specification so that simultaneous permeability studies could be made. The cell is illustrated in Figure 2.4 and the system is represented schematically in Figure 2.5. The cell used was cylindrical in shape (9 cm diameter, 14 cm long) and was constructed mainly from Perspex. Inside the cell there were two chambers approximately 6 cm in length and 4 cm, in diameter, which were separated by a membrane gasket. The test membrane was held in place by 2 silicone rubber gaskets (9 cm outer diameter, 4 cm inner diameter). The whole cylinder was then held in place by six bolts. It should be noted that the pressure applied by these bolts was critical. If the bolts were too loose then leakage between chambers occurred, whereas if they were too tight the membrane could be damaged. Each chamber had an inlet and outlet ports to allow the continuous circulation of fluid.

Figure 2.4 Diagramatic representation of the permeability cell

(Reproduced from reference 39)

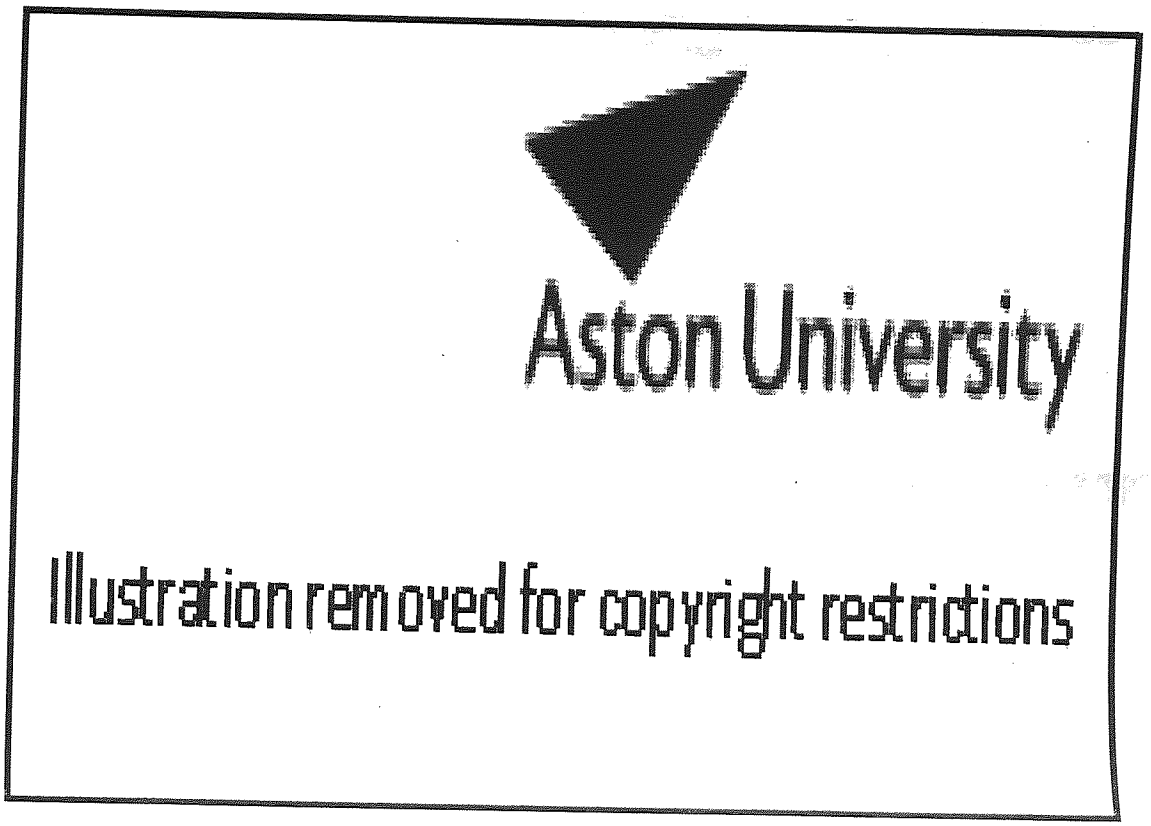

Aston University

Illustration removed for copyright restrictions

Figure 2.3 Schematic representation of permeability apparatus

(Reproduced from reference 39)

These ports were diametrically opposed to ease the removal of air bubbles. A standard salt solution was passed through the chamber on the right hand side. Initially, distilled water is passed through the left hand side. The solutions on each side of the membrane were continually stirred by paddles positioned close to the membrane surfaces. The paddles were driven, via a magnetic coupling system, by an external stirrer motor. The cell once assembled was immersed in a thermostated water bath set at 37^{o}C. This bath had been specially designed to allow the stirring system to function properly.

Each chamber was connected to a specially adapted separating funnel (250 cm^3). These funnels acted as a reservoir, once the tap had been opened, through which the system could be filled. Once the taps were closed solution simply flowed through the 'T' piece. The separating funnels were linked to the bottom ports of the channels via two sampling tubes. Samples could be taken from these tubes by inserting a syringe needle through the suba-seal at the top. However, in the course of this study when the permeation of single ions was studied, the conductivity of the solution at the low side (i.e. the chamber on left hand) was monitored. This was achieved by placing a conductivity flow-through cell (K=1), in between the top port of the chamber on the left hand side. The conductivity was then displayed on an αlpha 800 conductivity meter (range 200 $\mu s\ cm^{-1}$).

The closed fluid loops of each chamber were continually circulated by a peristaltic pump with a flow rate of (30 $cm^3 min^{-1}$). The stirring rate was approximately 150 rev min^{-1}.

2.11.2 Operation of the Ion Permeability Apparatus

The permeability cell was sealed and placed in a thermostated water bath (37 ^{o}C) overnight. A 5 cm diameter disc was cut from the membrane and was allowed to equilibrate in the distilled water at 37 ^{o}C overnight. The disc was then sandwiched

between the silicone rubber gaskets. The cell was assembled and immersed in the water bath as quickly as possible, to minimise cooling. Each chamber was then filled from the respective reservoirs, the right hand side containing the standard ion solution and the left hand side initially distilled water. The peristaltic pump was switched on and the sample tubes carefully filled. The hydrostatic pressure in each chamber was controlled by pinching the tubes connecting the outlet ports at the top of the cell to the reservoir. Great care was taken at this stage since the membrane easily bursts under an unequal pressure. The stop clock was started as soon as the cell was half full. Once the cell was virtually full the bubbles were eliminated from the chambers by tilting the cell, gently. The final adjustments to the hydrostatic pressure were made by alternating the height of the sample tubes. Finally, the stirrer motors were switched on. A speed setting in the order of 150 rpm was used.

For the first few hours the hydrostatic pressure was observed and adjustments made as necessary. Conductivity readings were made at least every fifteen for the first hour or so and care was taken to ensure that there were no air bubbles in the flow through cell when the reading was recorded since this would invalidate the reading. Once the system had become stable readings were taken every half hour or so over a period of 6-10 hours.

2.11.3 Errors Associated with the Measurement of Permeability Coefficients

The effects of experimental parameters upon permeation rates have been investigated so that any effects can be eliminated from these studies. Previous permeability studies on similar systems have indicated that the stirring rate at the membrane is not critical at 30 rpm or above[162]. Subsequent studies have illustrated that in particular it is essential to stir the membrane at the side with the highest ion concentration to remove any surface

layer effects[163,164]. Studies using this system have illustrated that there is a decrease of 3% for the final permeability coefficient if the membrane is stirred at the high side only and a decrease of 10% if the low side or neither side is stirred[156]. Similarly changes in the flow rate between 30 and 90 ml/min do not appear to be a critical factor[156]. The errors which arise from the swelling and deswelling effects of hydrogels in salt solutions were eliminated by measurement of the individual thickness at the end of each permeability run.

The reproducibility of the experimental data was also considered. The effects that dismantling, cleaning and reassembling the apparatus used in these studies have on the permeability coefficient was studied[39]. The permeability of KCl through poly HEMA under identical experimental conditions gave values for the permeability coefficient with a reproducibility of ± 2.5%[39]. Similarly, if a different sample membrane was used the experimental errors were again of the order of 2-3% . Finally, the reproducibility of the data over time and between workers was considered. The permeation of KCl through a crosslinked HEMA membrane of composition HEMA:EGDM (90:10) was studied. A value of 2.4 $x10^{-8}cm^2s^{-1}$ has been reported previously[39] and a value of $2.3x10^{-8}cm^2s^{-1}$ was obtained in this study. This corresponds to a difference of 4% and reflects the long term reproducibility of the permeability data obtained using this apparatus.

2.12 Measurement of Mechanical Properties

The mechanical properties of the hydrogels in tension were investigated using a Hounsfield HTi tensometer interfaced to an IBM 55SX computer. Dumbbell shaped specimens of gage length 8mm and width 3.3mm were cut from the hydrated sample under test. These test specimens were then equilibrated in distilled water to ensure complete hydration prior to testing. The mechanical testing of hydrated specimens of this

type presents problems which have been discussed in detail elsewhere[165]. However, these problems have been overcome and a standard test method was developed which involves the use of a fine spray to ensure complete hydration during the test. The samples were tested to break at an extension rate of 20mm/min and the reported values of tensile strength, initial modulus and elongation to break were calculated from the average of a minimum of six tests.

CHAPTER 3

Transport Properties of Unmodified and Crown Modified Hydrogel Membranes

3.1 Introduction

Crown ethers are a unique class of polyether which can selectively bind to ions, particularly alkali and alkaline earth metal cations. The concept of occluding ionophores within a polymer matrix has been exploited for many years in the design of permselective membranes for chemical sensor applications[166,167]. However, whilst the concept of the physical immobilisation of species within a hydrogel matrix is well known, there have been few attempts to study hydrogel systems which contain occluded crown ethers. As hydrogels contain imbibed water, through which aqueous species are transported, it is interesting to consider the effects of the inclusion of an ionophoric crown ether on the transport properties of these materials.

Previous studies within the Speciality Materials Group at Aston have investigated the possibility of preparing a range of hydrogel membranes in which crown ethers have been dispersed within the polymer matrix[39]. These studies have illustrated that a lipophilic crown ether, dicyclohexano-18-crown-6, DCH-18-C-6, could be dispersed within a poly HEMA membrane containing 10% ethylene glycol dimethacrylate (EGDM) crosslinker by weight, to produce a homogeneous membrane. In addition, these studies illustrated that ionophore loss whilst the polymer hydrates is insignificant within the duration of the permeability experiments[39]. A 5% (wt/wt) loading of this crown ether was used in the initial transport studies since the addition of this crown ether at this loading has a negligible effect on EWC (values of 24.3% and 24.6% at 37^{o}C for the unmodified and modified systems were reported[39]). Hence, direct comparisons could be made between the transport properties of both modified and unmodified membranes. A preliminary investigation of the transport properties of this membrane indicated that the crown has a significant effect on the transport of KCl. Initially, induction periods or 'lag-times' were

observed, where relatively little ion permeation occurred, which were followed by steady state diffusion in which ion permeation was significantly lower than for an unmodified membrane.

As the transport properties of the unmodified membrane HEMA:EGDM (90:10) had not been studied previously, the initial studies described in this Chapter consider the effects of both cation and anion variation on ion transport through this membrane. In addition, the reproducibility of the earlier studies of the cation transport through a DCH-18-C-6 modified membrane was examined and this study has been extended to look at the effect anion variation has on ion permeation through crown modified membranes.

3.2 Ion Permeation Studies Through a Crosslinked HEMA Membrane

This section will deal with the results obtained from the permeability studies on the unmodified membrane system.

3.2.1 Effect of Cation Variation on the Transport of Chloride Salts

The effect of cation variation on ion permeability through a poly HEMA membrane with 10% crosslinker, EGDM, referred to as HEMA:EGDM (90:10) was investigated using a range of chloride salts of the group I and II metal cations, namely Na^+, Li^+, K^+, Ca^{2+}, Mg^{2+} and Ba^{2+}. The chloride salts were chosen for historical reasons. The initial studies of transport phenomena in hydrogels arose from attempts to design reverse osmosis membranes for desalination purposes[138] and hence the chloride salts were of particular interest. The primary ion transport data obtained from these studies is illustrated in Figures 3.1 and 3.2. The gradients of these graphs were used to calculate the permeability coefficients by substituting the appropriate values into Equation 1.10 (Section 1.6.1).

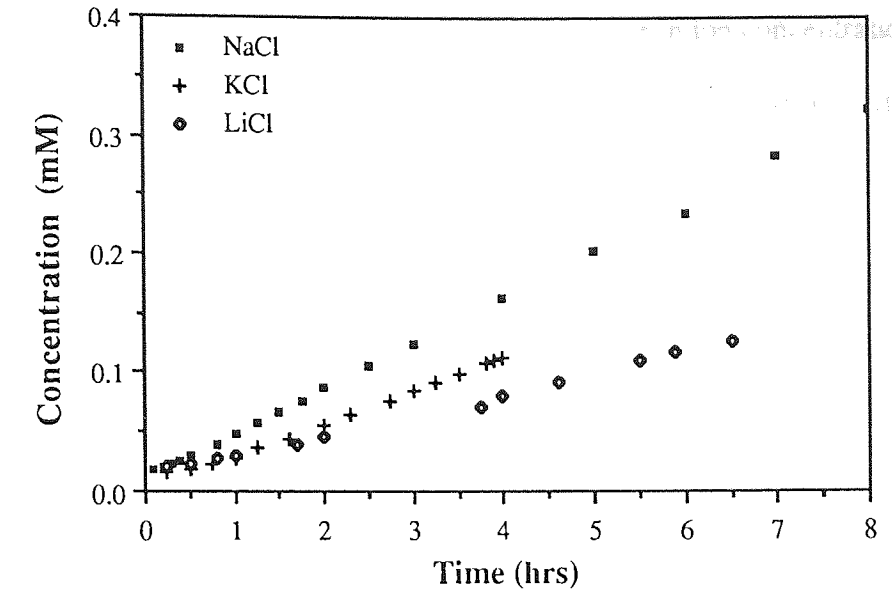

Figure 3.1 Primary data for the transport of group I metal chlorides across HEMA:EGDM (90:10)

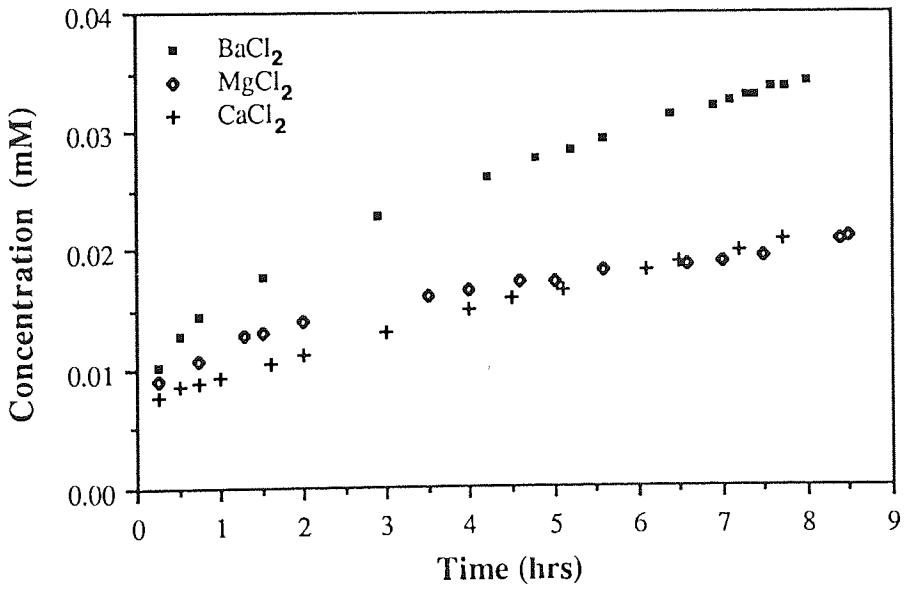

Figure 3.2 Primary data for the transport of group II metal chlorides across HEMA:EGDM (90:10)

The data obtained for the transport of group II metal cations (Figure 3.2) illustrates that initially there is a period where a relatively rapid increase in ion concentration is observed before ion permeability reaches a steady state. Since this may be attributed to the system attaining equilibrium the permeability coefficients were calculated from the gradient once this steady state has been reached.

The values obtained for the calculated permeability coefficients for group I and II metal cation variation are given in Table 3.1. These results illustrate that in all cases ion permeation is significantly lower for group II metal cations than for group I metal cations and that cation transport through these membranes decreases in the order :

$$Na^+ > K^+ > Li^+ >> Ba^{2+} > Ca^{2+} > Mg^{2+}$$

Table 3.1 Permeability coefficients for cation transport across HEMA:EGDM (90:10)

Salt (0.25M)	$Px10^8$ (cm^2s^{-1})
KCl	2.3
NaCl	2.7
LiCl	1.6
$CaCl_2$	0.14
$MgCl_2$	0.08
$BaCl_2$	0.19

In addition, both the calculated permeability coefficients and Figure 3.2 illustrate that the concentration of group II metal cations which permeate across the membrane over a period of 8 hours is extremely small. This implies that the transport of these ions is effectively blocked by this membrane system. This result might have been predicted since previous studies on HEMA:MMA (methyl methacrylate) copolymers illustrate that as the MMA

content is increased and EWC is reduced, 'cut-off' points in ion transport are observed[39,40]. The value predicted from these studies for the $CaCl_2$ cut-off point occurs when the EWC at 37°C is approximately 27% . Since the EWC of HEMA:EGDM (90:10) is 24.3% at 37°C[39], $CaCl_2$ permeation would, in fact, be expected to be minimal. Additionally, studies of the transport properties of poly HEMA based MMA and styrene copolymers[39] have illustrated that ion transport decreases in the order: $K^+ > Na^+ > Li^+ >> Ca^{2+}$. This behaviour has been related to the size of the cation permeating across the membrane. Although the crystallographic radii of these ions increases with an increase in atomic number, both the Stokes and Nightingale hydrated radii can be used to account for this trend. Table 3.2 gives the values for inoic radii quoted by Nightingale[168].

Table 3.2 Ionic radii of group I and II metal cations (reproduced from reference 168)

Ion	Crystallographic Radii / Å	Stokes' Hydrodynamic Radii / Å	Nightingale's Hydrodynamic Radii / Å
Li^+	0.60	2.38	3.82
Na^+	0.95	1.84	3.58
K^+	1.33	1.25	3.31
Mg^{2+}	0.65	3.47	4.28
Ca^{2+}	0.99	3.10	4.12
Ba^{2+}	1.13	2.90	4.04

Thus, if the permeability coefficients are compared with the values quoted in Table 3.2 for the hydrodynamic radii of these cations, the rate of ion permeability through HEMA:EGDM (90:10) appears to be influenced by the hydrated ionic radii of the cation with the exception of the transport of sodium ions. Initially, as the values obtained for the permeability coefficients for NaCl and KCl transport were similar it was thought that the

observed reversal in order might be attributed to the errors associated with the measurement and determination of the permeability coefficient, P. However, since these experimental errors are of the order of ± 4% (Section 2.11.3) the values quoted in Table 3.1 for group I metal cation transport are reproducible to $\pm 0.1 \times 10^{-8} cm^2 s^{-1}$. Hence, this reversal in the rate of cation permeation cannot be fully attributed to errors incurred during the measurement and calculation of the permeability coefficient, P. However, this copolymer contains a relatively high proportion of crosslinker, EGDM, and it is not unreasonable to expect the ion transport phenomena to be inherently complex. Previous studies have illustrated that water structuring effects play a dominant role in ion transport[39,40] for membranes with an EWC of about 25% measured at at 37°C. Thus, the transport of ions through HEMA:EGDM (90:10) would not be expected to be governed by diffusional size effects alone. Furthermore, as the proportion of crosslinker increases there will be an increase in both the number of chain entanglements and the stiffness of these chains; thus ion permeation might be expected to be further restricted by chain interference. Such considerations imply that it is perhaps unwise to place to much emphasis on this reversal in the order of sodium and potassium ion permeation. However, this study has illustrated that cation permeation through HEMA:EGDM (90:10) is generally influenced by diffusional size effects and has shown that group II metal cation transport is inhibited by this copolymer.

3.2.2 Permeation of a Mixed Salt Solution

The results discussed in the preceding Section refer to data obtained from permeation studies of single salt solutions. Such results highlighted some of the factors which affect ion transport and implied that group II ion transport through a membrane of composition HEMA:EGDM (90:10) is inhibited. In order to test this observation the mixed ion permeability of 0.25M solutions of KCl and $CaCl_2$ was studied. The increase in ion

concentration with time was monitored using flame ionisation atomic absorption spectroscopy and the primary ion transport data is illustrated in Figure 3.3.

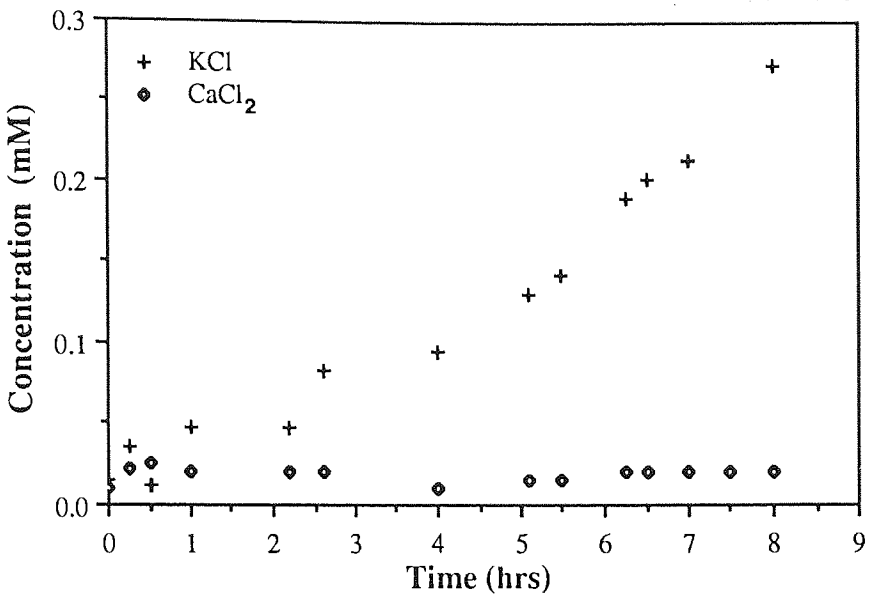

Figure 3.3 Primary data for the transport of a mixed salt solution across HEMA:EGDM (90:10)

These results indicate that although there is a broader degree of scatter in the experimental data than is observed with conductivity measurements, particularly at the lower ion concentrations, $CaCl_2$ permeation through this membrane is effectively blocked. Additionally, there appears to be a period of approximately four hours before the concentration of KCl at the low side increases linearly with time, i.e before a steady state of permeation is observed. The permeability coefficient was calculated once this steady state had been reached. A value of 3.1×10^{-8} cm^2s^{-1} was obtained. Since the value for single ion permeability is 2.3×10^{-8} cm^2s^{-1}, this result suggests that ion permeability in the steady state with mixed cations is greater than would be predicted on the basis of single salt studies. These results reflect the complex situation which arises when a mixed salt solution permeates across a hydrogel membrane. In addition to the factors described in

Section 3.2.1 the relative solubilities of these salts will also influence salt permeability. However, this study has demonstrated experimentally that it is possible to inhibit the transport of calcium ions and highlights the potential of hydrogels for use in a range of permselective applications.

3.2.3 Effect of Anion Variation on the Transport of Potassium Ions

Studies of the transport of a range of potassium salts through both poly HEMA and HEMA based MMA and styrene based copolymers have illustrated that anion variation has a significant effect on ion permeation[39,156]. In particular, anions which are said to structure water, for example SO_4^{2-}, were found to reduce potassium ion permeation, whereas if the co-anion is SCN^- which acts as a water structure breaker, potassium ion transport is enhanced. The studies of the effect cation of variation on ion transport through HEMA:EGDM (90:10) described in Section 3.2.1, have illustrated that ion transport may be influenced further by chain interference and water structuring effects. Hence, it is important to study the effects of a high concentration of crosslinking agent within a hydrogel membrane on the transport of anions. A range of potassium salts were used to study the effect of anion variation has on ion transport across a HEMA:EGDM (90:10) membrane (Figure 3.4). The primary ion transport data illustrated in Figure 3.4 was then used the calculate the permeability coefficients given in Table 3.3.

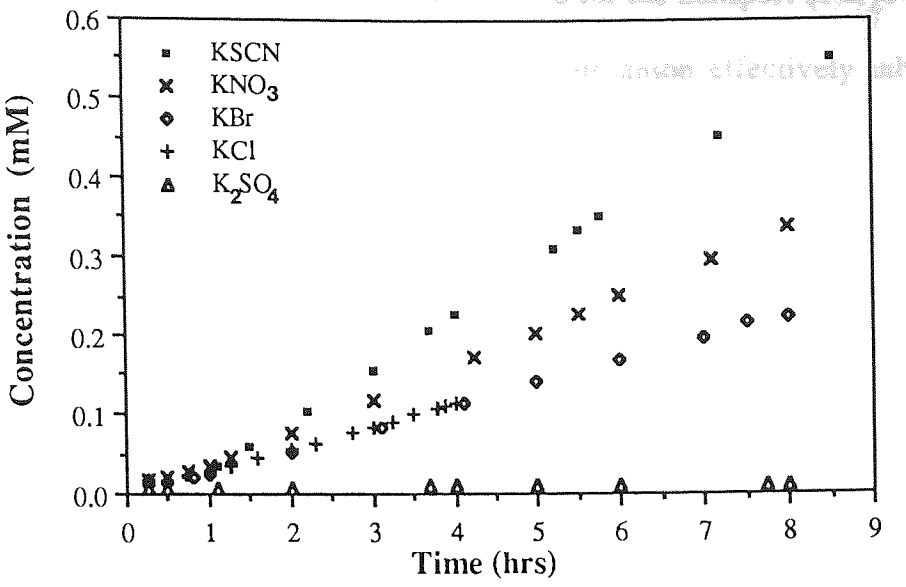

Figure 3.4 Effect of anion variation on cation transport through HEMA:EGDM (90:10)

Table 3.3 Permeability coefficients for the transport of potassium salts across HEMA:EGDM (90:10)

Salt (0.25M)	$Px10^8$ (cm^2s^{-1})
KSCN	6.4
KNO_3	3.6
KBr	2.5
KCl	2.3
K_2SO_4	0.01

These permeability coefficients may be used to arrange these anions in an order which reflects decreasing ion permeation. This series is given below;

$$SCN^- > NO_3^- > Br^- \sim Cl^- >> SO_4^{2-}$$

These results follow the same order observed in previous permeability studies where water structure breaking anions permeate more rapidly than water structure making anions

such as SO_4^{2-}. However, the value of P obtained for the transport of K_2SO_4 illustrate that in a highly crosslinked hydrogel the sulphate anion effectively inhibits cation transport.

3.3 Transport Phenomena in Hydrogels Containing Occluded Crown Ethers

Preliminary studies at Aston by Hamilton[39] have illustrated that it is possible to occlude a K^+ selective crown ether, dicyclohexano-18-crown-6, DCH-18-C-6, within a crosslinked HEMA membrane and that the presence of this crown has an interesting effect on the transport of cations across the membrane. It was essential, therefore, to test the reproducibility of these earlier observations and then to extend these studies to describe the effect of the nature of the anion on the transport properties of the membrane. In addition, attempts were made to extend the range of crown ethers which can be occluded in a crosslinked poly HEMA membrane. The results obtained from these studies will be presented and discussed in this below.

3.3.1 Effect of Cation Variation on the Transport of Chloride Salts Through a dicyclohexano-18-crown-6 Modified Membrane

In the introduction to this Chapter the occlusion of a potassium selective ionophore dicyclohexano-18-crown-6, DCH-18-C-6, in a crosslinked HEMA membrane of composition HEMA:EGDM (90:10) wt/wt was discussed. A 5% wt/wt loading of this crown ether was used and the transport of 0.25M solutions of NaCl and KCl was studied so that direct comparisons could be made with previous studies. The EWCs of both the unmodified and modified membranes were determined at room temperature and values of 26.8 ± 0.5 and $26.7 \pm 0.5\%$, respectively, were obtained. The primary ion transport data is illustrated in Figure 3.5.

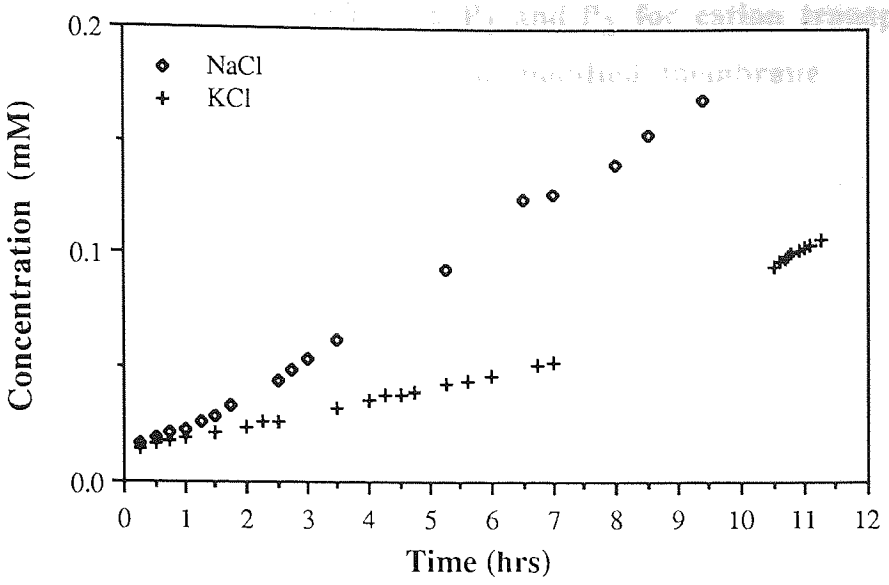

Figure 3.5 Effect of cation variation on ion transport through a dicyclohexano-18-crown-6 modified membrane

The results obtained from this study exhibit similar trends to those observed in the earlier study and indicate that the presence of this crown ether has a significant effect on the transport properties of this material. In both studies linear induction periods where ion transport is inhibited were observed, these were then followed by a final steady state of ion permeation. It is interesting to note that this behaviour contrasts with the enhanced ion transport which occurs with crown ethers dispersed in organic liquid membranes and reflects the competition between the imbibed water and the crown ether in the ion transport process. The gradients of the initial, and final slopes, m_1 and m_2, of the graphs illustrated in Figure 3.5 have been used to calculate the permeability coefficients P_1 and P_2 (Equation 1.10, Section 1.6.1). These values are compared with the values reported by Hamilton[39] in Table 3.4

Table 3.4 Permeability coefficients P_1 and P_2 for cation transport across a dicyclohexano-18-crown-6 modified membrane

Source of Data	0.25M KCl		0.25M NaCl	
	$P_1 \times 10^8$ / cm^2s^{-1}	$P_2 \times 10^8$ / cm^2s^{-1}	$P_1 \times 10^8$ / cm^2s^{-1}	$P_2 \times 10^8$ / cm^2s^{-1}
Figure 3.5	0.4	1.4	0.6	1.3
Hamilton	0.3	1.4	1.1	1.7

The duration of the initial induction period has also been determined and these values have been compared with those previously reported by Hamilton[39] (Table 3.5). In general there is good agreement between the two sets of data given in Tables 3.4 and 3.5. The discrepancies which do arise however, can be accounted for by considering the experimental errors.

Table 3.5 Extended 'lag-times' for the transport of cations across a dicyclohexano-18-crown-6 modified membrane

Source of data	0.25M KCl	0.25M NaCl
	t_{lag} / hrs	t_{lag} / hrs
Figure 3.5	7.3	1.7
Hamilton	4.5	2.0

Previous analyses of experimental error demonstrated that slight variations in membrane composition have little effect on the overall transport properties (Section 2.11.3). In contrast, it is anticipated that since the crown ether plays a dominant role in the ion transport process slight variations in the crown ether concentration of this system will affect the overall ion transport process. The crown ether is dispersed within the polymer matrix and will leach slowly from the membrane whilst the polymer hydrates. Since the pre-soaking times may vary it is difficult to produce an identical crown ether concentration

in each permeability experiment. Furthermore, assuming that the crown ether is dispersed evenly within the gel, variations in the membrane thickness will also alter the localised crown concentration. In fact the observed differences in the lag-times of 7.3 and 4.5 hours for KCl transport may, in part, be attributed to the differences in crown concentration caused by the variations in membrane thicknesses of 0.045 and 0.038 cm respectively. However, despite these considerations the results obtained in this study illustrate that the effects the presence of crown ether imparts on ion transport within a hydrogel membrane are reproducible.

3.3.2 Effect of Anion Variation on the Transport of Potassium Through dicyclohexano-18-crown-6 Modified Membranes

Variations in the counter anion have a significant effect on cation transport through unmodified membranes. Thus, it is important to consider the effects of anion variation on cation transport through crown ether modified membranes. A range of potassium salts were chosen to study this effect. This was in part due to the fact that potassium salts had been used in previous studies[39,156], but primarily because the crown ether, DCH-18-C-6, binds selectively to potassium ions. This section, therefore, will discuss the results obtained in a study of the effect of anion variation on the transport of K^+ ions through a membrane, HEMA:EGDM (90:10) containing 5% (wt/wt) DCH-18-C-6.

The primary ion permeability data is shown in Figure 3.6. This figure illustrates quite clearly that variations in the counter anion will affect the transport properties of this membrane. In general, there is a 'lag-time' or induction period followed by final steady state diffusion. However, the most obvious feature illustrated by this graph is the differences in the 'lag-times' as the anion is varied. Values for these 'lag-times' or induction periods were determined by taking the point at which the initial slope intersects

the slope of the final steady state and these values are presented in Table 3.6.

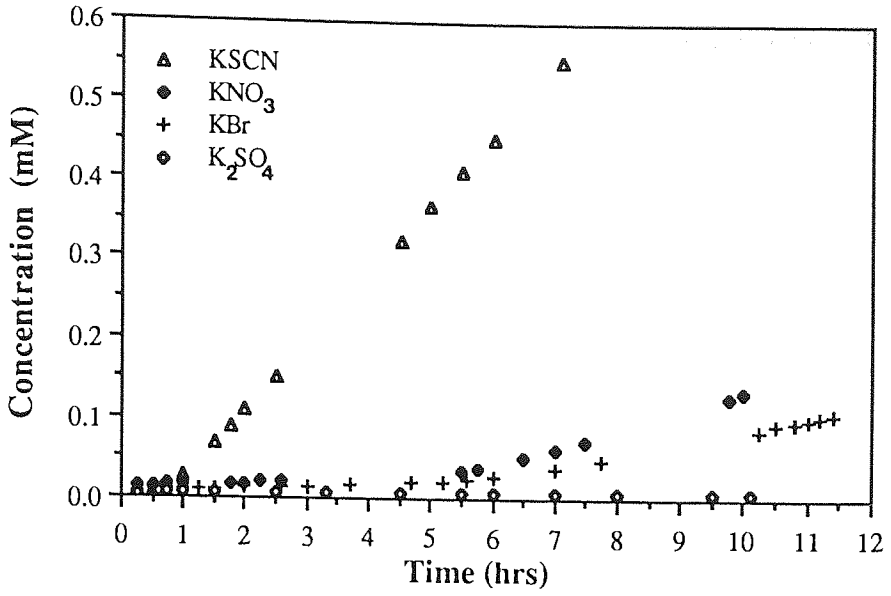

Figure 3.6 **Effect of anion variation on potassium ion transport across a dicyclohexano-18-crown-6 modified membrane**

Table 3.6 **Effect of anion variation on the 'lag-time' for potassium transport across a dicyclohexano-18-crown-6 modified membrane**

Salt (0.25M)	Lag-time / hrs
KSCN	0.9 ± 0.25
KCl	4.5 ± 1.0
KNO_3	5.3± 1.0
KBr	6.0± 1.0
K_2SO_4	> 24

The errors quoted for these 'lag-times arise since the change in the rate of ion permeation from the initial to final steady state occurs gradually. When these errors are considered the values for the 'lag-time' are observed to increase in the order;

$$SCN^- < NO_3^- \sim Br^- \sim Cl^- << SO_4^{2-}$$

The linearity of both the induction period and the final steady state indicates that this membrane may be regarded as having two permeability rates, one during the induction period, P_1 and the second, P_2, once a final steady state has been reached. Using the data illustrated in Figure 3.6 values for P_1 and P_2 were calculated and these values are presented in Table 3.7.

Table 3.7 Permeability coefficients P_1 and P_2 for the transport of potassium salts across a dicyclohexano-18-crown-6 modified membrane

Salt	$P_1 \times 10^8$ / $cm^2\ s^{-1}$	$P_2 \times 10^8$ / $cm^2\ s^{-1}$
KSCN	0.8	6.0
KNO_3	0.2	2.0
KBr	0.2	1.6
KCl	0.4	1.4
K_2SO_4	0.02	—

Previous studies of the effect of cation variation on ion transport through crown modified membranes (Section 3.3.1) indicated that the experimental error associated with the determination of permeability coefficients in these systems is higher than for the unmodified hydrogel copolymer systems. Thus, it is difficult to distinguish between the effects that Cl^-, $Br^-$and NO_3^- impart on potassium ion transport through crown ether modified membranes. However, the results in Table 3.7 show several similarities with those obtained for the unmodified membrane (Section 3.2.3) in that permeation appears to be greater when a structure breaking counter anion such as SCN^- is present and that the ion permeation in both systems is effectively zero with the water structure making anion SO_4^{2-}. In addition, if the values quoted for ion permeation in the unmodified membrane are compared with those obtained for permeation in the final steady state in the modified

membrane (Table 3.3 and 3.7) it is obvious that ion permeation is suppressed in the crown modified membranes. The values for the effective reduction in permeation in the final state are given in Table 3.8.

Table 3.8 Effective reduction in the permeability coefficient for the transport of potassium across a dicyclohexano-18-crown-6 modified membrane

Anion	Effective reduction in P_2 (%)
SCN^-	6
NO_3^-	44
Br^-	36
Cl^-	38

The values in Table 3.8 reflect the earlier observation and imply that K^+ ion transport in the final state is relatively unaffected by the presence of the crown ether when a highly soluble counter anion is present. Additionally, there is little distinction between the effect of Cl^-, Br^- and NO_3^- on ion permeation in the final state.

Previously, it has been postulated that the induction period might result from the gradual filling of ionophore sites[39]. A simple calculation may be used to determine the concentration of salt in the membrane at the 'lag-time' and this may be used to estimate the ratio of salt to crown ether at this point. The same ratio of 2:5 is observed for Cl^-, Br^- and NO_3^- taking into account the errors involved in this calculation. Since this ratio implies that each cation interacts with two crown ether molecules, this result suggests that the initial 'lag-time' might arise from partioning between the crown ether and the metal cations and that after the initial induction period cations participate in a site-hopping mechanism.

3.3.3 Occlusion of Other Crown Ethers in Hydrogel Membranes

The studies described in the preceding Sections illustrated that the presence of an occluded crown ether will influence the transport properties and in particular will inhibit the transport of the ion to which it selectively chelates. Thus, attempts were made to occlude two further crown ethers within a hydrogel membrane of composition HEMA:EGDM (90:10). This copolymer composition was used to facilitate comparisons with previous studies. The crown ethers benzo-15-crown-5 and dibenzo-18-crown-6 were chosen since these crowns were both available and are relatively inexpensive. However, dibenzo-18-crown-6 is insoluble in both monomers and hence could not be evenly dispersed within the hydrogel membrane. Attempts to occlude benzo-15-crown-5, a sodium selective crown ether, proved more successful and clear, homogeneous membranes were prepared. A loading of 5% by weight of this crown was used so that comparisons could be made with the work described in the preceding section.

Membranes were prepared and allowed to hydrate overnight before being used. The permeation of 0.25 M NaCl through this membrane was studied. The primary ion transport data is illustrated in Figure 3.7. This data appears to indicate that with this membrane system the 'lag-time' or induction period is no longer present. The permeability coefficient has been calculated and a value of 2.8×10^{-8} $cm^2 s^{-1}$ was obtained. Since a value of 2.7×10^{-8} $cm^2 s^{-1}$ was obtained for the unmodified system this result indicates that the majority of the ionophore might have leached from the membrane during hydration.

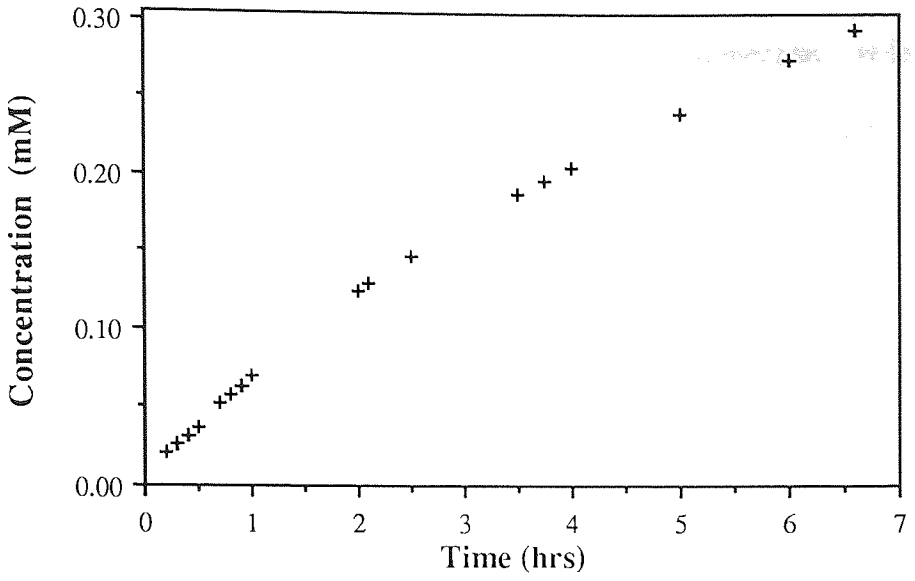

Figure 3.7 Transport of sodium chloride across a benzo-15-crown-5 modified membrane

In order to confirm this theory attempts were made to determine the rate of loss of crown ether from the membrane. At first, since neither of the unreacted monomers absorb at the same wavelength as the crown ether, efforts were made to monitor the loss of crown ether using UV spectroscopy. Unfortunately, this method proved to be inaccurate as the concentration of crown ether determined was dependent upon whether the sample of leaching water was removed from the bulk of the solution or from nearer the membrane surface. These results implied that the crown ether leaches from the membrane fairly quickly but tends to remain close to the polymer surface and does not diffuse into the bulk of the solution. A weight loss study as described in Section 2.9.3 was therefore used. The average weight loss from two samples was determined for both the modified and unmodified membranes and these values are illustrated in Figure 3.8. Although, there is an error of approximately ±1% in these results it would appear that the average weight loss from the unmodified membrane is lower from the membrane containing the crown

ether. In addition, these results indicate that after three hours soaking the majority of the crown ether, benzo-15-crown-5, has leached from the membrane. It is, therefore, reasonable to conclude that the primary transport data illustrated in Figure 3.7 is in fact that of the unmodified membrane since the ionophore would have leached from the membrane during the overnight soak.

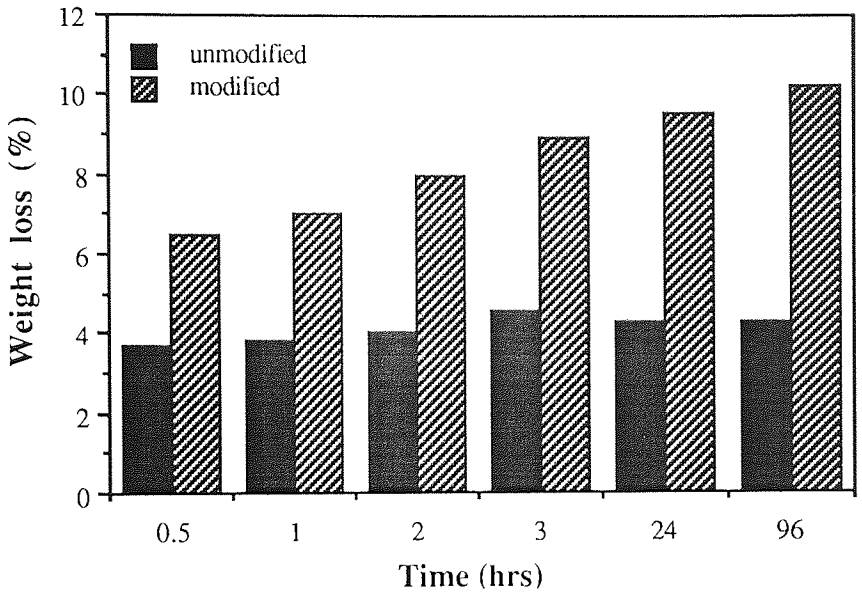

Figure 3.8 Average weight loss from unmodified and benzo-15-crown-5 modified membranes

3.4 Conclusions

The transport properties of the unmodified membrane HEMA:EGDM (90:10) have been reported and discussed in this Chapter. The results indicated group I and II metal cation transport through this membrane generally decreased as the hydrated ionic radii of the cation increased and that any deviations which arise are attributable to the presence of a high proportion of crosslinking agent. Additionally, the results illustrated that group II cation permeation through this membrane is significantly lower than that of group I metal cations. The mixed cation permeation study confirmed that for the transport of a mixed

solution of 0.25 M KCl and 0.25M $CaCl_2$, the permeation of Ca^{2+} ions was effectively blocked or screened by this membrane. These studies have highlighted the potential of hydrogel copolymers for use in the design of permselective membranes for group I metal cations.

The transport studies of the DCH-18-C-6 modified membrane, have illustrated that the presence of an ionophore will affect the transport properties of the material. However, this study suggests that the transport properties of this system might be more susceptible to slight variations in membrane composition than the unmodified system. The effect of the counter anion variation on the rate of K^+ ion transport was also studied. The results indicated that the induction period or 'lag-time' might be caused by an ionophore filling mechanism and that once approximately half the sites are occupied ions may be transported via a site-hopping mechanism.

Finally, this study has also illustrated the range of crown ethers which may be occluded within these membranes is limited by ionophore loss during hydration. Thus, in order to extend this study it is important to consider the physical immobilisation of these species within a hydrogel matrix.

CHAPTER 4

Synthesis and Preliminary Transport Studies of Monomeric Crown Ethers

4.1 Introduction

It was shown in the previous Chapter that the inclusion of crown ethers within a hydrogel matrix will affect the transport properties of the material, but it was apparent that these systems are limited by ionophore loss during hydration. It was decided, therefore, that compositions in which the crown ether was physically immobilised within the hydrogel should be studied.

Initially, two crown ethers, benzo-15-crown-5 and dibenzo-18-crown-6 were chosen. These crown ethers bind selectively to sodium and potassium ions respectively. Two factors determined this choice, firstly the relative cheapness and ready availability of these materials and secondly, these ionophores could be modified easily and attached to a hydrophilic polymer. Several routes to the synthesis of either acrylate or methacrylate monomers were considered and potential routes to the acrylate monomer are shown in Figs 4.1 to 4.5. Once synthesised it was intended that these monomers could be polymerised with HEMA via a free radical polymerisation. It was hoped that the reactivity ratios of these monomers might be similar to those of HEMA and EGDM so that a uniform distribution of the crown ether within the hydrogel matrix would be obtained. Furthermore, polymers obtained from these benzo-15-crown-5 and dibenzo-18-crown-6 derivatives would give an insight into differences between the properties of pendant and backbone chelating groups. In the following Sections the results obtained from the synthetic work and from the studies of the transport properties of these materials will be considered.

4.2 Synthesis of Crown Monomers

Several routes were investigated to obtain a suitable derivative which could be polymerised with HEMA. Of these the route via the nitro derivative of benzo-15-crown-5

was the most successful and this will be discussed below. The following synthetic route to 4'acryloylaminobenzo-15-crown-5 was followed (Figure 4.1);

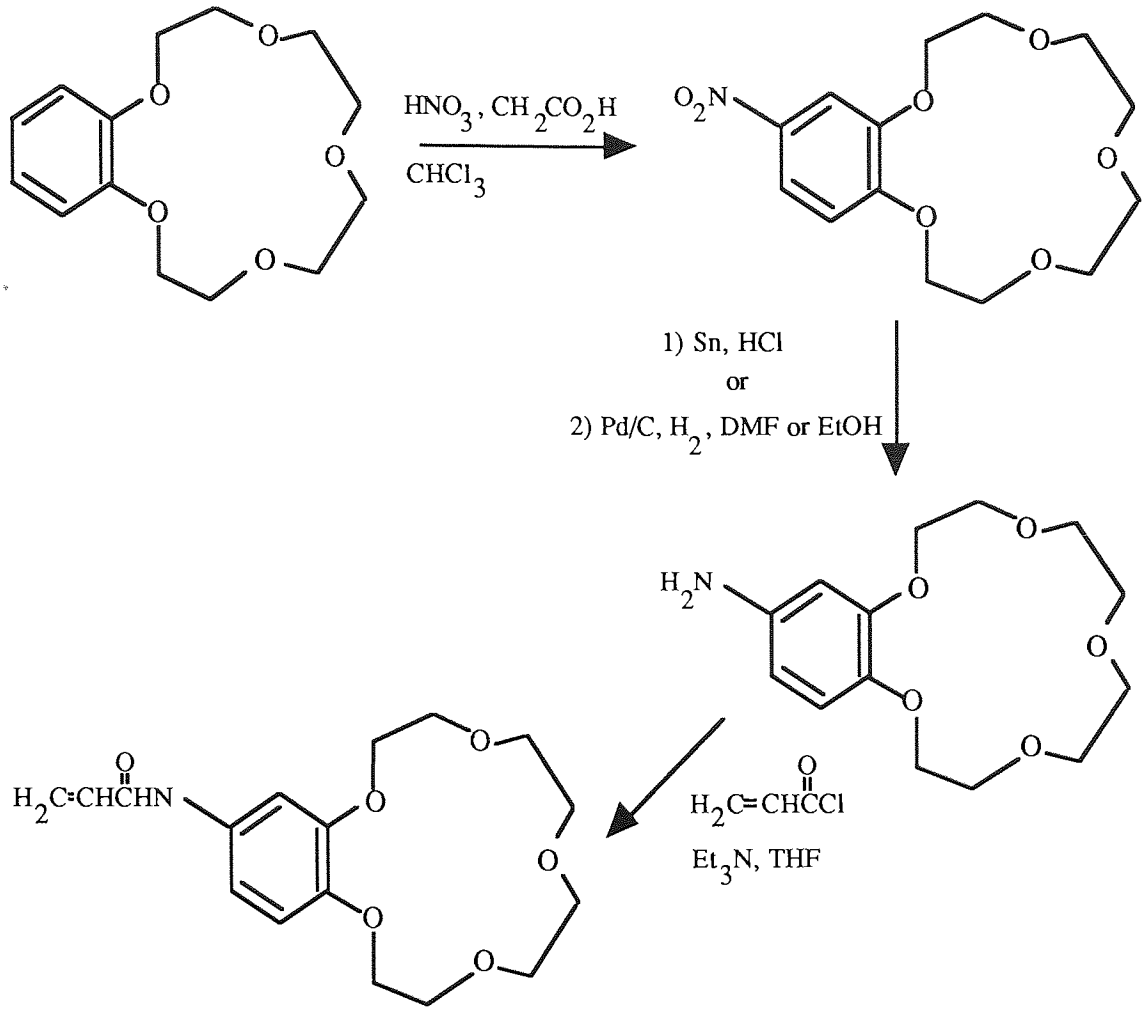

Figure 4.1 The synthesis of 4-acryloylaminobenzo-15-crown-5

The first stage in this reaction involves the aromatic nitration of benzo-15-crown-5. Although the IR and NMR spectra (Figures 1-3, Appendix 2) and the elemental analysis indicated that a pure product had been obtained, the melting point and aromatic proton splitting were initially thought to be anomalous.

Ungaro *et al* [160] reported a melting point of 84-85 ^{o}C for 4-nitrobenzo-15-crown-5, whereas the product obtained in this reaction had a melting point of 95-96 ^{o}C. However,

it would appear that these workers had obtained an impure sample of this material since the melting point obtained in these studies is consistent with the value quoted and observed for a sample of this compound supplied by Aldrich. The ^{1}H NMR contained two pairs of doublets in the aromatic region when a singlet and a doublet had been expected. A two dimensional COSY (correlation spectroscopy) NMR was obtained to resolve this splitting (Figure 4, Appendix 2). This spectrum and some decoupling experiments illustrated clearly that the product was substituted in the 4 position and that the splitting could be accounted for by long range coupling via the nitro group.

Tin and hydrochloric acid were initially used for the reduction, but it was apparent that the reduced product was impure and had been obtained in a low experimental yield. Catalytic hydrogenation was much more successful and a pure product was obtained using ethanol as the solvent. Previous workers had suggested that DMF (dimethyl formamide) was a suitable solvent for this reduction[114]. However, in these studies it was found that DMF was difficult to remove at the end of the reaction and hence contaminates the product.

The final stage in this synthesis involves a nucleophilic substitution to form a vinyl amide. The first attempts at this reaction produced products of varying purity. Initially, the purity of the monomer was not considered to be a critical factor, since it was hoped that any impurities present would leach out of the membrane whilst the polymer hydrated. Hence, hydrogels were prepared from samples which appeared from IR data to contain some monomer. However, the major contaminant in all cases was later found to be acrylic acid, obtained as acryloyl chloride hydrolyses, which will affect the properties of the polymer. It was necessary, therefore, to obtain the monomer in a pure form, this was achieved by carrying out the reaction under anhydrous conditions.

Other routes were investigated in an attempt to obtain other derivatives which could be copolymerised with HEMA. However, in each case rather surprisingly it was in the initial stages of the synthesis that problems arose. Some of these problems are discussed below.

The following synthetic scheme was considered for the synthesis of 4-acryloylacetylbenzo-15-crown-5 (Figure 4.2);

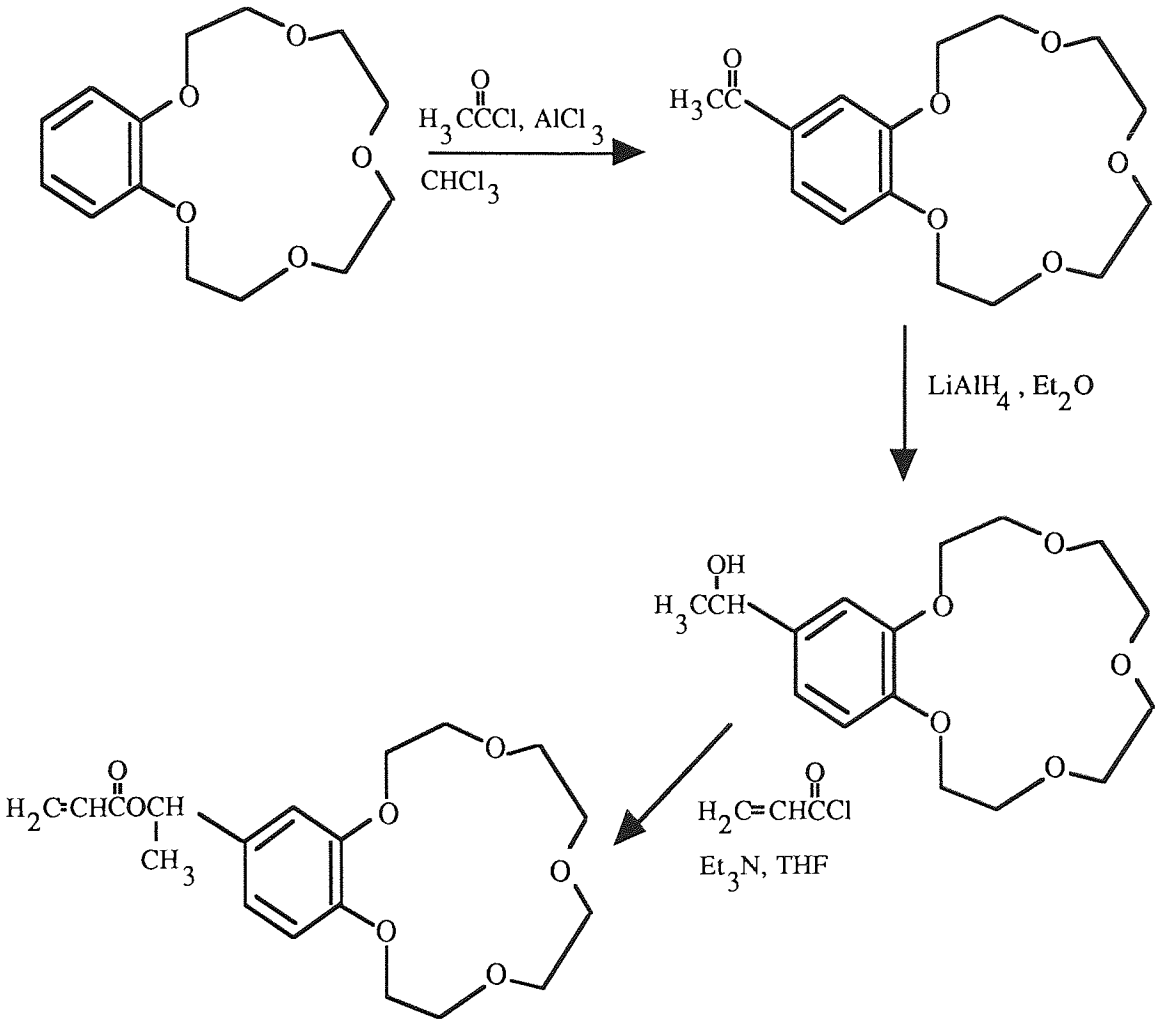

Figure 4.2 The synthesis of 4-acryloylacetylbenzo-15-crown-5

The first stage of this reaction involved the Friedel Crafts acylation of benzo-15-crown-5. Several attempts were made to prepare 4-acetylbenzo-15-crown-5, however, it was

apparent from both the spectra and the melting point data that each of the products still contained a significant amount of the starting material. Since it appeared difficult to obtain a pure product from this method a reaction scheme which would ultimately lead to the formation of a more reactive primary alcohol was considered. This scheme is illustrated in Figure 4.3;

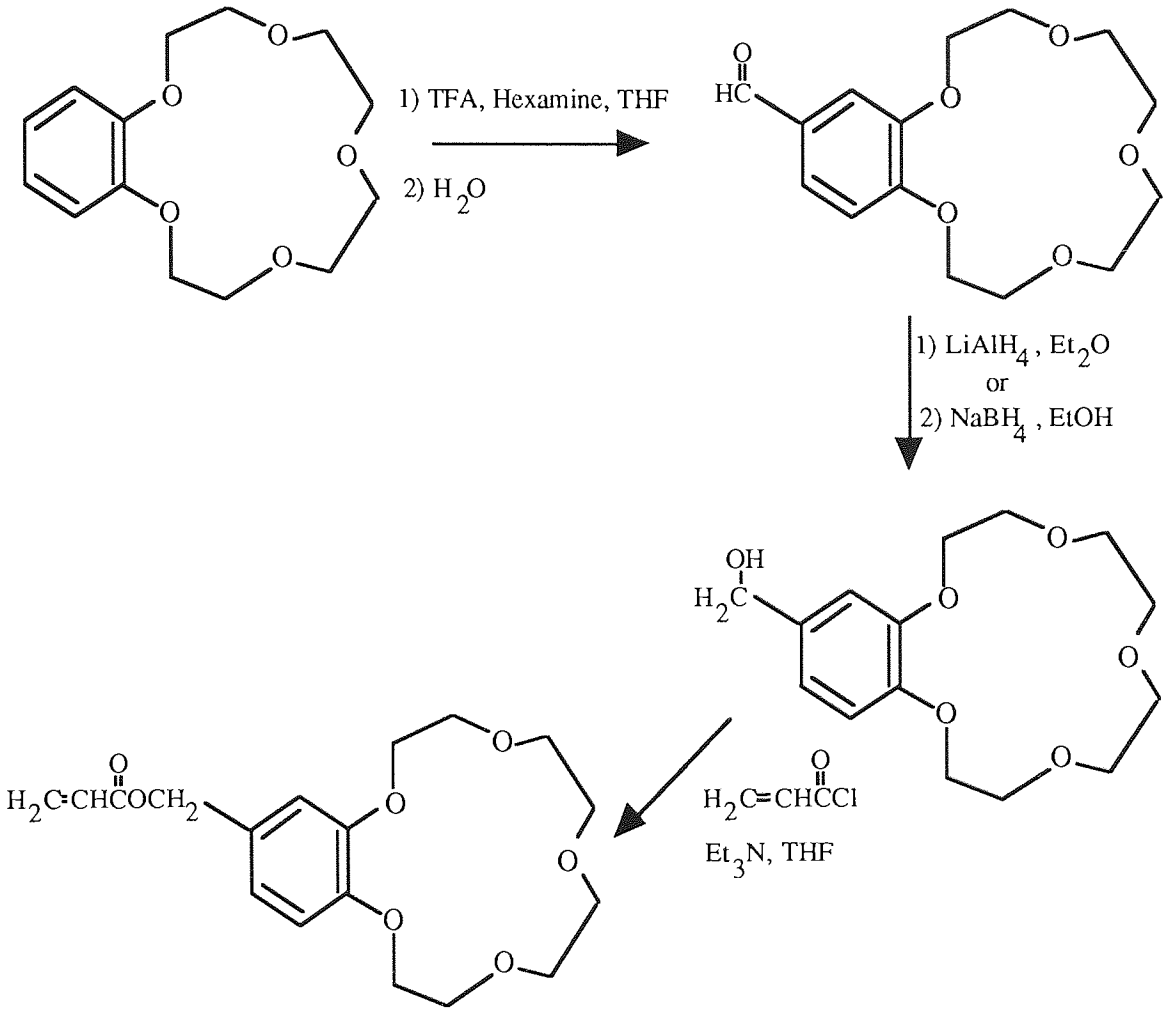

Figure 4.3 The synthesis of 4-acryloylmethylbenzo-15-crown-5

The formylation of benzo-15-crown-5 was attempted using a method reported by Wada and coworkers[161]. However, the initial attempts produced impure products in low yields which were contaminated with the starting material, benzo-15-crown-5 (Figure 5,

Appendix 2). It was found that purer products could be obtained if the reaction time was extended from 12 to 36 hours and if a greater excess of trifluoroacetic acid, TFA, was used. Attempts were made to synthesis both the hydroxyl and acryloyl derivatives but at no time was a pure product obtained.

Dibenzo-18-crown-6 was used in attempts to prepare suitable derivatives which could be polymerised as part of a poly HEMA backbone. Initially, attempts were made to synthesise 4,4'-diacryloyldiaminobenzo-18-crown-6 using the route outlined below in Figure 4.4.

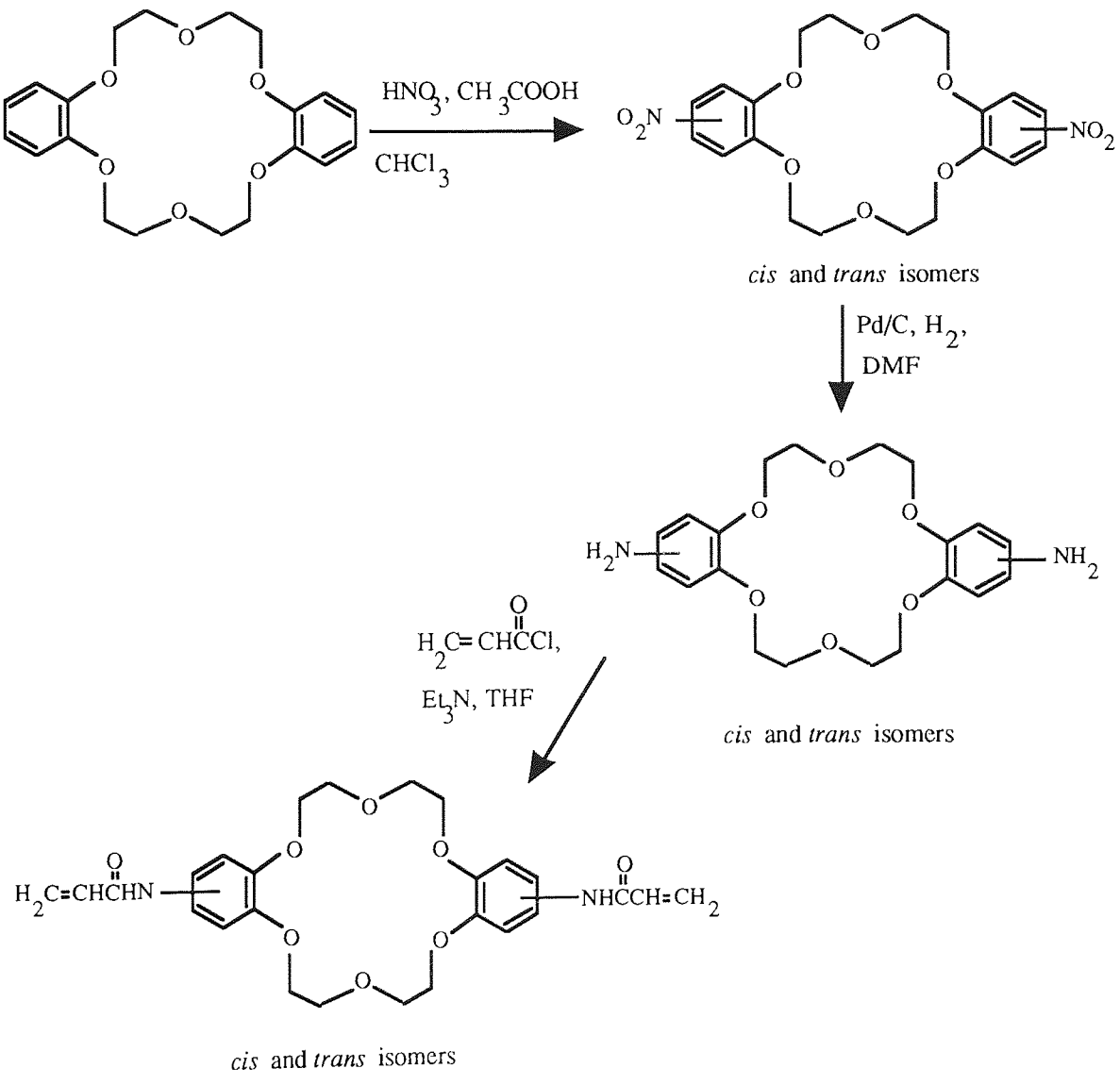

Figure 4.4 The synthesis of 4,4'-diacryloylaminodibenzo-18-crown-6

The preparation and separation of the *cis* and *trans* isomers of 4,4'-dinitrodibenzo-18-crown-6 was carried out using the method outlined by Feigenbaum and Michel[114]. The spectral data obtained for the two isomers illustrated that although the *trans* isomer had been obtained in a pure form the *cis* isomer was contaminated with the starting material dibenzo-18-crown-6. The subsequent catalytic reduction of the *trans* isomer, however, proved unsuccessful. Although there was insufficient time to investigate this reaction it is likely that both the yield and purity of the products might be improved if ethanol is used in place of DMF, as with the reduction of 4-nitrobenzo-15-crown-5.

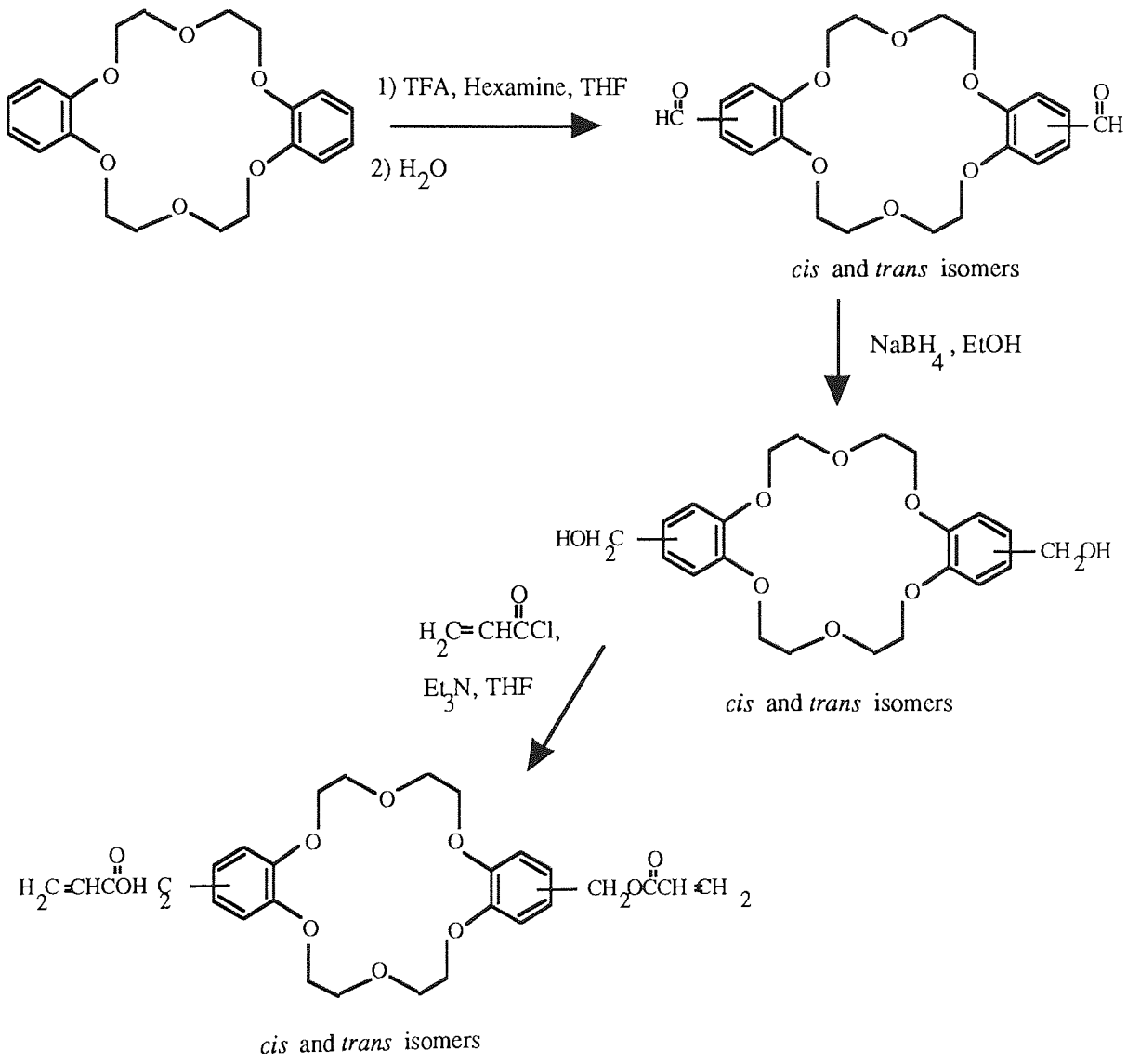

Figure 4.5 The synthesis of 4,4'-diacryloylmethyldibenzo-18-crown-6

An alternative route to a divinyl derivative was considered and is illustrated in Figure 4.5. The initial stage in this reaction scheme involves the bis formylation of dibenzo-18-crown-6. Several attempts were made to synthesise this derivative, however, although the IR spectra illustrated the presence of a small carbonyl peak, both the melting points and NMR data confirmed that the product had not been obtained and that the starting material had been recovered. Hence, the syntheses of both the bis hydroxy and the bis formyl derivatives were unsuccessful. It is likely, however, that the yield and purity of the bis formyl derivative could be improved if the same reaction conditions described for the synthesis of 4-formyl derivative were followed.

4.3 Summary of Monomer Synthesis

The results discussed in the preceding section illustrate some of the difficulties encountered during the synthesis of the monomers illustrated in Figures 4.1 to 4.5. After extensive preliminary investigations efforts were concentrated on the synthesis of 4-acryloylaminobenzo-15-crown-5. This was in part due to the fact that this synthesis appeared to be the most facile, but also resulted from the limited finance available for developing the other syntheses. The results described in the following Section were obtained from a range of 4-acryloylaminobenzo-15-crown-5 modified hydrophilic copolymers.

4.4 Hydrogels Containing 4'-acryloylaminobenzo-15-crown-5

Initially, membranes were prepared by adding the monomer to a mixture of HEMA and crosslinker EGDM, 90:10 (wt/wt). This composition was chosen to allow comparisons with the earlier work on occluded crown systems. Different batches of the monomer were used to prepare membranes with crown loadings of 2.5 and 5 %. The effect of this comonomer on the EWC's of the membranes was determined and the results are

illustrated in Table 4.1.

Table 4.1 The effect of bound crown on the EWC of HEMA:EGDM (90:10)

Polymer Composition	EWC (%)
HEMA:EGDM (90:10)	26.8 ± 0.5
HEMA:EGDM (90:10) + 2.5% 4-acrylolyaminobenzo-15-crown-5	27.4 ± 0.5
HEMA:EGDM (90:10) + 5% 4-acrylolyaminobenzo-15-crown-5	25.4 ± 0.5

Initially, this variation in EWC was explained by a competitive contribution between the 'chain stiffening' effect and the hydrophilicity of the monomer. However, with hindsight this effect is most likely attributable to the differences in purity between batches of the monomer. Higher concentrations of the acrylic acid impurity would enhance EWC. Thus, it would appear in retrospect that the terpolymer prepared with a 2.5% loading of the monomer contains a higher concentration of acrylic acid. This was confirmed by the IR spectrum of this monomer (Figure 6. Appendix 2) where the carbonyl stretch at $1732cm^{-1}$ is attributable to acrylic acid.

After studying EWC the transport properties of these membranes were examined. The transport of sodium across the membrane containing a 2.5% loading of the monomer was studied (Figure 4.6). The results suggest that when a crown is immobilised within a hydrogel matrix the 'lag-time' or induction period shown by the occluded system is no longer present. The permeability coefficient was calculated from the primary ion transport data and a value of $3.8x10^{-8}cm^2s^{-1}$ was obtained. Since the value for the unmodified membrane is $2.7x10^{-8}cm^2s^{-1}$, it would appear that sodium ion transport across this

crown modified membrane is enhanced. This result, however, may in part be explained by the higher water content of this membrane. Since the monomer used to prepare this membrane was impure this result illustrated that the purity of the crown monomer is a critical factor. It was, therefore, felt that a pure sample of the monomer had to be obtained before any further conclusions could be drawn from this study.

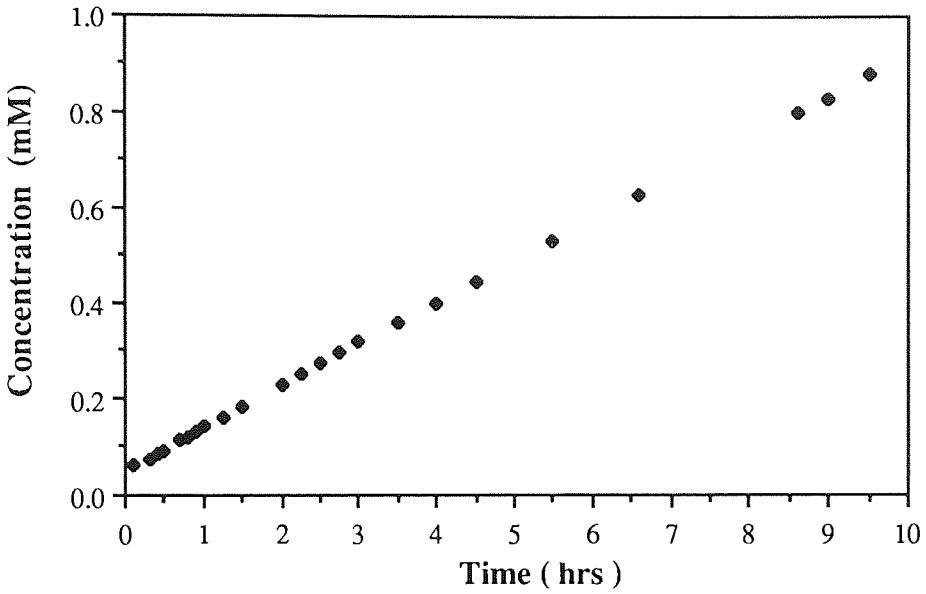

Figure 4.6 Transport of NaCl across HEMA:EGDM (90:10) modified with 2.5% 4-acryloylaminobenzo-15-crown-5

Further membranes were prepared from a pure sample of the crown monomer. Again the monomer was added to a mixture of HEMA:EGDM (90:10) to allow comparisons with earlier studies. Monomer loadings of 1 and 5% (wt/wt) were used. Sufficient crown monomer had been synthesised to extend this range, however, as the sample proved to be relatively insoluble in the comonomer mixture the range of compositions available for study was restricted. The effect the addition of this pure crown monomer to comonomer mix has on the EWC of the polymer was determined. The results obtained are given in Table 4.2 and indicate that at these loadings the addition of crown monomer has little effect on EWC.

Table 4.2 The effect of 4-acryloylaminobenzo-15-crown-5 on the EWC of HEMA:EGDM (90:10)

Polymer Composition	EWC (%)
HEMA:EGDM (90:10)	26.8 ± 0.5
HEMA:EGDM (90:10) + 1% 4-acryloylaminobenzo-15-crown-5	26.5 ± 0.5
HEMA:EGDM (90:10) + 5% 4-acryloylaminobenzo-15-crown-5	26.0 ± 0.5

The effect of sodium chloride solution on EWC has also been studied and the results are shown in Table 4.3. It is interesting to note that a 1% loading of crown monomer gives rise to a slightly greater suppression in EWC in the presence of sodium chloride. However, when a 5% loading of the pure monomer is added to the comonomer mix, there is effectively no change in EWC of the resultant membrane in the presence of sodium chloride. One possible explanation for this result is that at higher loadings the sodium ions interact preferentially with the crown hence reducing the effective water rejection observed in other hydrogel systems.

Table 4.3 The effect of 0.25M NaCl on the EWC of HEMA:EGDM (90:10)

Polymer Composition	EWC (%)
HEMA:EGDM (90:10)	25.3 ± 0.5
HEMA:EGDM (90:10) + 1% 4-acryloylaminobenzo-15-crown-5	24.5 ± 0.5
HEMA:EGDM (90:10) + 5% 4-acryloylaminobenzo-15-crown-5	25.9 ± 0.5

The transport of sodium chloride across a membrane with a 5% loading of the crown monomer was also studied (Figure 4.7)

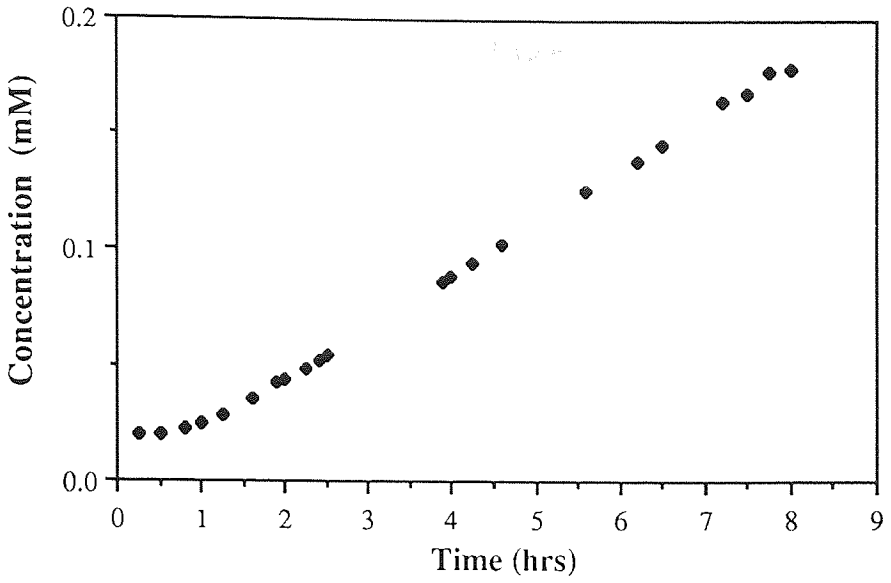

Figure 4.7 Transport of NaCl across HEMA:EGDM (90:10) modified with 5% 4-acryloylaminobenzo-15-crown-5

Figure 4.7 illustrates that for the transport of 0.25m NaCl across this membrane there appears to be a short induction or 'lag-time' period which is followed by a steady increase in sodium ion concentration. The permeability coefficient was calculated once the final steady state had been reached. A value of $1.7 \times 10^{-8} cm^2 s^{-1}$ was obtained . The value for sodium chloride transport through the unmodified membrane is $2.7 \times 10^{-8} cm^2 s^{-1}$, which suggests that in the final steady state sodium ion permeation through the modified membrane is inhibited. The initial 'lag-time' could arise from the gradual filling up of ionophore sites, implying that sodium ion transport is inhibited until these sites are occupied. However, since this 'lag-time' is less than 1 hour it might simply be attributable to the system reaching equilibrium. If this site filling hypothesis is correct then a reduction in the initial concentration of sodium chloride should give rise to an extended 'lag-time'. The subsequent steady state shows reduced ion permeation when compared with the unmodified membrane and since this result cannot be accounted for on

the basis of EWC it suggests that the presence of an immobilised crown ether has a significant effect on the transport of sodium chloride.

4.4 Conclusions

Although several problems were encountered with the synthesis of the monomers a pure sample of 4-acryloylaminobenzo-15-crown-5 was obtained. The studies to date on the bound crown systems have produced some interesting results and such systems appear to show some similarities in their transport properties with the unbound systems discussed in Chapter 3.

The problems encountered with the synthesis mainly arose from attempting these reactions on a relatively small scale, which in turn led to the associated problems observed in purifying these products in sufficient quantities of be use in further reactions. The preliminary transport studies highlighted some of the problems associated with using impure monomers in these studies. The initial results for the transport of NaCl across a hydrogel membrane containing a pure sample of 4-acryloylaminobenzo-15-crown-5, show that the crown ether significantly inhibits ion transport in the final steady state.

CHAPTER 5

Characterisation of 2-hydroxyethyl methacrylate Copolymers Containing Linear Polyethers

5.1 Introduction

Linear polyethers have been shown to be relatively inert toward biological species[11]. Additionally, diglyme and other poly(ethylene oxides) can form complexes with metal cations. Thus, it was hoped that the inclusion of monomeric linear polyethers within vinylic based hydrogel membranes might enhance their biocompatibility and influence their permselectivity. This Chapter is, therefore, primarily concerned with the use of linear polyethers in the synthesis of methacrylate based hydrogels. However, since these are novel hydrogel systems a detailed study of the effects of polyethers on some of the fundamental properties of vinylic hydrogels is of primary importance and will also be discussed in this Chapter.

A range of methacrylate based poly(ethylene oxide) monomers was initially chosen which could be copolymerised with other acrylate or methacrylate monomers, such as HEMA, via a free radical polymerisation. Their inclusion within a hydrogel matrix should yield some information about the effect of variations in the structure of the polyether side chain on the properties of hydrogel polymers. For example, these monomers would not only illustrate the effect of increasing polyether chain length on the properties of the polymer, but should also facilitate comparisons between the effects of hydroxyl and methoxy terminated poly(ethylene oxide) chains on the polymer's properties. Finally, hexapropoxylated hydroxypropylmethacrylate, HPHPMA, was chosen to illustrate the effect of the addition of a methyl substituent on the polyether chain on the properties of these materials.

The monomers used in this study are illustrated overleaf in Figure 5.1.

methoxy polyethylene glycol methacrylate (MPEG MA)

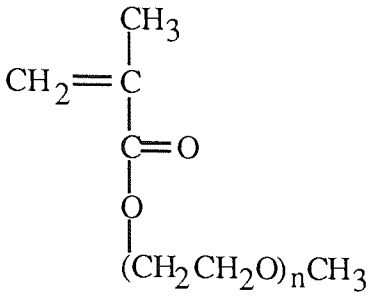

n=4 to 5 MPEG 200 MA
n=9 to 10 MPEG 400 MA
n=12 to 13 MPEG 550 MA
n=22 to 23 MPEG 1000 MA

ethoxylated hydroxyethyl methacrylate (HEMA 4,5 EO) and
polyethylene glycol monomethacrylate 10 moles EO (PEG MA 10 EO)

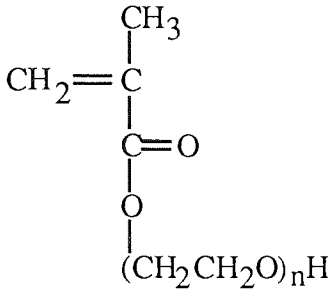

n=5 to 6 HEMA 4,5 EO

n=10 PEGMA 10 EO

hexapropoxylated hydroxypropyl methacrylate (HPHPMA)

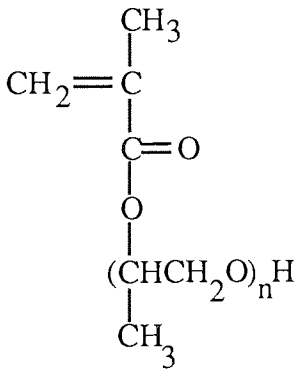

n = 7 HPHPMA

Figure 5.1 Structures of poly(ethylene oxide) monomers used in this work

5.2 Assessment of the Purity of Linear Polyether Monomers

The monomers illustrated in Figure 5.1 were used as supplied. However, gel permeation chromatograms, GPC's, were obtained for all of these monomers to provide some indication of the molecular weight distribution and purity of these monomers. The GPC traces for these monomers are illustrated in Appendix 3, Figures 1 to 4. The chromatograms illustrate that the molecular weight distributions are fairly narrow for the monomethoxy polyethylene glycol methacrylate derivatives of molecular weights 200, 400 and 550 (Figure 1, Appendix 3). However, the trace for the sample of molecular weight 1000 appears to indicate that lower molecular weight species may be present. The traces for both HEMA 4,5 EO, PEGMA 10 EO and HPHPMA (Figures 2, 3, and 4 respectively, Appendix 3) are slightly broader than those obtained for the monomethoxy polyethylene glycol methacrylate monomers which suggests that these polymers contain material with a broader range of molecular weights.

5.3 Effect of Linear Polyethers on EWC

This section deals with the results obtained from a systematic study of the effects of each of the monomers illustrated in Figure 5.1 on the EWC of HEMA based hydrogel membranes. A broad range of hydrogels were prepared which were based on HEMA containing either 1 or 10 % crosslinking agent, ethylene glycol dimethacrylate (EGDM). The compositions based on HEMA are referred to as HEMA:EGDM (99:1) and HEMA:EGDM (90:10) respectively for convenience. In addition, a few hydrogels based on HEMA:EGDM (95:5) were also studied. The effects of linear polyether monomers on the EWC of these copolymers will be discussed.

5.3.1 Effect of Polyethers on the EWC HEMA:EGDM (99:1)

A range of copolymers were prepared by adding 5 to 20% by weight, of each of the

monomers illustrated in Figure 5.1, to HEMA:EGDM (99:1) before copolymerising the mixture as described previously. The EWC's of these membranes were determined and the values are given in Table 5.1.

Table 5.1 The effect of polyether content on the EWC of HEMA:EGDM (99:1)

Membrane Composition	EWC (%)
HEMA:EGDM (99:1)	36.9
HEMA:EGDM (99:1) + 5% MPEG 200 MA	37.6
HEMA:EGDM (99:1) + 10% MPEG 200 MA	38.8
HEMA:EGDM (99:1) + 15% MPEG 200 MA	41.1
HEMA:EGDM (99:1) + 20% MPEG 200 MA	43.0
HEMA:EGDM (99:1) + 5% MPEG 400 MA	39.0
HEMA:EGDM (99:1) + 10% MPEG 400 MA	40.6
HEMA:EGDM (99:1) + 15% MPEG 400 MA	42.6
HEMA:EGDM (99:1) + 20% MPEG 400 MA	46.4
HEMA:EGDM (99:1) +5% MPEG 550 MA	40.6
HEMA:EGDM (99:1) +10% MPEG 550 MA	42.7
HEMA:EGDM (99:1) +15% MPEG 550 MA	45.8
HEMA:EGDM (99:1) +20% MPEG 550 MA	48.5
HEMA:EGDM (99:1) +5% MPEG 1000 MA	41.0
HEMA:EGDM (99:1) +10% MPEG 1000 MA	44.4
HEMA:EGDM (99:1) +15% MPEG 1000 MA	48.5
HEMA:EGDM (99:1) +20% MPEG 1000 MA	49.4
HEMA:EGDM (99:1) +5% HEMA 4,5 EO	37.7
HEMA:EGDM (99:1) +10% HEMA 4,5 EO	39.9
HEMA:EGDM (99:1) +15% HEMA 4,5 EO	40.6
HEMA:EGDM (99:1) +20% HEMA 4,5 EO	41.4
HEMA:EGDM (99:1) + 5% PEGMA 10 EO	38.4
HEMA:EGDM (99:1) + 10% PEGMA 10 EO	39.6
HEMA:EGDM (99:1) + 15% PEGMA 10 EO	41.0
HEMA:EGDM (99:1) + 20% PEGMA 10 EO	42.1

The results presented in Table 5.1 will be discussed in terms of the effect of both polyether chain length and polyether content on the EWC of these membranes. Finally, the effect variations in polyether structure impart on the EWCs of these membranes will also be discussed.

Methoxy polyethylene glycol methacrylates of molecular weights 200, 400, 550 and 1000 were chosen to illustrate the effect of increasing polyether chain length on the EWC of a series of terpolymers based on HEMA:EGDM (99:1). These monomers are referred to by the acronyms MPEG 200 MA, MPEG 400 MA, MPEG 550 MA and MPEG 1000 MA for convenience and contain 4 to 5, 9 to 10, 12 to 13 and 22 to 23 repeating CH_2CH_2O units respectively. The EWCs of copolymers have been presented in Table 5.1 but are plotted in Figure 5.2 to illustrate this effect more clearly.

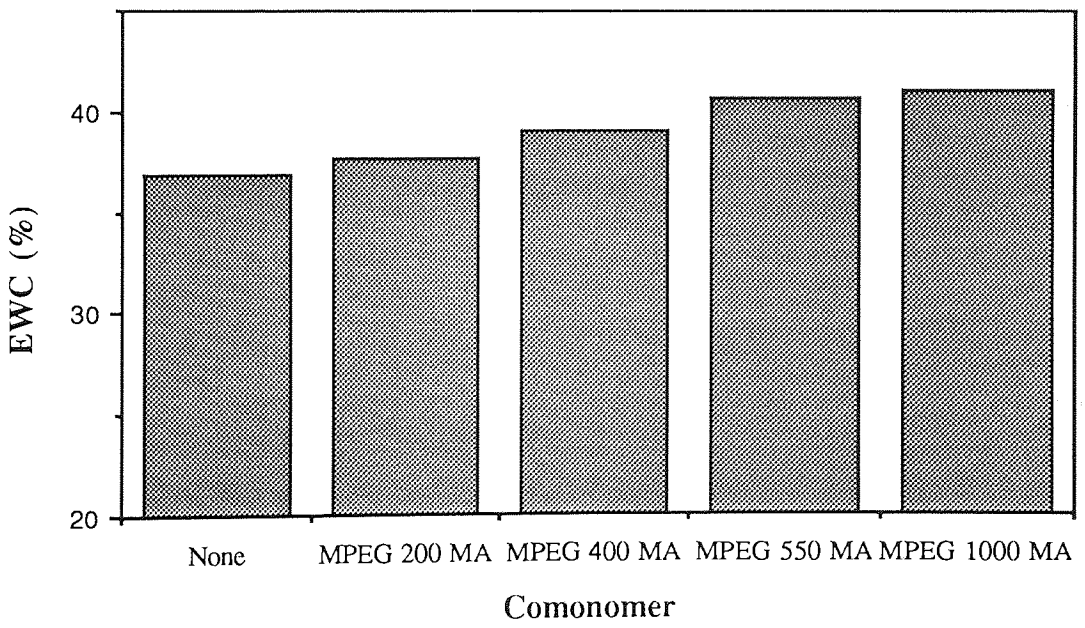

Figure 5.2 **Effect of polyether chain length on the EWC of HEMA:EGDM (99:1)**

Figure 5.2 illustrates that the HEMA terpolymers containing poly(ethylene oxide) have a higher EWC than the unmodified polymer HEMA:EGDM (99:1) and that this effect is more pronounced as the poly(ethylene oxide) chain length increases. This result might have been predicted since the CH_2CH_2O repeat unit is hydrophilic and can interact with water to form a range of hydrates[10,41,46,52,55]. Hence, increases in the number of polyether repeat units would be expected to enhance both the water binding and the EWC of these membranes.

The results in Table 5.1 also indicate that in all cases increasing the concentration of each poly(ethylene oxide) comonomer enhances the EWC of the membrane. Again such results are not unexpected since increasing the number of polyether groups within the gel would result in an increase in both the number of sites which can interact with water and the EWC of the membrane.

The monomers methoxy polyethylene glycol 200 methacrylate, MPEG 200 MA and ethoxylated hydroxyethyl methacrylate (HEMA 4,5 EO) are structurally similar since they both contain the same number of CH_2CH_2O repeat units. However, in the former case the polyether chain is terminated by a methoxy group whilst in the latter, it is terminated by a hydroxyl group. Similarly, the methoxy terminated methoxy polyethylene glycol 400 methacrylate (MPEG 400 MA) contains the same number of repeating CH_2CH_2O units as the hydroxy terminated polyethylene glycol methacrylate (PEGMA 10 EO). Hence, the EWC's of these two sets of copolymers were compared to illustrate the effects hydroxy and methoxy terminated polyether chains impart on EWC. The values obtained for the EWCs of membranes containing these monomers have been given in Table 5.1, however, these values are plotted in Figures 5.3 and 5.4 so that comparisons may be made more easily.

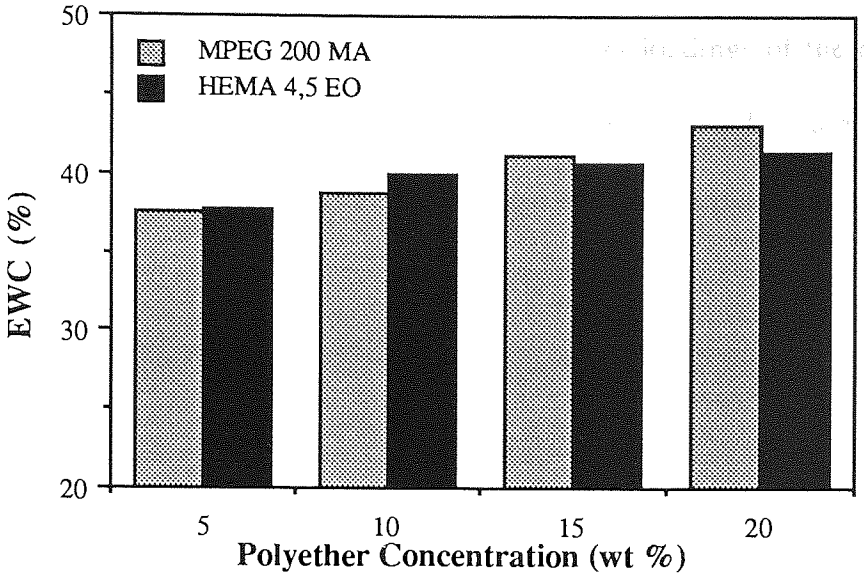

Figure 5.3 Effect of hydroxy vs methoxy end groups on the EWC of terpolymers with 4,5 repeating ether groups in the polyether side chain

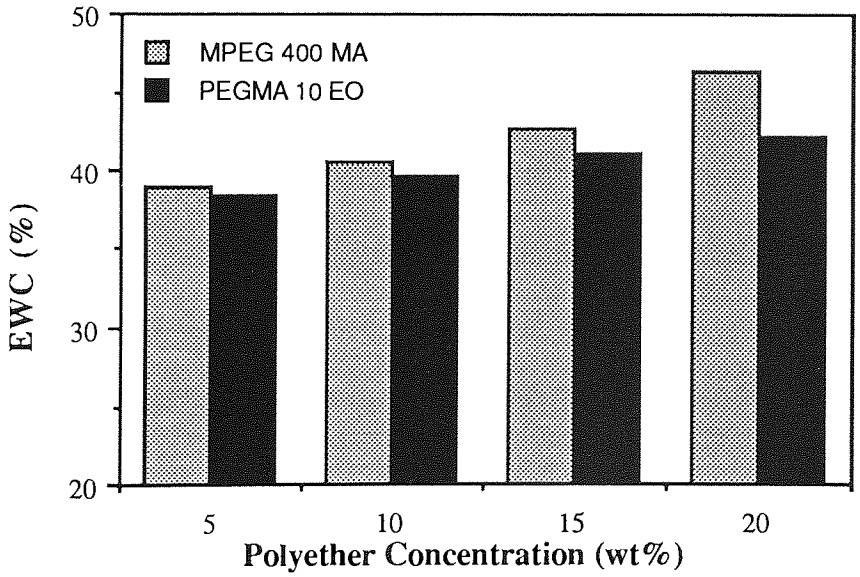

Figure 5.4 Effect of hydroxy vs methoxy end groups on the EWC of terpolymers with 9,10 repeating ether groups in the polyether side chain

When the errors associated with the measurement of EWC(± 0.5%) are taken into consideration there is very little difference in the observed EWCs of membranes containing 4,5 CH_2CH_2O repeat units especially at lower loadings of the monomers. However, when 10 CH_2CH_2O units are present in the polyether side chain, the values obtained for the EWCs of the methoxy derivatives are higher than those observed for the hydroxy derivatives. Initially, this result was suprising since it was anticipated that due to the greater hydrophilicity of the hydroxyl group, membranes containing methoxy terminated polyether chains might have lower EWC values. One possible explanation for the observed result is that the hydroxyl group interacts preferentially with the polyether side chain to form internal hydrogen bonds. Such hydrogen bond formation would result in the formation of a crown ether type structure for the polyether side chain and would restrict the water binding of the terminal hydroxyl group. In addition, this effect might be expected to be more pronounced with the longer ethylene oxide chains since steric factors would then be more favourable for ring formation. Thus, hydrogen bond formation would hence give rise to the observed suppressions in EWC.

Hexapropoxylated hydroxypropylmethacrylate (HPHPMA) (Figure 5.1) was obtained in order to determine the effect of a methyl substituent on the ethylene oxide group on EWC. The values for the EWC are given in Table 5.2 and these values are plotted in Figure 5.5.

Table 5.2 The effect of increasing HPHPMA content on EWC

Membrane Composition	EWC (%)
HEMA:EGDM (99:1) + 5% HPHPMA	37.1
HEMA:EGDM (99:1) + 10% HPHPMA	35.0
HEMA:EGDM (99:1) + 15% HPHPMA	34.2
HEMA:EGDM (99:1) + 20% HPHPMA	33.6

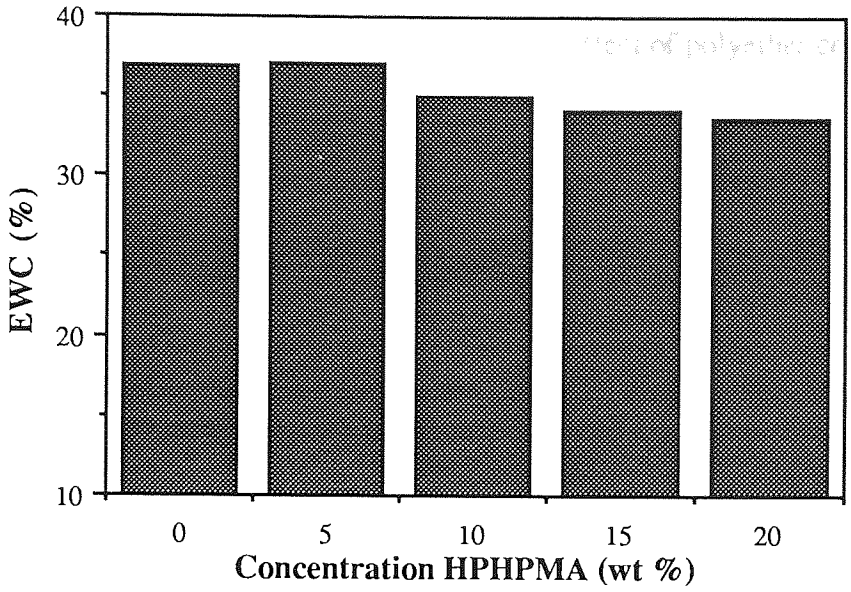

Figure 5.5 Effect of HPHPMA on the EWC of HEMA:EGDM (99:1)

Figure 5.5 clearly illustrates that increasing the concentration of HPHPMA reduces EWC. This result is not entirely unexpected since poly hydroxypropyl methacrylate (HPMA) has an EWC of 21.2%[169] and the introduction of the hydrophobic methyl substituent to the polyethylene oxide chain might be expected to reduce the EWC of the polymer.

5.3.2 The Effect of Polyether on the EWC of HEMA:EGDM (90:10)

In Chapters 3 and 4, 5% (wt/wt) loadings of the cyclic ethers were either occluded or copolymerised in a crosslinked HEMA membrane of composition HEMA:EGDM (90:10). These studies illustrated that the presence of cyclic ethers within a hydrophilic matrix has a significant effect on the transport properties of the polymer. Thus, a range terpolymers with a 5% wt/wt loading of poly (ethylene oxide) was initially prepared so that the effects these linear polyethers impart on the transport properties of the terpolymers could be studied. The EWCs of these terpolymers were also studied. Terpolymers containing 10

to 20% (wt/wt) of MPEG 200 MA, MPEG 400 MA and MPEG 1000 MA monomers were also prepared. Although a smaller range of densely crosslinked copolymers were synthesised, the compositions were chosen to enable the effect of polyether concentration, chain length and structure to be studied.

The effect of polyether chain length was studied using a series of membranes of composition HEMA:EGDM (90:10) with a 5% (wt/wt) loading of MPEG MA monomers. After hydration for three weeks the EWCs were determined and the values obtained are listed in Table 5.3 and are plotted on Figure 5.6

Table 5.3 Effect of polyether chain length on the EWC of HEMA:EGDM (90:10)

Membrane Composition	EWC (%)
HEMA:EGDM (90:10)	26.8
HEMA:EGDM (90:10) + 5% MPEG 200 MA	26.7
HEMA:EGDM (90:10) + 5% MPEG 400 MA	27.2
HEMA:EGDM (90:10) + 5% MPEG 550 MA	28.0
HEMA:EGDM (90:10) +5% MPEG 1000 MA	28.5

The results in Table 5.3 indicate that increases in the polyether chain length give rise to the expected increases in EWC. However, Figure 5.6 illustrates that this effect is less pronounced than for the HEMA:EGDM (99:1) series. Furthermore, in the HEMA:EGDM (90:10) series a 5% loading of MPEG 200 MA appears to have no effect on the EWC of the unmodified membrane and the addition of a 5% loading of MPEG 400 MA causes only a slight increase in the EWC of the membrane. These results suggest that at this loading the enhanced water structuring capabilities of the polyether chains make little contribution to the overall EWC of the terpolymer.

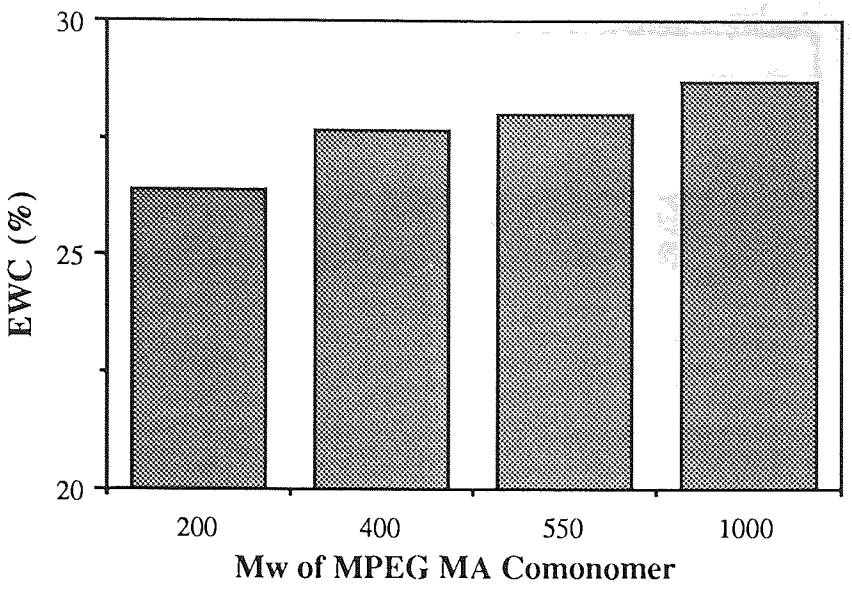

Figure 5.6 Effect of polyether chain length on the EWC of HEMA:EGDM (90:10)

Table 5.4 and Figure 5.7 give the values for the EWCs of terpolymers containing higher concentrations of the methoxy polyethylene glycol methacrylates of molecular weights 200, 400 and 1,000. These results illustrate that the increasing poly(ethylene oxide) content causes the EWC of the membrane to rise. This is attributable to the higher concentration of the hydrophilic poly(ethylene oxide) side chains. However, the overall increases in EWC are generally less pronounced than for the HEMA:EGDM (99:1) series. This may be attributed to the increased crosslink density which reduces the free-volume available for water within the polymer network.

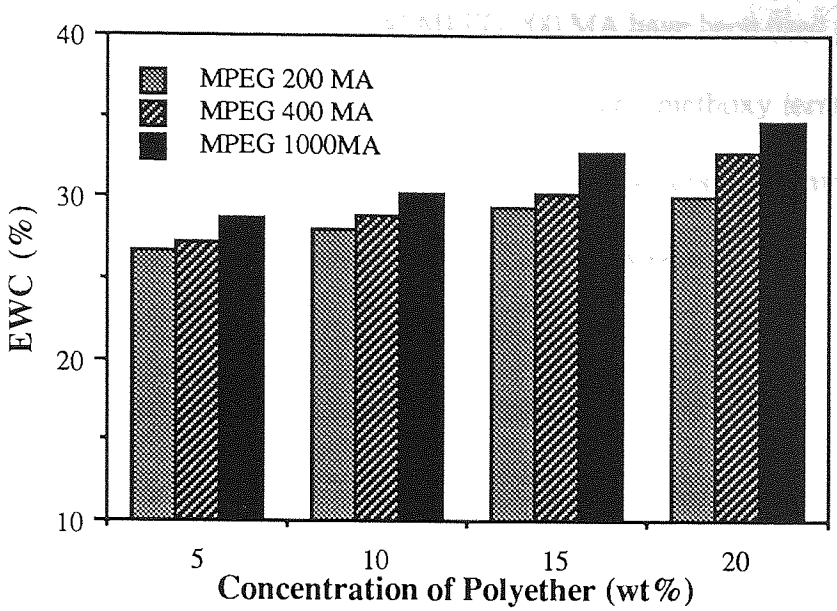

Figure 5.7 Effect of polyether content on the EWC of HEMA:EGDM (90:10)

Table 5.4 The Effect Polyethers on the EWC of HEMA:EGDM (90:10)

Membrane Composition	EWC (%)
HEMA:EGDM (90:10)	26.8
HEMA:EGDM (90:10) + 5% MPEG 200 MA	26.7
HEMA:EGDM (90:10) + 10% MPEG 200 MA	28.0
HEMA:EGDM (90:10) + 15% MPEG 200 MA	29.4
HEMA:EGDM (90:10) + 20% MPEG 200 MA	30.1
HEMA:EGDM (90:10) + 5% MPEG 400 MA	27.2
HEMA:EGDM (90:10) + 10% MPEG 400 MA	28.9
HEMA:EGDM (90:10) + 15% MPEG 400 MA	30.3
HEMA:EGDM (90:10) + 20% MPEG 400 MA	32.8
HEMA:EGDM (90:10) +5% MPEG 1000 MA	28.5
HEMA:EGDM (90:10) +10% MPEG 1000 MA	30.3
HEMA:EGDM (90:10) +15% MPEG 1000 MA	32.7
HEMA:EGDM (90:10) +20% MPEG 1000 MA	34.6

The monomers HEMA 4,5 EO and MPEG 200 MA have been used previously to illustrate the differences between the effects of hydroxyl and methoxy terminated polyether side chains on EWC. However, in the range of terpolymers containing a higher degree of crosslinker only the membranes which had been copolymerised with a 5% (wt/wt) loading of HEMA 4,5 EO were available for comparison with the MPEG 200 MA terpolymers. Hence, the EWC's of the membranes HEMA:EGDM (90:10) with 5% MPEG 200 MA and HEMA:EGDM (90:10) with 5% HEMA 4,5 EO were compared. Values of 26.7±0.5% and 27.5±0.5% respectively were obtained. Even when the experimental errors incurred during the measurement of EWC are taken into consideration the terpolymer containing the hydroxyl terminated polyether side chain has a slightly higher EWC. This result might have been anticipated since the hydroxyl group is more hydrophilic than the methoxy group. However, this result contrasts with the previous studies discussed in Section 5.3.1, which indicated that for terpolymers containing a lower crosslink density, membranes containing the methoxy terminated poly ethers have similar or slightly higher EWC's than those containing the hydroxyl terminated polyethers. This reduction in EWC has previously been attributed to the formation of internal hydrogen bonds between the terminal hydroxyl groups and the polyether side chain. Although, a broader range of compositions should be studied before any conclusions are drawn, this result may be rationalised. Increases in crosslink density will reduce chain flexibility and the formation of internal hydrogen bonds is sterically less favourable with a polyether chain length of 4, 5 repeat units. Hence, as the concentration of crosslinker increases it might be anticipated that due to steric factors the hydroxyl group will interact preferentially with water molecules, thus giving rise to the observed increase in the EWC.

The introduction of a methyl substituent to the polyether side chain will produce a more

hydrophobic monomer and hence the EWC would in turn be expected to fall for terpolymers containing propylene oxide side chains. However, the addition of 5% (wt/wt) HPHPMA to HEMA:EGDM (90:10) produces a terpolymer with the same EWC as the unmodified copolymer. This result suggests that at this loading the water structuring is again dominated by the densely crosslinked HEMA membrane.

5.3.3 Effect of Crosslinker Content on EWC

A range of hydrogels was prepared by copolymerising 5% (wt/wt) loadings of the methoxy polyethylene glycol methacrylate (MPEG MA) monomers of molecular weights 200, 400 and 1000 with a mixtures of HEMA and EGDM in the proportion HEMA:EGDM (95:5) (wt/wt). The use of this series enabled the effect of increasing crosslinker concentrations on the EWC of polyether containing terpolymers to be measured. The results illustrated in Figure 5.8, confirm that EWC decreases as the concentration of crosslinker increases. Similar results have been obtained with other hydrogel polymers[39,169] and have been attributed to a reduction in free volume in the hydrogel network as the chain length between crosslinks decreases.

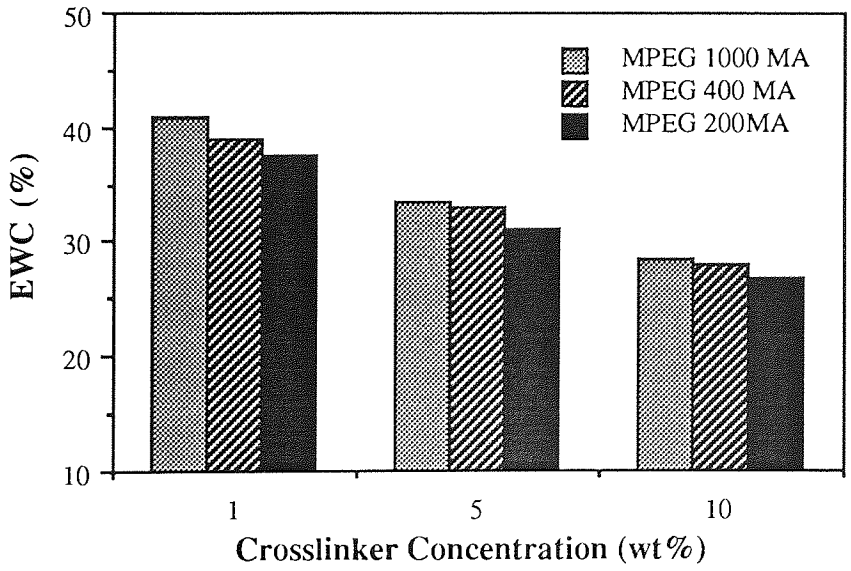

Figure 5.8 Effect of crosslinker concentration on the EWC of polyether terpolymers

5.4 Effect of Salt on EWC

Several studies have illustrated that hydrogel membranes can swell or deswell in salt solutions[39,138,170-172]. Hence, a range of group I and II metal chlorides, LiCl, NaCl, KCl, $CaCl_2$, $BaCl_2$ and $MgCl_2$ has been used to study the effect salts have on the EWC of both an unmodified membrane of composition HEMA:EGDM (90:10) and membranes modified with 5% wt/wt loadings of methoxy polyethylene glycol methacrylates of molecular weight 200, 400 and 1000. The EWC's of these membranes, in a range of salt solutions were determined using the method outlined in Section 2.9.1 and the results are presented below.

The EWC of a HEMA:EGDM (90:10) copolymer in a range of salt solutions was determined and the results are presented in Table 5.5 and Figure 5.9. These results indicate that EWC is suppressed by the addition of metal chloride salts and that this effect is greatest with group II metal chlorides. In addition, these results illustrate that within the limits of experimental error, the individual cations within an elemental group exert a similar effect on EWC.

Table 5.5 The Effect of Salt on the EWC of HEMA:EGDM (90:10)

Solution	EWC(%)
Distilled Water	26.8
0.25M NaCl	25.3
0.25M KCl	26.4
0.25M LiCl	26.0
0.25M $CaCl_2$	23.0
0.25M $BaCl_2$	23.8
0.25M $MgCl_2$	23.9

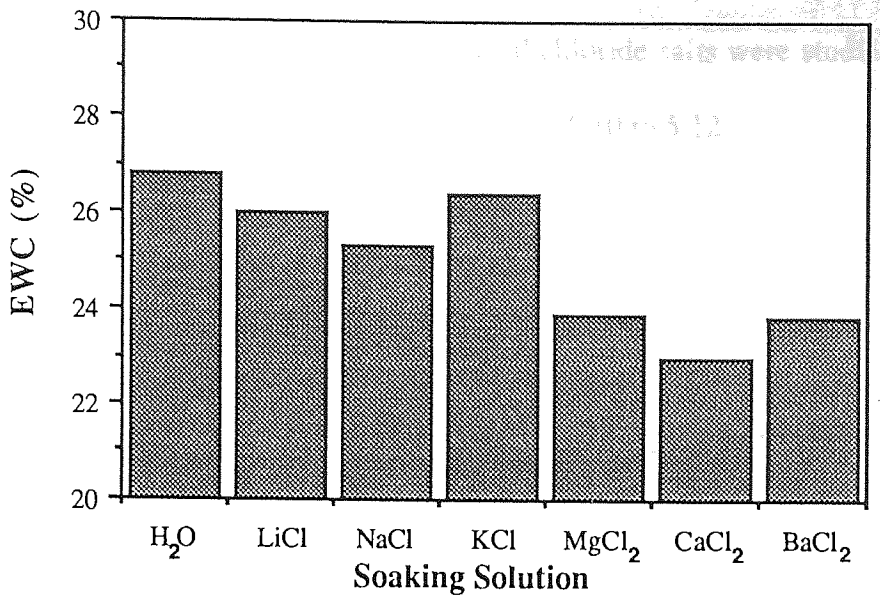

Figure 5.9 Effect of salt on the EWC of HEMA:EGDM (90:10)

Several workers have previously observed similar deswelling effects when hydrogels are transferred from pure water to solutions of the chloride salts of sodium[138,170-172] and other metals[39]. It has been suggested that this may be attributed to the water structuring effects of the salt, which may in turn promote enhanced hydrophobic binding within the hydrogel matrix[170]. Furthermore, Hamilton[39] reported that a group II metal cation, Ca^{2+}, exerts a greater water structuring effect than the group I metal cations and that in the presence of a common anion the water structuring effects of each individual group I metal cation are subsumed by those of the anion. The results obtained in this study, therefore, show similar trends to those observed by previous workers; the group II metal cations suppress EWC to the greatest extent and within each group the cations suppress EWC to a similar extent.

After studying the effect of salt solutions on HEMA:EGDM (90:10) copolymers a range crosslinked HEMA membranes of composition HEMA:EGDM (90:10) with 5% wt/wt

loadings of either MPEG 200 MA, MPEG 400 MA and MPEG 1000 MA were prepared. Their EWC's in the presence of group I and II metal chloride salts were studied and the results are presented in Table 5.6 and plotted in Figures 5.10 to 5.12

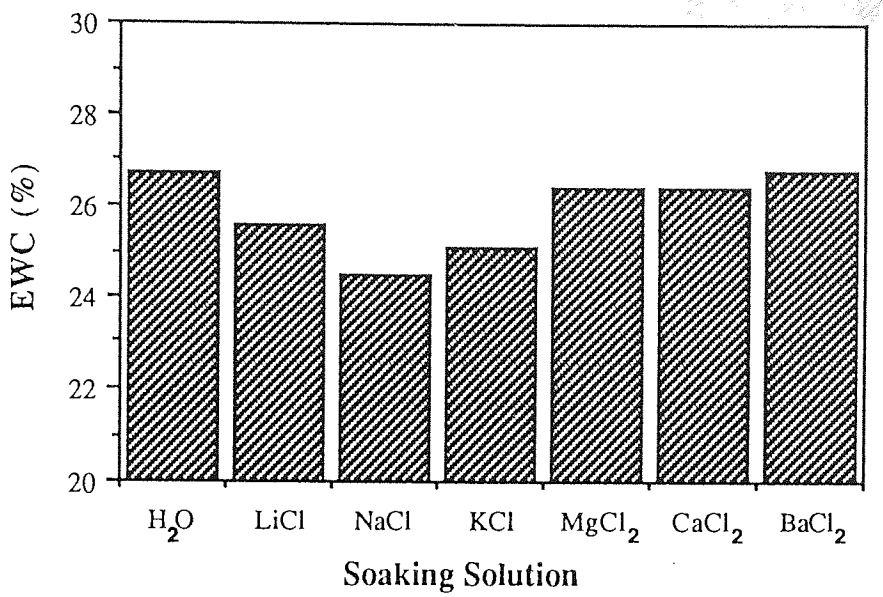

Figure 5.10 Effect of salt on the EWC of MPEG 200 MA modified HEMA:EGDM (90:10)

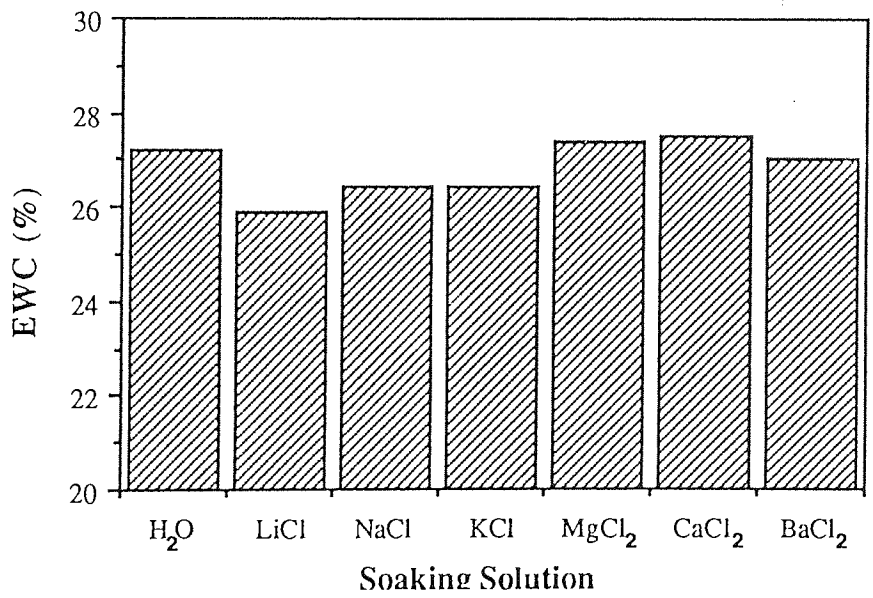

Figure 5.11 Effect of salt on the EWC of MPEG 400 MA modified HEMA:EGDM (90:10)

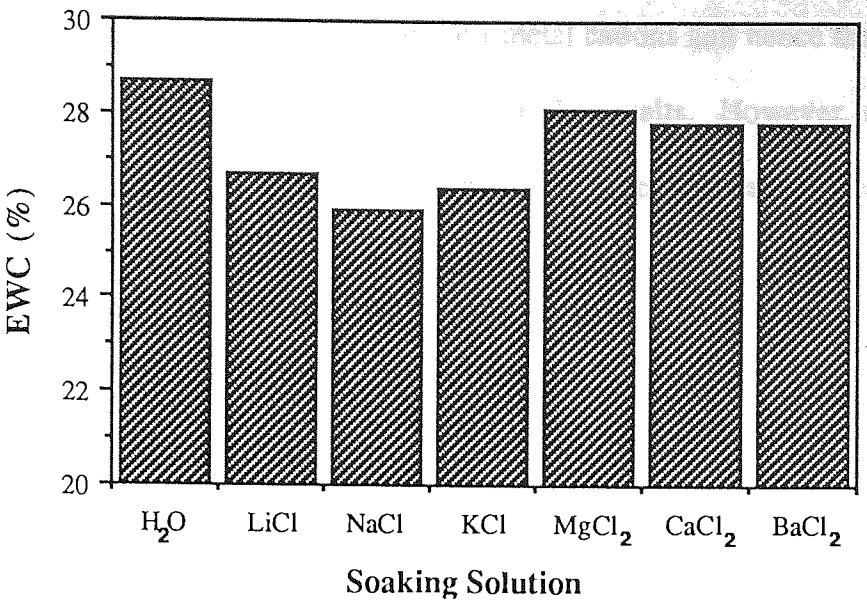

Figure 5.12 Effect of salt on the EWC of MPEG 1000 MA modified HEMA:EGDM (90:10)

Table 5.6 The effect of salt on the EWC of MPEGMA modified membranes

Membrane Composition	EWC(%)						
	H_2O	250 mM					
		LiCl	NaCl	KCl	$MgCl_2$	$CaCl_2$	$BaCl_2$
HEMA:EGDM (90:10) + 5% MPEG 200 MA	26.7	25.6	24.5	25.1	26.4	26.4	26.8
HEMA:EGDM (90:10) + 5% MPEG 400 MA	27.2	25.9	26.4	26.4	27.4	27.5	27.0
HEMA:EGDM (90:10) + 5% MPEG 1000 MA	28.5	26.7	25.9	26.4	28.1	27.8	27.8

When the results in Table 5.6 are compared with those obtained for the modified membrane (Table 5.5) it is apparent that in both the unmodified and modified membranes group I metal cations cause a slight depression in EWC. However, group II metal cations deviate from the behaviour observed in the unmodified system, no longer causing a deswelling effect in the modified membranes. Generally, group II metal cations exert a

greater water structuring effect than group I metal cations and hence the EWC of these membranes would be expected to be lower in these salts. However, since this is no longer observed with the modified membranes it is logical to assume that the water structuring effects of the cation must be reduced. There are two possible explanation for this result;

i) either the cations are unable to partition in these membranes or

ii) the ions interact preferentially with the poly(ethylene oxide) groups in the polymer backbone thus, restricting the water structuring effects of the cation.

Previous studies have indicated that the EWC of the HEMA:EGDM (90:10) copolymer is close to the 'cut-off' point for group II ion transport[39,40], which suggests that these ions might not partition readily in these membranes. However, suppressions in EWC are observed for the unmodified membrane which implies that ions will partition within the imbibed water even though the net ion transport is inhibited. Thus, since ion partitioning is not restricted by the EWC of the membrane these results suggest that this effect may be attributed to interactions between the polyether side chains and the cation.

5.5 Partition Coefficients of HEMA:EGDM (90:10) Containing Linear Polyethers

The partition coefficient is a measure of the solutes ability to dissolve in a membrane matrix and is an important parameter since it also affects the transport properties of the membrane. In a hydrated polymer it is often assumed that most salts will have a minimal interaction with the polymer matrix and will be solvated exclusively by the imbibed water. Hence, the partition coefficient would be expected to be related to the overall EWC of the polymer. Two methods for calculating the partition coefficients of hydrogels have generally been used in the literature. Yasuda *et al*[138] suggest that the partition

coefficient, Sm, may be calculated using the following equation;

$$Sm = \frac{\text{weight of salt in membrane / volume of membrane}}{\text{weight of salt / volume of solution}} \quad (5.1)$$

whereas Hamilton *et al*[39,40,156] suggest that the partition coefficient may be calculated by;

$$Sm = \frac{\text{moles of salt in the membrane / weight of membrane}}{\text{moles of salt /g of equilibrating solution}} \quad (5.2)$$

Due to the broad range of polymer compositions available for study, it was not possible to determine values for partition coefficients using both of the equations described in the literature, for all the group I and II metal cations studied in Section 5.4. Hence, one metal chloride salt from group I and II was chosen from each group so that comparisons could be made between the values calculated from Equations 5.1 and 5.2. Such salts would also give some indication of the contributing effects of both univalent and divalent cations to the partition coefficient, Sm. The partition coefficients in 0.25M solutions of NaCl and $CaCl_2$ of a range of polyether modified membranes has been determined using the method outlined in Section 2.9.2. Terpolymers based on HEMA:EGDM (90:10) with a 5% loading of each of the monomers illustrated in Figure 5.1 were studied. The effect of increasing MPEG 200 MA content was also studied using membranes which have been copolymerised with 10,15 and 20% wt/wt of this monomer. The experimental data has been used to calculate values for the partition coefficients using both of these equations. Sm_1 and Sm_2 are used to designate the values calculated from equations 5.1 and 5.2 respectively. The values for three discs were obtained and the average of these values is given in Table 5.7. The errors associated with these measurements were found to vary,

however, all measurements produced values σ_{n-1} of 0.002 or better.

Table 5.7 Partition coefficients, Sm, for 0.25M solutions of NaCl and $CaCl_2$

Membrane Composition	Sm_1 NaCl	Sm_1 $CaCl_2$	Sm_2 NaCl	Sm_2 $CaCl_2$
HEMA:EGDM (90:10)	0.019	0.008	0.014	0.007
HEMA:EGDM (90:10) + 5% MPEG 200 MA	0.028	0.011	0.018	0.009
HEMA:EGDM (90:10) + 10% MPEG 200 MA	0.021	—	0.015	—
HEMA:EGDM (90:10) + 15% MPEG 200 MA	0.023	—	0.017	—
HEMA:EGDM (90:10) + 20% MPEG 200 MA	0.022	—	0.016	—
HEMA:EGDM (90:10) + 5% MPEG 400 MA	0.045	0.010	0.031	0.011
HEMA:EGDM (90:10) + 5% MPEG 550 MA	0.033	0.012	0.026	0.009
HEMA:EGDM (90:10) + 5% MPEG 1000 MA	0.032	0.012	0.020	0.010
HEMA:EGDM (90:10) + 5% HEMA 4,5 EO	0.026	0.010	0.022	0.009
HEMA:EGDM (90:10) + 5% HPHPMA	0.019	0.007	0.014	0.007

The values obtained for Sm_1 and Sm_2 tabulated in Table 5.7 show that $CaCl_2$ partitions less readily than NaCl. This data also illustrates that whilst the values obtained for Sm_1 and Sm_2 for the partitioning of $CaCl_2$ are fairly similar, the values obtained for Sm_1 NaCl derived from Yasuda's equation (Equation 5.1) are generally slightly higher than those obtained using Hamiltons method (Equation 5.2). Since the same discs were used to

determine values of Sm_1 and Sm_2 these discrepancies cannot be attributed to errors incurred in the measurement of the concentration of leached salt. However, the membrane volume (Equation 5.1) has been determined by assuming that all the discs have the same surface area and that deswelling effects due to the salts are negligible. Thus, the higher values for $Sm_{1\ NaCl}$ may be attributed to errors in the determination in the volume of the membrane.

These values, however, do show similar trends with the values for Sm_1 and Sm_2 being generally greatest for the MPEG 400 MA modified membrane and lowest for HEMA:EGDM (90:10) and a HPHPMA modified membrane. This result might have been anticipated for the partition coefficient in NaCl on the basis of the observed EWC's in salt solution (Tables 5.5 and 5.6) Although, these EWC's were determined at room temperature, similar trends would be expected at 37^{o}C and hence, since the EWC in 0.25M NaCl is greatest for the MPEG 400 MA modified membrane, Sm_{NaCl} might also be expected to be greatest with this membrane. However, careful examination of the data in Tables 5.5, 5.6 and 5.7 indicates that Sm no longer falls with decreasing EWC. Whilst there is evidence in the literature to suggest that Sm might be related to the overall EWC of the polymer[138], in general deviations between EWC an Sm are observed at lower EWC's around the region considered in this study. This point is also illustrated by the results for the MPEG 200 MA modified membranes, where the partition coefficient Sm initially increases and then drops to an approximately constant value as EWC in the salt increases (Table 5.8).

Unfortunately, due to the narrow range of EWC's studied it is difficult to rationalise these results further and ideally, the effects of a broader range of salt solution on both EWC and Sm should be studied before any conclusions are drawn.

Table 5.8 The effect of MPEG 200 MA content on the EWC of modified HEMA:EGDM (90:10) in 0.25M NaCl at room temperature

Membrane Composition	EWC (%)
HEMA:EGDM (90:10) + 5% MPEG 200 MA	24.5
HEMA:EGDM (90:10) + 10% MPEG 200 MA	26.2
HEMA:EGDM (90:10) + 15% MPEG 200 MA	27.6
HEMA:EGDM (90:10) + 20% MPEG 200 MA	28.1

5.6 Mechanical Properties of Hydrogels Containing Linear Polyethers

The mechanical properties of a range of poly HEMA based hydrogels were tested on a Hounsfield tensometer as described in Section 2.12. Typical load-extension curves for poly HEMA and a polyether modified membrane are illustrated in Figure 5.13. A computer programme calculated values of tensile strength, T_s, elongation to break, E_b, and initial modulus, E_m. As the materials investigated all had similar structures and covered a fairly narrow range of EWC's from 36.9% to 49.4%, large variations in mechanical properties would not be expected. The measured values for T_s, E_m and E_b were in the range 0.55 to 0.83 MPa, 0.48 to 0.77 MPa and 112 to 184 % respectively. However, some differences and trends were apparent and these are discussed below.

The values obtained for the tensile strength, T_s, indicated that initially T_s increases with the addition of the polyether and then falls of as the EWC increases. The values for initial modulus, E_m, generally fall as the EWC increases and increasing concentrations of the more flexible polyether are added.

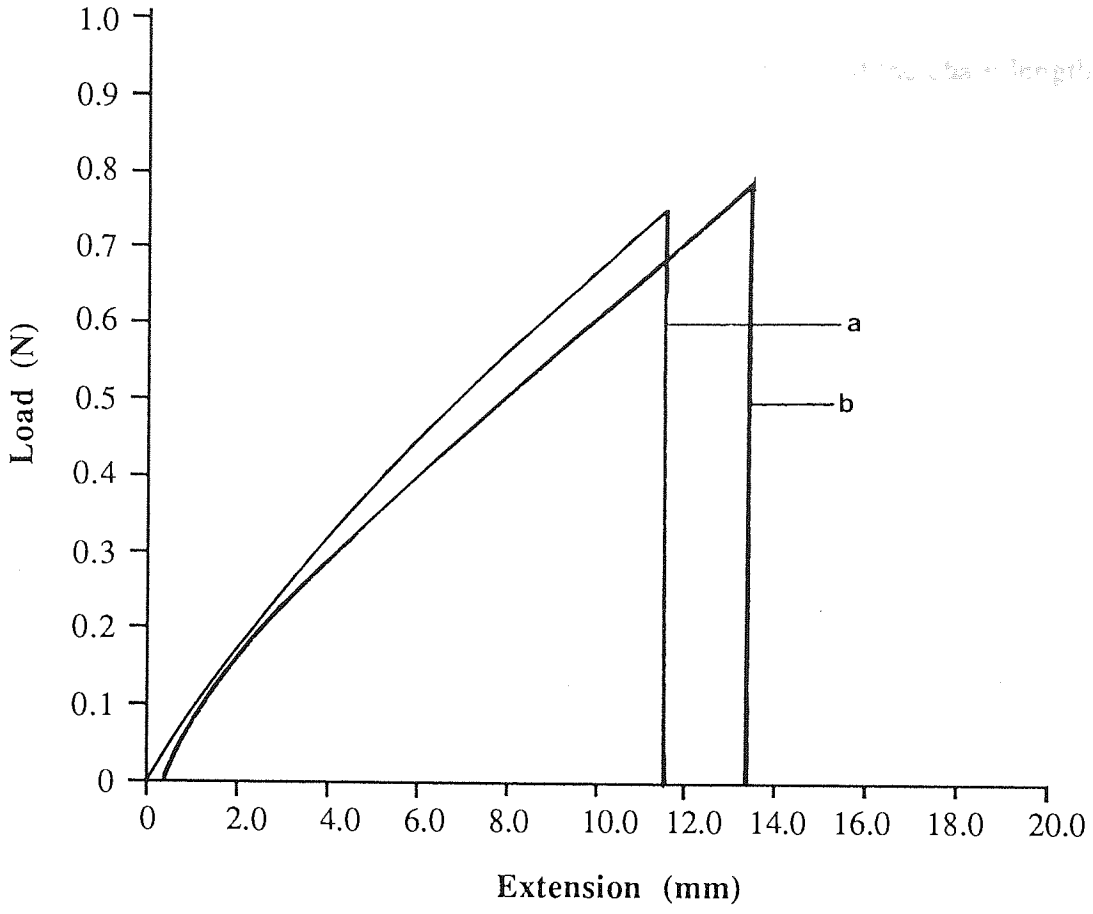

Figure 5.13 Typical load / extension curves for (a) HEMA:EGDM (99:1) and (b) HEMA:EGDM (99:1) + 5% MPEG 1000 MA

This would be expected as the addition of a plasticer should reduce the stiffness of the polymer. Finally, the elongation to break, E_b, would be expected to increase as the concentration of plasticising polyether increases. However, whilst increases in E_b are generally observed with the addition of small amounts of polyether (5 to 10% wt/wt) when the concentration was increased further to 20% wt/wt the values for E_b decreased. As it proved difficult to prepare complete membranes by copolymerising these polyethers with EGDM, it is likely that this tail off in E_b may be attributed to impurities in these monomers which cause a 'chain-stopping' effect during polymerisation. The mechanical properties of all the membranes containing polyethers are not, however, markedly different from those of HEMA:EGDM (99:1).

5.7 Conclusions

This study has illustrated that increases in both the content and the chain length of poly (ethylene oxide) monomers in the HEMA:EGDM system, enhances EWC and this effect may be attributed to the greater hydrophilicity of the linear polyether side chain. Additionally, the study of the effect of structural variations on EWC has illustrated that the addition of a hydrophobic methyl substituent to the polyether side chain reduces EWC and that 'mobile' hydroxy terminated linear polyether side chains have lower EWC than values the methyl terminated derivatives. This latter effect has been attributed to the formation of internal hydrogen bonds, thus giving rise to a pseudo crown ether type structure for the polyether side chain.

The studies of the effect of salt on EWC have indicated that whilst the unmodified membrane exhibits similar trends to those observed in previous studies, in modified membranes the EWC is unaffected by group II metal cations. This effect is attributable to interactions between these ions and the polyether side chain.

The data obtained for the partition coefficients illustrates that both literature methods produce similar values for Sm and that the values obtained using Equation 5.1 may be slightly higher due to the errors incurred in the determination of the polymer volume. These results have also indicated that the divalent cation, Ca^{2+}, partitions less readily than the univalent cation Na^{+}.

Finally, the mechanical properties of polyether modified HEMA:EGDM (99:1) membranes whilst, being similar to those of HEMA:EGDM (99:1) illustrate that initially increases in T_s, E_m and E_b are observed with the addition of poly (ethylene oxide).

CHAPTER 6

Transport Studies of Linear Polyether Modified Hydrogel membranes

6.1 Introduction

The ability of linear polyethers such as polyethylene glycol and glyme to solvate and complex with alkali and alkaline earth metal cations has been known for many years. Generally, values for the stability constants of complexation between linear polyethers and metal cations are much lower than those observed for their cyclic analogues. For example, Frensdorff[77,78] obtained values of 2.0 and 6.1 for the constants of complexation for potassium ions by pentaglyme and 18-crown-6, respectively. Hence, the uses of poly(ethylene oxides), PEO's, in chemistry as ionophores are less common than those of crown ethers. Although this ability to form complexes with metal cations may be advantageous in the fabrication of permselective membranes, if polyethers sequester metal cations, particularly group II metal cations, from biological fluids this may lead to biointolerance. Thus, it is important to study the effects linear polyethers on the transport properties of their copolymers.

Three methoxy polyethylene glycol methacrylates (MPEG MA) of nominal Mw 200, 400 and 1,000 (MPEG 200 MA, MPEG 400 MA and MPEG 1000 MA) were chosen (Figure 6.1). These monomers were selected so it would be possible to compare how the transport properties vary with polyether chain length.

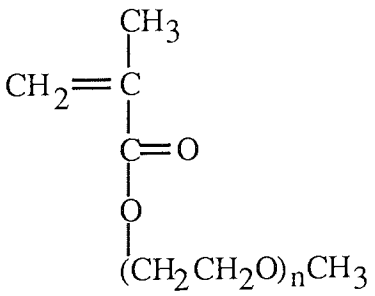

n=4 to 5 MPEG 200 MA
n=9 to 10 MPEG 400 MA
n=22 to 23 MPEG 1000 MA

Figure 6.1 The structure of the MPEG MA's used in this study

Initially, terpolymers were prepared by copolymersing a 5% (wt/wt) loading of each monomer illustrated in Figure 6.1 with a mixture HEMA:EGDM (90:10). This composition was chosen so that direct comparisons could be made with the previous investigations of cyclic or crown ether systems. The transport of a range of group I and II metal chlorides across membranes containing these linear polyethers was studied and the results obtained will be discussed in this Chapter. Additionally, the effect of increasing the poly (ethylene oxide) concentration on the transport of NaCl has been studied and the results will be presented and discussed in this Chapter.

6.2 Effect of Linear polyethers on the Transport of Group I Metal Cations Across HEMA:EGDM (90:10)

The permeability of a range of group I metal chlorides, LiCl, NaCl and KCl, across methoxy polyethylene glycol methacrylate modified crosslinked HEMA copolymers was studied. The ion permeability studies were all carried out at 37^{o}C using membranes which had been soaked for at least three weeks prior to use. Initially, the effect of increasing polyether chain length on ion transport will be discussed.

The primary ion transport data for the permeation of 0.25M solutions of NaCl, KCl and LiCl across membranes containing 5% (wt/wt) of these linear polyethers is illustrated in Figures 6.2 to 6.4.

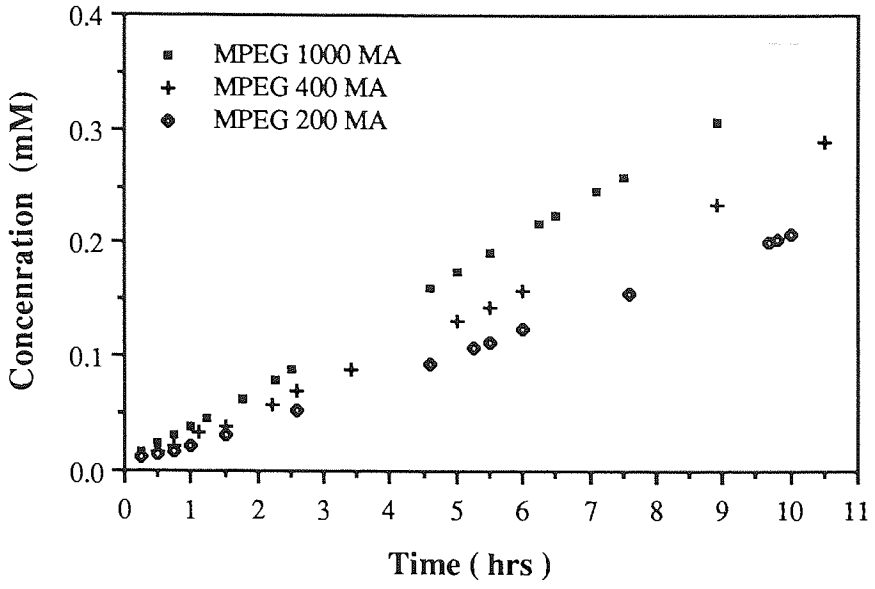

Figure 6.2 **Primary transport data for the permeation of NaCl across methoxy polyethylene glycol methacrylate modified HEMA:EGDM (90:10)**

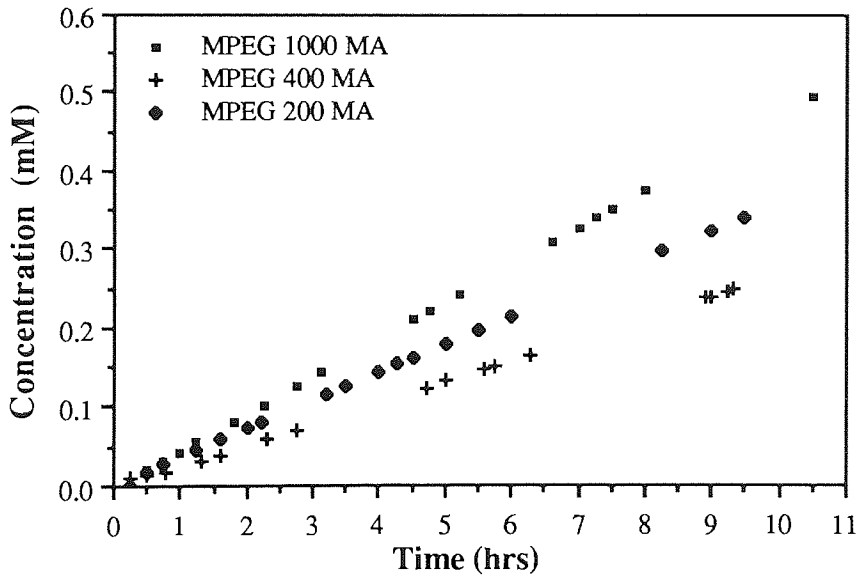

Figure 6.3 **Primary transport data for the permeation of KCl across methoxy polyethylene glycol methacrylate modified HEMA:EGDM (90:10)**

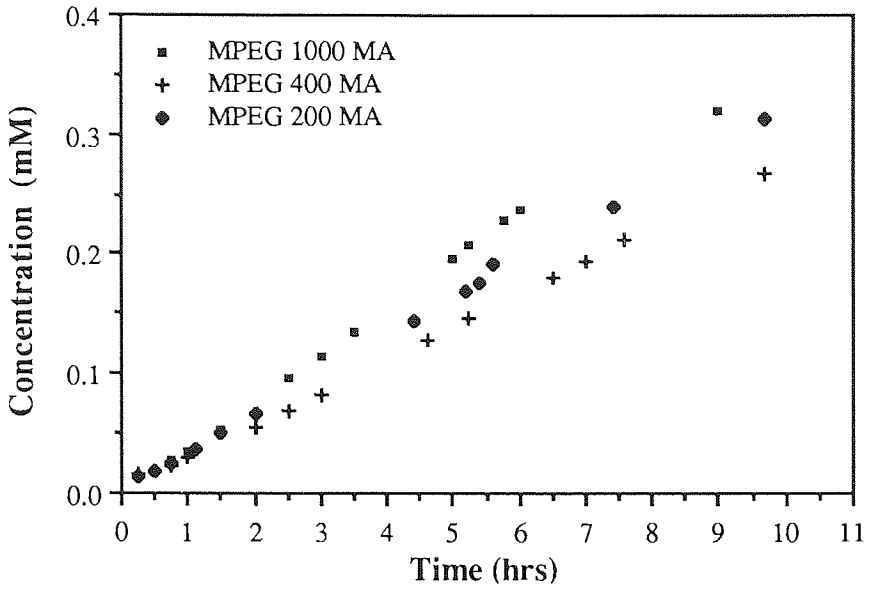

Figure 6.4 Primary transport data for the permeation of LiCl across methoxy polyethylene glycol methacrylate modified HEMA:EGDM (90:10)

In Chapter 5 it was shown that increases in polyether chain length also lead to an increase in EWC. Other workers have shown that ion transport is enhanced as EWC rises[40,156] thus enhanced ion transport would be expected as the polyether chain length increases. Figure 6.2 clearly illustrates that this is, in fact, the case for the transport of NaCl, while, Figures 6.3 and 6.4 show that for KCl and LiCl permeation, increases in EWC do not lead to the expected increases in ion permeation. However, it is important to take care at this stage to avoid placing undue emphasis on small variations in both EWC and ion permeability.

The graphs shown in all of these Figures indicate that in all cases ion permeability increases linearly with time and hence the gradients of these graphs may be used to calculate the permeability coefficients. The values obtained along with the values reported

in Section 3.2.1 for the unmodified crosslinked HEMA copolymer are presented in Table 6.1

Table 6.1 The effect of polyether chain length on the calculated permeability coefficients, P for the transport of 0.25 M solutions of NaCl, KCl and LiCl across HEMA:EGDM (90:10)

Membrane composition	$P \times 10^8$ / cm^2s^{-1}			EWC / %
	NaCl	KCl	LiCl	
HEMA:EGDM (90:10)	2.7	2.2	1.6	26.8
HEMA:EGDM (90:10) + 5% MPEG 200 MA	1.7	3.2	2.3	26.7
HEMA:EGDM (90:10) + 5% MPEG 400 MA	2.0	2.7	2.2	27.2
HEMA:EGDM (90:10) + 5% MPEG 1000 MA	3.0	4.2	2.8	28.5

The experimental data presented in Table 6.1 clearly illustrates that the induction periods observed with systems containing cyclic ethers do not occur in these systems. However, the presence of a linear polyether can led to a suppression in ion permeability despite increases in the EWC of the polymer. This is particularly illustrated by the results obtained for the transport of NaCl. In these studies the permeability coefficients obtained for the permeation of Na^+ ions are lower for membranes containing 5% (wt/wt) of both MPEG 200 MA and MPEG 400 MA, than is observed for unmodified membrane, HEMA:EGDM (90:10).

Previous studies of transport phenomena in hydrogels have illustrated that ion permeability is related to the volume fraction of water present within the polymer matrix. A simple plot of the permeability coefficient, P, against the volume fraction of water, H,

is therefore shown in Figure 6.5.

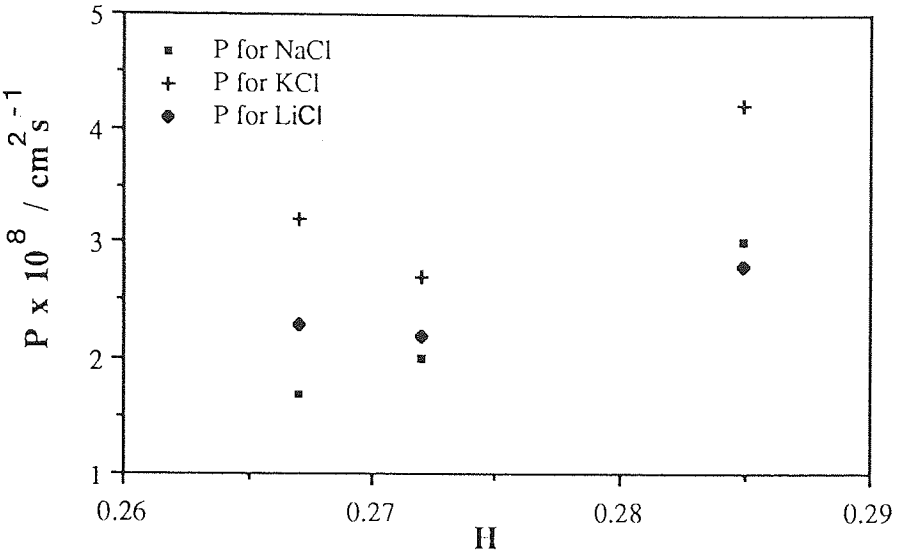

Figure 6.5 Plot of P vs H for the transport of group I metal chlorides through MPEG MA modified membranes

Figure 6.5 illustrates that the results for NaCl transport are remarkably linear, while dips in ion permeability are observed for the transport of KCl and LiCl through MPEG 400 MA modified membranes. Although these dips in ion permeation may be significant it is important to obtain results from a broader range of copolymers and consider the influence that other factors such as monomer purity may have on ion transport before any conclusions are drawn. More detailed relationships have been derived to describe ion permeability data[148,149], however, previous studies on similar systems have indicated that the free volume of diffusion theory gives the best fit with experimental data[39,40]. This theory predicts a linear relationship between the natural logarithm of the permeability coefficient, P and the inverse of the EWC, expressed as the volume fraction of water (Equation 3.1).

$$\text{Ln } P \propto H \qquad (3.1)$$

where P is the permeability constant and

H is the volume fraction of water

This relationship can be used to predict values for P if the EWC of the hydrogel is known. However, this theory assumes that ion permeation occurs in the aqueous phase only and does not account for the water structuring effects of either the ions permeating or the hydrophilic groups within the polymer backbone. Since the bulk of ion permeability data has previously been obtained from hydrogel membranes containing hydroxyl water structuring groups, it is important to consider the water structuring effects within these membranes before any comparisons are made.

There is a great deal of evidence in the literature to suggest that poly (ethylene oxide) groups will structure water[10], with each OCH_2CH_2 interacting to form numerous hydrates. Hence, before any conclusions are drawn from this study it is necessary to examine the experimental data to assess the applicability of the free volume of diffusion theory. The data in Table 6.1 have been used to calculate LnP against 1/H for the transport of NaCl, KCl and LiCl and the values are plotted Figure 6.6.

Whilst it is perhaps unwise to place too much emphasis on the information available from three data points, it would appear from this graph, as in Figure 6.5, that a linear relationship is only observed for NaCl transport. Again the the results for KCl and LiCl appear to show a dip which corresponds to the depressed value obtained for the permeability coefficient for ion transport across the membrane containing 5% (wt/wt) of MPEG 400 MA.

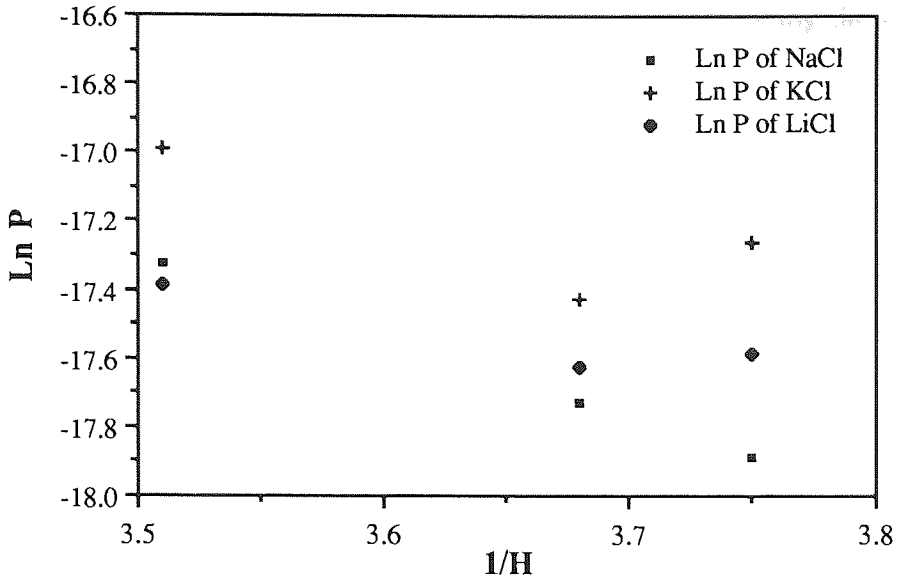

Figure 6.6 Plot of LnP vs 1/H for the transport of group I metal chlorides through MPEG MA modified membranes

Several workers have suggested that ion transport occurs predominantly in the gel's bulk or freezing water[25,145]. Hence, this suppression in ion permeation may result from a reduction in the bulk or freezing water of the polymer due to enhanced water structuring by the polyether side chains. However, the suppression of ion transport may also be attributable to the formation of cation:polyether complexes or a combination of both these factors. If ion transport is hindered by a chelation effect, these results suggest that the formation of such complexes must occur more rapidly than in the systems containing cyclic ethers. Hence, the 'lag-times' exhibited by the cyclic systems are no longer observed in these studies and the values obtained for the permeability coefficients, P, are similar to the values obtained for permeation in the final steady state through the systems containing cyclic ethers (Chapters 3 and 4). In addition, if increased water structuring within the polymer causes this effect it is reasonable to suggest that the free volume theory might still account for ion transport. Hence, these results appear to illustrate that whilst

NaCl transport is apparently reduced by water structuring effects, there are clearly additional factors which must be considered when rationalising the results for KCl and LiCl transport.

The overall effect of each linear polyether on the order of ion transport through a modified HEMA:EGDM (90:10) membrane was investigated. The permeability coefficients given in Table 6.1 for both the modified and unmodified membranes are illustrated in Figure 6.7.

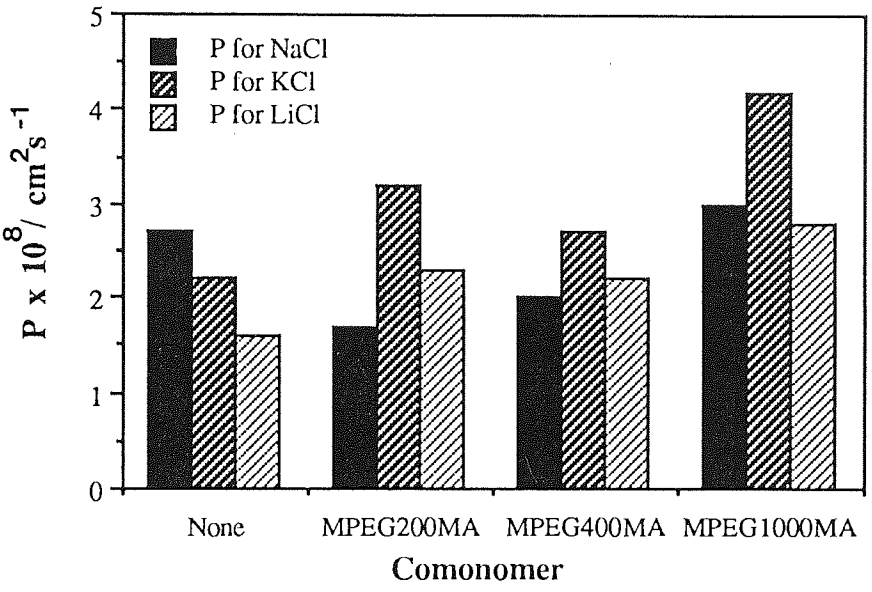

Figure 6.7 Effect of composition on the permeability coefficients, P, for the transport of group I metal cations across modified and unmodified HEMA:EGDM (90:10)

This diagram shows that for the unmodified membrane ion permeation follows the order; $Na^+ > K^+ > Li^+$.

However, this order is clearly not observed for membranes containing 5% (wt/wt) of these polyethers. For membranes containing either MPEG 200 MA or MPEG 400 MA

the rate of ion transport follows the order; $K^+ > Li^+ > Na^+$.

Whereas, for a membrane containing MPEG 1000 MA the order of ion permeation is; $K^+ > Na^+ > Li^+$.

Thus whilst variations in the exact order of ion permeation are observed, in general the presence of poly (ethylene oxide) side chains has the greatest effect on the transport of sodium ions. Finally, it is worth noting that the order for ion permeation through MPEG 1000 MA modified membranes, whilst differing from that illustrated by the unmodified membrane, is the same as the order through poly HEMA and HEMA:MMA copolymers[39].

6.3 Effect of MPEG 200 MA on Sodium Transport Across HEMA:EGDM (90:10)

It would appear from previous observations that sodium ion transport is suppressed by copolymerisation with all the methoxy polyethylene glycol methacrylates, but that this effect is most pronounced with MPEG 200 MA. A range of hydrogels was prepared with the basic composition HEMA:EGDM (90:10) to which either 10, 15 or 20% (wt/wt) of the MPEG 200 MA comonomer was added. All membranes were allowed to soak for at least three weeks prior to use and the transport of 0.25M NaCl at 37^{o}C was studied. The primary ion transport data is illustrated in Figure 6.8 shows that the concentration of Na^+ ions permeating across each terpolymer increases linearly with time. In addition, enhanced NaCl transport occurs as the concentration of MPEG 200 MA and hence the EWC of the terpolymer increases. Permeability coefficients have been calculated from this data and are given in Table 6.2.

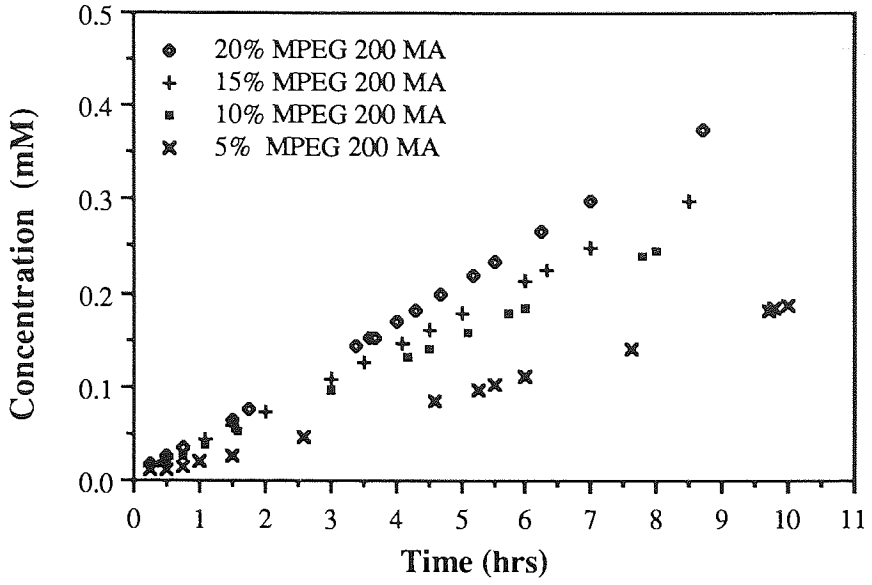

Figure 6.8 Effect of increasing MPEG 200 MA content on the transport of NaCl

Table 6.2 Effect of increasing MPEG 200 MA content on the permeability coefficient for the transport of 0.25M NaCl at 37°C across HEMA:EGDM (90:10)

Amount of MPEG 200 MA in the co-monomer mix / %	P x 10^8 / cm^2s^{-1}	EWC (%)
0	2.7	24.3
5	1.7	26.7
10	2.5	28.0
15	3.1	29.4
20	3.7	30.1

It is interesting to note that the values for the permeability coefficients presented in Table 6.2 indicate that up to 10% of the MPEG 200 MA may be added to HEMA:EGDM (90:10) before NaCl permeation exceeds that of the unmodified membrane. The data given in Table 6.2 has also been used to calculate values for LnP and 1/H. These values

have been plotted in Figure 6.9. Since a linear relationship is obtained it would appear that NaCl transport is governed by the volume faction of water present within the polymer and that the transport properties of this range of polymers can be described by a free volume of diffusion model.

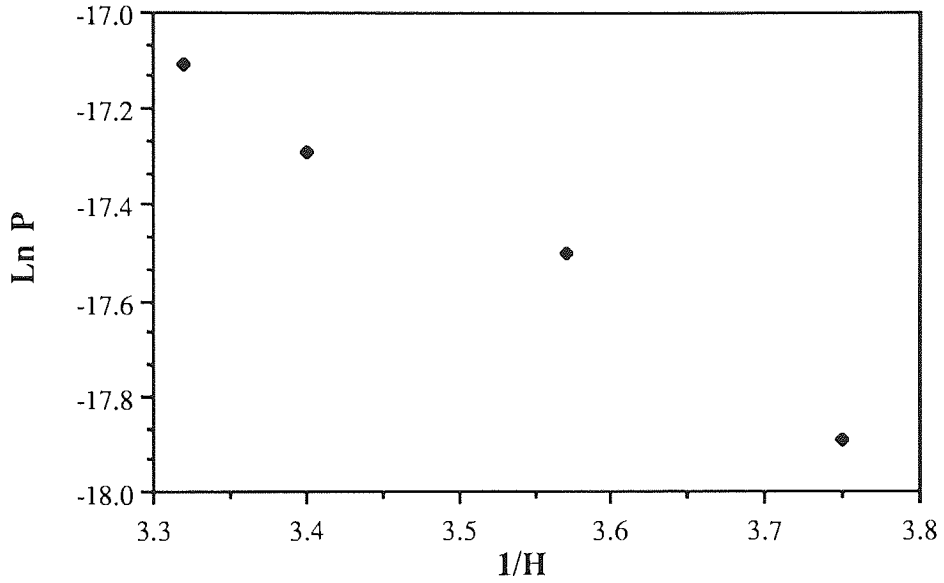

Figure 6.9 Plot of Ln P vs 1/H for the transport of NaCl across MPEG 200 MA modified terpolymers

6.4 Effect of Linear Polyethers on the Transport of Group II Metal Cations Across HEMA:EGDM (90:10)

The results from a study of the transport of a range of group II metal cations through the unmodified membrane, HEMA:EGDM (90:10) indicated that the transport of these metal cations are effectively screened by the membrane. However, the incorporation of poly (ethylene oxide) monomers within the backbone of a crosslinked HEMA copolymer enhances EWC. Additionally, these monomers may form complexes with group II metal cations. Consequently, the effect of the addition of these monomers to HEMA:EGDM (90:10) on the transport properties of a range of group II chloride salts was studied.

The transport of 0.25M solutions of $MgCl_2$, $BaCl_2$ and $CaCl_2$ across a membrane of composition HEMA:EGDM (90:10) with 5% (wt/wt) of either MPEG 200 MA, MPEG 400 MA or MPEG 1000 MA was investigated and the results obtained will be discussed below. As before all membranes were soaked for at least three weeks prior to use and the transport of these ions was studied at 37°C. The results will be discussed in terms of the effect of polyether chain length (or molecular weight) on the transport properties. In addition, the effect of poly (ethylene oxide) monomer on the rate of ion transport through poly ethylene oxide modified terpolymers was also studied.

The primary ion transport data for the permeation of 0.25M solutions of $CaCl_2$, $MgCl_2$, and $BaCl_2$ across these membranes is illustrated in Figures 6.10, 6.11 and 6.12.

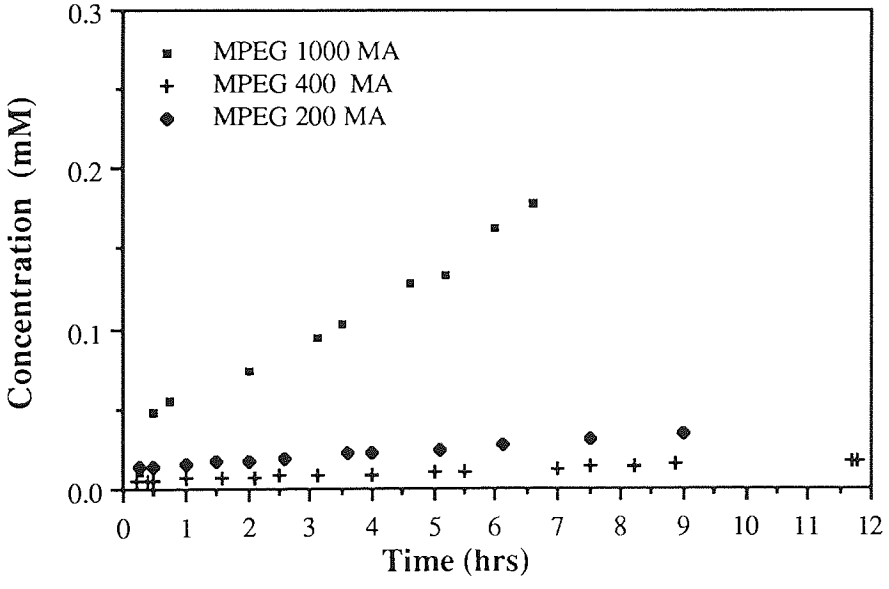

Figure 6.10 Primary transport data for the permeation of $CaCl_2$ across methoxy polyethylene glycol methacrylate modified HEMA:EGDM (90:10)

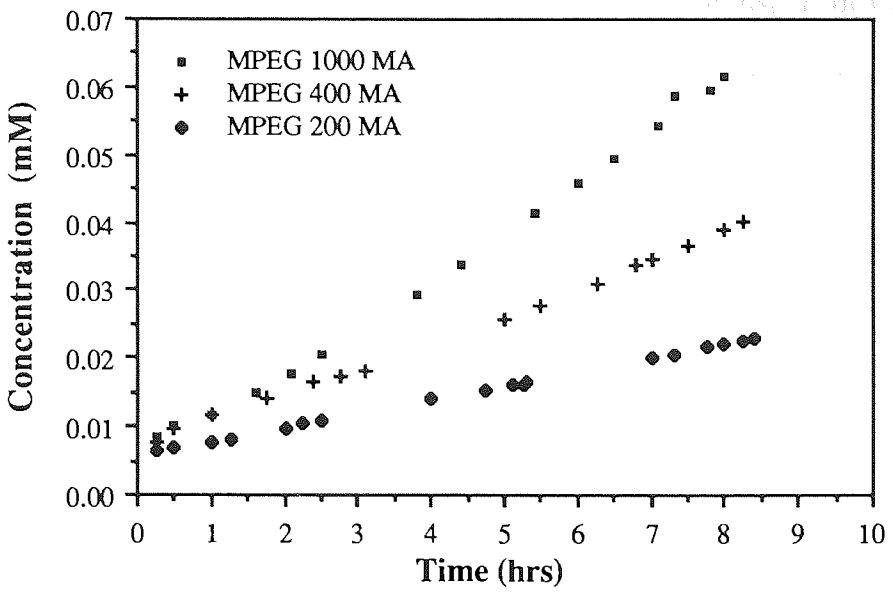

Figure 6.11 Primary transport data for the permeation of $MgCl_2$ across methoxy polyethylene glycol methacrylate modified HEMA:EGDM (90:10)

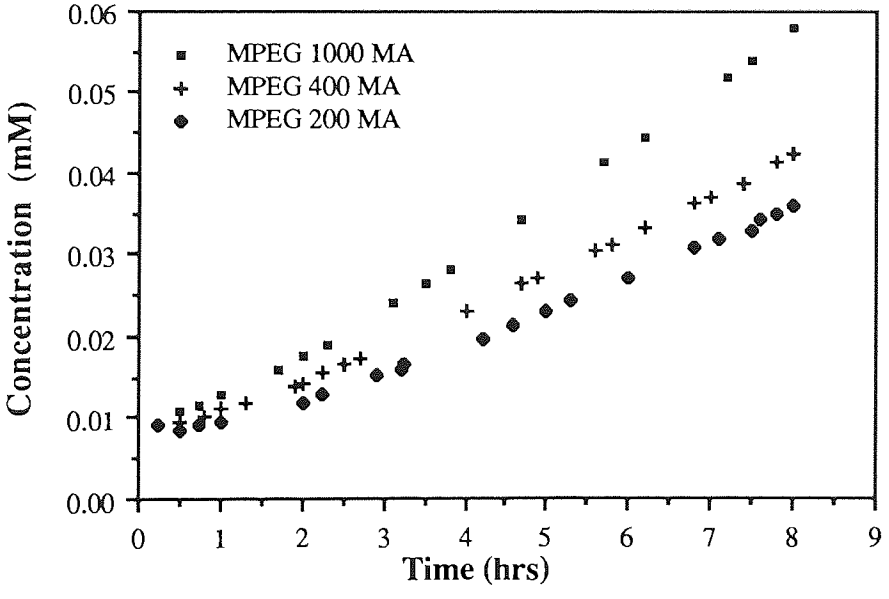

Figure 6.12 Primary transport data for the permeation of $BaCl_2$ across methoxy polyethylene glycol methacrylate modified HEMA:EGDM (90:10)

The effect of increasing chain length (or M_w) on the transport of $CaCl_2$ is illustrated in Figure 6.10. The graph shows that Ca^{2+} ion permeation through membranes containing 5% (wt/wt) of either MPEG 200 MA or MPEG 400 MA varies linearly with time. However, for Ca^{2+} ion transport through a membrane containing 5% (wt/wt) MPEG 1000 MA, there is an initial period where ion permeation is low before a slight increase in the rate of ion transport is observed. Similar induction periods or 'lag-times' have been observed for ion permeation through hydrogels containing cyclic polyethers, but in the latter case these changes in the rate of ion permeation are more pronounced. Figures 6.11 and 6.12 illustrate that $MgCl_2$ and $BaCl_2$ transport is affected in a similar manner. Figure 6.11 shows that for the transport of $MgCl_2$ induction periods are observed for ion permeation through MPEG 400 MA and MPEG 1000 MA modified membranes, while for Ba^{2+} ion permeation, initial induction periods are observed for all of the MPEG MA modified membranes (Figure 6.12). Since these initial periods illustrate linear variations in ion concentration with time, this data can be used to calculate the initial and final permeability coefficients P_1 and P_2. The values obtained are illustrated in Table 6.3.

In the preceding Sections in this Chapter the permeability data has been used to test whether the free volume model of diffusion is applicable to ion permeation through membranes containing these poly (ethylene oxide) monomers. The data given in Table 6.3 for the permeability coefficients once a final steady has been reached and the EWC of these polymers have been used to calculate values for LnP_2 and 1/H. Figure 6.13 illustrates the results obtained for the transport of $MgCl_2$, $BaCl_2$ and $CaCl_2$.

Table 6.3 Calculated values of P_1 and P_2 for group II metal chloride transport across HEMA:EGDM (90:10) modified terpolymers

Membrane Composition	BaCl2		$MgCl_2$		$CaCl_2$		EWC
	P_1x10^8/ cm^2s^{-1}	P_2x10^8/ cm^2s^{-1}	P_1x10^8/ cm^2s^{-1}	P_2x10^8/ cm^2s^{-1}	P_1x10^8/ cm^2s^{-1}	P_2x10^8/ cm^2s^{-1}	/%
HEMA:EGDM (90:10)	—	0.19	—	0.08	—	0.14	24.3
HEMA:EGDM (90:10) + 5% MPEG 200 MA	0	0.20	—	0.14	—	0.14	26.7
HEMA:EGDM (90:10) + 5% MPEG 400 MA	0.16	0.33	0.17	0.20	—	0.11	27.2
HEMA:EGDM (90:10) + 5% MPEG 1000 MA	0.36	0.67	0.34	0.54	0.32	0.49	28.5

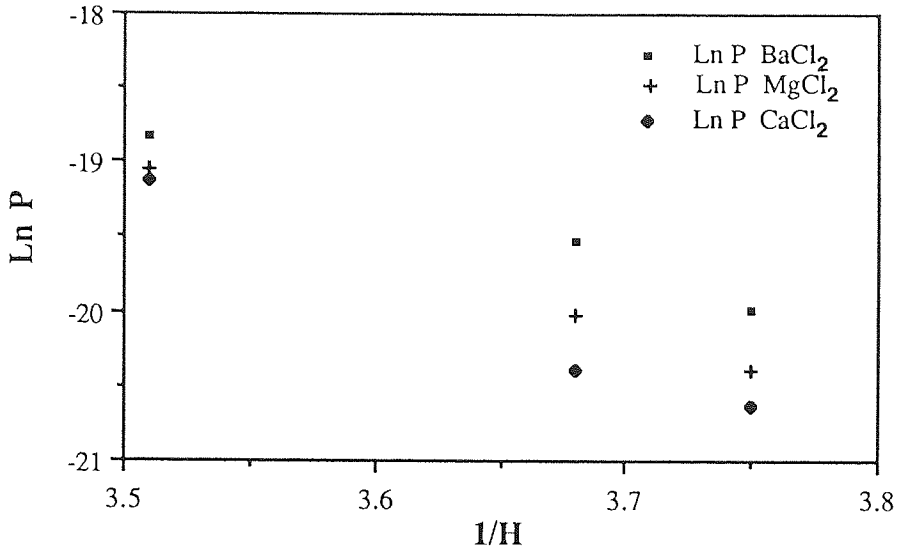

Figure 6.13 Plot of LnP_2 vs 1/H for the transport of group II metal chlorides through MPEG MA modified membranes

Although it is necessary to obtain more data points before any conclusions are drawn, the graphs for the transport of both Ba^{2+}, Ca^{2+} and Mg^{2+} appear to be linear. Such results would imply that in the final steady state these ions permeate at a rate determined by the EWC of the hydrogel and hence the diffusion of these ions could be described by a free volume model of diffusion.

In previous studies of transport phenomena in hydrogels containing cyclic polyethers similar induction periods have been observed and this effect has been attributed to the gradual filling of ionophore sites. Hence, the lag-times observed in this study might also be caused by the formation of complexes between poly (ethylene oxide) donor groups and the cations permeating through the membrane. In addition, 'lag-times' may be observed with these ions because the overall rate of ion transport is reduced to such an extent that

the partitioning process between the polyether and the cation can be observed. The duration of these 'lag-times' have been estimated and the values are given in Table 6.4

Table 6.4 Extended 'lag-times' for the permeation of group II chlorides through MPEG MA modified membranes

Membrane Composition	T_{lag} / hrs		
	$BaCl_2$	$MgCl_2$	$CaCl_2$
HEMA:EGDM (90:10) +5% MPEG 200 MA	1.5		
HEMA:EGDM (90:10) +5% MPEG 400 MA	1.4	3.5	
HEMA:EGDM (90:10) +5% MPEG 1000 MA	2.8	2.5	3.1

The results in Table 6.4 appear to indicate that longer polyether chains cause an initial inhibiting effect on the cation flux across the membrane. Furthermore, these results also indicate that as the size of the hydrated cation increases in the order;

$$Ba^{2+} < Mg^{2+} < Ca^{2+}$$

the smaller chained poly (ethylene oxide) monomers apparently have little effect on the initial rate of ion flux and hence the 'lag-times' or induction periods are no longer observed. This result is not suprising as studies of complex formation by both linear and cyclic polyethers have illustrated that there is generally an optimum number of repeating (OCH_2CH_2) units required for stable complex formation. However, such studies have been based on the ionic radii of the cation and would predict that small chained polyethers would exhibit the following preferences for these ions;

$$Mg^{2+} < Ca^{2+} < Ba^{2+}$$

which is in fact the reverse of the observed preferences. Hence, these results appear to indicate that if this initial rate of transport is caused by a chelation effect, complex formation is determined by the hydrated ionic radii of the cation.

The effect of group II metal cation variation on the rate of ion transport through the unmodified membrane, HEMA:EGDM (90:10) has been discussed previously in Section 3.2.2. Group II metal cations were found to permeate this membrane in the order;

$$Ba^{2+} > Ca^{2+} > Mg^{2+}$$

which implied that ion permeability was related to the hydrated ionic radii with smaller cations permeating more rapidly than larger cations.

Once a final steady state of diffusion has been obtained the calculated values for the permeability coefficients through both the unmodified and modified membranes can be used to illustrate the order in which these ions permeate. The values given Table 6.4 have been plotted in Figure 6.14 to illustrate these trends more clearly.

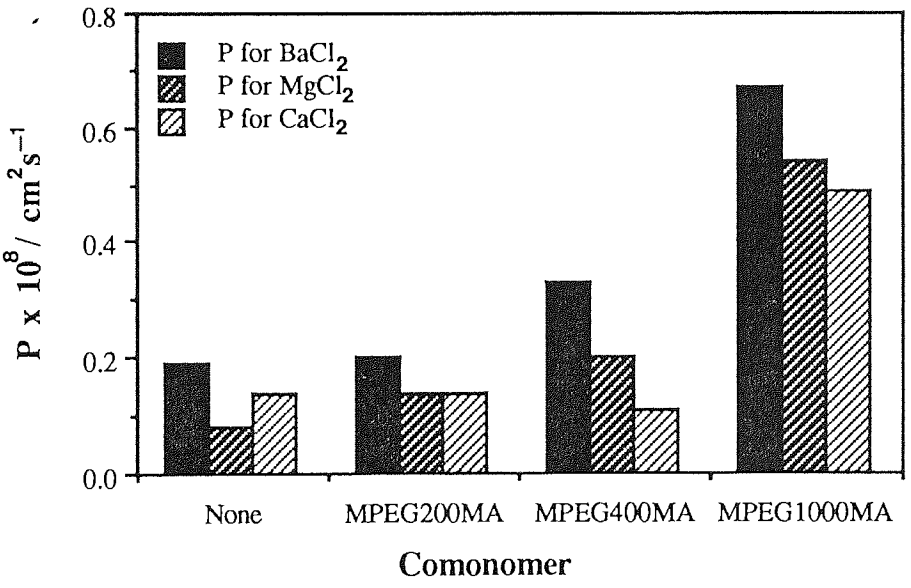

Figure 6.14 Effect of composition on the permeability coefficient, P, for the transport of group II metal cations across modified and unmodified HEMA:EGDM (90:10)

Figure 6.14 illustrates that these ions permeate through a membrane containing 5%

(wt/wt) MPEG 200 MA follows in the order;

$$Ba^{2+} > Ca^{2+} = Mg^{2+}$$

and through membranes containing MPEG 400 MA and MPEG 1000 MA in the order;

$$Ba^{2+} > Ca^{2+} > Mg^{2+}$$

Thus, in general ion permeation in the final steady state follows the same order as for the unmodified membrane. Figure 6.14 also appears to indicate that even though EWC is enhanced with the addition of MPEG 200 MA to HEMA:EGDM (90:10) there is no overall increase in the rate of Ba^{2+} and Ca^{2+} ion permeation. Similarly, the enhanced EWC which arises from the addition of 5% (wt/wt) MPEG 400 MA does not affect the final rate of Ca^{2+} ion transport.

Finally, it is interesting to note that despite variations in the initial 'lag-times' (Table 6.4) the values for the initial steady state permeation, P_1 are approximately the same for both Ba^{2+} and Mg^{2+} through the MPEG 400 MA modified membrane and for the transport of all the cations studied through the MPEG 1000 MA modified membrane (Table 6.3).

6.3 Discussions and Conclusions.

The results obtained in these studies clearly indicate that the presence of linear poly (ethylene oxide) side chains can affect the transport properties of the material. In all of these studies the values obtained for the permeability coefficients are lower than would be predicted on the basis of previous studies. However, the explanation for these results remains unclear.

Poly (ethylene oxide) units are thought to interact with at least three molecules of water, hence their presence in a hydrogel might be anticipated to not only increase the overall EWC but also the increase the fraction of structured or bound water within the gel's

matrix. If ion permeation does occur predominantly in the gel's freezing water or bulk water as previously postulated then ion transport would be expected to be reduced by the inclusion of further water structuring groups. This relationship between ion transport and freezing water has been highlighted by previous studies which illustrated that salt rejection is enhanced when the freezing water content is low[23]. The results obtained for the transport of NaCl through these membranes appear to imply that permeation is in fact related to EWC and suggests that the observed reduction in ion permeation may result from the water structuring effects of the polyether monomer. Similarly, the values determined for the final steady state of permeation of group II metal cations across the membranes containing MPEG 400 MA and MPEG 1000 MA imply that in the final steady state ion permeation can be described by a free volume model for diffusion.

Where deviations are observed for example for KCl and LiCl transport, ion permeation may also be affected by the formation of complexes between the metal cation and the polyether side chains. If the formation of metal cation:PEO complexes can affect the transport of the membrane then MPEG 200 MA might also be expected to form complexes with Li^+, Na^+, Ca^{2+} and Mg^{2+} since it most resembles 15-crown-5. However, these results tend to imply that complexation may be influenced by steric factors and suggests complex formation occurs at the end of the polyether side chain farthest from the HEMA backbone. However, the purity of the linear polyethers used in this study should also be considered before any conclusions can be drawn.

The results obtained for the transport of group II metal cations show some similarities with the systems containing cyclic polyethers which are discussed in Chapters 3 and 4. However, the variations in ion permeation illustrated by these system are less pronounced than in the systems containing cyclic polyethers. These studies also indicate that if the

induction periods are caused by a chelation effect, then this process is related to the hydrated ionic radii of the cation.

This study has highlighted the potential applications of these polymers in the design of both permselective membranes and membranes whose transport properties mimic those of the systems containing the more expensive crown ethers. Finally, it has also highlighted the need to gain further information concerning the water structuring in these membranes in order to rationalise some of these results.

CHAPTER 7

Surface Properties of Hydrogels Modified with Linear Polyethers

7.1 Introduction

One of the major applications of hydrogels is in the field of biomedical applications, with their use in the design and fabrication of soft contact lens being perhaps the most commercially successful venture. Hydrogel surfaces are, therefore, often in intimate contact with biological fluids. Hence, it is important to study the surface properties of these materials.

Recently workers have indicated that thrombogenic reactions to synthetic polymers are significantly reduced by the presence of linear polyether side chains. Furthermore, it has been suggested that this reduction in thrombogenic reactions might be attributed to the presence of flexible hydrated polyether chains which serve to reduce protein adsorption at the polymer surface. Studies in the ocular environment indicate that calcium plays a significant role in the formation of white surface film deposits[8] and discrete elevated deposits or 'white spots'[9]. Additionally, the transport studies described in the preceding Chapter illustrated that linear polyethers, specifically those with longer chains, interact with calcium ions. Hence, if linear polyether chains are able to sequester calcium ions it is likely that as a direct result ocular compatibility may be reduced. This Chapter is primarily concerned with the results obtained from a study of the surface properties of a range of linear polyether terpolymers and attempts to elucidate the relationship between the structure of the poly(ethylene oxide) comonomer and the surface properties of these materials. However, the results obtained from a study of the effects of linear polyethers on the ocular compatibility of HEMA based terpolymers will also be discussed. Finally, the rational of the techniques used to probe the surface properties of these materials both on a macroscopic and molecular level will be described.

7.2 Determination of Surface Energy

Contact angle goniometry has been used to determine the surface energy of hydrogel copolymers and the practical details associated with this technique are described in Section 2.10. In this preliminary study contact angles have been determined in the dehydrated state. The detailed theory associated with the determination of surface energy from contact angles is beyond the scope of this project but has been described elsewhere by Corkhill[169]. However, for measurements on dehydrated polymer surfaces the Owens and Wendt equation (Equation 7.1) is generally used[173].

$$1+\text{Cos}\theta = (2/\gamma_{lv} [(\gamma_{lv}^{d}.\gamma_{s}^{d})^{0.5} + (\gamma_{lv}^{p}.\gamma_{s}^{p})^{0.5}] \qquad (7.1)$$

where, γ_{lv} is the liquid -vapour interfacial free energy,

γ_{lv}^{d} is the dispersive component of the liquid and finally,

γ_{lv}^{p} is the polar dispersive component of the liquid.

This equation relates the contact angle, θ, to the polar, γ_{s}^{p} and dispersive, γ_{s}^{d}, forces of the solid. Hence, if the contact angles with two wetting solutions whose polar and dispersive components have been determined previously, are measured, the polar and dispersive forces of the solid can then be calculated by solving the Owens and Wendt equation simultaneously. Finally, the total surface free energy, γ_{s}^{t}, can be obtained by adding the values for γ_{s}^{d} and γ_{s}^{p} (Equation 7.2).

$$\gamma_{s}^{t} = \gamma_{s}^{d} + \gamma_{s}^{p} \qquad (7.2)$$

Several liquids have been used in surface free energy determinations[174] but in these studies distilled water and methylene iodide were chosen. The reason for this choice is

because of their high surface free energies and the appropriate balance in their polar and dispersive components. The values of γ_s^d, γ_s^p and γ_s^t for these liquids are given in Table 7.1

Table 7.1 Polar and dispersive components of water and methylene iodide

Liquid	γ^d (mN/m)	γ^p (mN/m)	γ^t (mN/m)
Water	21.8	51.0	72.8
Methylene Iodide	48.1	2.3	50.8

The results obtained from a study of the effect of a range of monomethyl polyethylene glycol methacrylate, MPEG MA, monomers of Mw 200, 400 and 1,000 on the surface energies of HEMA based hydrogels will be presented and discussed in this section. Unfortunately, due to the hydrophilicity of terpolymers of composition HEMA:EGDM (99:1) copolymerised with an added 5 to 20 % (wt/wt) of MPEG MA's, it was impossible obtain accurate results for their contact angles with water. However, the contact angles with water and methylene iodide were successfully obtained for a range of copolymers with a basic composition HEMA:EGDM (90:10) to which x% (wt/wt) MPEG MA (where x = 5 to 20 for MPEG 200 and 400 MA and 5 to 15 for MPEG 100 MA) had been added. The results are presented in Table 7.2. Figures 7.1, 7.2 and 7.3 illustrate the variations in γ_s^d, γ_s^p, and γ_s^t as a function of the mole % of polyethylene oxide present in the terpolymer.

Table 7.2 Polar, dispersive and total surface free energies for dehydrated poly (ethylene oxide) modified copolymers

Copolymer Hydrogel Composition	Water Contact Angle	Methylene Iodide Contact Angle	Dispersive Component of Surface Free Energy (mN/m)	Polar Component of Surface Free Energy (mN/m)	Total Surface Free Energy (mN/m)
HEMA:EGDM 90:10	60	39	31.5	15.8	47.3
HEMA:EGDM 90:10 + 5% MPEG200MA	62	35	34.0	13.5	47.5
HEMA:EGDM 90:10 + 10% MPEG200MA	59	36	32.9	15.8	48.7
HEMA:EGDM 90:10 + 15% MPEG200MA	47	36	30.4	24.7	55.1
HEMA:EGDM 90:10 + 20% MPEG200MA	45	41	27.6	27.7	55.3
HEMA:EGDM 90:10 + 5% MPEG400MA	59	37	32.4	16.0	48.4
HEMA:EGDM 90:10 + 10% MPEG400MA	54	34	32.8	18.9	51.7
HEMA:EGDM 90:10 + 15% MPEG400MA	51	33	32.6	20.9	53.5
HEMA:EGDM 90:10 + 20% MPEG400MA	47	37	29.9	25.0	54.9
HEMA:EGDM 90:10 + 5% MPEG1000MA	57	35	32.9	17.0	49.9
HEMA:EGDM 90:10 + 10% MPEG1000MA	41	31	31.7	27.7	59.4
HEMA:EGDM 90:10 + 15% MPEG1000MA	38	32	30.7	30.1	60.8

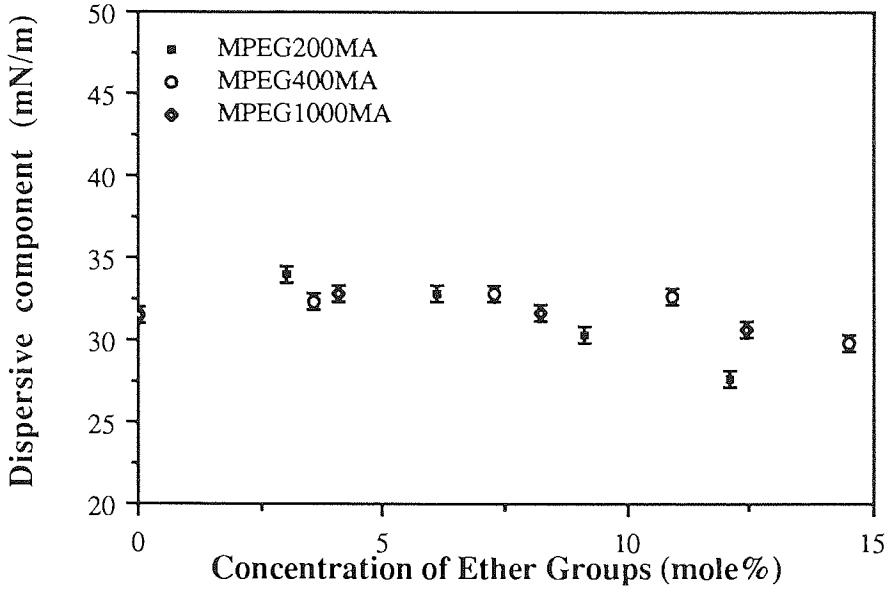

Figure 7.1 Effect of composition on γ_s^d of poly (ethylene oxide) terpolymers

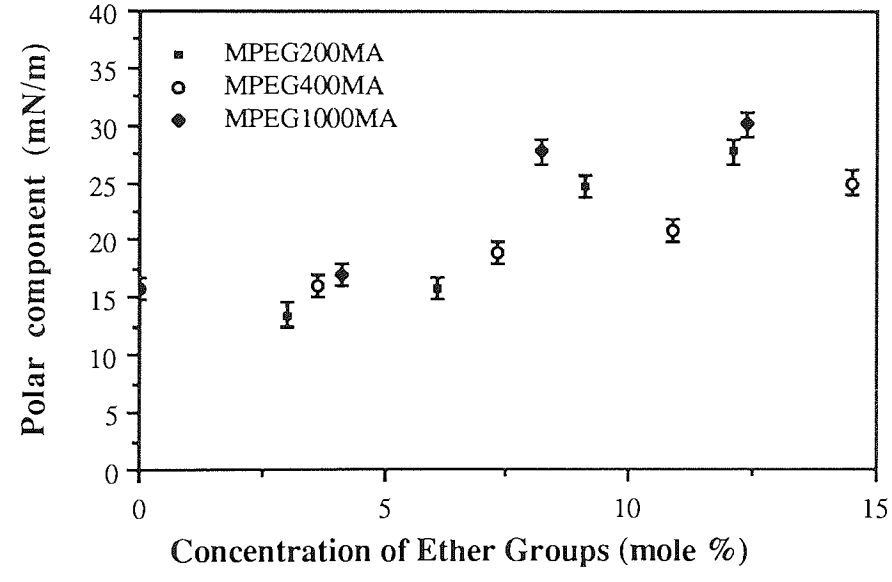

Figure 7.2 Effect of composition on γ_s^p of poly (ethylene oxide) terpolymers

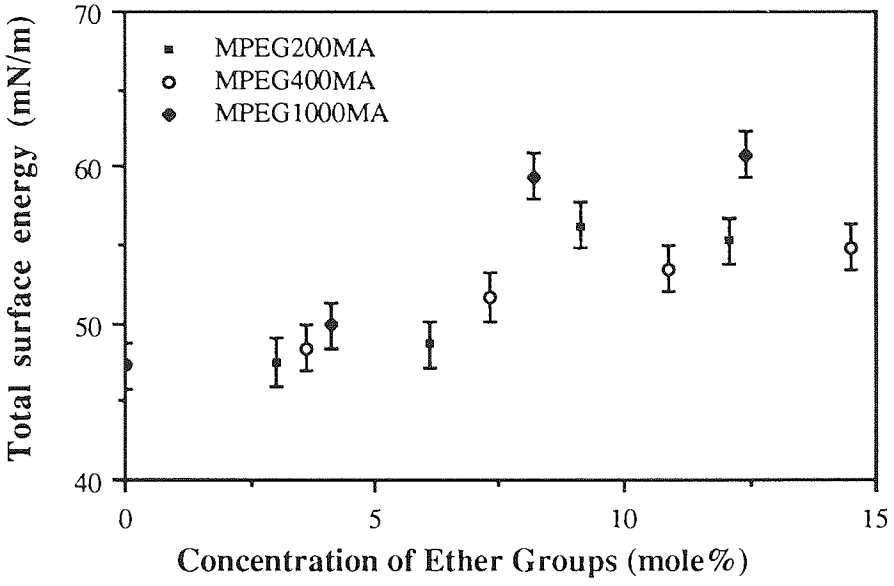

Figure 7.3 Effect of composition on γ_s^t of poly(ethylene oxide) terpolymers

Figure 7.1 illustrates that at lower concentrations of poly(ethylene oxide) there is little change in the dispersive component of the surface free energy, γ_s^d, however, further increases in ether content cause a slight decrease in γ_s^d. Conversely, the polar component, γ_s^p, gradually increases with the addition of poly(ethylene oxide) (Figure 7.2). Hence, the observed increase in the total surface free energy, γ_s^t, is due to the increases in the polar component of the surface free energy (Figure 7.3). This is also reflected by the increase in the polar fraction of the total surface free energy, γ_s^t, with the addition of the polyether monomers. The results obtained in this study indicate that both the polar component and the polar fraction of the total surface free energy of the dehydrated polymer are increased by copolymerisation with poly(ethylene oxide) comonomers. Such results, therefore, imply that the polar ether groups must express themselves at the polymer surface. Furthermore, since the dispersive component arises predominately from contributions to the surface energy from non-polar groups, in this

case the α methyl group and the CH_2 on the polymer backbone, it is reasonable to suggest that the observed suppression in γ_s^d, results from a shielding effect by the polyether side chains. At higher polyether concentrations both γ_s^p and γ_s^t appear to level off. Although it is important to confirm this by determining the surface free energies of a broader range of terpolymers, it is reasonable to suggest that γ_s^t should reach a maximum which corresponds to the values for the homopolymer. This value should be less than the value for water. In addition, it is worth noting that difficulties in determing an accurate value for the surface energy of the homopolymer are envisaged since the homopolymer will be hydrophilic hence it will be difficult to determine water contact angles for the dehydrated polymer accurately. Furthermore several unsuccessful attempts have been made to prepare lightly crosslinked (1%) hydrogel membranes from these monomers. In all cases fragments of polymer were obtained due to chain stopping effects caused by monomer impurities. Finally, it is interesting to note that there is no clear cut evidence to suggest that increases in the polyether chain length affect the total surface energy (Figure 7.3).

Most hydrogels are used in their hydrated state, hence, it is often advantageous to be able to compare biocompatibility data with values for the surface energies of the hydrated polymer. Barnes *et al* [12] have illustrated that it is possible to derive accurate values for the polar and dispersive components of the hydrated polymer from a combination of the measured values for the dehydrated surface and the known values for bulk water. The components are then calculated on the basis of the volume fractions of both water and polymer present in the membrane, using Equation 7.3

$$\gamma_h = [\,(1\text{-}H) \times \gamma_s\,] + H \times \gamma_{lv} \qquad (7.3)$$

where, γ_h is the calculated value for the polar or dispersive component of the surface

free energy of the hydrated polymer,

H is the EWC expressed as a fraction,

γ_s is the measures polar or dispersive component of the dehydrated polymer and

γ_{lv} is the polar or dispersive component of water.

Table 7.3 Calculated values for the polar, dispersive and total surface free energies of hydrated poly (ethylene oxide) modified terpolymers in their hydrated state

Membrane Composition	γ_{hs}^{d} (mN/m)	γ_{hs}^{p} (mN/m)	γ_{hs}^{t} (mN/m)
HEMA:EGDM (90:10)	28.9	25.2	54.1
HEMA:EGDM (90:10) +5%MPEG 200 MA	30.7	23.5	54.2
HEMA:EGDM (90:10) +10%MPEG 200 MA	29.8	25.7	55.5
HEMA:EGDM (90:10) +15%MPEG 200 MA	27.9	32.4	60.3
HEMA:EGDM (90:10) +20%MPEG 200 MA	28.9	34.7	60.6
HEMA:EGDM (90:10) +5%MPEG 400 MA	29.5	25.5	55.0
HEMA:EGDM (90:10) +10%MPEG 400 MA	29.6	29.2	57.8
HEMA:EGDM (90:10) +15%MPEG 400 MA	29.3	30.0	59.3
HEMA:EGDM (90:10) +20%MPEG 400 MA	27.2	33.5	60.7
HEMA:EGDM (90:10) +5%MPEG 1000 MA	29.7	26.7	56.4
HEMA:EGDM (90:10) +10%MPEG 1000 MA	28.7	34.8	63.5
HEMA:EGDM (90:10) +15%MPEG 1000 MA	27.8	36.9	64.6

The values derived for the polar, γ_{hs}^{p} and dispersive, γ_{hs}^{d} components of the hydrated polymers surface free energy using Equation 7.3 are given in Table 7.3. The predicted values for the polar and total surface free energy given in Table 7.3 are generally higher than those determined for the dehydrated polymer surface, while the values predicted for the dispersive component of the surface free energy are lower. These values obviously illustrate similar trends. These increases, in γ_{s}^{p} and γ_{s}^{t}, however, are not unexpected and are a direct consequence of the addition of water whose polar component is significantly enhanced.

7.3 Horizontal ATR FTIR of poly (ethylene oxide) Terpolymers

Attenuated total reflectance (ATR) or multiple pass internal reflectance (MIR) fourier transform infra-red (FTIR) spectroscopy is a technique which has been used increasingly to study the surfaces of polymers. For successful results the sample should be in intimate contact with a prism (a zinc selenide crystal). An IR beam is then directed at an angle to the polymer surface through the prism. The beam is then reflected numerous times between the polymer surface and the prism until it is collected at the opposite end to the incoming beam. The depth of penetration by the beam is dependent on a number of factors including the angle of incidence, the wavelength of the incident radiation and finally the refractive indices of both the sample and the crystal. When coupled with FTIR it is possible to obtain IR spectra of a polymer surface quickly and by making use of the subtraction procedures available with FTIR spectrometers it should be possible to study the variations in chemistry at the polymer surface.

In this Section the results obtained from a preliminary study which assesses whether it is possible to detect ether groups at the surface of poly (ethylene oxide) terpolymers using this technique, will be discussed.

Figure 7.4 Horizontal ATR FTIR of HEMA:EGDM (99:1)

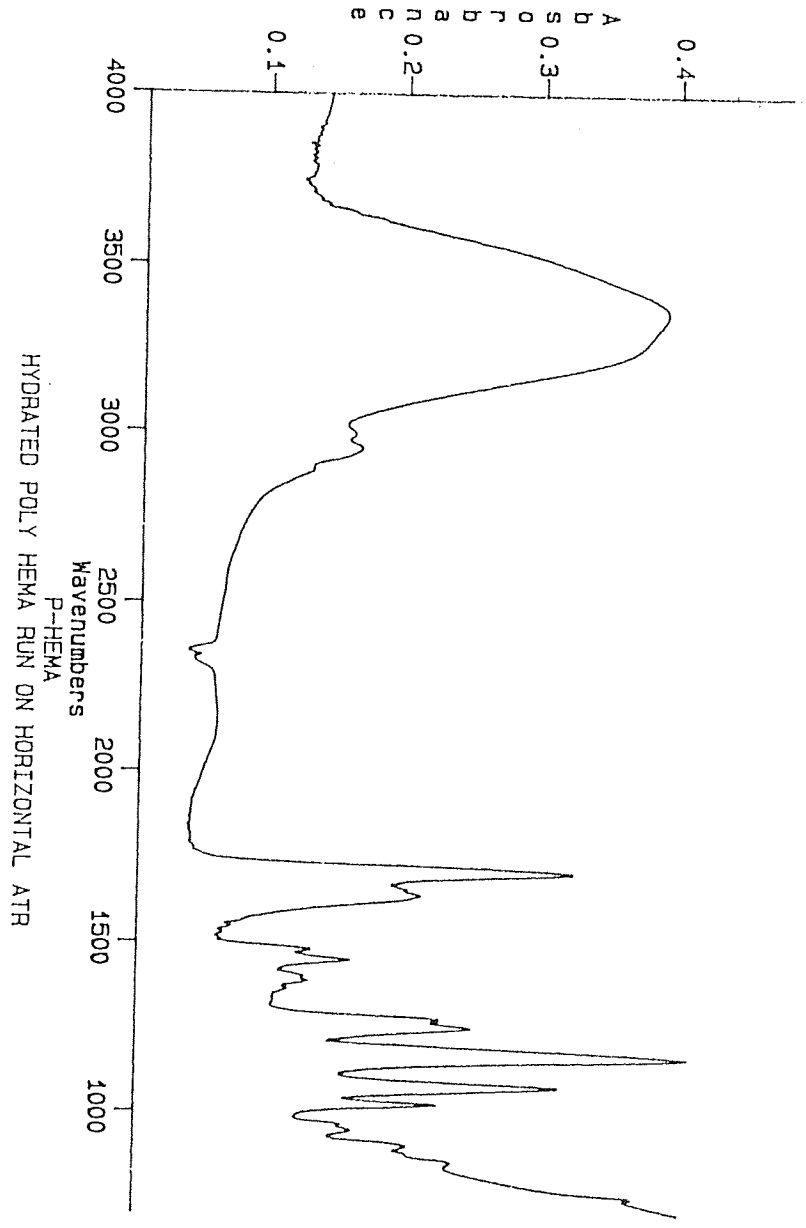

Figure 7.5 Horizontal ATR FTIR of HEMA:EGDM (99:1) modified with 5% MPEG 200 MA

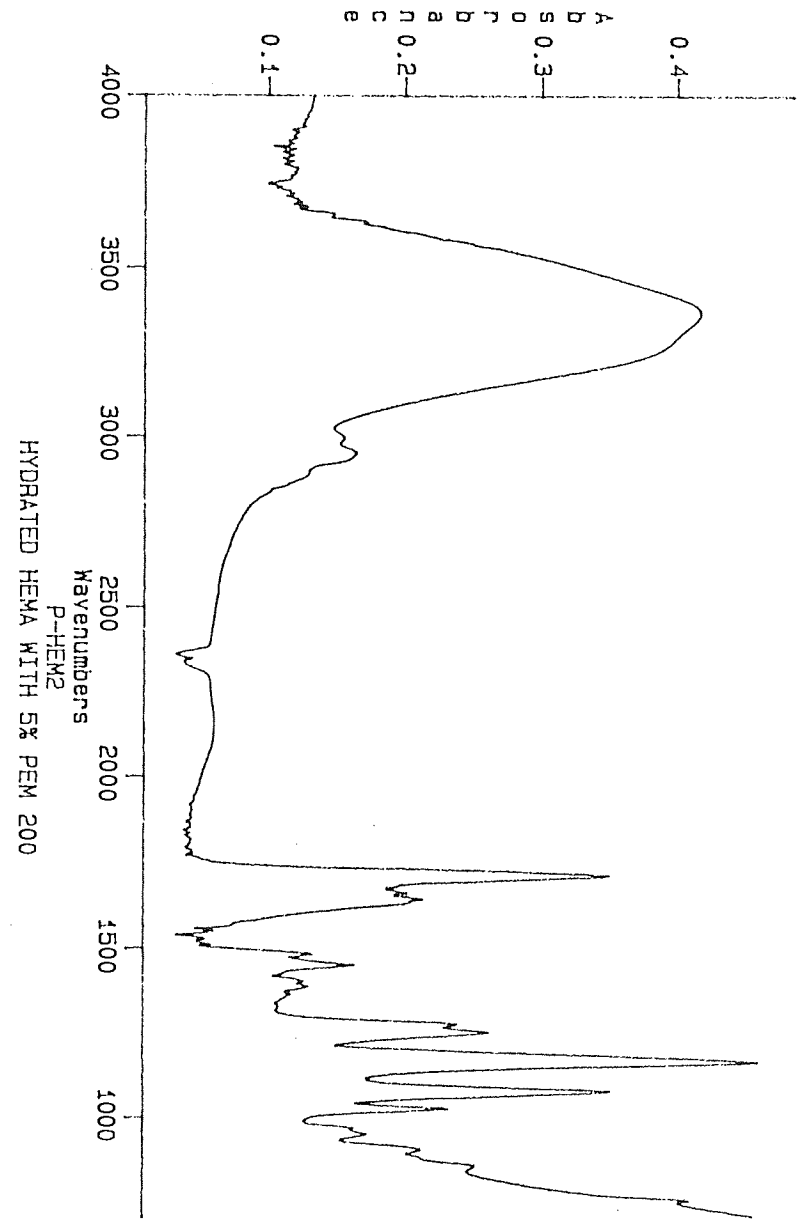

Figure 7.6 Horizontal ATR FTIR Subtraction spectra for HEMA:EGDM (99:1) with 5% MPEG 200 MA and HEMA:EGDM (99:1)

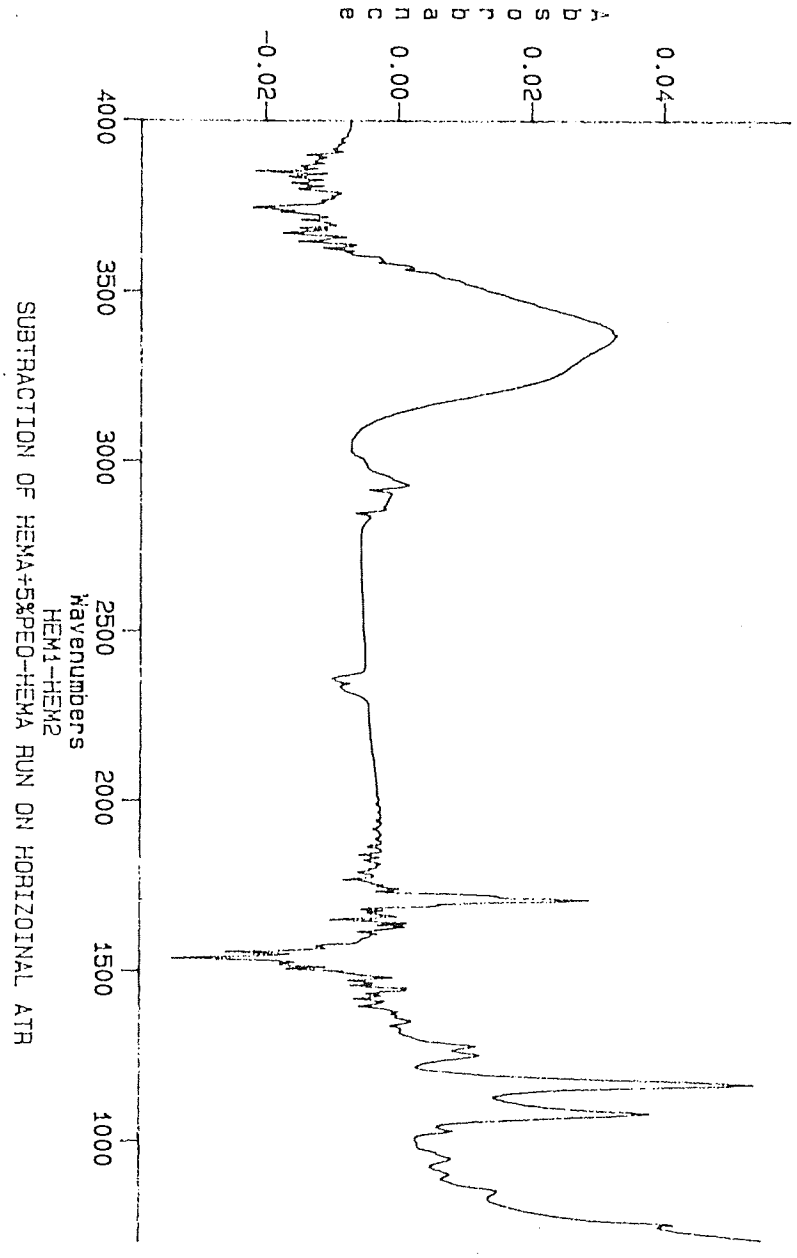

For this purpose the ATR FTIR spectra of HEMA:EGDM (99:1) (wt/wt) and a mixture of the monomers HEMA:EGDM (99:1) (wt/wt) which have been copolymerised with 5% (wt/wt) of MPEG 200 MA were obtained. These spectra are illustrated on Figures 7.4 and 7.5.

By comparing these spectra it is obvious that any differences in their surface chemistry are not immediately apparent. However, since these spectra had been obtained from identically sized samples and are both based on HEMA:EGDM (99:1) it is possible to apply subtraction techniques to illustrate the differences between the surface chemistry of these samples. This spectrum is illustrated in Figure 7.6. The peaks at 1050 cm^{-1} and 1150 cm -1 clearly indicate that ether peaks can be detected at the polymer surface. The OH stretch at around 3400 cm^{-1} appears since the MPEG 200 MA terpolymer has a slightly higher EWC than HEMA:EGDM (99:1) (37.6% and 36.9% respectively). Finally, the peak at 1720 cm^{-1} is attributable to the C=O stretch of the carbonyl group in MPEG 200 MA. This study has, therefore, illustrated that it is possible to detect ether groups at the polymer surface using this technique and suggests that the explanation proposed in the preceding section for the increase in the surface energies of these terpolymers may well be valid.

7.4 Lipid and Protein Deposition Studies

The use of hydrogels in the fabrication of soft contact lenses is perhaps the most successful application of these materials. However, the range of monomers used in their fabrication has to date been somewhat limited and most of commercial materials 'spoil' in the ocular environment. Hence, considerable efforts have been made within the Speciality Materials group at Aston to primarily understand the spoilation process and to synthesise

new materials with enhanced ocular compatibility. Linear polyethers have already been shown to exhibit enhanced biocompatibility and hence such monomers may offer a unique opportunities in the design of new contact lens materials. However, the transport studies discussed in Chapter 6 illustrated that these polyethers may also sequester calcium ions and thus reduce the ocular compatibility of linear polyether terpolymers. This Section, therefore, is concerned with the results obtained in a study of the ocular compatibility of a range of linear poly (ethylene oxide) based terpolymers and assesses their potential uses in the quest for materials with enhanced are ocular compatibility. Initially, however, the techniques used to study these properties will be described.

The chemistry of tears is extremely complex since their composition not only varies between individuals but will also alter if tears are stimulated by external factors. For example the chemistry of tears which result from exposure to onions are quite different from that of the unstimulated tear film. Thus, it is difficult to obtain consistent and reproducible results for *in vivo* ocular spoilation studies. This problem, however, has been circumvented at Aston with the development of an *in vitro* spoilation model. The exact details of this model are beyond the scope of this thesis but have been described in greater detail by Franklin[175]. This model is used to mimic the ocular spoilation process and employs a standard artificial tear solution based on fœtal calf serum and phosphate buffered saline (pH 7.4). This solution is similar to natural tears and offers further opportunities to 'spike' the system with other tear components such as mucin, lactoferrin and lysozyme. The deposition of both protein and lipids can be detected non destructively using fluorescence spectroscopy. In addition, by exciting at both 360 nm and 280 nm and monitoring the growth of the lipid and protein spoilation peaks at 400-600 nm, it is possible to gain further information about the spoilation process. Finally, since this model is *in vitro* it offers the opportunity to test a broader range of copolymer

compositions than *in vivo* methods would allow.

The *in vitro* ocular spoilation model has been used here to assess whether the artificial tear film compatibility of HEMA based hydrogels might be improved by copolymerisation with linear polyethers monomers. A range of HEMA based terpolymers which contained a variety of poly (ethylene oxide) monomers were studied. These monomers were chosen so that the effects, if any, of increasing polyether chain length, increasing polyether content, structural variations in the polyether side chain and increases in crosslinker content on the properties of these materials could be assessed.

The deposition of both lipids and proteins from spiked and unspiked artificial tear solutions was monitored every 7 days for 28 days using fluorescence spectroscopy. Typical examples of the spectra obtained are illustrated in Figures 7.7 and 7.8. It is interesting to note that the fluorescence spectra indicated that in all cases the deposition of both lipids and proteins is greater than would be observed with commercial lenses. This effect has been attributed to both 'edge effects' and the surface rugosity of these samples. These results highlight the advantages of having a smooth optical surface. After 28 days the samples were removed from the model. The results indicated that in some cases lipid deposition had not been initiated even after the equivalent of up to 3 weeks simulated continuous wear. A typical pattern for lipid deposition is illustrated by Figure 7.9.

Figure 7.7 Fluorescence spectra excited at 360nm

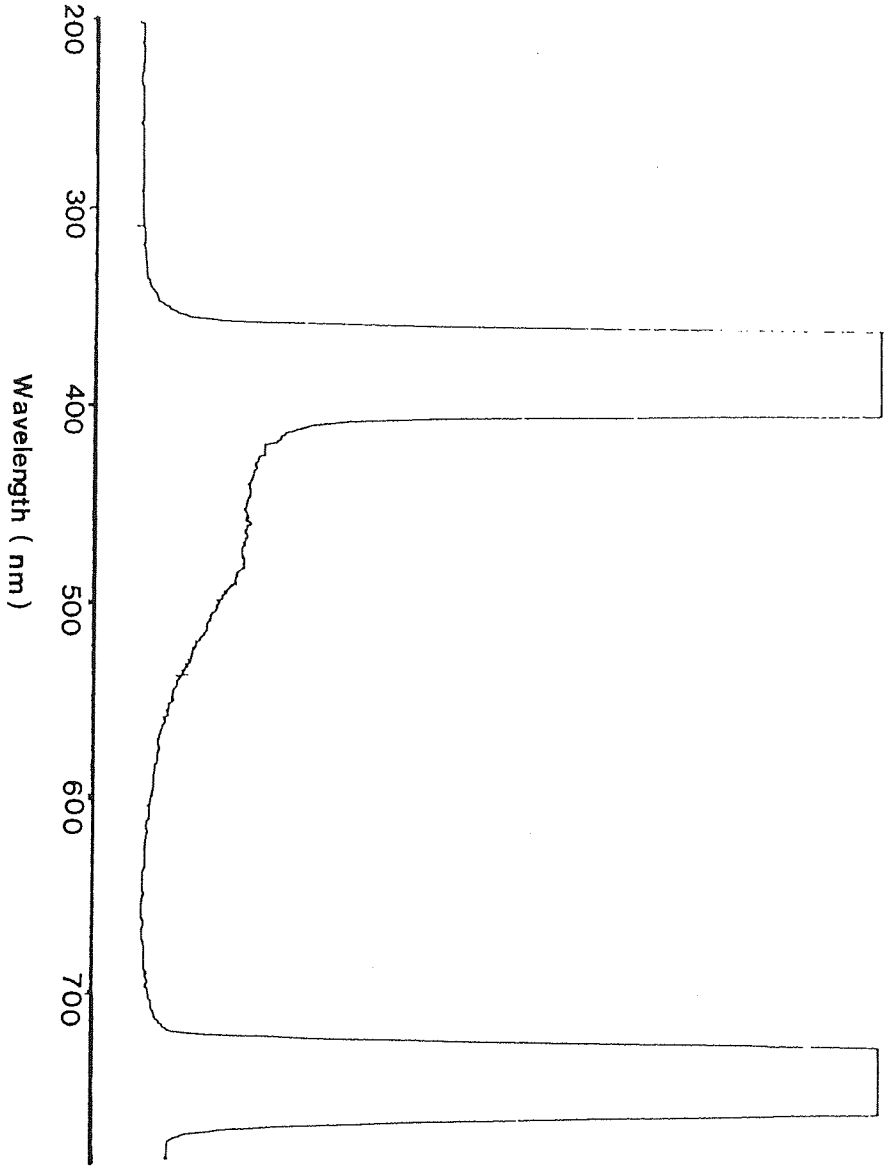

Figure 7.8 Fluorescence spectra excited at 280nm

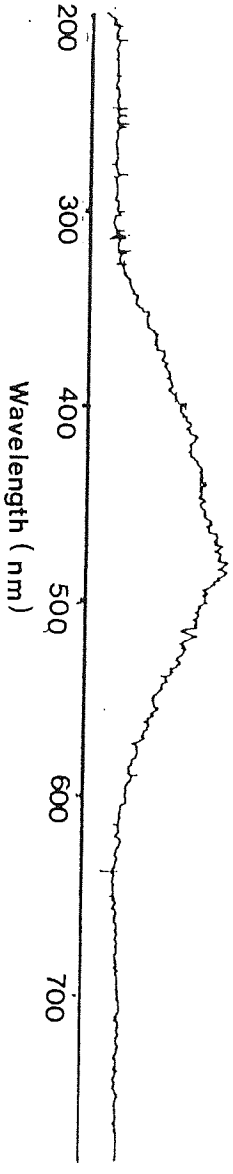

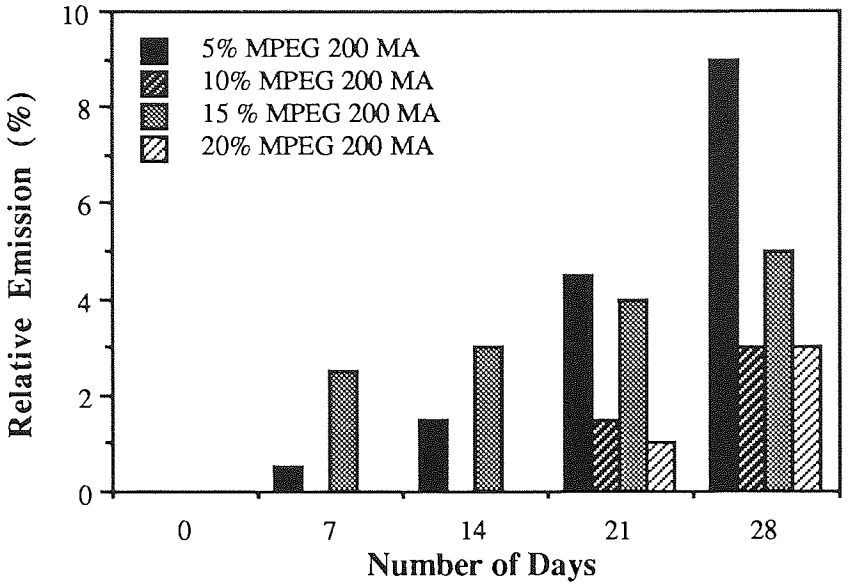

Figure 7.9 Typical deposition of lipid on a poly (ethylene oxide) modified HEMA copolymer with time

7.4.1 Effect of Poly (ethylene oxide) Chain Length on Ocular Spoilation

Monomethoxy polyethylene glycol methacrylates (MPEG MA's) which contain 4 to 5, 9 to 10, 11 to 12 and 22 to 23 repeating OCH_2CH_2 units respectively were chosen to study the effects of increases in polyether chain length on the tear film compatibility of HEMA based hydrogels. The monomers HEMA and EGDM in the ratios of either 99:1 or 90:10 were copolymerised with 5 to 20% (wt/wt) of these monomers. The ocular compatibility of these materials was then assessed using the *in vitro* ocular spoilation model. The fluorescence spectra were determined over a period of 28 days. The average height of emission peaks was taken to indicate the lipid deposition and these values were then used to obtain values for the combined average lipid deposition from both spiked and unspiked tear solutions. The results for a range of terpolymers based on HEMA:EGDM (99:1) are illustrated in Figure 7.10.

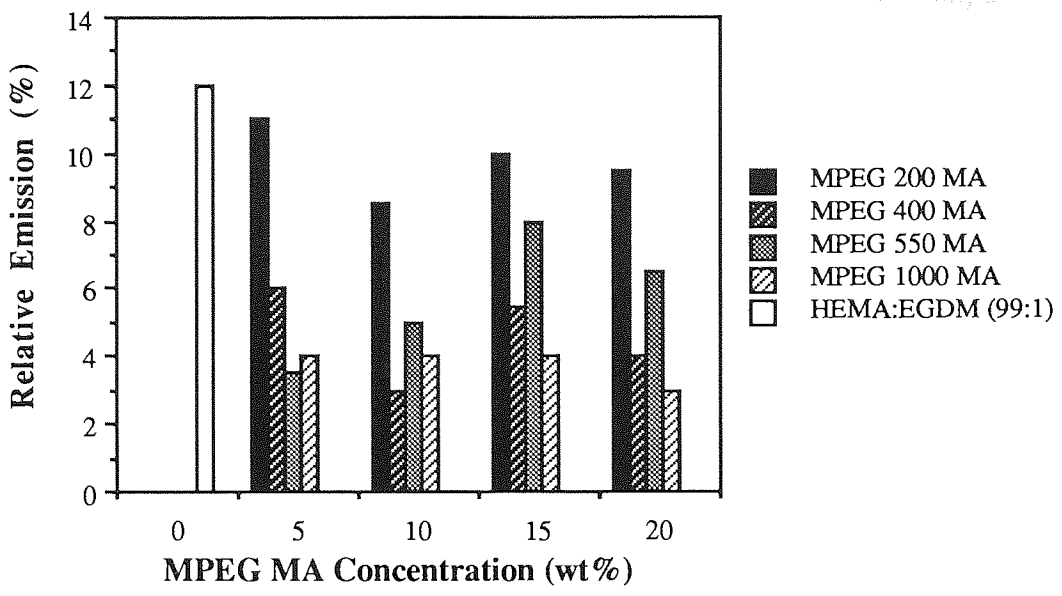

Figure 7.10 Effect of polyether chain length on lipid deposition to methoxy polyethylene glycol methacrylate modified HEMA:EGDM (99:1) terpolymers

The experimental error associated with the determination of percentage emission is approximately 5%. Hence, Figure 7.10 illustrates that in all cases, with the exception of the terpolymer with MPEG 200 MA, the relative emission for these terpolymers is lower than the value obtained for the unmodified membrane HEMA:EGDM (99:1). This, suggests that lipid deposition is reduced by copolymerisation with linear polyether monomers. Furthermore, these results also imply that in all cases the MPEG 200 MA comonomer is least effective in preventing the deposition of lipids. In addition, whilst there generally appears to be a gradual reduction in lipid deposition as the polyether chain length increases for the MPEG 200 MA, MPEG 400 MA and MPEG 10000 MA series, when the experimental errors are again considered it is apparent that MPEG 400 MA and MPEG 1000 MA are equally effective in suppressing lipid deposition. MPEG 550 MA copolymers, however, produce anomalously high lipid depositions. One plausible

explanation for this result is that the monomer MPEG 550 MA contains impurities which inhibit polymerisation and hence the effective concentration of the polyether at the surface is reduced. There is some evidence support this explanation. Whilst MPEG MA's with poly ethylene glycols (PEG's) of Mw 200, 400 and 1000 were obtained from the same supplier, a different source was used to obtain the MPEG 550 MA monomer and difficulties have been observed in preparing homopolymers using similar monomers from this source. Finally, the results shown in Figure 7.10 also imply that increasing concentrations of polyether apparently have little effect on lipid deposition.

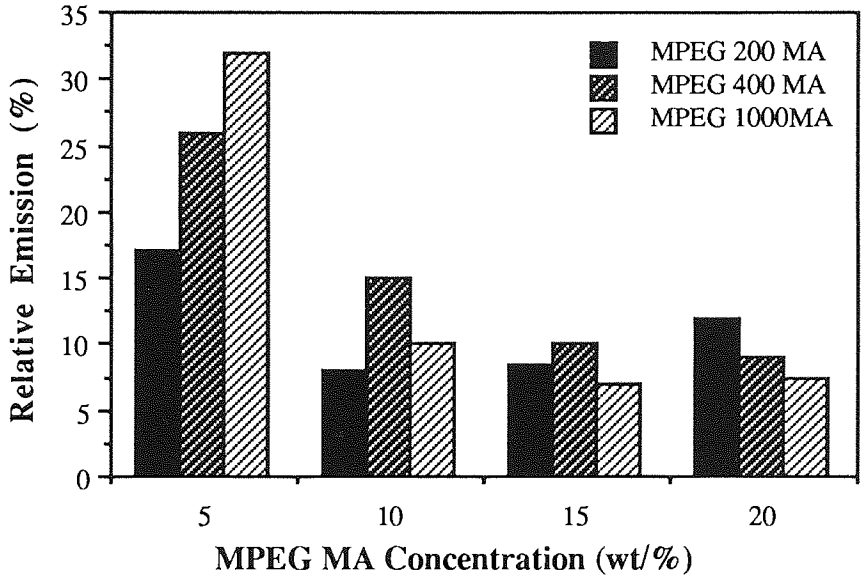

Figure 7.11 Effect of polyether chain length on lipid deposition to methoxy polyethylene glycol methacrylate modified HEMA:EGDM (90:10) terpolymers

Figure 7.11 shows the lipid deposition after 28 days for a range of HEMA:EGDM (90:10) copolymers. These results indicate that the relationship between increasing polyether chain length and decreasing lipid deposition observed in Figure 7.10, is no longer

apparent except at a 20% loading of these monomers. In addition, in this series the MPEG 200 MA copolymers are no longer most susceptible to lipid deposition. These results do, however, suggest that lipid deposition for the MPEG 400 MA and MPEG 1000 MA terpolymers, is generally reduced as the concentration of polyether increases.

The deposition of proteins on some of these copolymers was also studied. The results for the combined average for protein deposition from both spiked and unspiked tears after 28 days of simulated continuous wear for both HEMA:EGDM (99:1) and HEMA:EGDM (90:10) based terpolymers are illustrated in Figures 7.12 and 7.13 respectively.

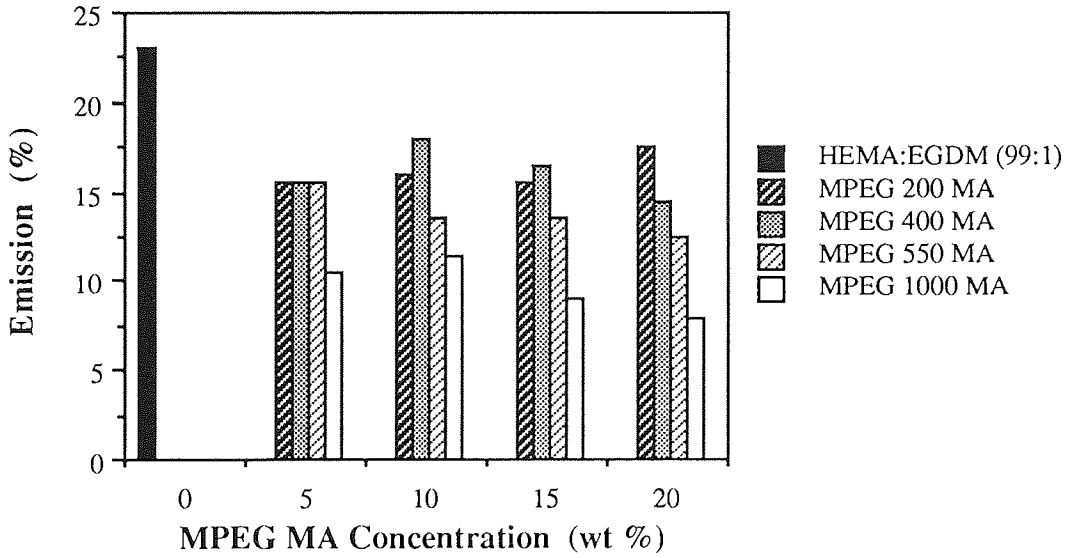

Figure 7.12 Effect of polyether chain length on protein deposition to methoxy polyethylene glycol methacrylate modified HEMA:EGDM (99:1) terpolymers

It is interesting to note that Figure 7.12 illustrates that protein deposition on the MPEG 1000 MA copolymers is significantly lower for all compositions. This is also true for the HEMA:EGDM (90:10) copolymers with the exception at 5% (wt/wt) loading of the MPEG 1000 MA comonomer (Figure 7.13), thus, suggesting that longer chained polyethers might be more effective at restricting protein deposition.

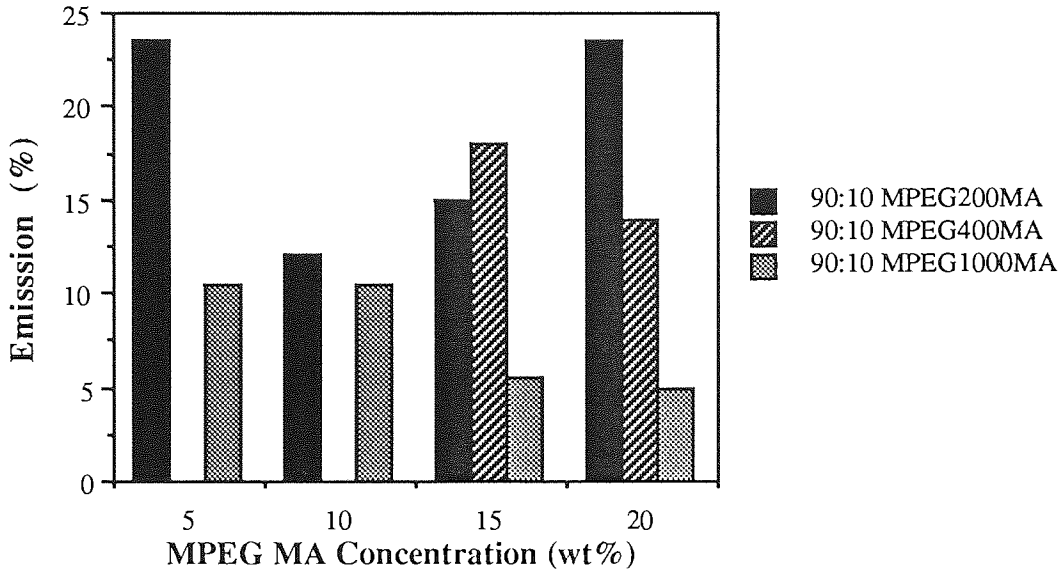

Figure 7.13 Effect of polyether chain length on protein deposition to methoxy polyethylene glycol methacrylate modified HEMA:EGDM (90:10) terpolymers

This argument is enhanced further by the general trend of decreasing protein deposition with increasing polyether chain length. However, there are notable exceptions. Primarily, the results in Figure 7.12 imply that protein deposition to terpolymers with 5% loadings of MPEG 200 MA, MPEG 400 MA and MPEG 550 MA is unaffected by increasing polyether chain length. Secondly, the results in Figure 7.13 show that the MPEG 400 MA copolymers exhibit enhanced protein deposition as the polyether chain length increases from 4, 5 to 9, 10 OCH_2CH_2 repeat units.

7.4.2 Effect of Crosslinker Content on the Deposition of Proteins and Lipids.

The effect of increasing crosslinker concentrations on the deposition of both proteins and lipids was studied. The monomers HEMA and EGDM in the ratios of 99:1, 95:5 and

90:10 were copolymerised with 5% (wt/wt) of either MPEG 200 MA, MPEG 400 MA or MPEG 1000 MA. The results for the lipid and protein deposition after 28 days are illustrated in Figures 7.14 and 7.15 respectively.

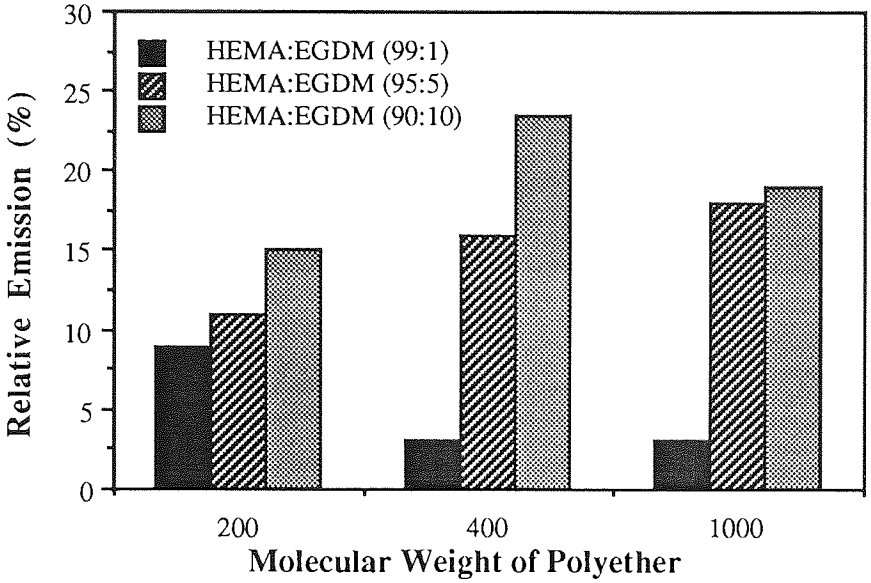

Figure 7.14 Effect of crosslinker concentration on lipid deposition to methoxy polyethylene glycol methacrylate modified terpolymers

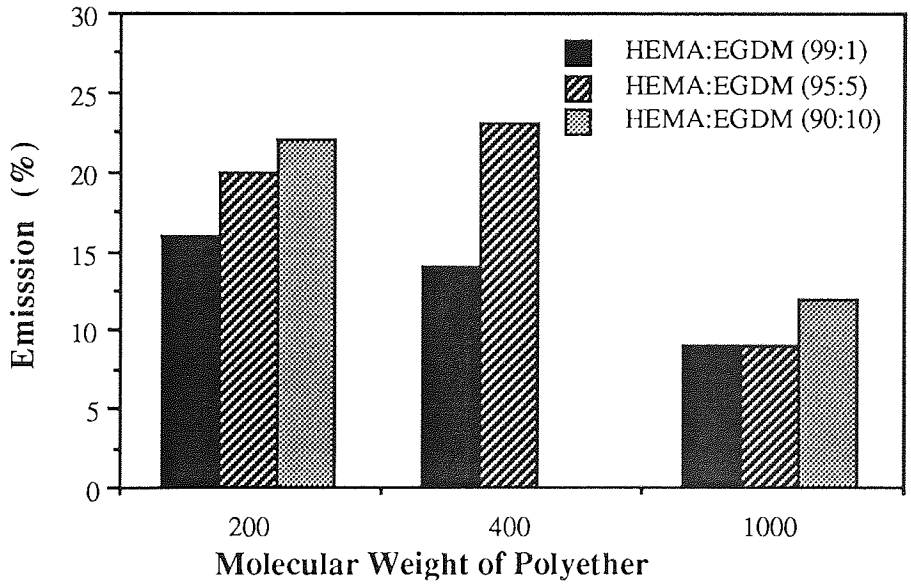

Figure 7.15 Effect of crosslinker concentration on protein deposition to methoxy polyethylene glycol methacrylate modified terpolymers

These Figures illustrate that both lipid and protein deposition are enhanced as the concentration of crosslinker, EGDM, increases. This result, however, is not unexpected. Lipid and protein deposition is thought to be reduced by the presence of long flexible poly(ethylene oxide) chains at the polymer surface. Moreover, increases in crosslinker concentration will restrict chain mobility within the gel, thus reducing the expression of poly(ethylene oxide) groups at the surface. Additionally, as the concentration of crosslinker increases the hydrophobicity of the surface is enhanced. Hence, lipid and protein deposition would be expected to increase as the crosslinker concentration rises.

7.4.3 Effect of Structural Variations in the Polyether Side Chain on Ocular Compatibility

This Section is concerned with the results which were obtained from a study of the effects of structural variations in the polyether side chain on the ocular compatibility of range of HEMA:EGDM (99:1) based terpolymers. Of particular interest were the effects, if any, of either substituting a hydroxyl for a methoxy end group or replacing a hydrogen in the polyether side chain with a methyl group, on the deposition of both proteins and lipids. For this purpose the monomers HEMA 4,5 EO, PEGMA 10 EO and HPHPMA were chosen.

The monomers HEMA 4,5 EO and PEGMA 10 EO are structurally similar to MPEG 200 MA and MPEG 400 MA in that they both contain similar numbers of repeating OCH_2CH_2 units. However, in the former case the polyether side chain is terminated by a hydroxyl group and in the latter it is terminated by a methoxy group. The lipid deposition after 28 days for a range of these terpolymers prepared from these monomers was determined. The results are illustrated in Figure 7.16.

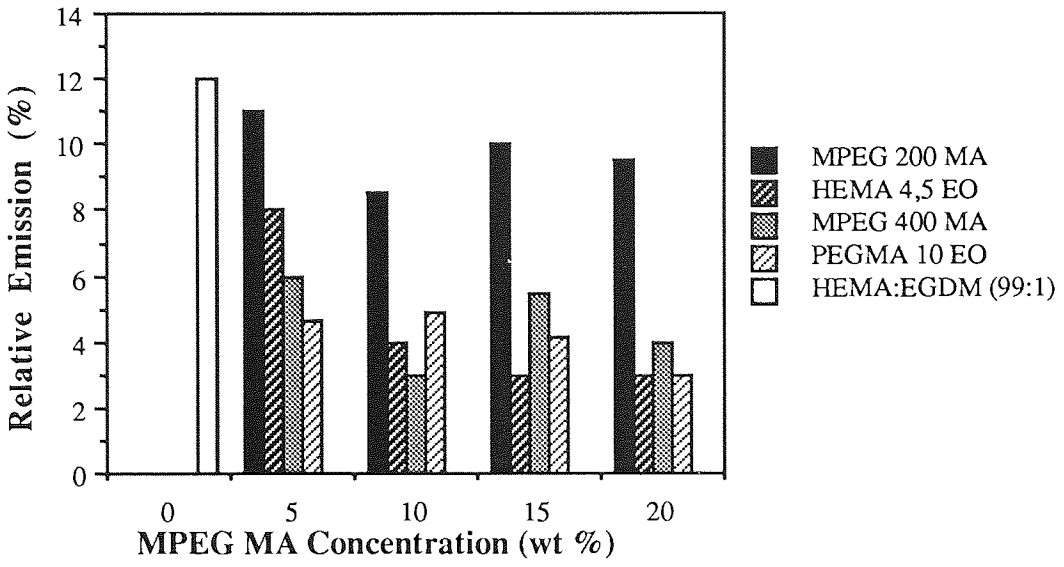

Figure 7.16 Effect of hydroxy vs methoxy end groups on lipid deposition to poly(ethylene oxide) modified HEMA:EGDM (99:1)

Figure 7.16 indicates that in general lipid deposition is reduced with hydroxyl terminated polyethers. In particular, by substituting the methoxy group of MPEG 200 MA with a hydroxyl as in HEMA 4, 5 EO, lipid deposition is significantly reduced. Increases in the poly ethylene glycol chain length of the hydroxyl terminated side chain, however, except at 5% (wt/wt) loadings of the do not reduce lipid deposition further.

The protein deposition has also been studied and the results are illustrated in Figure 7.17.

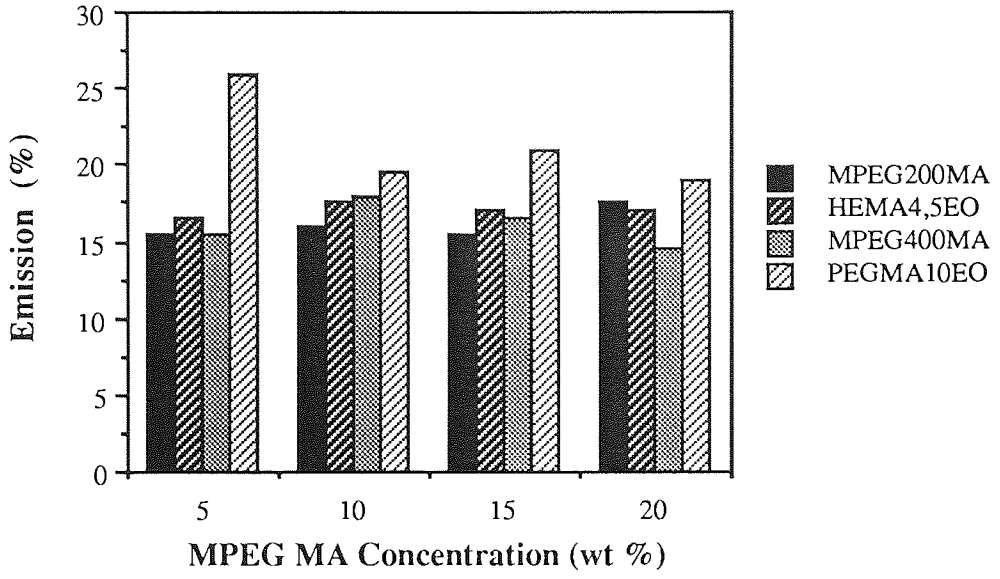

Figure 7.17 Effect of hydroxy vs methoxy end groups on protein deposition to poly(ethylene oxide) modified HEMA:EGDM (99:1)

Figure 7.17 illustrates that protein deposition, unlike lipid deposition, is enhanced by the presence of a hydroxyl group at the end of the polyether side chain. However, when the errors associated with the measurement of these emission peaks are taken into consideration it is apparent that this effect is only significant with the PEGMA 10 EO terpolymers. This result is not, however, entirely unexpected since previous studies discussed in Section 5.3.1 have highlighted the affinity of hydroxyl terminated monomers for hydrogen bond formation. Therefore, since protein molecules readily form hydrogen bonds it is likely that protein deposition in this case is enhanced via the formation of hydrogen bonds. Furthermore, it might anticipated that this effect might be greatest as chain flexibility i.e the poly (ethylene oxide) chain length increases. Since the PEGMA 10 EO terpolymers do show generally show enhanced protein deposition, the results obtained in this study suggest that protein deposition is enhanced via the formation of

hydrogen bonds between the hydroxyl groups at the ends of the polyether side chains and protein molecules.

A range of terpolymers containing a propyl ether was prepared by adding various concentrations of the monomer hexapropoxylated hydroxypropylmethacrylate, HPHPMA to a mixture of HEMA:EGDM (99:1) (wt/wt). The lipid and protein deposition from 'spiked' and 'unspiked' tears were studied to illustrate the effect of replacing an ethereal hydrogen with a methyl substituent, on the surface properties of these terpolymers. Unfortunately, terpolymers containing 6 repeating OCH_2CH_2 units were not available for comparison. However, since MPEG 200 MA and MPEG 400 MA contain 4 to 5 and 9 to 10 repeat units respectively, the values obtained for lipid and protein fluorescence for terpolymers containing these terpolymers are given for comparison. Figures 7.18 and 7.19 illustrate the lipid and protein deposition after 28 days respectively.

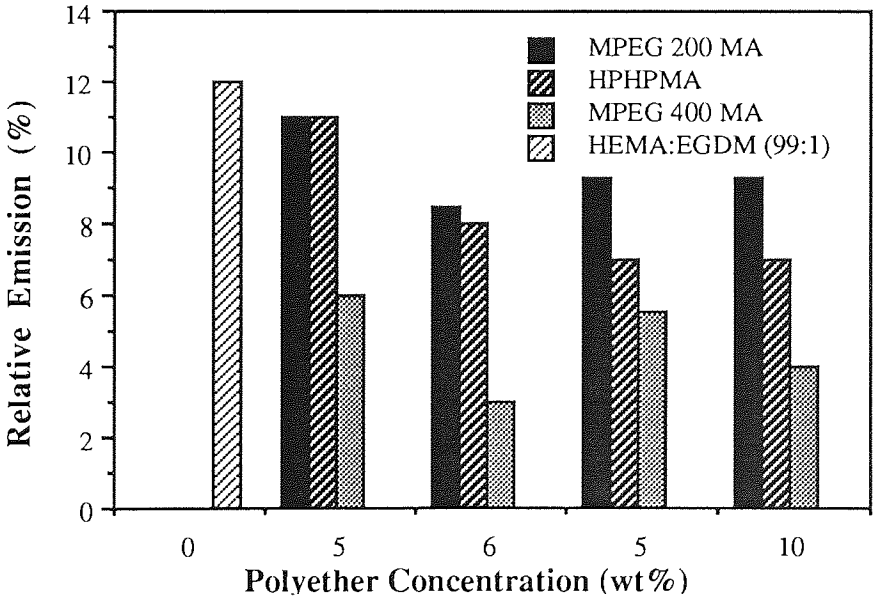

Figure 7.18 Effect of a methyl substituent in the polyether side chain on lipid deposition to poly(ethylene oxide) modified HEMA:EGDM (99:1)

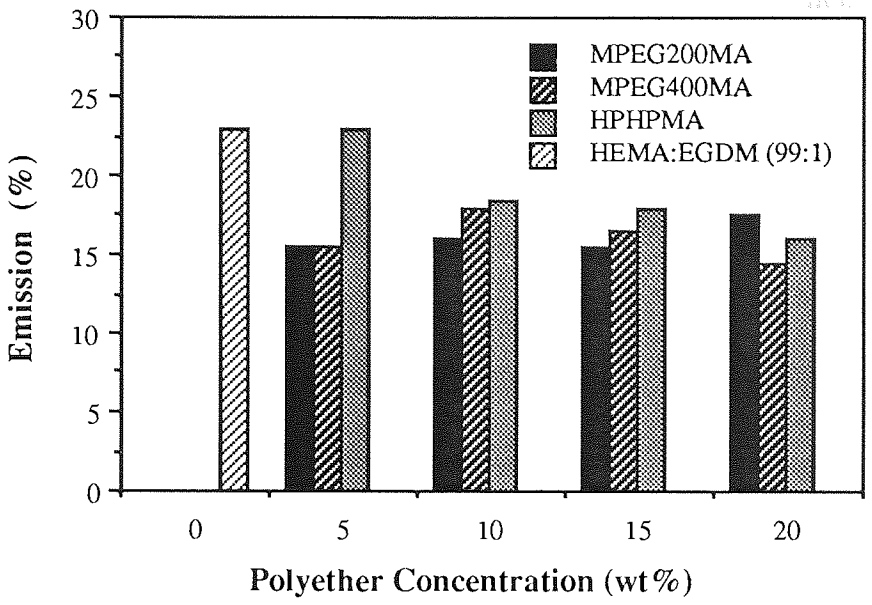

Figure 7.19 Effect of a methyl substituent in the polyether side chain on protein deposition to poly(ethylene oxide) modified HEMA:EGDM (99:1)

Figure 7.18 illustrates that in all cases lipid deposition on HPHPMA terpolymers is lower than for the unmodified poly HEMA membrane. However, when the experimental errors are taken into consideration it is apparent that the presence of a methyl substituent does not significantly effect lipid deposition on ether containing terpolymers. Similar results are observed for protein deposition where with the exception of the terpolymers modified with 5% (wt/wt) of HPHPMA the methyl substituent in the polyether side chain has little effect on protein deposition.

7.4.4 Ocular Spoilation Studies on Novel Soft Contact Lenses

The results described in the preceding Sections have highlighted the potential improvements in ocular compatibility which result from copolymerisation with linear polyether monomers. The results also indicated that in all cases the lipid and protein

depositions were higher than for commercial lenses a factor which is probably due to the surface rugosity of these materials and 'edge effects' produced during the polymerisation. Lathe cut lenses were fabricated using PEGMA 10 EO and MPEG 400 MA. Care was taken to ensure that the EWC of these lenses matched that of poly HEMA. This was achieved by copolymerising with methyl methacrylate and n-vinyl pyrrolidone. The *in vitro* ocular spoilation of these materials was then studied. The results obtained in this study are compared with those obtained for poly HEMA lenses in Figure 7.20. Figure 7.20 illustrates that lipid and protein deposition is reduced for the lenses containing linear polyethylene oxides. In addition, if these results are compared with the results obtained for the hydrogel membranes (Figures 7.10 to 7.20) it is apparent that the overall fluorescence due to both lipid and proteins are reduced if the edge effects and the surface rugosity are reduced. Finally, these results illustrate the great potential of these materials for applications in the ocular environment and these lenses are currently being evaluated in *in vivo* trials.

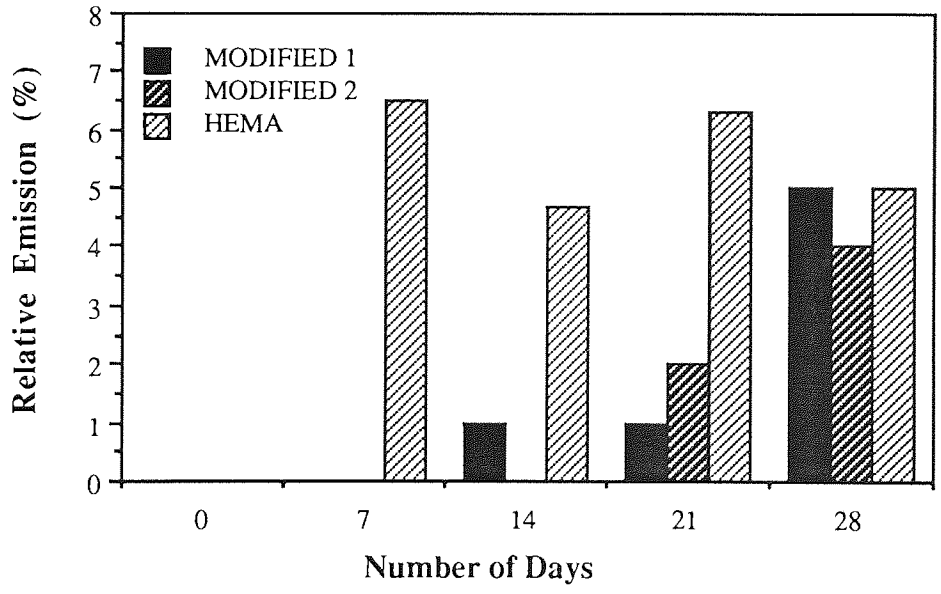

Figure 7.20 Deposition of lipid with time on novel contact lenses containing poly (ethylene oxides)

7.5 Cell Adhesion to poly(ethylene oxide) Terpolymers

Cell culture or tissue culture is a technique which has been developing rapidly during the past decade. This technique makes use of the fact that under certain well defined conditions cells can be kept alive *in vitro*. Such cells can then be used to probe the surface properties of materials on a molecular scale. This Section is concerned with the results obtained from some preliminary investigations to assess the effects of various poly(ethylene oxide) comonomers on the adhesion of 3T3 cells. A complete description of the experimental technique used in these studies is beyond the scope of this thesis, however, they have been well documented elsewhere by Thomas[176].

A range of monomethyl polyethylene glycol methacrylate terpolymers was prepared by copolymerising 20% (wt/wt) loadings of MPEG MA's of Mw 200, 400 and 1000 with a mixture of HEMA:EGDM (99:1). The effect of polyether chain length on the adhesion of 3T3 cells was then studied. In addition, a terpolymer containing 20% HEMA 4,5 EO (wt/wt) which contains the same number of repeating OCH_2CH_2 units as MPEG 200 MA, was also studied to assess the effect of a polyether terminated with a hydroxyl group as opposed to a methoxy group on cell adhesion. After 4 hours the cell growth was determined and the results are illustrated in Figure 7.21. This Figure indicates that cell adhesion ceases abruptly once the Mw of the polyether chains exceeds 200. These results also indicate that cell adhesion to the terpolymer containing the hydroxyl terminated polyether is greater than to the methoxy terminated derivative. Although these results are significant it is inadvisable to draw too many conclusionsusing the data from only one set of experiments. However, it is interesting to note that these results are in agreement with the earlier studies discussed in Section 7.4.1 and 7.4.3. In Section 7.4.1 it was shown that lipid deposition like cell adhesion , in the MPEG MA series, is greatest for MPEG 200 MA terpolymers and that further increments in the polyether chain length i.e as the

Mw increases from 400 to 1000 have a negligible effect on lipid deposition. Additionally, the results discussed in Section 7.4.3, indicate that protein deposition is enhanced with hydroxy terminated polyether monomers. Since cell adhesion is known to be enhanced once a protein layer has been deposited on the polymer surface[176], it reasonable to expect that enhanced protein deposition will be mirrored by enhanced cell adhesion.

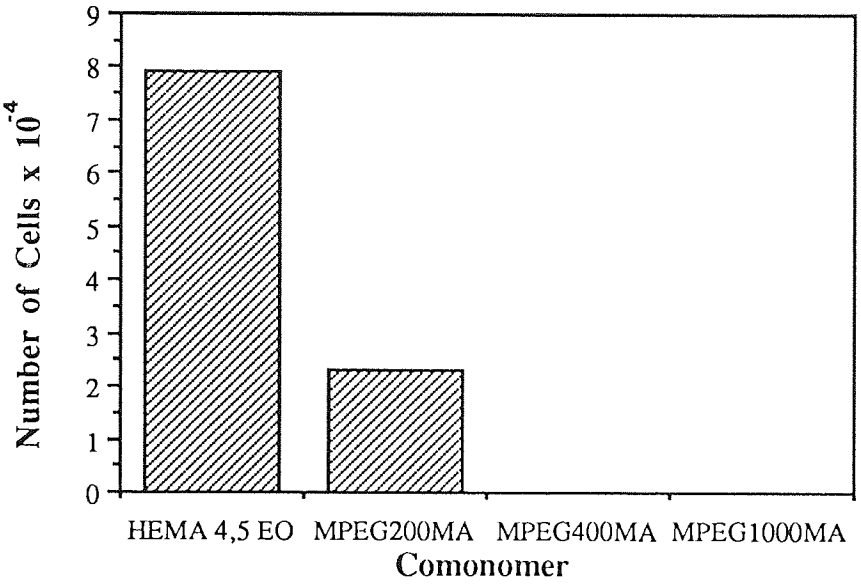

Figure 7.21 Adhesion of 3T3 cells to poly(ethylene oxide) modified terpolymers

7.6 Conclusions

The surface properties of a range of poly(ethylene oxide) terpolymers have been studied on both a macroscopic and molecular level. The macroscopic surface properties were probed using both contact angle goniometery and horizontal ATR FTIR. The contact angle measurements indicated that the polar component of the surface free energy, γ_s^p, generally increases with increasing polyether content, whislt the dispersive component, γ_s^d, increases with the initial addition of poly(ethylene oxide) but falls as the

concentration of poly(ethylene oxide) added to the comonomer mix increases. The values for γ_s^p and γ_s^d have been used to calculate the corresponding values for the hydrated polymer, γ_{hs}^p and γ_{hs}^d. The total surface free energy for both the dehydrated and hydrated polymer surfaces were also calculated and the values obtained indicated that the total surface free energy increases with increasing concentration of polyether in the copolymer mix. In addition, the polar fraction of the total surface free energy increases dramatically with relatively small increments in EWC. These results suggested that the polar OCH_2CH_2 repeat units in the polyether side chain must have a significant effect on the surface energy of the polymer and that such groups are expressed at the polymer surface. The preliminary horizontal ATR FTIR studies illustrated that it is possible to detect subtle changes in chemistry at the surface of a hydrated polymer using this technique. The subtraction spectrum indicated that ether groups can be detected at the polymer surface and this evidence supports the explanation for the observed increases in the total surface free energy.

Ocular spoilation and cell adhesion studies were used to study the surface properties of these terpolymers on a molecular scale. The *in vitro* ocular spoilation model was used to study the ocular compatibilities of a range of poly(ethylene oxide) based terpolymers. These results have demonstrated the potential of this model for the use in the assessment of new materials for ocular devices. In addition, the results obtained in this study indicated that copolymerisation with poly(ethylene oxide) monomers does enhance the ocular compatibility. Further analysis of this experimental data indicates that some general conclusions may be drawn concerning the structure-property relationships of these materials. Firstly, the ocular compatibility of HEMA:EGDM (99:1) based copolymers is not significantly enhanced by copolymerisation with MPEG 200 MA, but ocular compatibility increases as the Mw of the poly ethylene glycol, PEG increases from 200 to

400 i.e. as the polyether chain length increases. However, further increments in the Mw of the PEG, from 400 to 1000, do not appear to enhance the ocular compatibility of HEMA:EGDM (99:1) based terpolymers. Secondly, increasing the crosslinker concentration of the gel enhances ocular spoilation and this effect has been attributed to restrictions in chain mobility and the increase in hydrophobicity as the degree of crosslinks within the polymer was increased. Thirdly, lipid deposition is reduced if the methoxy group at the end of the polyether chain is replaced with a hydroxyl group. Protein deposition, however, is enhanced if the polyether side chain is terminated by a hydroxyl group. Furthermore, this effect is more pronounced as the length of the polyether side chain is increased and has been attributed to the formation of hydrogen bonds between the hydroxyl end group of the polyether chains and protein molecules. Finally, substituting a hydrogen on the ether group with a methyl group to form a propyl ethylene oxide, does not appear to effect either protein or lipid deposition.

The preliminary results from the cell adhesion studies show similar trends to those observed in the *in vitro* spoilation studies. Cell adhesion cuts of dramatically as the molecular weight of the PEG in MPEG MA increase from 200 to 400. In addition, as with lipid and protein deposition further increments in Mw have no discernable effect on cell adhesion. Similarly, if the methoxy group at the end of the polyether chain is replaced with a hydroxyl group the adhesion of cells is further enhanced, an effect which has been attributed to the preferential formation of hydrogen bonds between the hydroxyl group of the polyether side chain and the protein .

In conclusion, the results described in this Chapter have highlighted some of the unique surface properties of these linear polyether terpolymers. These studies have illustrated that the properties of acrylate based hydrogels may be significantly enhanced by adding

relatively small amounts of these monomers to the comonomer mix. Finally, this study has illustrated the potential applications of acrylate:linear polyether copolymers not only in the fabrication of novel ocular devices but also in the design of materials for low affinity separation polymers.

CHAPTER 8

Conclusions and Suggestions for Further Work

8.1 Conclusions and Final Discussions

A range of hydrogel copolymers based on 2-hydroxyethyl methacrylate (HEMA) which contain either linear or cyclic polyethers was synthesised. Because both cyclic and linear polyethers are known to complex with metal cations, particular emphasis was placed on the ion transport properties of these copolymers. A detailed study of the transport properties these materials has been completed. The results from this study are not only consistent with results obtained in previous studies but have highlighted a potential mechanism for ion transport through crown ether modified membranes.

Other workers have shown that linear polyethers enhance the biotolerance of synthetic polymers. In general two methods have been used to synthesise polymers containing poly (ethylene oxides). These methods are copolymerisation with isocyanates to form a polyether polyurethane network and grafting of the poly(ethylene oxide) on to the polymer surface. In these studies, however, methacrylate derivatives of poly (ethylene oxides) have been copolymerised with other methacrylates, HEMA and EGDM. Thus, a range of synthetically versatile terpolymers were prepared and characterised. Particular emphasis was placed on the surface properties of these terpolymers and the conclusions which may be drawn from these studies will now be discussed in greater detail.

Previous studies at Aston had illustrated that it is possible to occlude a potassium selective ionophore, dicyclohexano-18-crown-6, within a crosslinked HEMA membrane. Preliminary studies of the transport properties of crown ether modified membranes indicated that the presence of a crown ether has a significant effect on ion transport. Linear induction periods, or 'lag-times' in potassium ion transport were observed before a final steady state was reached in which ion transport was significantly lower than for the unmodified membrane. It was essential, therefore, to consolidate and extend these earlier

observations. However, since the effect of a high crosslink density on ion transport had not been fully investigated, it was first necessary to study the factors affecting ion transport through an unmodified crosslinked HEMA copolymer.

The results obtained from studies of salt transport through an unmodified crosslinked HEMA copolymer illustrated that, in general, ion transport is governed by the relative size of the hydrated cation and the nature of the counter anion. However, these studies also implied that the transport group II metal cations and of sulphate salts through this copolymer is inhibited. A study of the transport of a mixed solution of group I and II metal chlorides confirmed that group II metal cation transport through this copolymer is effectively 'blocked' and highlighted the potential of hydrogels for use in range of permselective applications.

Further investigations illustrated conclusively that the effect that the presence of an occluded crown ether, dicyclohexano-18-crown-6, imparts on ion transport is a reproducible phenomenon and suggested that ion transport through the modified membranes may be described by a dual-sorption mechanism. However, the results indicated that the exact values for both 'lag-times' and permeability coefficients are less reproducible than for the unmodified membranes due to localised variations in crown ether concentration. This study was then extended to consider the effect of anion variation on ion transport. The results indicated that at the extremes of the Hoftmeister series the anion affects ion transport in different ways: the 'lag-time' decreases and rate of ion transport in the final steady state increases with the water structure breaking anion SCN^-, while 'lag-times' in excess of 24 hours were observed for the water structure making anion $S_2O_4^{2-}$. However, the anions Cl^-, Br^- and NO_3^{2-} all affect ion transport in a similar manner. A simple calculation of the salt to crown ether ratio at the 'lag-time' produced a value of 2:5.

This result suggests that the initial induction period might arise from a gradual partitioning of the metal cation with the crown ether. In addition, this ratio implies that after the initial induction period ion transport may be facilitated by a site-hopping mechanism. The attempts made to extend these studies using other crown ethers established that the range of crown ethers which can be occluded in this copolymer are limited by both ionophore loss during hydration and the solubility of the crown ether in the comonomer mix. Hence attempts were made to overcome this problem with the synthesis of a range of monomeric crown ethers.

Initially, several reaction schemes were considered based on benzo-15-crown-5 and dibenzo-18-crown-6, which selectively bind to sodium and potassium respectively. However, problems were encountered with the reactions outlined in these schemes due to relatively small scales on which these reactions were carried out and the aqueous solubilities of the products. The route to 4-acryloylaminobenzo-15-crown-5 proved most accessible and hence efforts were concentrated on the synthesis of this monomer. Preliminary studies of the effect of 4-acryloylaminobenzo-15-crown-5 on the transport of sodium ions through crosslinked HEMA membranes produced anomalous results. The results suggested that the linear induction periods observed for systems containing unbound crown ether were no longer present with the systems containing a bound crown ether. Furthermore, sodium ion transport through the bound crown ether system appeared to be enhanced. However, these results were attributed in part to the presence of acrylic acid as an impurity in the monomer 4-acryoylaminobenzo-15-crown-5. Considerable efforts were made, therefore, to ensure that a pure sample of the monomer was prepared. Further transport studies indicated that for terpolymers which were synthesised using a pure sample of the monomer ion transport is modified in a similar way to the systems which contain unbound crown ether with ion transport being

described by a dual-sorption mechanism.

Linear polyethers can also form complexes with metal cations. Although this process may be advantageous in applications which require permselectivity, if linear polyethers are able to sequester metal cations from biological solutions this may lead to long term biointolerance. Hence, the transport properties of a range of HEMA, poly ethylene glycol methacrylate based terpolymers were studied. The primary data for the transport of group I metal cations across these membranes illustrated that although the transport of sodium ions is inhibited the linear induction periods observed for systems containing cyclic ethers are no longer present. Group II metal cation permeation mimics the dual-sorption behaviour observed for the systems containing cyclic ethers. However, for the transport of group II metal cations through copolymers modified with linear polyethers the changes in the rate of ion permeation are much less pronounced.

Extensive studies were made of the effects of both copolymer composition and polyether structure on EWC. In general, increases in EWC are observed as both the concentration and chain length of the polyether increase. Subtle variations in EWC were observed when the hydroxyl group at the end of the polyether chain was replaced by a methoxy group. Terpolymers containing the hydroxyl terminated polyether were expected to have enhanced EWC's. However, compositions with a low degree of crosslinking agent and hence greater chain mobility were found to have lower EWC's than the comparable copolymers containing methoxy terminated polyether side chains. This effect was attributed to the formation of a internal crown ether type structure for the polyether side chain. Conversely, as the proportion of crosslinker increased and hence chain mobility decreased, EWC was enhanced due to the preferential water-hydroxyl group interactions. Finally, reductions in EWC were observed with the introduction of a methyl substituent to

the polyether side chain.

The surface properties of terpolymers containing methacrylate derivatives of poly ethylene glycols were studied on both a macroscopic and a molecular scale. Macroscopic properties were probed using contact angle measurements on the dehydrated terpolymers and FTIR. The contact angle measurements illustrated that both the polar component of the total surface energy, γ_S^p and total surface energy, γ_S^t, increased as the polyether chain length and concentration of polyether increased. This effect has been attributed to the expression of the polar ether groups at the polymer surface and FTIR confirmed that ether group can be detected at the polymer surface. Although the dispersive component of the total surface energy remains relatively unaffected by the addition of polyether, slight depressions in γ_S^d are observed as the concentration of polyether increases, due to shielding of the α methyl group and the CH_2 groups in the polymer backbone by the polar ethereal side chains.

The surface properties were studied on a molecular level using *in vitro* ocular spoilation techniques and some preliminary cell adhesion studies. A systematic study of the effects of variations in terpolymer composition and polyether structure on the ocular compatibility was completed using an *in vitro* spoilation model. The results illustrated conclusively that ocular compatibility is improved by the presence of the polyether . Furthermore, a number of conclusions can be drawn relating ocular compatibility to terpolymer composition.

1) While ocular compatibility is improved as the molecular weight of the poly ethylene glycol increases from 200 to 400, further increases in Mw of the glycol do not enhance compatibility.

2) Increases in polyether concentration over the range studied in this work do not

significantly enhance ocular compatibility.

3) Increases in the concentration of crosslinker give rise to enhanced lipid and protein deposition.

4) Lipid deposition on terpolymers containing hydroxyl terminated polyether side chains is lower than for terpolymers containing the corresponding methoxy terminated derivative. Conversely, protein deposition to terpolymers containing the hydroxyl terminated polyether side chains is enhanced. This effect has been attributed to the formation of hydrogen bonds between the polyether side chains and the protein molecules.

5) The addition of a methyl substituent on the polyether side chain does not significantly enhance lipid and protein deposition.

Although the cell adhesion studies described in this thesis are of a preliminary nature it is encouraging to note that the results obtained are in agreement with the *in vitro* ocular spoilation studies. A dramatic 'cut-off' in cell adhesion was observed as the molecular weight of the poly(ethylene oxide) increased above 200. Additionally, cell adhesion to a terpolymer containing a hydroxyl terminated polyether was significantly higher than to a similar terpolymer containing methoxy terminated polyether side chains.

8.2 Suggestions for Further Work

In general crown ethers interact selectively with one metal cation and this process is governed by both the size of the crown cavity and the metal cation. However, crown ethers can also form 2:1 complexes with larger cations and there is evidence in the literature to suggest that polymeric crown systems modulate the transport of cations via the formation of 2:1 complexes. Hence, the transport studies of the bound crown systems described in this thesis should be extended to investigate whether crown ethers

immobilised within hydrophilic polymer matrices impart a similar effect on the transport of group I and II metal cations.

The synthetic route developed for the synthesis of a pure acryloyl derivative of benzo-15-crown-5 can be adapted to provide a series of crown ether based monomers. A range of monobenzo crown ethers are available and the final stage of the synthesis can be used to extend the series of monomers to include the methacryloyl derivatives. With a range of monomers it should be possible to modulate ion transport for a variety of metal cations and thus produce permselective membranes. Another potential application of hydrophilic immobilised crown systems is in the fabrication of chemical sensors. The two methods used to look at the interactions of hydrophilic polymers in previous studies namely, fibre optic and coated wire electrodes, could be used to test the suitability of hydrophilic linear polymers containing 4-acryloylamino-benzo-15-crown-5 for this application.

Ethylene oxide groups interact with water to form a number of hydrates and some water binding studies have been made on the polyether-polyurethane based hydrogels. However the water structuring or binding in the hydroxyalkyl methacrylate-linear polyether, polymers studied in this thesis might be expected to be more complex since the hydroxyl group can also structure water. In addition, an understanding of water structuring is important in the interpretation of the results obtained in studies of the transport properties. Hence, the water binding in these terpolymers should be studied. Furthermore, a study of the effects of salts on water binding might help elucidate the observed EWC's for the terpolymers described in these studies in the presence of group II metal cations.

The studies of the macroscopic surface properties of hydroxyalkyl methacrylate based

linear poly (ethylene oxide) copolymers suggest that the polyether groups are expressed at the surface. It would, therefore, be of interest to extend this study using both FTIR ATR and ESCA to see whether the concentration of these groups at the surface is dependent upon the concentration of polyether in the copolymer or the number of repeat units in the polyether side chain. Both the *in vitro* ocular spoilation and cell adhesion studies have illustrated the low affinity of the linear poly (ethylene oxide) terpolymers for biological species. One possible application of these materials is in the fabrication of low affinity chromatographic solid support phases.

Finally, an understanding of the copolymer structure at a molecular level is important. By determining the reactivity ratios of the monomers containing poly (ethylene oxide) units it should be possible to predict the copolymer structure using computative techniques.

APPENDIX 1

Nomenclature of Crown Ethers

Table 1 Nomenclature of crown ethers

STRUCTURE	NOMENCLATURE ACCCORDING TO		
	PEDERSEN	VOGTLE AND WEBER	IUPAC
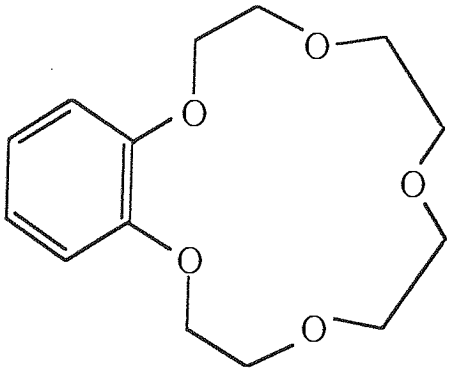	benzo-15-crown-5	15<O_5-(1,2)benzeno.2_4 coranand-5>	2,3,benzo-1,4,7,10,13-pentaoxacyclopenta-decane

APPENDIX 2

Spectral Data For Synthesis of Crown Ether Monomers

Infra-red Spectra

All infra-red spectra described in this thesis were obtained from a Perkin-Elmer FTIR spectrometer model 1710 coupled to a 3600 data station using the KBr disc method.

NMR Spectra

The nmr spectra described in this thesis were obtained using a Bruker AC 300 MHz spectrometer. Unless otherwise stated $CDCl_3$ was used as the solvent.

Figure 1 Infra-red spectrum of 4-nitrobenzo-15-crown-5

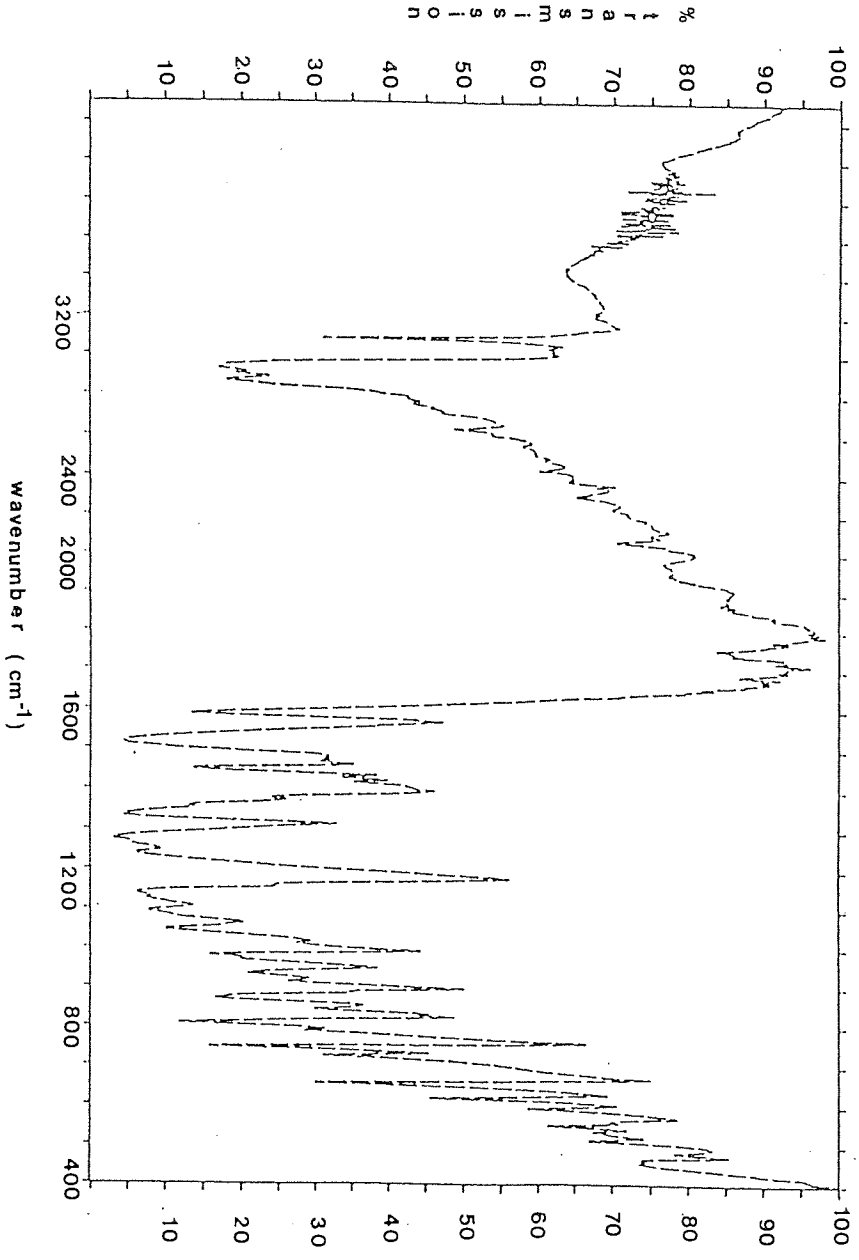

Figure 2 ^{1}H nmr spectrum of 4-nitrobenzo-15-crown-5

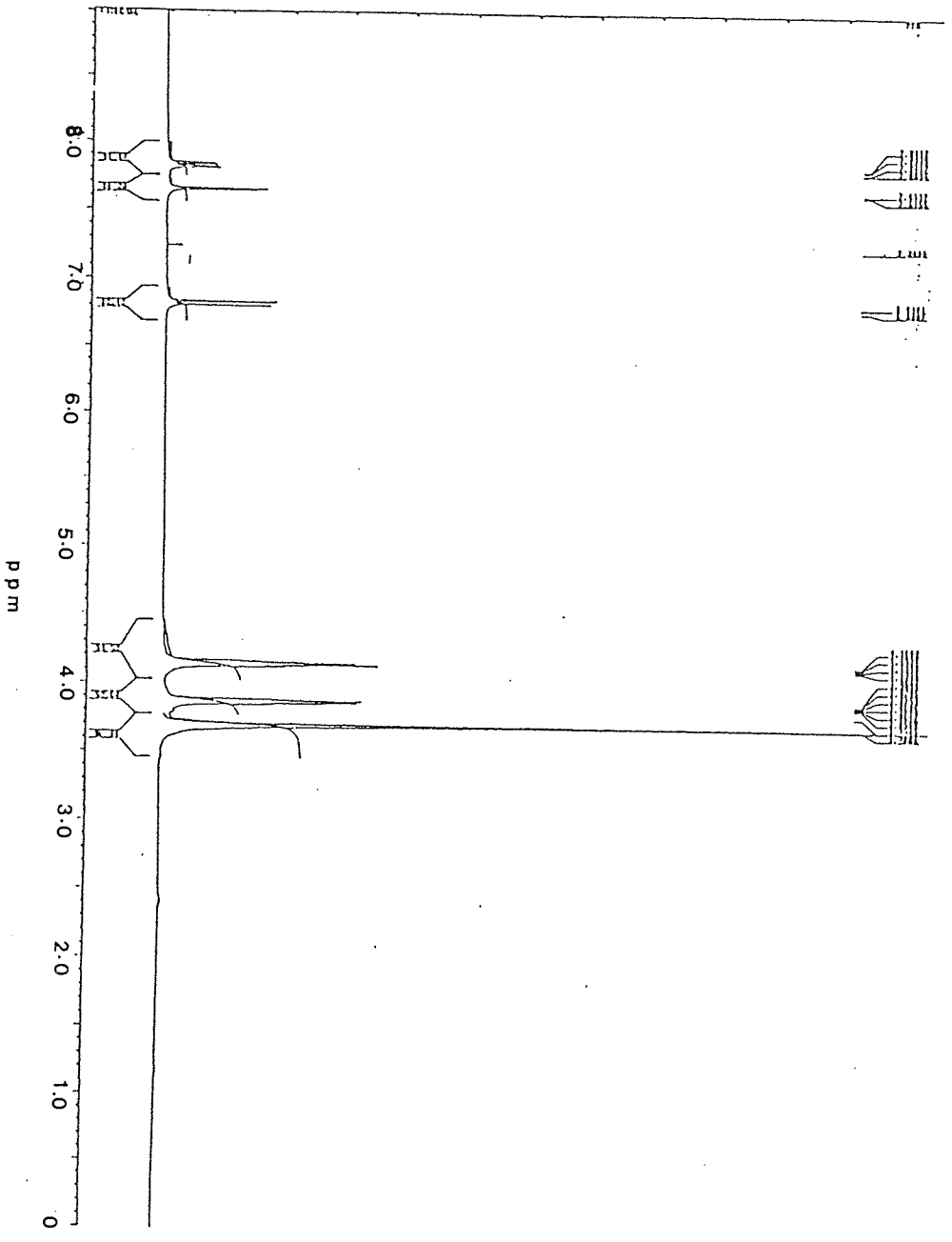

Figure 3 ^{13}C spectrum of 4-nitrobenzo-15-crown-5

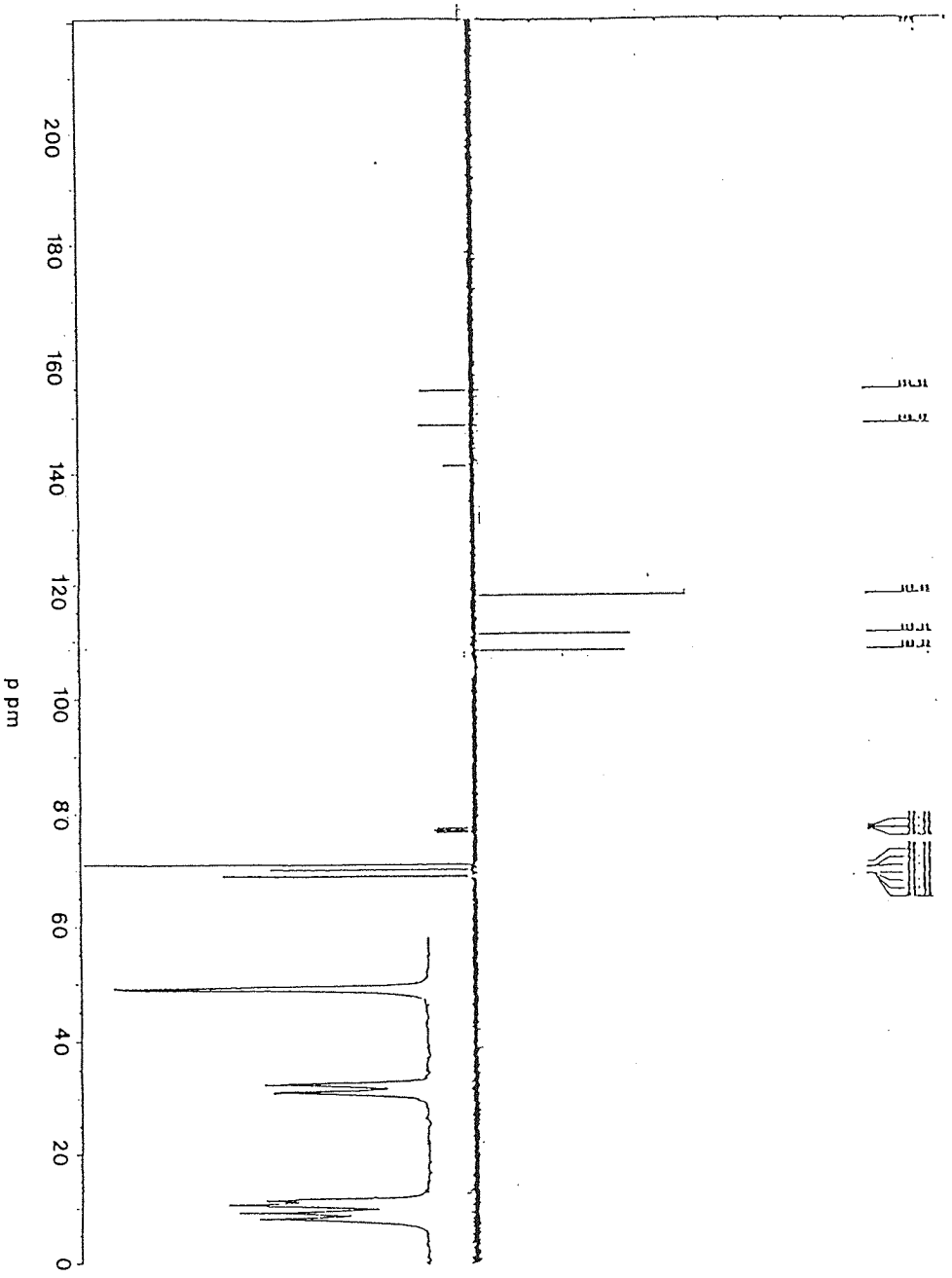

Figure 4 A two dimensional COSY spectrum of 4-nitrobenzo-15-crown-5

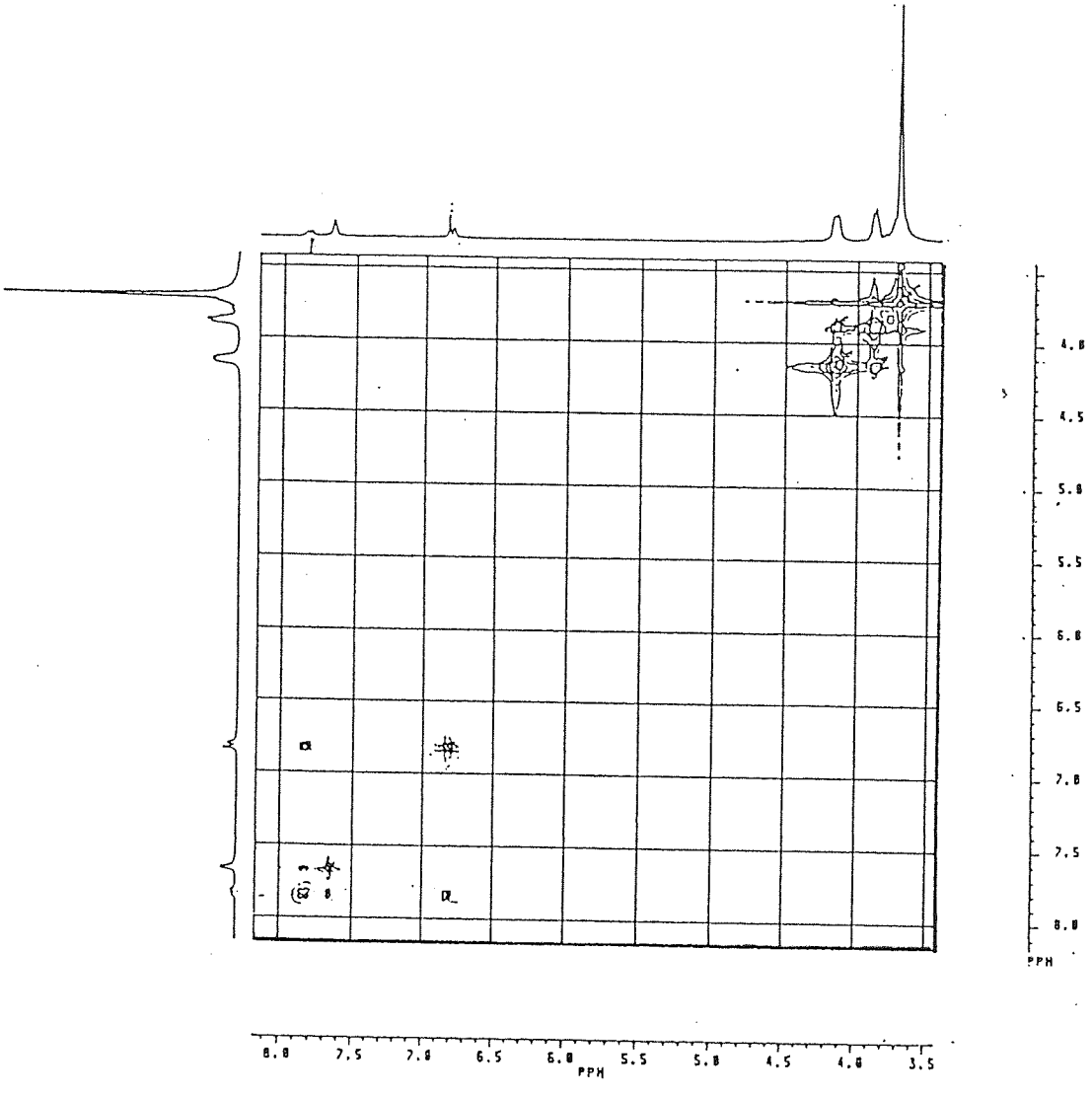

Figure 5 ^{13}C spectrum of 4-formylbenzo-15-crown-5

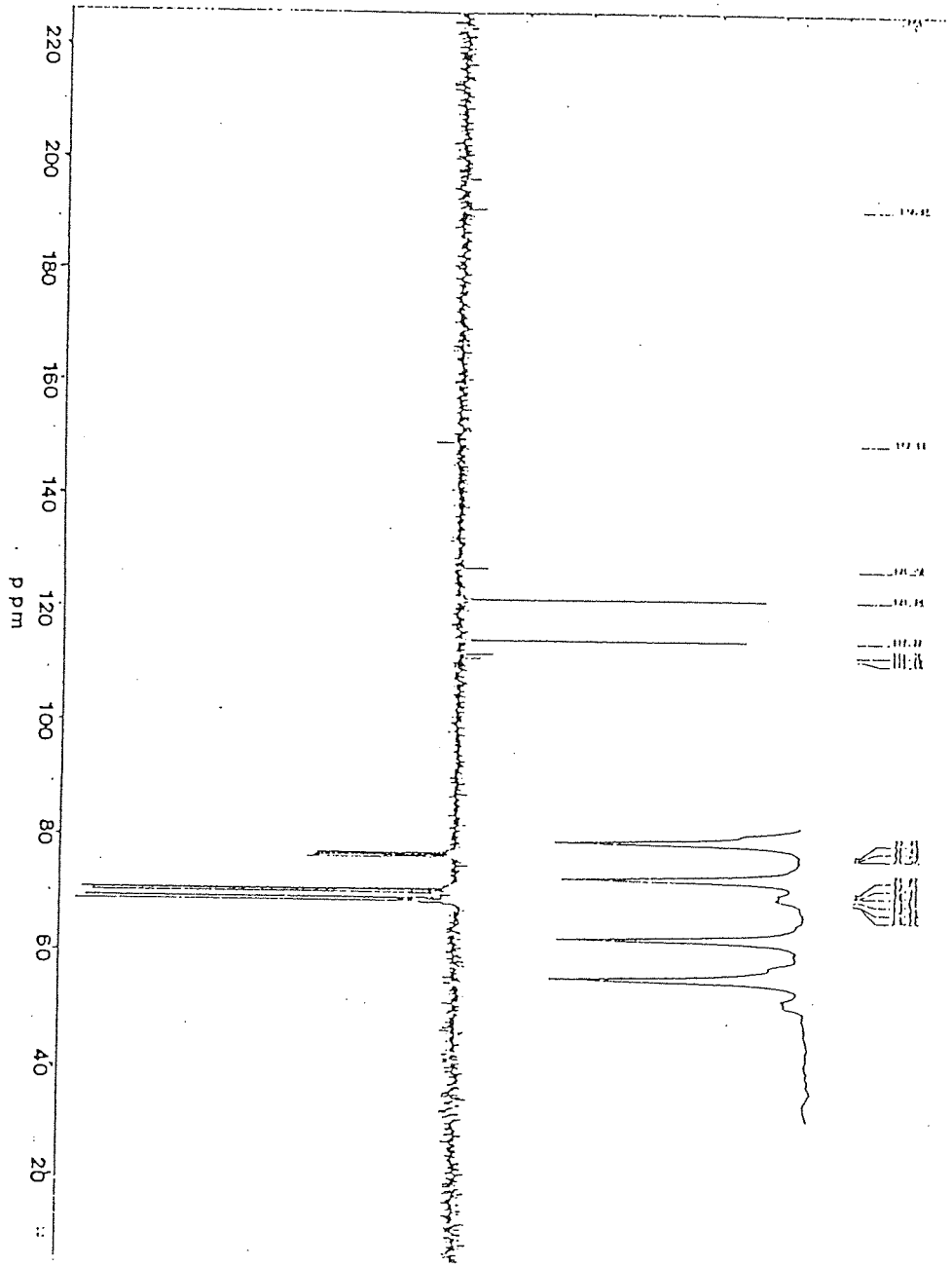

Figure 6 Infra-red spectrum of contaminated 4-acryloylaminobenzo-15-crown-5

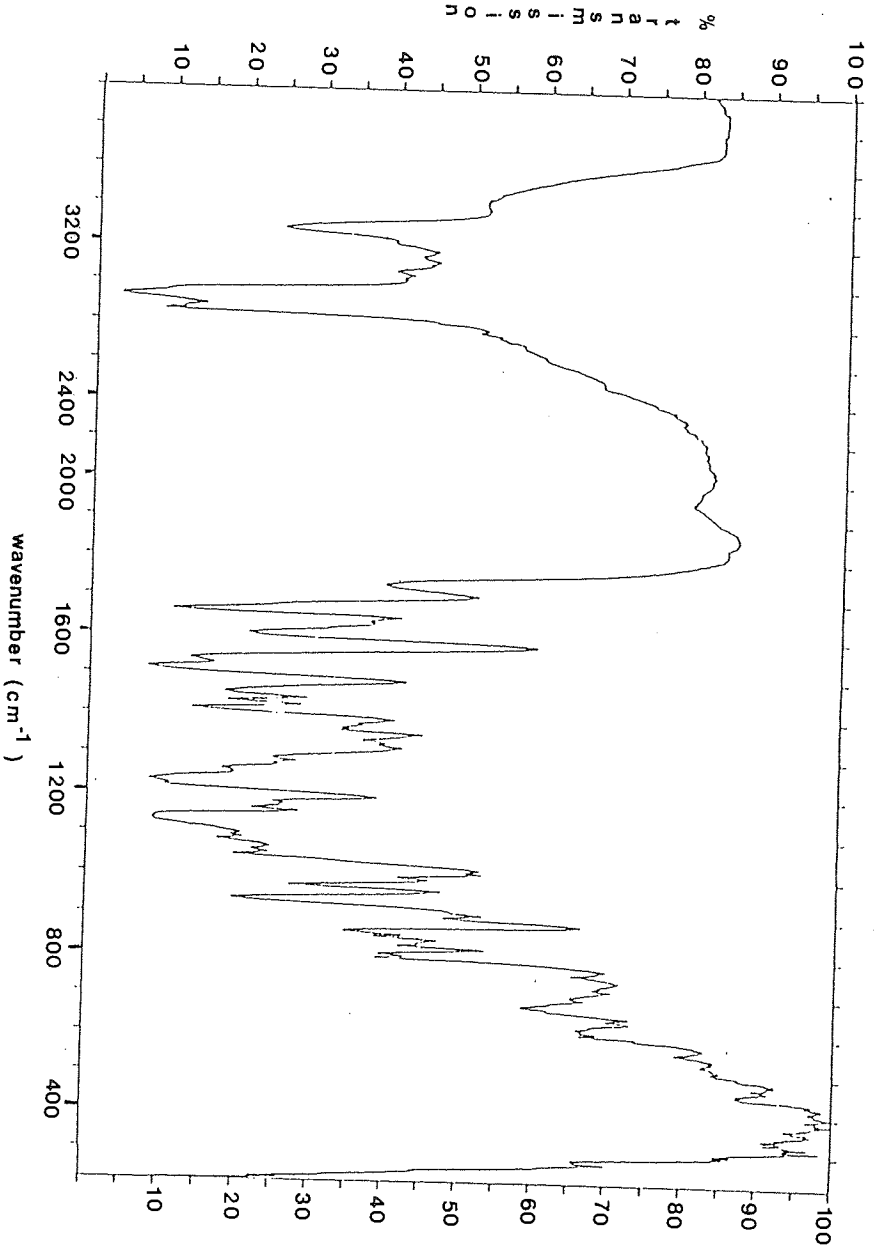

APPENDIX 3

Gel Permeation Chromatograms for Linear Polyether Monomers

Figure 1 Gel permeation chromatograms for the methoxy polyethylene glycol methacrylates (MPEG MA's)

Molecular weights are polystyrene equivalent molecular masses
Column - Pl gel 2 x mixed gel, solvent - THF, flow rate - 1 ml/min, refractive index detector and concentration 2mg/ml

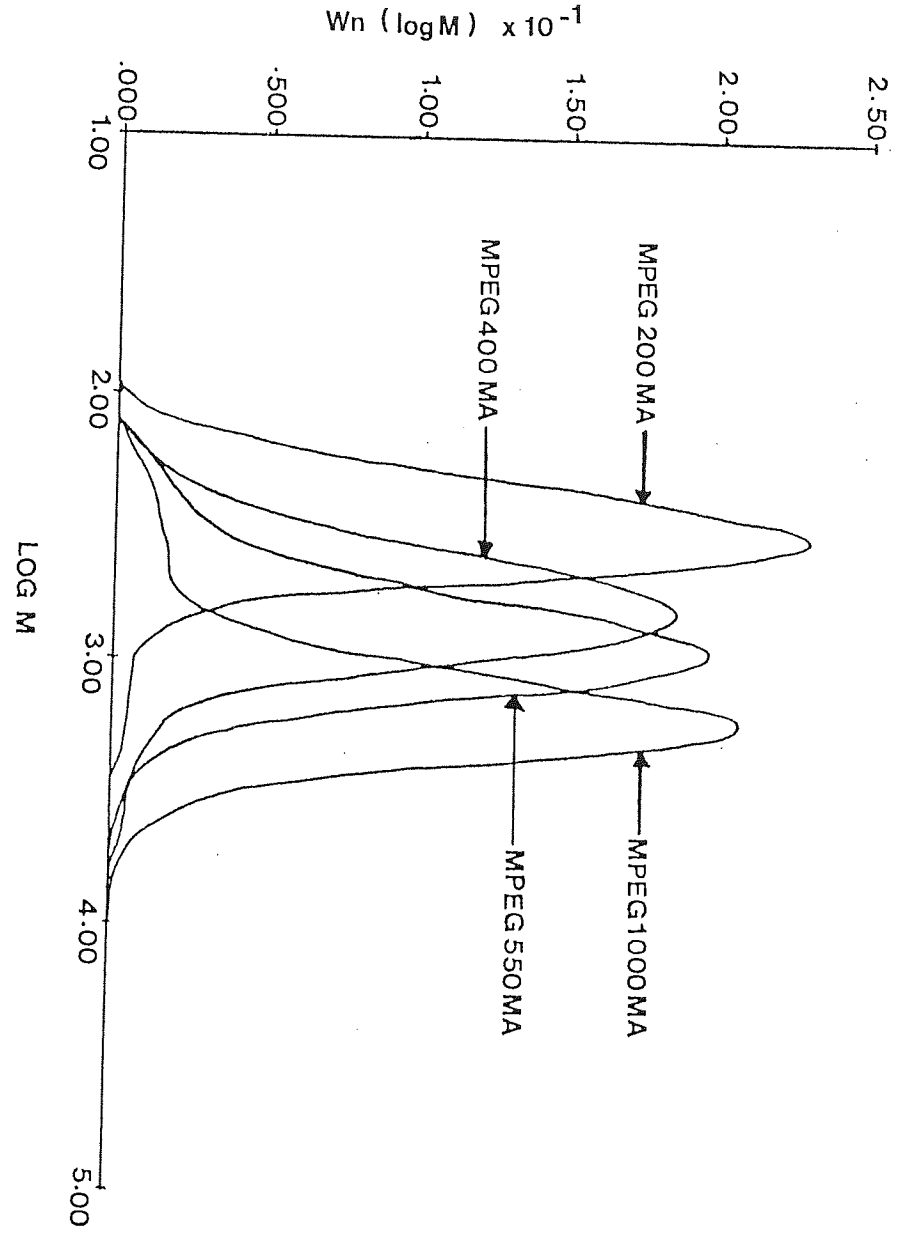

Figure 2 Gel permeation chromatogram for ethoxylated hydroxyethyl methacrylate (HEMA 4,5 EO)

Molecular weight is a polystyrene equivalent molecular mass
Column - Pl gel 2 x mixed gel, solvent - THF, flow rate - 1 ml/min, refractive index detector and concentration 2mg/ml

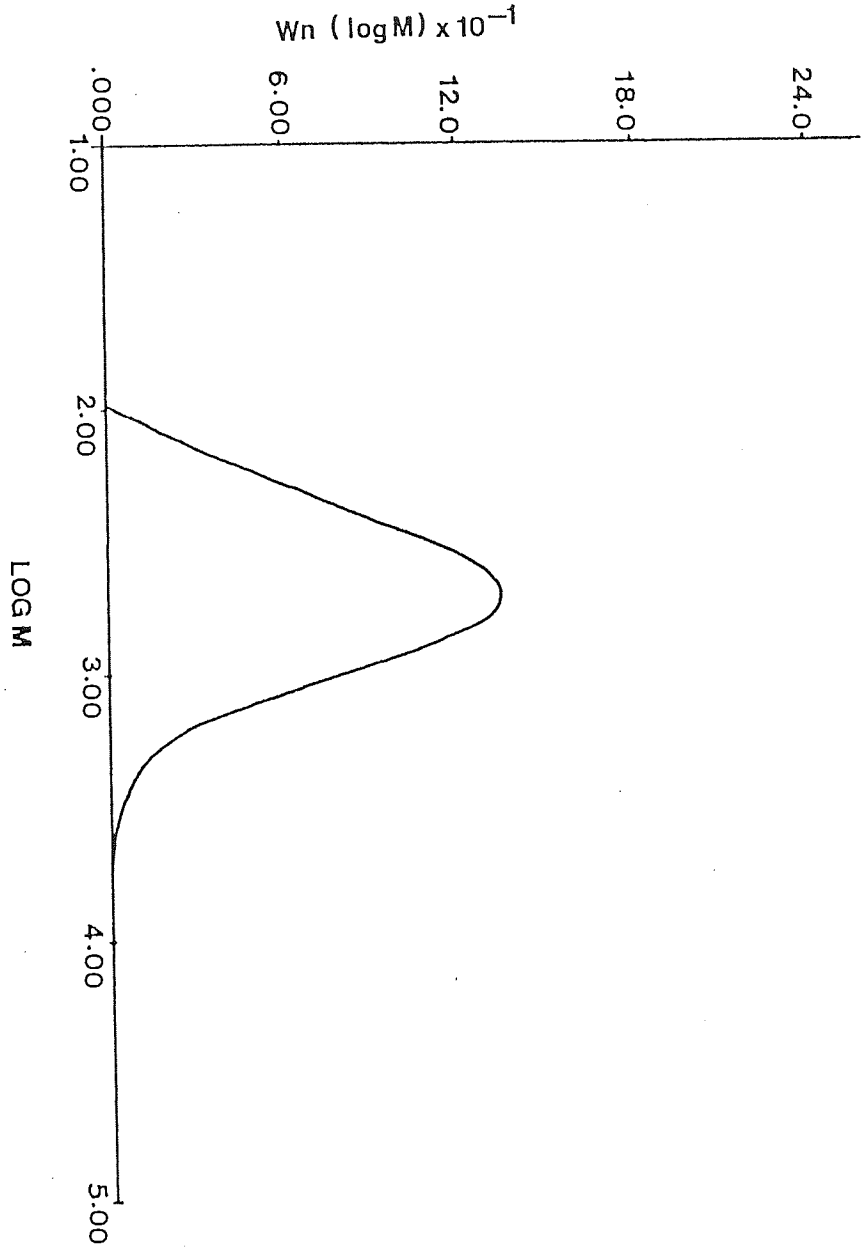

Figure 3 Gel permeation chromatogram for polyethylene glycol methacrylate (PEGMA 10 EO)

Molecular weight is a polyethylene glycol equivalent molecular mass
Column - Pl gel 2 x mixed gel, solvent - DMF, flow rate - 1 ml/min, refractive index detector and concentration 2mg/ml

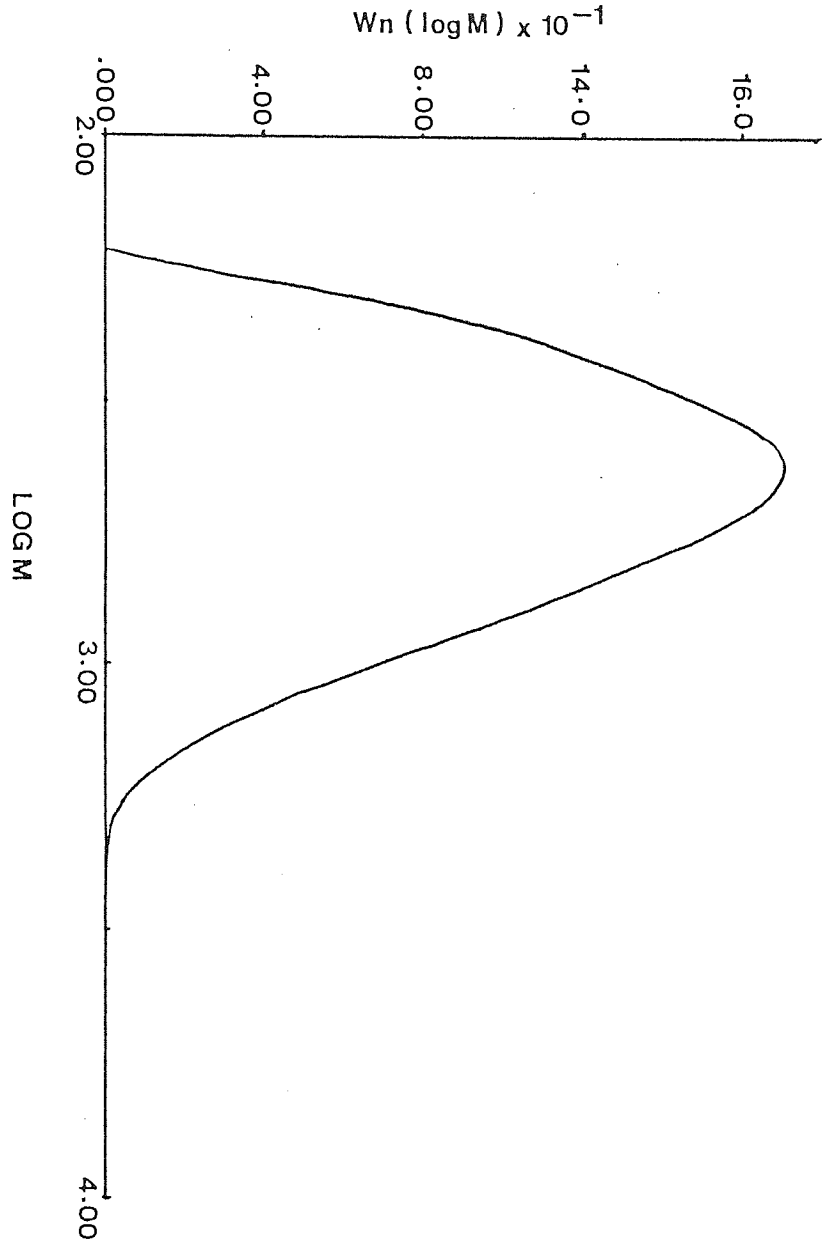

Figure 4 Gel permeation chromatogram for hexapropoxylated hydroxypropyl methacrylate (HPHPMA)

Molecular weight is a polystyrene equivalent molecular mass
Column - Pl gel 2 x mixed gel, solvent - THF, flow rate - 1 ml/min, refractive index detector and concentration 2mg/ml

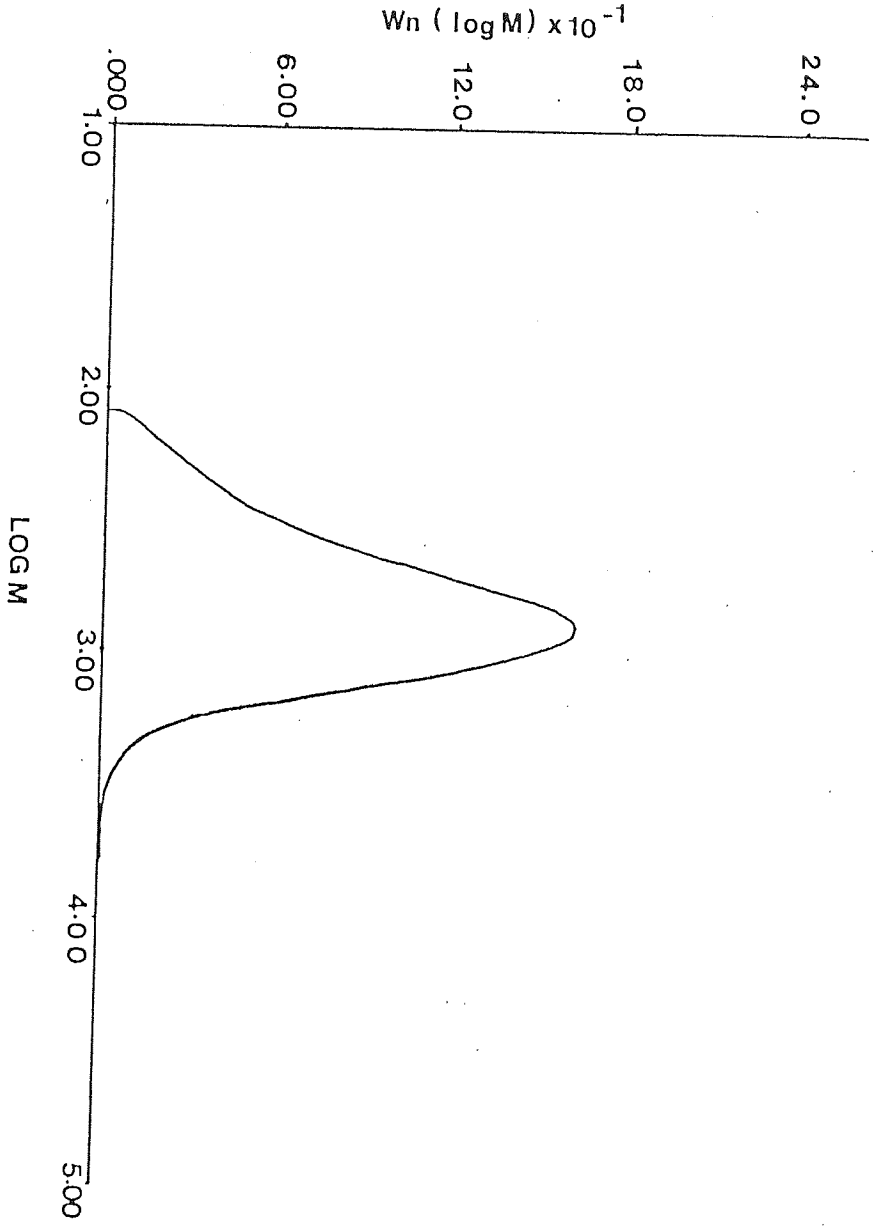

References

1 Wichterle, O. and Lim, D., Hydrophilic gels for biological use, Nature, 1960, 185 , 117-118

2 Tighe, B.J., Hydrogels as contact lens materials, in Hydrogels in Medicine and Pharmacy, Vol. III, Ed. Peppas, N.A., CRC Press, Boca-Raton, Florida, 1987, 53-82

3 Roorda, W.E., Boddé, H.E., de Boer, A.G. and Junginger, H.E., Synthetic hydrogels as drug delivery systems, Pharm. Weekbl. Sci Ed., 1986, 8 , 165-189

4 Corkhill, P.H., Hamilton, C.J. and Tighe, B.J., Synthetic hydrogels VI. Hydrogel composites as wound dressing and implant materials, Biomaterials, 1989, 10 , 3-10

5 Singh, H., Vasudevan, P., Misro, M., Ray, A.R. and Guha, S.K., Novel mode of contraception using polymeric hydrogels I, J. Biomed. Mater. Res., 1982, 16 , 3-9

6 Corkhill, P.H., Trevett, A.S. and Tighe, B.J., The potential of hydrogels as synthetic articular cartilage, Proc. Instn. Mech. Engrs., Part H, J. Engineering in Medicine, 1990, 204 , 147-155

7 Corkhill, P.H., Hamilton, C.J. and Tighe, B.J., The design of hydrogels for medical applications, in Critical Reviews in Biocompatibility, Vol. 5 (Issue 4), Ed. Williams, D.F., CRC Press, Boca Raton, Florida, 1990, 363-436

8 Abbott, J.M., Bowers, R.W.J., Franklin, V.J.and Tighe, B.J., Studies in the ocular compatibility of hydrgels (IV) Observations on the role of calcium in desposit formation, J. Br. Contact Lens Assoc., 1991, 14 , 21-28

9 Bowers, R.W.J. and Tighe, B.J., Studies of the ocular compatibility of hydrogels. White spot deposits - incidence of occurrence, location and gross morphology, Biomaterials, 1987, 8 , 89-93

10 Graham, N.B., Poly (ethylene oxide) and related hydrogels, in Hydrogels in Medicine and Pharmacy, Vol II, Ed. Peppas, N.A., CRC Press, Boca Raton, Florida, 1987, 95-113

11 Merrill, E.W., Pekala, R.W. and Mahmud, N.A., Hydrogels for blood contact, in Hydrogels in Medicine and Pharmacy, Vol. III, Ed. Peppas, N.A., CRC Press, Boca Raton, Florida, 1987, 1-16

12 Barnes, A., Corkhill, P.H. and Tighe, B.J., Synthetic hydrogels: 3. Hydroxyalkyl acrylate and methacrylate copolymers: Surface and mechanical properties, Polymer, 1988, 29 , 2191-2202

13 Lee, H.B., Jhon, M.S. and Andrade, J.D., Nature of water in synthetic hydrogels I. Dilatometry, specific conductivity and differential scanning calorimetry of polyhydroxyethyl methacrylate, J. Colloid Interface Sci., 1975, 51 , 225-231

14 Hatakeyama, T., Yamauchi, A. and Hatakeyema, H., Studies on bound water in poly (vinyl alcohol) hydrogel by DSC and FT-NMR, Eur. Polym. J., 1984, 20 , 61-64

15 Nagura, M., Nagura, M. and Ishikawa, H., State of water in highly elastic poly (vinyl alcohol) hydrogels prepared by repeated freezing and melting, Polymer Comms., 1984, 25 , 313-314

16 Sung, Y.K., Pulse NMR and thermal analysis of water-swelling polymers for biomedical applications, Polymer (Korea). 1986, 10 , 576-583

17 Sung, Y.K., Gregonis, D.E., Jhon, M.S. and Andrade, J.D., Thermal and pulse NMR analysis of water in poly (2-hydroxyethyl methacrylate), J. App. Polymer Sci., 1981, 26 , 3179-3728

18 Kim, E.H., Jeon, S.I., Yoon, S.C. and Jhon, M.S., The nature of water in tactic poly (2-hydroxyethyl methacrylate) hydrogels, Bull. Korean Chem. Soc., 1981, 2 , 60-66

19 Jhon, M.S., Hattori, S., Ma, S.M., Gregonis, D. and Andrade, J.D., The role of water in the osomotic and viscoelastic behaviour of gel networks, Polymer Preprints, 1975, 16 , 281-285

20 Pathmanathan, K. and Johari, .P., Dielectric and conductivity relaxations in poly (hema) and of water in its hydrogels, J. Poylmer. Sci: Part B: Polymer Phys., 1990, 28 , 675-689

21 Kim, E.H., Moon, B. Y., Jeon, S. and Jhon, M.S., The nature of water copolymer hydrogels, Bull. Korean Chem. Soc., 1983, 4 , 251-256

22 Nakamura, K., Hatakeyama, T. and Hatakeyama, H., Studies on bound water of cellulose by differential scanning calorimetry, Textile Res. J., 1981, 51 , 607-613

23 Frommer, M.A. and Lancet, D., Freezing and nonfreezing water in cellulose acetate membranes, J. Appl. Polymer Sci., 1972, 16 , 1295-1303

24 Takizawa, A, Kinoshita, T., Nomura, O., Tsujita,.Y., Characteristics of water in copoly(methyl methacrylate-N-vinylpyrrolidone) membranes, Polymer J., 1985, 17 , 747-752

25 Pedley, D.G. and Tighe, B.J., Water binding properties of hydrogel polymers for reverse osmosis and related applications, Br. Polym. J., 1979, 11 , 130-136

26 Bouwstra, J.A., van Miltenburg, J.C., Roorda, W.E. and Junginger, H.E., Polymer-water interactions in cross-linked gels determined by calorimetric measurements, Polym. Bull., 1987, 18 , 337-341

27 Corkhill, P.H., Jolly, A.M., Ng, C.O. and Tighe, B.J., Synthetic hydrogels: 1. Hydroxyalkyl acrylate and methacrylate copolymers-water binding studies, Polymer, 1987, 28 , 1758-1766

28 Roorda, W.E., Bouwstra, J.A., de Vries, M.A. and Junginger, H.E., The thermal analysis of water in p(HEMA) hydrogels, Biomaterials, 1988, 9 , 494-499

29 Roorda, W.E., Bouwstra, J.A., de Vries, M.A. and Junginger, H.E., Thermal behaviour of poly hydroxy ethyl methacrylate (pHEMA) hydrogels, Pharm. Res., 1988, 5 , 722-725

30 Aizawa, M. and Suzuki, S., Properties of water in macromolecular gels III. Dilatometric studies of the properties of water in macromolecular gels, Bull. Chem. Soc. Jpn, 1971, 44 , 2967-2971

31 Carles, J.E. and Scallan, A.M., The determination of the amount of bound water within cellulosic gels by NMR spectroscopy, J. App. Polymer Sci., 1973, 17 , 1855-1865

32 Nagashima, N. and Suzuki, E.I, Studies of hydration by broad-line pulsed NMR, Appl. Spec. Rev., 1984, 20 , 1-53

33 Quinn, F.X., Kampff, E., Smyth, G. and McBrierty, V.J., Water in hydrogels. 1. A study of water in poly (N-vinyl-2-pyrrolidone/methylmethacrylate) copolymers, Macromolecules, 1988, 21 , 3191-3198

34 Yamada-Nosaka, A., Ishikiriyama,K., Todoki, M.and Tanzawa, H., ^{1}H-NMR studies on water in methcrylate hydrogels. I, J. App. Polym. Sci., 1990, 39 , 2443-2452

35 Roorda, W.E., de Bleyser, J., Junginger, H.E. and Leyte, J.C., Nuclear magnetic relaxation of water in hydrogels, Biomaterials, 1990, 11 , 17-23

36 Tanaguchi, Y. and Horigome, S., The states of water in cellulose acetate membranes, J. Appl. Polym. Sci., 1975, 19 , 2743-2748

37 Jhon, M.S. and Andrade, J.D., Water and hydrogels, J. Biomed. Mater. Res., 1973, 7 , 509-522

38 Mack, E.J., Okano, T. and Kim, S.W., Biomedical applications of poly (2-hydroxyethyl methacrylate) and its copolymers, in Hydrogels in Medicine and Pharmacy Vol. II. Properties and Applications, Ed Peppas, N.A., CRC Press, Boca-Raton, Florida 1987, 65-93

39 Hamilton, C.J., Transport Phenonema in Hydrogel Membranes, PhD Thesis, The University of Aston in Birmingham. 1988

40 Murphy, S.M., Hamilton, C.J. and Tighe, B.J., Synthetic hydrogels: 5. Transport processes in 2-hydroxyethyl methacrylate copolymers, Polymer, 1988, 29 , 1887-1893

41 Boehmke, G. and Heusch, R., Hydration of poly glycol ethers, Fette. Seifen. Anstrichmittel, 1960, 62 , 87-91

42 Cunninghame, R.G. and Malcolm, G.N., The heats of mixing of aqueous solutions of polypropylene glycol 400 and polyethylene glycol 300, J. Phys. Chem., 1961, 65 , 1454-1456

43 Bailey, F.E., Lundberg, R.D. and Callard, R.W., Some factors affecting the molecular association of poly (ethylene oxide) and poly (acrylic acid) in aqueous solution, J. Polym. Sci : Part A, 1964, 2 , 845-851

44 Nakayama, H., Temperatue dependence of the heats of solution of poly (ethylene glycol) and of related compounds, Bull. Chem. Soc. Jpn., 1970, 43 , 1683-1686

45 Maron, S.H. and Filisko, F.E., Heats of solution and dilution for polyethylene oxide in several solvents, J. Macromol. Sci - Phys., 1972, B6 ,79-90

46 Hager, S.L. and Macrury, T.B., Investigation of phase behaviour and water binding in poly (alkylene oxide) solutions, J. App. Polym. Sci., 1980, 25 , 1559-1571

47 Kjellander, R. and Florin, E., Water structure and changes in the thermal stability of the system poly (ethylene oxide)-water, J.Chem Soc., Faraday Trans., 1981, 77 , 2053-2077

48 Fernandez-Berridi, M.J., Otero, T.F., Guzman, G.M.and Elorza, J.M., Determination of the solubility parameter of poly (ethylene oxide) at 25^{o}C by gas-liquid chromatography, Polymer, 1982, 23 , 1361-1366

49 Bogdanov, B. and Mihailov, E.M., Light microscopy studies of water oligo (ethylene oxide) eutectic system, J. Macromol. Sci., 1986, B-29 , 59-74

50 Bogdanov, B. and Mihailov, M., Structure and structural transformations of the systems of water and polyoxyethylene, J. Macrmol. Sci.-Phys, 1986, B-25 , 89-132

51 Graham, N.B., Nwachuku, N.E. and Walsh, D.J., Interaction of poly (ethylene oxide) with solvents: 1. Preparation and swelling of a crosslinked poly (ethylene oxide) hydrogel, Polymer, 1982, 23 , 1345-1349

52 Graham, N.B., Zulfiqar, M., Nwachuku, N.E and Rashid, A., Interaction of poly (ethylene oxide) with solvents: 2. Water-poly (ethylene glycol), Polymer, 1989, 30 , 528-533

53 Graham, N.B. and Zulfiqar, M., Interaction of poly (ethylene oxide) with solvents: 3. Synthesis and swelling in water of croslinked poly (ethylene oxide) urethane networks, Polymer, 1989, 30 , 2130-2135

54 Graham, N.B., Zulfiqar, M., Nwachuku, N.E and Rashid, A., Interaction of poly (ethylene oxide) with solvents: 4. Interaction of water with poly (ethylene oxide) crosslinked hydrogels, Polymer, 1990, 31 , 909-916

55 Schreiner, L. J., Milkovic, L. and Peemoeller, H., A determination of hydration stoichiometry in aqueous PEG_{400} solutions, Polymer Commun., 1991, 32 , 105-107

56 Liu, K-J. and Parsons, J.L., Solvent effects on the preferred conformation of poly (ethylene glycols), Macromolecules, 1969, 2 , 529-533

57 Koenig,J.L. and Angood, A.C., Raman Spectra of poly (ethylene glycols) in solution, J. Polymer Sci: Part A-2, 1970, 8 , 1787-1796

58 Baier, R.E., Dutton, R.C. and Gott, V.L., Surface chemical features of blood vessels walls and of synthetic materials exhibiting thromboresistance, in Advances in Experimental Medicine, Vol. 7, Surface chemistry of biological surfaces, Plenum Press, New York, N.Y., 1970, 235-260

59 Andrade, J.D., Interfacial phenomena and biomaterials, Medical Instrumentation, 1973, 7 , 110-120

60 Ratner, B.D., Hoffman, A.S., Hanson, S.R., Harker, S.R. and Whiffen, J.D., Blood compatibility-water content relationships for radiation grafted hydrogels, J. Polym. Sci. Polym. Symp., 1979, 66 , 363-375

61 Coleman, D.L., Gregonis, D.E. and Andrade, J.D., Blood-materials interactions: The minimum interfacial free energy and the optimum polar/apolar ratio hypothesis, J. Biomed. Mater. Res., 1982, 16 , 381-393

62 Hiatt, C.W., Shelokov, A., Rosenthal, E.J. and Galimore, J.M., Treatement of controlled pore glass with poly (ethylene oxide) to prevent the adsorption of rabies virus, J. Chromatogr., 1971, 56 , 362-364

63 Whicher S.J. and Brash, J.L., Platelet-foreign surface interactions: Release of granule constituents from adherent platelets, J. Biomed. Mater. Res., 1978, 12 , 181-201

64 Sa Da Costa, V., Brier-Russell, D., Trudel, G., Waugh, D.F., Salzman, E. W and Merrill, E.W., Polyether-polyurethane surfaces: Thrombin adsorption, Platelet adsorption, and ESCA Scanning, J. Coll. Interface. Sci., 1980, 76 , 594-596

65 Sa Da Costa, V., Brier-Russell, Salzman, E.W and Merrill, E.W., ESCA studies of Polyurethanes: Blood platelet activation in relation to surface composition, J. Coll. Interface. Sci. 1981, 80 , 445-452

66 Okkema, A.Z., Grasel, T.G., Zdrahala, R.J., Solomon, D.D. and Cooper, S.L., Bulk, surface, and blood-contacting properties of polyetherurethanes modified with polyethylene oxide, J. Biomater. Sci. Polymer Edn., 1989, 1 , 43-62

67 Liu, S.Q., Ito, Y. and Imanishi, Y., Synthesis and non-thrombogenicity of polyurethanes with poly (oxyethylene) side chains in soft segment regions, J. Biomater. Sci. Polymer Edn., 1989, 1 , 111-122

68 Brinkman, E., Poot, A. van der Does, L. and Bantjes, A., Platelet deposition studies on copolyether urethanes modified with poly (ethylene oxide), Biomaterials 1990, 11 , 200-205

69 Nakao, A., Nagaoka, S. and Mori, Y., Hemocompatibility of hydrogel with polyethyleneoxide chains, J. Biomater. Appl., 1987, 2 , 219-234

70 Nagaoka, S and Nakao, A., Clinical applications of antithrombogenic hydrogel with long poly (ethylene oxide) chains, Biomaterials, 1990, 11 , 119-121

71 Nojiri, C., Okano, T. Jacobs, H.A., Park, K.D., Mohammad, S.F., Olsen, D.B. and Kim, S.W., Blood compatibility of PEO grafted polyurethane and HEMA/styrene block copolymer surfaces, J. Biomed. Mater. Res., 1990, 24 , 1151-1171

72 Allmer, K., Hilborn J., Larsson, P.H., Hult, A. and Ranby, B., Surface modification of polymers. V. Biomaterial applications, J. Polymer Sci.: Part A: Polymer Chem., 1990, 28 , 173-183

73 Nagaoka, S., Mori, Y., Takiuchi, H., Yokota, K., Tanzawa, H. and Nishiumi, S., Interaction between blood components and hydrogels with poly (oxyethylene) chains, in Polymers as Biomaterials, Shalaby, S. W., Hoffman, A. S., Ratner, B. D. and Horbett, T. A., Eds., Plenum Press, New York, NY, 1984, 361-374

74 Lee, J.H., Kopeckova, P., Kopecek, J. and Andrade, J.D., Surface properties of copolymers of alkyl methacrylates with methoxy (polyethylene oxide) methacrylates and their protein-resistant coatings, Biomaterials, 1990, 11 , 455-464

75 Pedersen, C.J., Cyclic polyethers and their complexes with metal salts, J. Am. Chem. Soc., 1967, 89 , 2495-2496

76 Pedersen, C.J., Cyclic polyethers and their complexes with metal salts, J. Am. Chem. Soc., 1967, 89 , 7017- 7036

77 Frensdorff, H.K., Stability constants of cyclic polyether complexes with univalent cations, J. Am. Chem. Soc., 1971, 93 , 600-606

78 Pedersen, C.J. and Frensdorff, H.K., Macrocyclic polyethers and their complexes, Angew. Chem. Internat. Edit., 1972, 11 , 16-25

79 Bajaj, A.V., and Poonia, N.S., Comprehensive co-ordination chemistry of alkali and alkaline earth metal cations with macrocyclic multidentates : Latest position, Co-ord.Chem. Revs., 1988, 87 , 55-213

80 Synthetic multidentate macrocyclic compounds, Ed. Izatt, R.M. and Christensen, J.J., Academic Press, London, 1978

81 Progress in macrocylic chemistry, vol. 2, Ed. Izatt, R. M. and Christensen, J.J., Wiley-Interscience, New York, 1981

82 Hiraoka, M., Studies in organic chemistry 12: Crown compounds, their characteristics and applications, Elsevier, Amsterdam, 1982

83 Lindoy, L.F., The chemistry of macrocyclic ligand complexes, Cambridge University Press, Cambridge, Great Britain, 1988

84 Timko, J.M. and Cram, D.J., The furanyl unit in host compounds, J. Am. Chem. Soc., 1974, 96 , 7159-7160

85 Browne, C.M., Ferguson, G., McKervey, A.M., Mulholland, D.L., O'Conner, T. and Parvez, M., Molecular receptors. Synthesis, X-ray crystal structures, and chemical properties of crown ethers bearing an intraannular phenolic group, J. Am. Chem. Soc., 1985, 107 , 2703-2712

86 Kimura, E., Kimura, Y., Yatsunami, T. Shionoya, M. and Koike, T., A new Mg^{2+} ion receptor. Macrocyclic polyamines bearing an intraannular phenolic group, J. Am. Chem. Soc. 1987, 109 , 6212-6213

87 Fronczek, F.R., Gatto, V.J., Minganti, C., Schultz, R.A., Grandour, R.D. and Gokel, G.W., Ester side-arm participation in a crystalline lariat ether-sodium bromide complex, J. Am. Chem. Soc.,1984, 106 , 7244-7245

88 Nakatsuji, Y., Nakamura, T., Yonetani, M., Yura, H. and Okahara, M., Molecular design of the electron-donating sidearm of lariat ethers: Effective co-ordination of the quinoloine moiety in complexation toward alklai-metal cations, J. Am. Chem. Soc., 1988, 110 , 531-538

89 Dix, J. P. and Vogtle, F., Ion-selective crown ether dyes, Angew. Chem. Int. Ed. Engl, 1978, 17 , 857-859

90 Nakamura, H., Nishida, H., Takagi, M. and Ueno, K., Chromogenic crown ether reagents for spectro-colourimetric derterminations of sodium and potassium ions, Anal. Chim. Acta., 1982, 139 , 219-227

91 Dietrich, B., Lehn, J.M., and Sauvage, J.P., Diaza-polyoxa macrocycles et macrobicycles, Tet. Lett., 1969, (34) , 2885-2888

92 Walba, D.M., Richards, R.M., Hermsmeier, M., and Haltiwanger, R.C., Conformational properties of THYME polyethers. The bis- THYME cylinder: A three-dimensional analogue of 18-crown-6, J. Am. Chem. Soc., 1987, 109 , 7081-7087

93 Moore, C., and Pressman, B.C., Mechanism of action of valinomycin on mitochondria, Biochem. Biophys. Res. Commun,. 1964, 15 , 562-567 ?

94 Izatt, R.M., Lamb, J.D., Hawkins, R.T., Brown, P.R., Izatt, S.R. and Christensen, J.J., A selective M^{+}-H^{+} coupled transport of cations through a liquid membrane by macrocyclic calixarene ligands, J. Am. Chem. Soc., 1983, 105 , 1782-1785

95 Asfari, Z. and Vicens, J., Isolation and characterisation of bishomooxacalix[4]arene from the condensation product of 4-octadecylphenol with formaldehyde, Makromol. Chem., Rapid Commun., 1989, 10 , 177-179

96 Asfari, Z. and Vicens, J. Calix[7]arenes from 4-methyl- or 4-ethylphenols and formaldehyde, Makromol. Chem., Rapid Commun., 1989, 10 , 181-183

97 McKervey, M.A., Seward, E.M., Ferguson, G., Ruhl, B. and Harris, S.J., Synthesis , X-ray crystal structures and cation transfer properties of alkyl calixaryl acetates, a new series of molecular receptors, J. Chem. Soc., Chem. Commun., 1985, 388-390

98 Ferguson, G., Kaitner, B., McKervey, M.A., and Seward, E.M., Synthesis, X-ray crystal and cation transport properties of a Calix[4]arene tetraketone, a new versatile molecular receptor, J. Chem. Soc., Chem. Commun., 1987, 584-585

99 Diamond, D., Svehla, G., Seward, E.M., and McKervey, M.A., A sodium ion-selective electrode based on methyl p-t-butylcalix[4]aryl acetate as the ionophore, Anal. Chim. Acta., 1988, 204 , 223-231

100 Grandjean, J., Laszlo, P., Vogtle, F., and Sieger, H., Wrapping of noncyclic donor molecules around the sodium cation, Angew. Chem. Internat. Edit., Engl. Ed., 1978, 17 , 846-847

101 Weber, E., and Vogtle, F., Classification and nomenclature of coronands, cryptands, popands and of their complexes, Inorg. Chim. Acta. Lett., 1980, 45 , L-65 - L-67

102 Shchori, E., and Jagur-Grodzinski, J., Permeabilities to salts and water of macrocyclic polyether-polyamide membranes, J. App. Poly. Sci., 1976, 20 , 773-778

103 Shchori, E., and Jagur-Grodzinski, J., Polymeric alloys of poly (vinyl pyrrolidone) with a macrocylic polyether-polyamide, J. App. Poly. Sci., 1976, 20 , 1665-1671

104 Kimura, K., Maeda, T., Tamura, H. and Shono, T., Potassium-selective PVC membrane based on bis and poly(crown ether)s, J. Electroanal. Chem., 1979, 95 , 91-101

105 Peramunage, D., Fernandez, J.E. and Garcia-Rubio, L.H., Poly (crown ether): A potenetial candidate for solid-state electrolytes, Macromolecules, 1989, 22 , 2845-2849

106 Blasius, E., Janzen, K.-P., Klein, W., Klotz, H., Nguygen, V.B., Nguygen-Tein, T., Pfeiffer, R., Scholten, G., Simon, H., Stockemer, H. and Toussaint, A., Preparation, characterisation and applications of ion exchangers with cyclic polyether anchor groups, J. Chromatogr., 1980, 201 , 147-166

107 Blasius, E. and Janzen, K.-P. Analytical applications of crown cmpounds and cryptands in Topics in current Chemistry, 98 , Ed. Vogtle, Springer-Verlag, New York, 1981

108 Wen, J.-S, and Hsiue, G.-H., Liquid-crystal polymers containing macrocyclic polyethers, 1. Side-chain liquid-crystaline copolysiloxanes containing benzo-[15]-crown-5 based mesogenic side groups, Makromol. Chem., Rapid Commun., 1990, 11 ,151-157

109 Rodenhouse, R., Percec, V. and Feiring, A.E., Liquid crystal polymers containing macrohetrocyclic ligands 4. Synthesis of mesomorphic polymers containing crown ethers by cationic cyclopolymerisation of 1,2-bis(2-ethenyloxyethoxy) benzene with mesogenic vinyl ethers, J. Polymer. Sci: Part C: Polymer Letts, 1990, 28 , 345-355

110 Anzai, J., Suzuki,Y., Ueno, A., and Osa, T., Cation transport through liquid membranes mediated by photoreactive crown ethers, Polym. Commun., 1984, 25 , 254-256

111 Shirai, M., Kuwahara, M., and Tanaka, M., Synthesis and alkali cation binding properties of photodimerizable polymers with differently sized crown ethers, Eur. Polym. J., 1988, 24 , 403-410

112 Shirai, M., Moriuma, H. and Tanaka, M., Photoinduced release of alkali picrates uisng photoreactive poly (crown ether)s, Macromolecules, 1989, 22 , 3184-3186

113 Kragten, U.F., Roks, M.F.M. and Nolte, R.J.M., Facilitated ion transport in a biomembrane model. Artificial ion channels as pores in dihexadecyl phosphate vesicles, J. Chem. Soc., Chem. Commun. 1985, 1275-1276

114 Feigenbaum, W.M., and Michel, R.H., Novel polyamides from macrocyclic ethers., J. Polymer Sci. A-1, 1971, 9 , 817-820

115 Ergozhin, E.E., Kurmanaliev, M., Dyusebaev, Kh.A. and Khazrenova, G.G., New polymers with crown ether groups, Internat. Polym. Sci and Techn., 1989, 16 , T/100-T/101

116 Kopolow, S., Hogen Esch, T.E., and Smid, J., Cation binding properties of poly (vinyl macrocyclic polyethers), Macromolecules, 1971, 4 , 359-360

117 Kopolow, S., Hogen Esch, T.E., and Smid, J., Poly (vinyl macrocyclic polyethers). Synthesis and cation binding properties, Macromolecukes, 1973, 6 , 133-142

118 Wong, K.H., Yagi, K. and Smid J., Ion transport through liquid membranes facilitated by crown ethers an their polymers, J. Membrane Biol., 1974, 18 , 379-397

119 Talma, A.G., van Vossen, H., Sudholter, E.J.R., van Eerden, J., and Reinhoudt, D.N., Synthesis of 4'-vinylbenzo-3n-crown-n ethers ($4 \leq n \geq 10$), Syn. Commun., 1986, 680-683

120 Kikukawa, K., Nagira, K., and Matsuda, T., Synthesis of 4'-vinylbenzo-15-crown-5 from benzo-15-crown-5, Bull. Chem. Soc. Jpn. 1977, 50 , 2707

121 Tomoi, M., Abe, O., Ikeda, M., Kihara, K., and Kakiuchi, H., Synthesis of hydroxy group-containing crown ethers and polymer-supported crown ethers, Tet. Lett. 1978, (33), 3031-3034

122 Varma, A.J., Majewicz, T., and Smid, J., Polysalt complexes of poly (vinyl benzo-18-crown-6) and of poly (crown acrylates) with polyanions , J. Polymer Sci., Polymer Chem. Ed., 1979, 17 , 1573-1581

123 Yagi, K., Ruiz, J.A., and Sanchez, M.A., Cation binding properties of polymethacrylamide derivatives of crown ethers, Makromol. Chem., Rapid Commun., 1980, 1 , 263-268

124 Nakatsuji, Y., Furuyoshi, S. and Okahara, M., Synthesis and polymerisation of N-acryloyl-and N-methacryloylaminomethyl crown ethers, Makromol. Chem. 1986, 187 , 105-109

125 Oue, M., Ishigaki, A., Kimura, K., Matsui, Y., and Shono, J., Synthesis and cation-binding properties of poly and bis (thiacrown ether)s, J.Polymer Sci., Polymer Chem. Ed., 1985, 23 , 2033-2042

126 Herweh, J E., Synthesis, characterization and complexing properties of polymethacrylate bearing pendant macroheterocyclic strucures, J. Polymer Sci., Polymer Chem. Ed., 1985, 23 , 2767-2778

127 Chujo, Y. Nakamura, T. and Yamshita, Y., Synthesis of crown ether-terminated poly (methyl metahcrylate) by radical chain transfer polymerization, J. Polymer Sci: Part A: Polymer Chem. 1990, 28 , 59-65

128 Molinari, H., Montanari, F. and Tundo, P., Heterogeneous phase-transfer catalysts: High efficacy of catalysts bonded by a long to a polymer matrix, J. Chem. Soc., Chem. Comm., 1977, 639-641

129 Warshawsky, A., Kalir, R., Deshe A., Berkovitz, H. and Patchornik, A., Polymeric pseudocrown ethers. 1. Synthesis and complexation with transition metal anions, J. Am. Chem. Soc., 1979, 101 , 4249-4258

130 Kahana, N., Deshe, A., and Warshawsky, A., Synthesis of polymeric crown ethers and thermoregulated ion complexation effects, J. Polym. Sci.: Polym. Chem. Ed., 1985 , 23 , 231-253

131 Yokota, K., Kakuchi, T., Sasaki, H., Ohmori, H., Asymmetric induction in the cyclopolymerization of divinyl ethers derived from (R)- or (S)-3,3'-dimethyl-1,1'-bi-2-naphthol, Makromol. Chem., 1989, 190 , 1269-1275

132 Kakuchi, T., Hasegawa, T., Sasaki, H., Ohmori, H., Yamaguchi, K. and Yokota, K, Polymeric chiral cown ethers, 4. Subsituent effects of methyl and phenyl groups in the 3,3'-positions on chiral recognition of poly (crown ether)s synthesized by copolymerization of divinyl ethers derived from 1,1'-bi-2-naphthol, Makromol. Chem., 1989, 190 , 2091-2097

133 Kakuchi, T., Takaoka, T. and Yokota, K., Polymeric chiral crown ethers, 5. Synthesis of polymers cyclopolymerization of divinyl ethers containing moities deriving from L-tartric acid, and the chiral recognition toward amino acids, Makromol. Chem., 1989, 190 , 2449-2454

134. Kimura, K., Yoshinaga, M., Kitazawa, S., and Shono, T., Synthesis of poly (vinyl alcohol) based poly (crown ethers) and permeability of their polymeric membranes, J. Polymer Sci., Polymer Chem. Ed.,1983 , 21 , 2777-2785

135 Atkins, P.W., Chap 25 in Physical Chemistry, 2nd ed, Oxford University Press, Oxford, 1978, 874-875

136 Kubín, M. and Specek, P., Structure and properties of hydrophilic polymers and their gels V. Diffusion in gels, Collection Czechoslov. Chem. Commun, 1965, 30 , 3294-3302

137 Spacek, P. and Kubin, M., Diffusion in gels, J. Polym. Sci: Part C., 1967, 16 , 705-714

138 Yasuda, H., Lamaze, G.E. and Ikenberry, L.D., Permeability of solutes through hydrated polymer membranes. Part I. Diffusion of sodium chloride, Makromol. Chem., 1968, 118 , 19-35

139 Yasuda, H., Ikenberry, L.D. and Lamaze, C.E., Permeability of solutes through hydrated polymer membranes. Part II. Permeability of water soluble organic solutes, Makromol. Chem., 1969, 125 , 108-118

140 Yasuda, H., Peterlin, A., Colton, C.K., Smith, K.A. and Merrill, E.W., Permeability of solutes through hydrated polymer membranes. Part III. Theoretical background for the selectivity of dialysis membranes, Makromol. Chem.,1969 , 126 , 177-186

141 Ratner, B.D. and Miller, I.F., Transport through crosslinked poly (2-hydroxyethyl methacrylate) hydrogel membranes, J. Biomed. Mater. Res., 1973, 7 , 353-367

142 Ng, C.O., and Tighe, B.J., Polymers in contact lens applications VI. The 'dissolved' oxygen permeability of hydrogels and the design of materials for use in continuous-wear lenses, Br. Polym. J., 1976, 8 , 118-123

143 Refojo, M.F. and Leong, F.L., Water-dissolved-oxygen permeability coefficients of hydrogel contact lenses and boundary layer effects, J. Membrane Sci., 1979, 4 , 415-426

144 Kim, S.W., Cardinal, J.R., Wisniewski, S. and Zentner, G M., Solute permeation through hydrogel membranes, hydrophilic vs hydrophobic solutes, in Water in Polymers, Rowland, S. P., Ed., ACS Symposium Series, Vol. 127, American Chemical Society, Washington D.C., 1980, 347-359

145. Wisniewski, S., and Kim, S.W., Premeation of water-soluble solutes through poly (2-Hydroxyethyl Methacrylate) and poly (2-Hydroxyethyl Methacrylate) crosslinked with ethylene glycol dimethacrylate, J. Membr. Sci., 1980, 6 , 299-308

146 Yoon, S.C. and Jhon, M.S., The transport phenomena of some model solutes through postcrosslinked poly (2-hydroxyetyl methacrylate) membranes with different tactic precusors, J. App. Polym. Sci., 1982, 27 , 3133-3149

147 Yoon, S.C. and Jhon, M.S., Temperature effect on the permeation through poly (2-hydroxyetyl methacrylate) membrane, J. Appl. Polymer Sci., 1982, 27 , 4661-4668

148 Kojima, Y., Furuhata, K. and Miyasaka, K., Hydraulic permeability of water in poly(vinyl alcohol) membranes as a function of the degree of hydration, J. Appl. Polym. Sci., 1983, 28 , 2401-2410

149 Kojima, Y., Furuhata, K. and Miyasaka, K., Diffusive permeability of solutes in poly(vinyl alcohol) membranes as a function of the degree of hydration, J. Appl. Polym. Sci., 1984, 29 , 533-546

150 Moynihan, H.J. and Peppas, N.A., Transport phenomemna in polymers PHEMA membranes: Diffusive characteristics, Polymer News, 1984, 9 , 236-239

151 Peppas, N.A. and Moynihan, H.J., Solute diffusion in swollen membranes IV. Theories for moderately swollen networks, J. Appl. Polymer Sci., 1985, 30 , 2859-2606

152 Moynihan, H.J., Honey, M.S. and Peppas, N.A., Solute diffusion in swollen membranes. Part V: Solute diffusion in poly(2-hydroxyethyl methacrylate), Polym. Eng. Sci., 1986, 26 , 1180-1185

153 Uragami, T., Furukawa, T., and Sugihara, M., Studies on syntheses and permeabilities of special polymer membranes: 57. Permeability of solute through polymer membranes and state of water in their membranes, Polym. Comm., 1984, 25, 30-32

154 Uragami, T., Moriyama, K., Wada, T., Nakashima A., and Sugihara, M., Studies on syntheses and permeabilities of special polymer membranes, 60. Active transport of alkali metal ions through poly(vinyl alcohol) membranes, Makromol. Chem., Rapid Commun., 1985, 6 , 321-324

155 Tighe, B.J., The role of permeability and related properties in the design of synthetic hydrogels for biomedical applications, Brit. Polym. J., 1986, 1 , 8-13

156 Hamilton, C.J., Murphy, S.M., Atherton, N.D. and Tighe, B.J., Synthetic hydrogels: 4. The permeability of poly(2-hydroxyethyl methacrylate) to cations-an overview of solute-water interactions and transport processes, Polymer, 1988, 29, 1879-1886

157 Yasuda, H., Lamaze, C.E., and Peterlin, A., Diffusive and hydraulic permeabilities of water in water-swollen polymer membranes, J. Polym. Sci: Part A-2, 1971, 9 , 117-1131

158 Yoshikawa, M., Ochiai, S., Tanigaki, M. and Eguchi, W. Application and development of synthetic polymer membanes, 4. Relation between permselectivity for aqueous ethanol solution and state of water in synthetic polymer membranes, Makromol. Chem., Rapid. Commun., 1988, 9 , 559-564

159 Ogston, A.G. , The spaces in a uniform random suspension of fibres, Trans. Faraday Soc., 1958, 54 , 1754-1757

160 Ungaro, R., El Haj, B. and Smid, J., Substituent effects on the stability of cation complexes of 4'-substituted monobenzo crown ethers, J. Am. Chem. Soc., 1976, 98 , 5198-5202

161 Wada, F., Hirayama, H., Namiki, H., Kikukawa, K., and Matsuda, T., New Applications of Crown Ethers II. Synthesis of 4' Formylbenzocrown Ethers, Bull. Chem. Soc. Jpn. 1980, 53 , 1473-1474

162 Kumanoto, E., Effect of unstirred layers on the membrane-potential in a concentration cell, J. Membr., Sci., 1981, 9 ,43-51

163 Flynn, G. and Smith, E.W., Membrane diffusion I: Design and testing of a new multifeatured difussion cell, J. Pharm. Sci., 1971, 60 , 1713-1717

164 Artherton, N.D., Drug-water interactions in hydrogel membranes, Ph.D. Thesis, the universty of Aston in Birmingham, 1982

165 Tighe, B.J. and Trevett, A.S., The characterisation of mechanical properties of soft contact lenses, Trans. Br. Contact Lens Assoc.Annual Clinical Conference, Glasgow, 1990, 57-61

166 Petranek, J., and Ryba, O., Potassium selective electrodes based on macrocyclic polyethers : The effect of structure of the neutral carrier on selectivity, Anal. Chim. Acta., 1974, 72 , 375-380

167 Mascini, M., and Pallozzi, F., Selectivity of neutral carrier-PVC membrane electrodes, Anal. Chim. Acta., 1974, 73 , 375-382

168 Nightingale, E.R., Phenomenological theory of ion solvation. Effective radii of hydrated ions, J. Phys. Chem., 1959, 63 ,1381-1387

169 Corkhill P.H., Novel hydrogel polymers, Ph.D. Thesis, The Universty of Aston in Birmingham, 1988

170 Ng, C.O., Synthetic hydrogels in contact lens applications, Ph.D. Thesis, The Universty of Aston in Birmingham, 1974

171 Adamcova, Z., Structure and properties of hydrophilic polymers and their gels. X. Gel filtration of ethylene glycol methacrylate gels, Coll. Czech. Chem. Commun., 1968, 33 ,336-340

172 Dusek, K., Vosicky, V., Bohdanecky, M., Solubilization of poly (2-hydroxyethyl methacrylate) with aqueous salt solutions; Swelling of gels, Coll. Czech. Chem. Commun., 1977, 42 , 1599-1614

173 Owens, D.K. and Wendt, R.C., Estimation of the surface free energy of polymers, J. Appl. Polym. Sci. 1969, 13 , 1741-1747

174 Panzer, J., Components of solid surface free energy from wetting measurements, J. Colloid and Interface. Sci., 1973, 44 ,142-161

175 Franklin, V.J., Ph.D. Thesis, Lipoidal species in ocular spoilation process, Aston Universty, 1990

176 Thomas, K.D., Biological Interactions with Synthetic Polymers, PhD Thesis, University of Aston, 1988